The impacts of climate change on coffee: trouble brewing

James Rising,
Tim Foreman, John Simmons, Manuel Brahm, Jeffrey Sachs
The Earth Institute
Columbia University

October 1, 2016

Contents

Executive Summary

This report provides new evidence on the present and predicted future impacts of climate change on coffee production and markets.

Coffee is sensitive to climate. Arabica coffee is grown at high elevations, in warm regions, with sensitive quality, and multiple positive and negative ecosystem interactions 1.1. All of these cause high-quality coffee to be threatened by climate change.

Temperatures are already causing shifts. Recent temperatures in the coffee belt have been increasing by 0.16°C per decade (1.2), representing an average shift of 46km per decade. In Brazil, low elevation farms are already being impacted (3.2).

Temperature across the coffee belt is expected to rise by 2.1°C (likely range 1.7 - 2.5°C) by 2050 (3.1). Average future temperatures have high predictability, but not their spatial pattern. 60-64% of recent temperatures is explained by a trend, but most of the rest is uncertain year-to-year (1.2.2).

Precipitation across the coffee belt is expected to increase 1.7% (likely range -0.1 - 3.2%), but dry periods will often be drier (3.1). Average future precipitation has low predictability. Only 1% of precipitation can be explained by long-term trends, but decadal cycles predictable in the short-term (like El Niño) play a large role.

We develop a new database of spatial coffee production. The database combines spatial data from 3 global sources and 8 detailed country sources, and temporal data from 2 global sources and 5 country sources (2.1).

We present a new technique for coffee suitability analysis. The technique incorporates properties of soil, climate, and elevation for a statistical model, and combines it with biological conditions from the Global Agro-ecological Zones (GAEZ) project (2.2).

Nearly 20 countries could lose all highly naturally suitable coffee land. Globally, suitable regions will decrease by 56% for Arabica, including 24% of current cultivation, while they increase by 87% for Robusta. (4.2).

New coffee growing regions will become available further from the equator. For Arabica coffee, the countries with the most new coffee regions are Brazil, Mexico, and Angola. While many countries will gain new suitable land, globally this is only be 10 - 20% of what may be lost (4.2).

On average, El Niño years produce 30% hikes in coffee prices and drops in coffee yields. No corresponding effect is seen globally across La Niña years, except in their interactions with the PDO and AMO signals (3.4).

Higher temperatures may lead to larger coffee rust outbreaks. In addition, vigilant farmer action against these outbreaks will decrease small infestations but may increase the probability of large ones (2.4).

Hot days produce non-linearly large yield losses. In Brazil, days over 38°C cause serious losses, and some countries receive losses at temperatures as low as 33°C (3.3.2). Climate change will cause more of these days. There is evidence that some countries have adapted to high temperatures with lower sensitivity to them.

Under temperatures in 2050, average yields in existing growing areas are expected to drop 20%. The variation between countries is large, with some countries losing the majority of their production potential, and others seeing increases.

Globally, prices paid to farmers are driven much more by international prices than local competition. We also find that international prices and consumer demand are more self-determined than driven by changes in production and retail prices, respectively (3.6).

Most of the markup associated with producer countries does not go to farmers. Trade relations suggest that 21% of consumer prices go to production, 44% to distribution, and 35% to the organizations in the consumer's country (3.6.3).

Introduction

Coffee plays a vital role in many countries, providing necessary income to 25 million members of tropical countries and supporting a $81 billion industry (Sharf, 2014), making it one of the most valuable commodities in the world. However, coffee is extremely vulnerable to climate change, with disease outbreaks becoming more common and suitable regions beginning to shift (Guilford, 2014; Malkin, 2014). The coffee industry consists of a complex web of small-holder farmers, multinational corporations, government policies, and a diverse consumers. As coffee demand continues to expand, the international coffee system will experience pressure from all of these elements.

This research studies the effects of climate change on coffee from a global perspective. As productive coffee region shift, every aspect of the coffee system will be impacted, from developing country farmers to developed country consumers. By 2050, these long-term shifts will reshape the global coffee market.

The effects of climate on coffee also include shorter time-scales. Climatic cycles with global origins and global effects have long impacted coffee production. Production in different regions vary in their degree of sensitivity to climatic cycles and extreme temperatures, and understanding these differences is an important input to global planning.

Coffee production has considerable potential for supporting sustainability and economic opportunities for the future, but planning requires a better understanding of the interconnections between production, trade, and the environment. The future of coffee depends on understanding the risks, instituting high-resolution monitoring, and acting in anticipation of future impacts.

This report is organized into multiple chapters, exploring different aspects of the climate-coffee connection.

- **Chapter 1** introduces the basics of coffee growth and its vulnerability to climate change.
- **Chapter 2** describes the approach, methods, and data collection used for the new research in this report.
- **Chapter 3** presents our results on the impacts coffee will experience under future climate scenarios.
- **Chapter 4** presents our results on the potential for shifting cultivation to new regions.
- **Chapter 5** provides an overview of the strategies available to coffee growers to adapt to climate change.
- **Chapter 6** discusses future research and data needs in the coffee sector and future research opportunities.
- **Chapter 7** offers a series of recommendations to the coffee industry, as informed by our research.

A number of additional analyses are reported in Appendix A, many of which offer avenues for future research. Appendix B describes the coffee production database we generated and the principles behind it.

Maps disclaimer

Throughout this report, we display maps using the Gall-Peters projection to highlight features in the tropics and improve the readability of the maps. This projection distorts regions in the tropics to take up more vertical space. Also, to optimize the page realestate, we hide regions of the Atlantic and Pacific Oceans without islands or where small islands are not producers of coffee.

Chapter 1

Coffee growth and vulternability

1.1 Coffee and coffee production

Two species make up the vast majority of commercial coffee. *Coffea arabica* (Arabica coffee) originates from an area around the southern borders of Ethiopia and Sudan, and is known for its fine taste. *Coffea canephora* (Robusta coffee) is native to central and western Africa, just south of the Sahel, and is hardier and has a higher caffeine content than Arabica. From these regions, coffee has spread through the tropics, with cultivation in 78 countries (see figure 1.1).

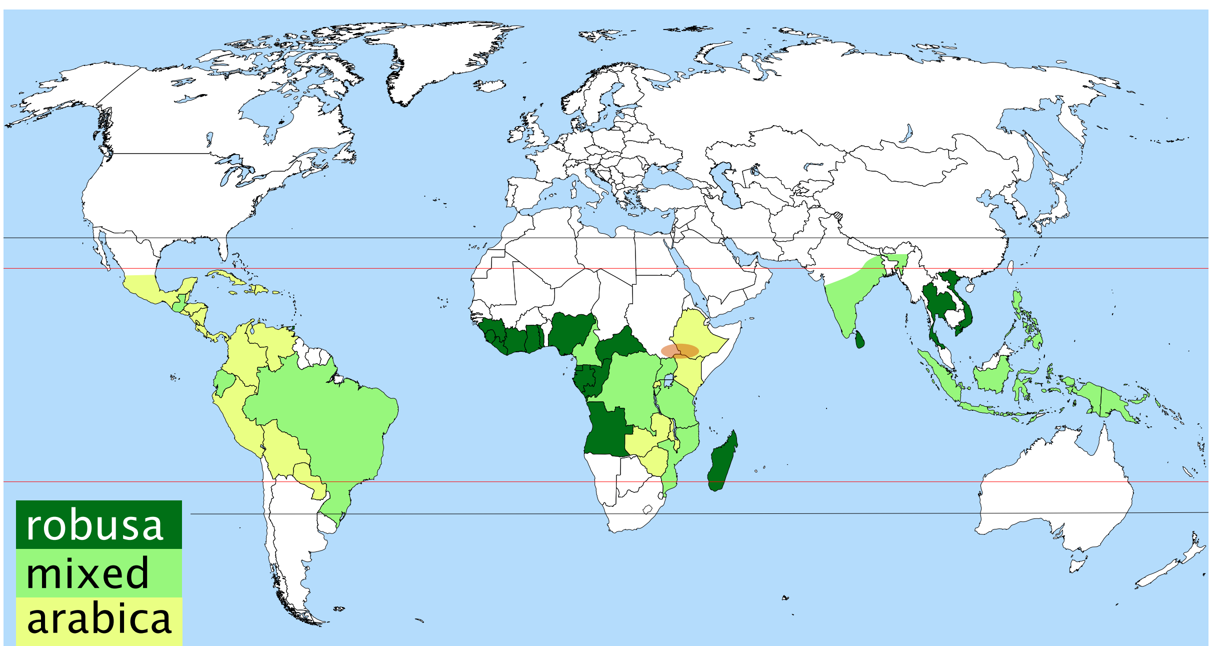

Figure 1.1: Coffee production, colored by species (Arabica, Robusta, and both). Tropics of Cancer and Capricorn shown in red, and latitudes of 30°N and S shown in black. Red oval identifies the native region of Arabica coffee. Adapted from Wikimedia Commons.

In figure 1.1, the red lines of longitude lines designate the tropics of Cancer and Capricorn, encompassing the traditional zone of coffee production. Throughout this report, we show results between the black lines, at 30°N and 30°S. This broader range is necessary as regions suitable for coffee cultivation shift toward the poles under climate change.

Many aspects of the production capacity, climatic response, and future suitability described in this report depend on the unique needs of the coffee plant. Since the quality of the coffee bean matters, as well as its quantity, the conditions for producing high quality coffee have been studied in multiple forms. Even slight changes in temperature, precipitation, and humidity can lower coffee quality, increase the risk of damage from frosts and pests, and undermine the sensitive flowering and berry growing phases.

Coffee plants require particular ranges of temperature, rainfall, and soil conditions to produce a high quality product. Arabica grows best in regions with mean annual temperatures of 18 to 22°C. High temperatures can accellerate the berry production process, and lower coffee quality. Lower temperatures slow the berry production process, allowing flavors to accummulate. However, frosts damage the plant, so temperatures need to be remain moderate (Pendergrast, 1999).

Himidity should be low, but heavy precipitation (over 1400 mm per year) is important. The rain requirements of coffee plants vary with the varieties grown in areas that have year-around rain and areas that have distinct rainy and dry seaons. In areas with dry seasons, precipitation should be common for at least 7 months of the year. However, too much precipitation (over 3000 mm in a year) is harmful to the coffee plant, causes soil erosion, and supports coffee diseases (Wrigley, 1988). In areas with distinct wet and dry seasons, the transition is important to promote growth in the wet season and ripening in the dry season. In areas without such a division, berries form year-around.

Robusta coffee grows in hotter temperatures, between 22 and 30°C for the mean annual temperature. They also tolerate higher levels of humidity, and as well as greater direct sunlight, common in open monocultures. Historically, Robusta coffee spread in response to the devastation left by coffee leaf rust (*Hemileia vastatrix*), to which the species has a greater resistence.

Wind speed is an important issue, with high winds reducing leaf area and hot winds increasing water requirements (Pohlan and Janssens, 2012).

Soils can embody many of these other climatic conditions, but the coffee plant has additional requirements for optimal soils. Soils should drain quickly, such as volcanic soils in Brazil and Hawaii. Slightly acidic soils are also beneficial, so long as the pH is not below 4 or above 8 (Willson, 1985).

Elevation is generally considered to be a primary concern, with Arabica commonly grown above 1000 m and Robusta at lower elevations. However, this is largely explained by the differences in temperatures: higher elevations in the tropics benefit from tropic and mountain-effect rains but have a low enough temperature for coffee flavors to develop.

Lower temperatures slow the coffee berry production process and improve bean quality by allowing flavors to accumulate (Muschler, 2001). This effect is also seen in shade-grown coffee, which allow the coffee plant to experience lower temperatures without increasing the risk of frosts.

Timing is important throughout the production process. Coffee plants take 3-4 years before they generate fruit, and do not fully mature until 9-12 years. Blossoming occurs after a drop in temperature, often induced by rainfall, and the fruit is available for harvest 6-8 months later for Arabica plants and 10-11 months for Robusta plants.

Coffee is being exposed to a growing list of threats under climate change. High temperatures are the most obivious, which accellerate berry production at a loss to its equality, increase water requirements, and ultimately damage the plant. Climate change is likely to increase the threat of pest and diseases.

Fungus, like the coffee rust *Hemileia vastatrix*, and pests, such as the coffee berry borer *Hypothenemus hampei*, are both expected to increase their activity under higher temperatures.

Both droughts and floods are expected to become more common under climate change. Coffee needs a consistent pattern of rainfall, with distinct rainy and dry seasons in the subtropics and continuous rainfal below latitudes of 10°. Climate change is expected to change precipitation in many regions (some expected to receive more rain, some less), but also the timing of rainfall over the year and increase the risk of both torrential downpours and extended droughts.

1.2 Recent climate change and uncertainties

The coffee belt, the band of coffee suitable regions between the tropics of Cancer and Capricorn, has experienced a sharp increase in temperatures since the 1960s, and this trend is expected to increase. Figure 1.2 displays the yearly average temperature in this belt over the instrumental record. The average increase in recent decades has been 0.16°C per decade. The equator is generally expected to warm more slowly than the poles, and this represents an intermediate rate, greater than the rate of ocean warming at 0.11°C per decade and less than the global average for land at 0.28°C per decade (GISTEMP Team, 2015; Hansen et al., 2010).

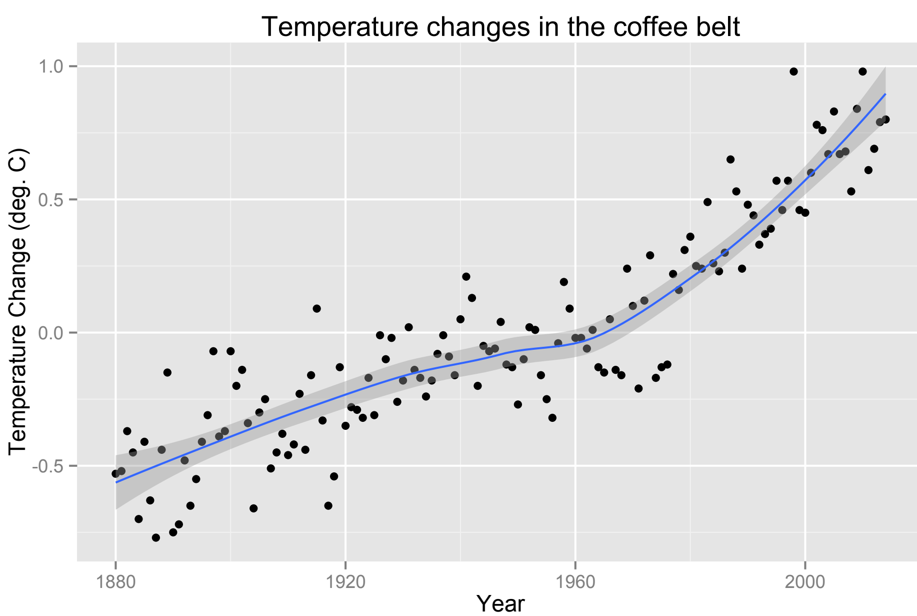

Figure 1.2: Yearly average temperatures in the coffee belt (dots), including temperatures over land and oceans, and a smooth running average with 95% confidence intervals.

As temperatures increase, coffee production will be forced toward the poles and to higher elevations. On average, to adapt to an increase of 0.16°C degrees per decade, coffee production will need to shift 46km per decade toward the poles or 29m higher per decade.[1]

[1] Average change in temperature with latitude and elevation from `http://landterms.com/Articles_and_FAQ_s/Conservation_and_Ecology_Articles_and_FAQ_s/Latitude__Elevation_and_Temperature/`, reported as 3°F / 300 miles

1.2.1 Counterbalancing effects

Not all of the effects of climate change are necessarily detrimental to coffee production. One of the major threats to coffee farms is frost (Varangis et al., 2003), and where minimum temperatures shift away from frosts without otherwise affecting conditions, coffee production will benefit. Elsewhere, the variability of temperature will become greater, increasing the risk of cold snaps and frost damage even as average temperatures warm.

Carbon fertilization will also have uncertain effects. Many crops see yield benefits from carbon fertilization (McGrath and Lobell, 2013), as plant produce more carbohydrates (Körner et al., 2007). However, a wider carbon-to-nitrogen ratio can produces a loss of quality for agricultural products. Quality coffee production may need to move to higher elevations to offset this increase in carbohydrate productivity. At higher elevations, bean development slows and flavors have more time to accumulate, but this also placing coffee back into zones of high frost risk.

As temperatures rise, coffee will be forced generally up slopes and away from the equator. Under 2-2.5°C of warming, the minimum altitude suitable for coffee production in Central America and Kenya is expected to increase by around 400m (IPCC, 2014). However, this will open up new areas to coffee production, even as it eliminates traditional areas, for example in high-elevation regions of Guatemala.

1.2.2 Climate predictability

The primary drivers of yields, suitability, and other responses of coffee to climate are through temperature and precipitation. Although we have extensive predictions of future temperature and precipitation patterns through the end of the century, these need to be treated with some circumspection. Our understanding of the future impacts of climate on coffee is limited by the fundamental predictability of the climate system.

Climate change and the long-term increase in global average temperatures are a virtual certainty. However, predictions for change in global temperature resulting from a doubling of CO_2 range from 1°C to 6°C (Stocker et al., 2014, Box 12.2). Many feedback loops in the climate are poorly understood, and predictions that agree on eventual changes in the climate can disagree on the timing. Furthermore, the patterns of weather changes are more uncertain than the global average. The uncertainty around how society will respond to climate change is even greater than uncertainty in climate.

One way to understand the amount of uncertainty for coffee-growing regions that results from the natural climate system is to identify the kinds of variability in historical temperature and precipitation. We can separate the average temperature and precipitation into components that are driven by (1) long-term trends, (2) decadal cycles, and (3) interannual variation. Long-term trends can be predicted many years in advance. Decadal cycles are more difficult to predict, but forecasts are often available months or years ahead. The remaining unpredicted changes in temperature and precipitation are idiosyncratic to a particular year, and typically unpredictable before that year.

The table below shows the portion of variability over the past hundred years that falls into each of these three components for land areas between 30°N and 30°S.

Temperature and precipitation show very different patterns of uncertainty. A large part of the region's temperature is predicted by the long-term trend (60-64%), reflecting the relative certainty of long-term temperature increases. Most of the remaining uncertainty for temperature is represented by inter-annual variation, and this portion of each year's temperature is very difficult to predict.

latitude and 3°F / 1000 ft elevation. This equates to 290 km / °C and 183 m / °C.

In contrast, there is very little long-term trend in precipitation. While climate change is expected to increase the rate of precipitation on average, observed changes are very small. However, in this case, decadal cycles provide some amount of predictability (17-25%), with changes in ocean temperatures driving decade-long increases and decreases in precipitation. There remains still a large fraction of each year's precipitation which is unpredictable.

Component	Annual Average	Sep. - Nov.
Long-term Trend	64%	60%
Decadal Cycles	6%	11%
Inter-Annual Variation	29%	26%
Long-term Trend	1%	1%
Decadal Cycles	17%	25%
Inter-Annual Variation	81%	69%

Table 1.1: From http://iridl.ldeo.columbia.edu/maproom/Global/Time_Scales/temperature.html and http://iridl.ldeo.columbia.edu/maproom/Global/Time_Scales/precipitation.html. Blossoming has been found to be the most sensitive time for coffee plants[2], and Sep. - Nov. is this period in Brazil, the largest coffee producer.

It is also possible to look at this patterns of predictability as they vary in space. The Time Scales Maproom from the International Research Institute for Climate and Society (IRI) provides a way of decomposing variability in temperature and precipitation over space. Decompositions for temperature and precipitation, against the long-term trend and decadal cycles drivers, are shown in figures 1.3 and 1.4.

The temperature maps show that little of the year-to-year variation is explained by a long-term trend in many coffee-growing regions. In particular, this historical analysis shows almost no explanatory capacity for Colombia and much of Indonesia. However, coffee growing regions of Brazil and India are strongly explained by the long-term trend, suggesting that the results from these areas will be most reliable. As above, almost none of the the year-to-year variation in precipitation is explained by the long-term trend, but moderate amounts driven by decadal cycles, particularly in Colombia and India.

[2] E.g., for Nicaragua: http://www.academia.edu/2243528/Coffee_yield_variations_and_their_relations_to_rainfall_events_in_Nicaragua.

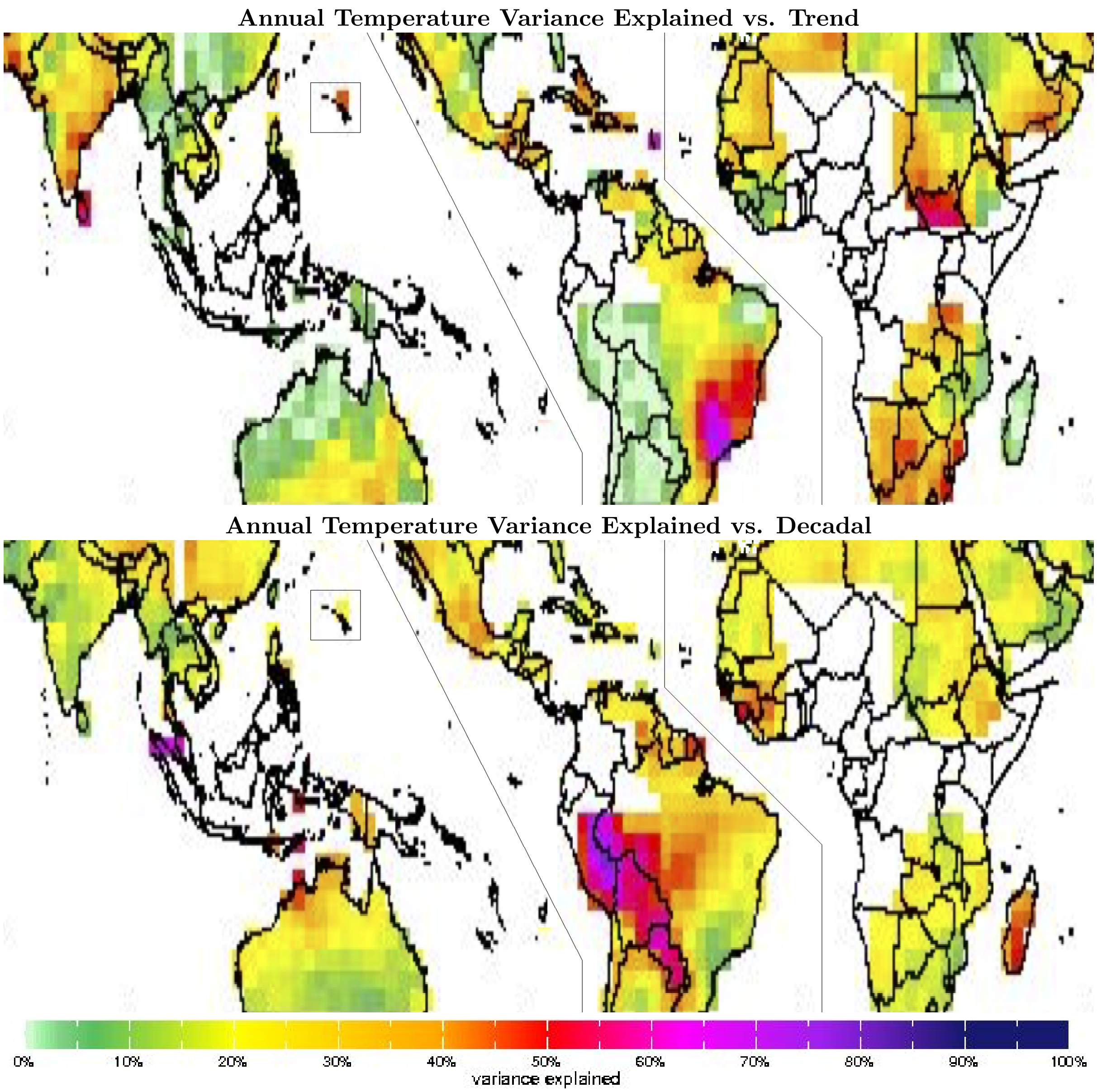

Figure 1.3: Long-term and decadal predictability for temperature, from `http://iridl.ldeo.columbia.edu/maproom/Global/Time_Scales/temperature.html`.

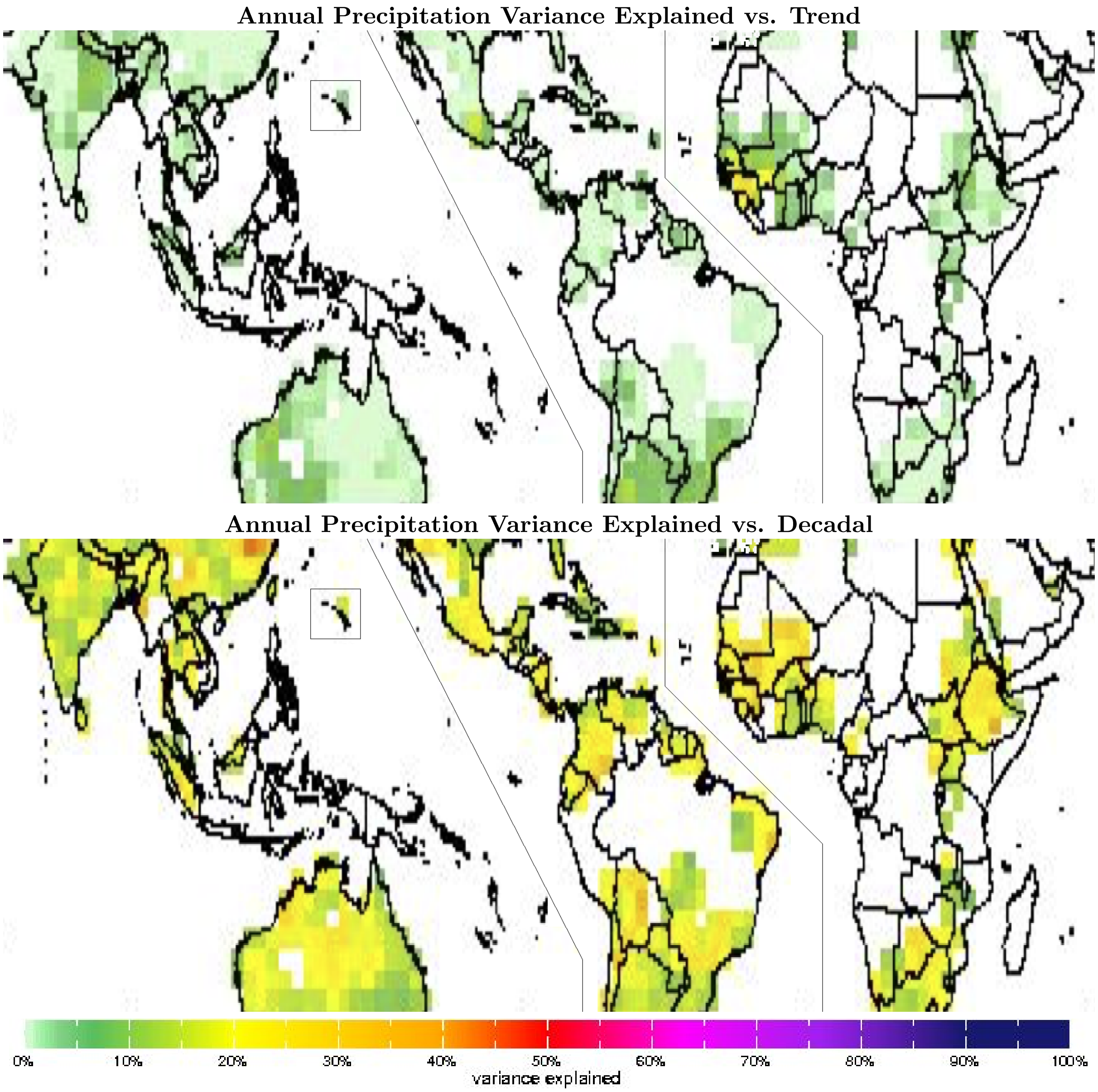

Figure 1.4: Long-term and decadal predictability for precipitation, from `http://iridl.ldeo.columbia.edu/maproom/Global/Time_Scales/precipitation.html`.

1.3 The importance of variability

While long-term climate change is going to alter the landscape of coffee, many climate impacts are already occurring and represent shifts on shorter time-scales. While the most commonly known cycle in the coffee industry is the biennial production cycle, climate has internal cycles that affect coffee production. These are produced by climate decadal variability, and are some of the most important climate dynamics for the coffee industry.

We find that the most important of these cycles is the El Niño/La Niña cycle, known as ENSO. The ENSO cycle produces vast weather changes over much of the tropics. ENSO is of particular concern today, as we approach what may be the largest El Niño event in a generation. During the last large El Niño in 1997-98, the tropics were hit by both droughts and floods, as shown in figure 1.5. It also coincided with infectious outbreaks in Africa (Epstein, 1999), megafires in Indonesia (Page et al., 2002), crop failures across the tropics (Hsiang and Meng, 2015). El Niño and La Niña events can often be predicted before their impacts are felt, and knowing what to expect can make a big difference in the outcomes.

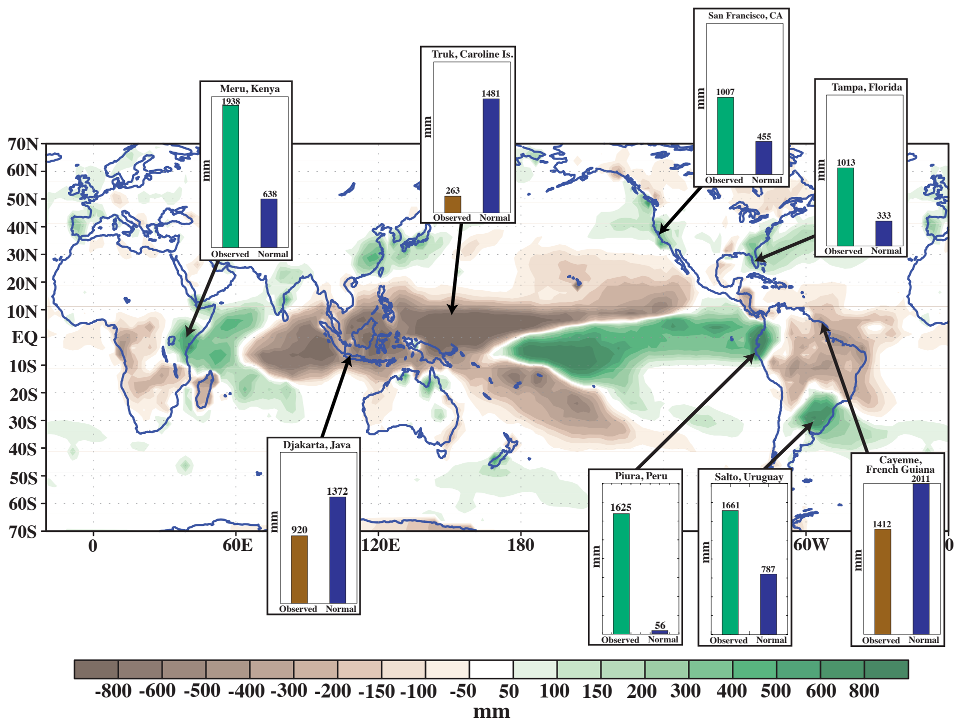

Figure 1.5: Rainfall anomalies from November 1997 to April 1998. Reproduced from Bell et al. (1999).

Climate indices, such as NINO 3.4 (a measure of the strength of the El Niño signal), correlate with the weather and weather impacts of coffee-growing countries. They are often more predictable than weather months in advance as well, allowing farmers and markets to glean information about their production prospects. In some areas, weather prediction is still poor, but global climate indices are always available, and can be used to more clearly identify the impacts of climate without the confounding role of local weather feedbacks.

Chapter 2

Research approach and data

We take a quantitative, empirical approach to produce the new research of this report and to address questions about the current and future state of the global coffee system. We identify relationships that are closely tied to the physical world, drawing on the strengths of the Earth Institute. Furthermore, the relationships we study are as they are reflected in aggregated data, often at the country-wide level. There are important impacts of climate change on farms and farmers that only appear implicitly in this data and our results.

We emphasize a number of elements underrepresented in the coffee literature. First, we focus on the pervasive uncertainty underlying coffee and climate analyses. This stems from a combination of the inherent variability of climate, the heterogeneity of coffee farming practices, and uncertainty in the statistical results relating them. Without this, the true risk of climate change to coffee can both be misestimated and misattributed. We have incorporated the analysis of uncertainty throughout our work.

Second, and related to this, is the state of coffee production knowledge. Coffee data is often not available at high resolution and not available comprehensively within regions. It is also likely to have considerable bias, since coffee production is highly politicized in many countries. We have developed a new spatial coffee production database to address these problems, and emphasize statistical techniques and tools that account for the erratic data quality.

Third, we have drawn from multiple academic literatures to apply innovative approaches to questions around coffee and climate. These include our Bayesian approach to estimating suitability; our study of interactions between multiple signals to understand variability; and our use of the most robust methods of econometrics to study production.

For future climate and suitability projections, we target the year 2050. Much of the climate change that will occur by 2050 is a result of emissions which have already occurred. These thirty-five years will be instrumental to the future of coffee, as we learn to adapt to rapid climate change.

By 2050, if the international community has not enacted strong, effective carbon controls, the rate of warming will be even greater. 2050 could be the beginning of additional, catastrophic climate impacts on coffee and elsewhere. However, this year provides a useful road mark, far enough into the future to see the impacts but close enough that planning for those impacts can start now.

We distinguish three broad scales of impacts of climate change on coffee, and present different threads of results for each. Most year-to-year changes in yields are the result of variability in weather, and we study how coffee responds to historical year-to-year variation to understand how it will respond in the future. Climatic cycles can also span multiple years or decades, producing the weather patterns that affect yields, and we study the impacts of relevant climate indices on production. Finally, long-term trends will shift the suitable regions for coffee, and we study these impacts distinctly from those that determine yields.

2.1 Coffee production database

In this report, we want to identify the relationships between climate and coffee through careful, empirically-grounded methods. Identifying the locations of coffee production is essential for understanding how coffee is already interacting with the climate and how it will respond to climate change. High resolution weather station and gridded weather data are readily available, to identify regions subjected to high temperatures, frosts, precipitation, and humidity, but their impacts will be most clear when the weather and coffee data are closely aligned in space. Similarly, climate change suitability maps are more useful when compared to high-resolution information about the current location of coffee growing areas.

Applying robust spatial methods requires a new global database of coffee production. We develop an initial version of this database, combining existing records of coffee production with geospatial maps of coffee producing areas. The framework we develop for combining multiple sources of spatial and temporal data invites an ongoing evolution of this database.

Previous global datasets only provide coarse information on coffee production. The most reliable global information on coffee production, at the ICO, the FAO, and the USDA Foreign Agricultural Service, is only available on a per-country basis. CIAT has constructed a database of information on coffee farms (see figure B.1), but our analysis requires production information as it changes over time. To our knowledge, there is no existing dataset of coffee producing regions at a high resolution.

Monfreda et al. (2008) provide an approximate geographic distribution for coffee, by first identifying global cropland at high resolution (5'), and then using country-specific databases of coffee production, where available, to refine the areas. The quality of the resulting production areas varies widely by country, as shown in figure B.2. For most countries, only country-level production is available. Four countries have county-level data on coffee production, and 13 others have state-level production information.

We have combined the information from the FAO, the UDDA, the CIAT farm map, and Monfreda et al. with detailed maps of coffee production regions for 8 major coffee producing countries. These countries produce roughly 85% of the world's coffee. These high-resolution country-specific maps allow us to assess the characteristics of coffee production at much greater detail, both in terms of climate variables such as temperature and precipitation, and geographical variables, such as latitude and elevation. Combining these factors with data on yields in these areas allows us to estimate the effects of weather patterns on coffee growing, as well as study the range of climates where coffee can be grown successfully.

A summary of this information is provided in table 2.1 and some production area maps are included in appendix B, along with a description of the process for combining these maps.

Similarly, yield data for coffee at a finer resolution than the country level helps identify more closely the impact of existing climate dynamics on yield. Table 2.2 summarizes the data collected on yields, production, area planted and harvested, and fertilizer use.

To provide a visual summary of the combined harvest maps, we use average country-wide total harvest areas from FAO to translate harvest patterns to units of harvested hectares. Where information is detailed, hectare harvests in intensely cultivated coffee regions approach the land area of the grid cells. Where only diffuse, country-level data is available, the entire country has a uniform low average harvested

Country	Production	Coverage	Resolution	Source
Brazil	2,720 kt	country-wide	municipality (5503)	IBGE
Vietnam	1,650 kt	country-wide	raster image	Cafecontrol
Colombia	696 kt	country-wide	raster image	Oficina de E. y P. Básicos Cafeteros
Indonesia	411 kt	6 regions	raster image	Schroth (2014)
Ethiopia	390 kt	country-wide	raster image	GAIN (2013)
India	300 kt	country-wide	state (13)	Coffee Board (India Gov.)
Mexico	270 kt	country-wide	raster image	Gonzalez (2010)
Guatemala	240 kt	country-wide	vector layers	MFEWS
El Salvador	82 kt	country-wide	raster image	Poyecto Programa Ambiental
Nicaragua	78 kt	country-wide	raster image	MFEWS
Tanzania	50 kt	country-wide	raster image	Caparo et al. (2015)
Haiti	21 kt	country-wide	vector image	Coffee Supply Chain Risk Ass. Miss.
Rwanda	21 kt	country-wide	points	Nzeyimana (2014)
Yemen	14 kt	country-wide	raster image	Maxey (2015)
Total	7,766 kt	global	country	ICO, FAO, USDA FAS
		global	inferred raster	Monfreda et al. (2008)
		global	points	Bunn et al. (2015), CIAT

Table 2.1: Sources of spatial coffee production, from academic literature, government agencies, and NGO reports. Average production values are taken over the past decade. The resolution is listed as either a reporting level (municipality, state, country), as a graphical map (raster image, vector layers), a gridded analysis (inferred raster), or individual points (points).

Country	Variables	Time	Space	Organization
India	Planted, Produced, Yield	32 years (1951 - 2013)	15 growing regions	Knoema
Brazil	Harvested, Produced	yearly (1990 - 2012)	5624 municipalities	IBGE
Indonesia	Area, Produced, Yield	2011	20 districts (Kecamatan)	Dinas Pertanian
Rwanda	Area, Agroforested, Yield	2005	10 growing regions	NAEB
Vietnam	Area	2012, 2013	11 provinces + other	GAIN
Brazil	Fertilizer use	2002	5 regions	FAO
global	Harvested, Produced, Yield	1961 - 2012	86 countries	FAO
global	Produced (by variety), Stocks, Export, Consumption	1960 - 2013	79 countries	USDA FAS
global	Fertilizer use	1995 - 2002	24 countries	FertiStats

Table 2.2: Sources of global and sub-country data on coffee yields, total production, and planted and harvested area.

area. These values are used as weights to aggregate climate impacts when comparing country production with spatially distributed weather data.

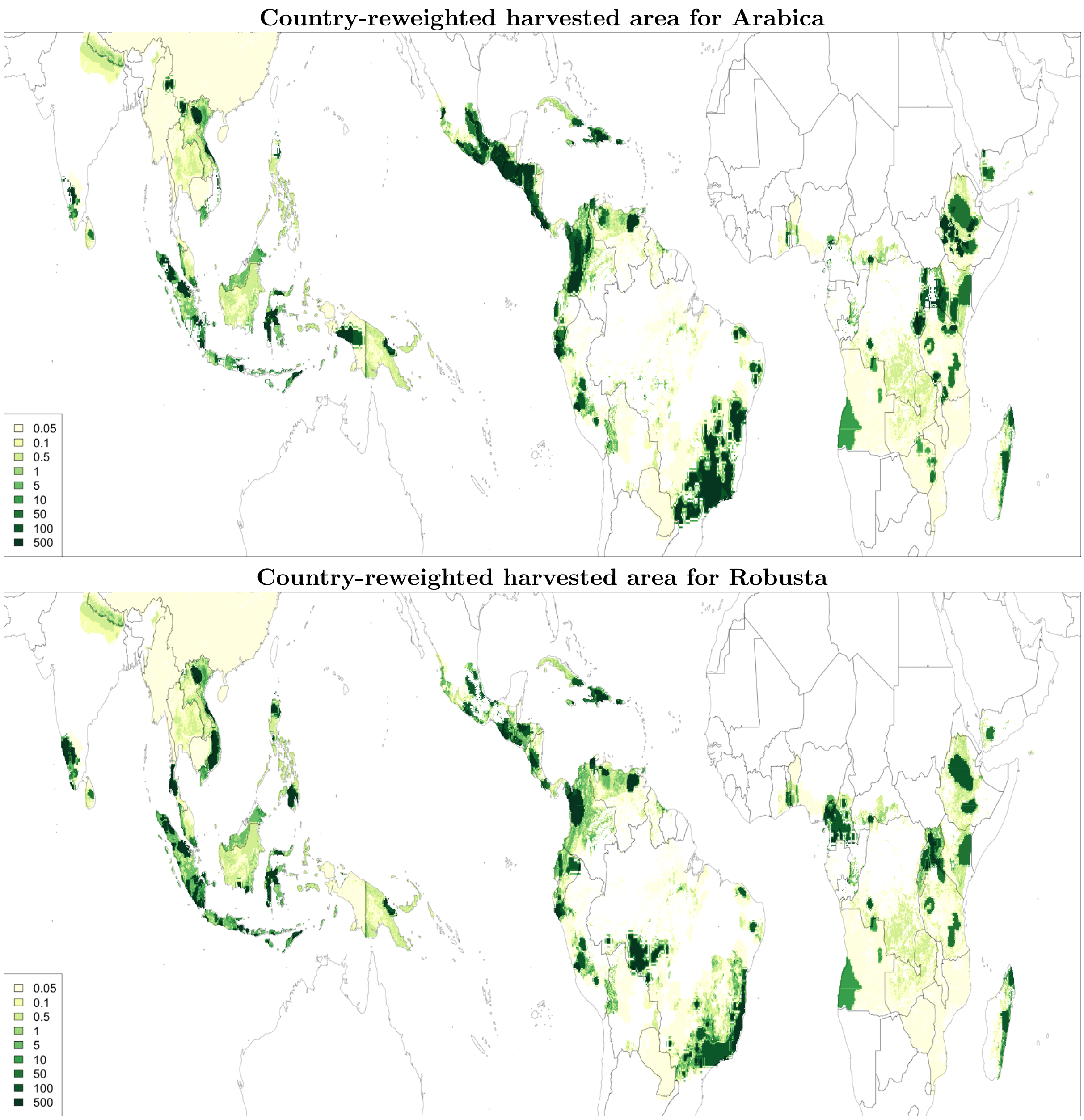

Figure 2.1: Harvest maps combined across all months, and re-weighted so that the sum of grid cell values within a country is equal to the average harvested area in the most recent year of harvest.

2.2 A Bayesian suitability approach

Our approach to estimating suitability is diagrammed in figure 2.2. Using existing environmental characteristics, we compute a statistical model, which we apply to future environmental characteristics and compare the result to previous estimates. This section describes the basic principles used to construct that model.

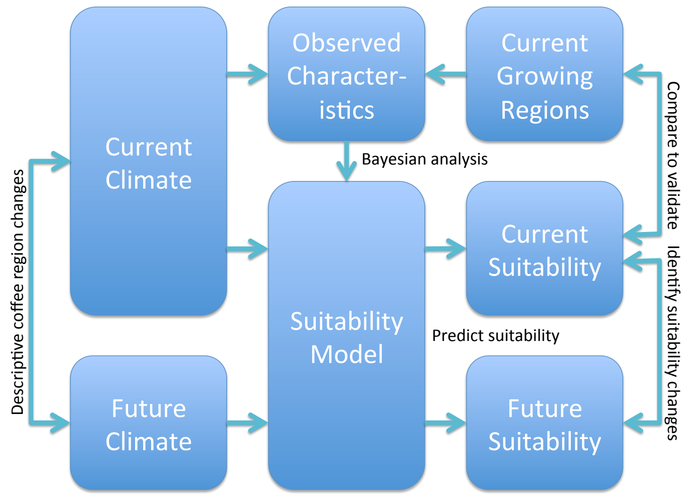

Figure 2.2: Diagram of the process for determining future climate suitability for coffee. On the left is global weather data, fed into both the model creation process and the model itself in the center. These then are used to produce current and future suitability maps.

2.2.1 Comparing MaxEnt and Bayesian odds techniques

Both the MaxEnt and Bayesian techniques are sophisticated and represent the uncertainty of their result with high integrity. Table 2.3 provides a comparison of the main strengths and weaknesses of the two techniques.

MaxEnt has been used to study species suitability for a long time, and is designed for situations where a species is observed only at particular locations. The spatial coffee database gives us a much clearer picture of where coffee currently is grown and is not.

MaxEnt is most appropriate when there are underlying motivations for the constraints that are used as a central part of the method: for example, a common constraint is to require that that the mean and variance of temperatures for observed coffee match the mean and variance for future coffee. Unfortunately, MaxEnt constraints are often chosen arbitrarily and without a physical foundation. The Bayesian odds approach incorporates the entire distribution of environmental indicator values where coffee is grown, rather than a small collection of moments.

	MaxEnt	Bayesian Odds
Form of observation data	A set of point locations, for where the species was observed	A weighted grid of presence across all space
Use of environmental data	Mean and other moments of the environmental data are used, based on the constraints chosen	The full distribution of values for any environmental indicators are included
Use of constraints	Constraints are central to the technique	Constraints are not used
Result uncertainty	Fully maintained	Fully maintained
Key simplification	Only chosen constraints describe the distribution of environmental indicators	Dependence between indicators is assumed to be captured by a rank correlation.

Table 2.3: Comparison between the features of MaxEnt and Bayesian odds methods.

2.2.2 Suitability data

We calculate suitability using the following environmental variables, all available at 5 arc-minute resolution. These are shown in figure 2.3.

- Soil texture data from the Harmonized World Soil Database (FAO/IIASA/ISRIC/ISSCAS/JRC, 2012). This consists of three macro-soil components (sand, silt, and clay), and three trace components (organic carbon, calcium carbonate, and gypsum). These six properties are available at high resolution (a 0.5' or about 1km grid) for the topsoil (0 cm to 30 cm) and again for the subsoil (30 cm to 100 cm).
- Land elevation from the SRTM elevation database (Jarvis et al., 2008).
- Gridded bioclimatic data from the WorldClim dataset (Hijmans et al., 2005). This database includes 19 variables, including annual mean temperature, diurnal range, maximum and minimum temperatures, annual precipitation, maximum and minimum precipitations, temperatures in wet and dry months, and precipitation in hot and cold months.
- Urban areas from Natural Earth and derived from 2002-2003 MODIS satellite data (Schneider et al., 2003).
- Protected regions from the World database on protected areas (WDPA Consortium, 2004). Protected areas and urban areas are important both as constraints on current coffee producing regions and on future ones.

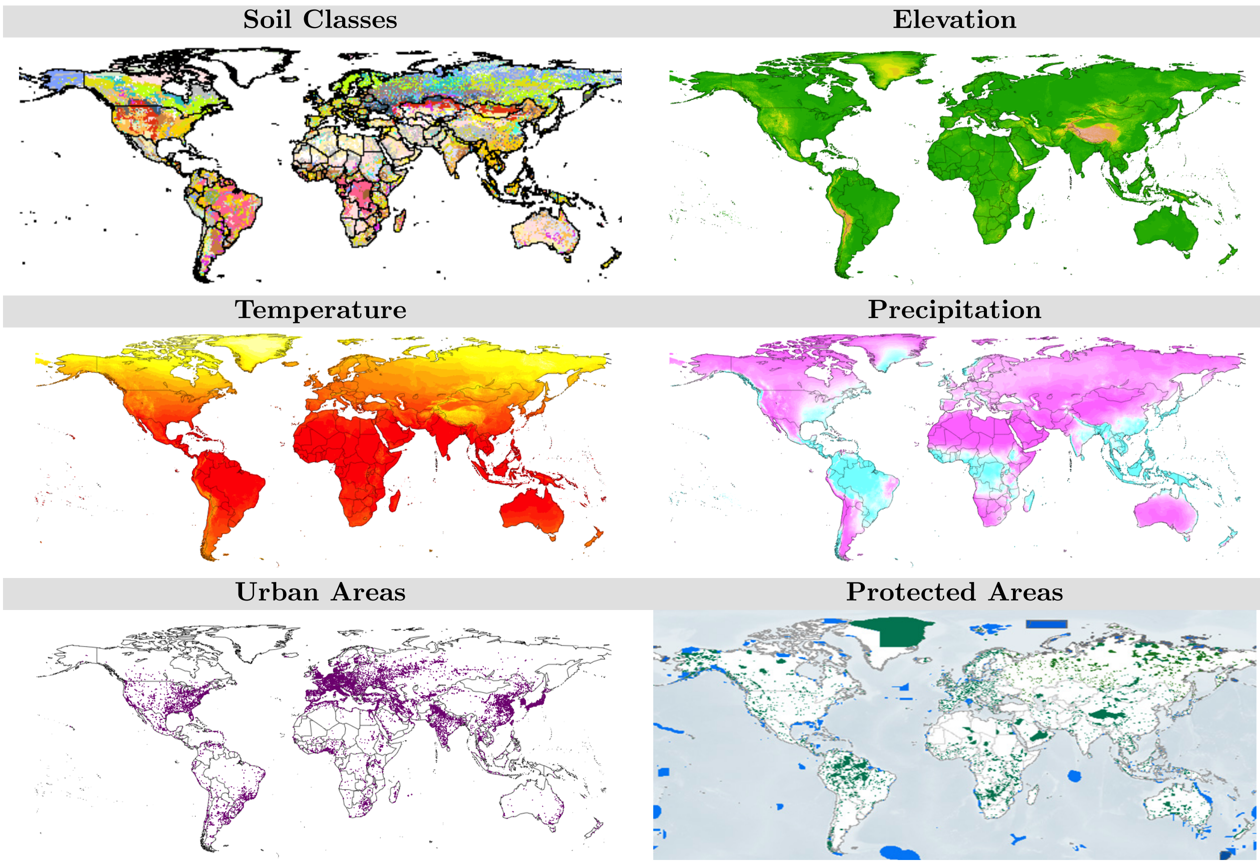

Figure 2.3: Inputs to the suitability analysis. See the text for details.

2.3 Crop modeling approaches

The suitability analysis describes how regions may need to shift under long time horizons. We also want to understand how exiting coffee growing regions will respond. Higher temperatures will reduce yields, weather patterns could affect berry production, and water requirements will change. This requires a model of production from weather data.

One broad approach to predicting crop development and providing decision-support tools to farmers is through biological process models. These models capture the process of plant development (phenology) at the individual plant level, and are available for many crops as models for DSSAT, APSIM, and CERES.

Biological process models of coffee production appear to be in their early stages. The most advanced may be the one developed by Rodríguez et al. (2011), with a "tri-trophic, physiologically-based system perspective", capable of studying water and light needs and pest impacts. The next generation of biological models, represented by Dauzat et al. (2014) and Maro et al. (2014) are still under development. This state of the literature motivated our focus on statistical models.

A statistical production model relates high-resolution weather data (such as temperature and precipitation) with observed yields (Schlenker and Roberts, 2009). The most advanced of these estimate the effect of growing degree-days and "killing degree-days" in a non-linear fashion, and account for varying unobserved characteristics that are idiosyncratic to each region, such as management, elevation, and soil properties. Econometric approaches have been used to study individual regions (e.g., Gay et al., 2006; Guzmán Martínez et al., 1999). We use our global coffee production database and a new technique we call hierarchical modeling to generate global estimates.

The models are estimated using natural experiments, by comparing observed yields in years with different distributions of weather to estimate the effect of weather in general. These experiments completely inform our models of production. The models below include daily minimum and maximum temperatures, precipitation, and humidity. We do not include elevation because it is impossible to do statistical experiments where elevation varies in the same region, to see its effects.

This approach puts a "black box" around the complicated system surrounding production, and makes no attempt to disentangle the effects of farmers responding to weather, the effects of that weather on the crops themselves, and the effects that these have on the plant's susceptibility to disease. This black box is both a strength and a limitation. It captures realistic relationships between weather and yields, rather than theoretical responses of the crops in an experimental setting. It can capture the environmental determinants of coffee disease spread, and their impacts implicitly. It can also be used to predict yields under climate change and weather events. However, because it cannot distinguish the social and natural causes, it makes an implicit assumption that yields will continue to respond the same way to increasing temperatures over time.

The production model can also be used to predict yields months before a harvest. By combining climatological signals, like ENSO, for which there is some capacity of prediction, with yearly averages (climatologies), it is possible to generate plausible weather patterns to apply to the model. The biennial cycle of coffee is not explicitly captured in our model, which considers only effects driven by weather (Bernardes et al., 2012).

It is reasonable to expect different countries to have different effects from temperatures. We could estimate each country independently, and this would be an "unpooled" model. However, we also want the model for one country to inform, to an extent supported by the data, the model for another country. To capture this, we will construct a "hierarchical model", where each country's sensitivity to temperature will be drawn from a common distribution, simultaneously estimating each country's parameters and the distribution across all of them.

Furthermore, we allow varieties in different regions to operate differently, as supported by the data. For example, where plentiful data supports a higher optimal growing temperature for Robusta, the model should represent this. If very little data is available, the predicted response should by default conform to an average for that region and variety. Finally, we want to incorporate higher resolution data where it is available. The municipality data in Brazil informs the same common coefficients as the Brazil-specific country-level yield data.

We have developed a technique for allowing this kind of data-driven multiple levels of aggregation and degrees of generalization, based on Bayesian Hierarchical Modeling (Gelman et al., 2014) and Inversion Theory (Menke, 2012). Under this technique, each country and sub-country region has its own parameters, but the parameters are further modeled as being related to each other.

2.4 Pest growth and control

An associated project for this report explored the effects of temperature in agricultural pest outbreaks. The project focuses coffee rust fungus, La Roya, in Guatemala, an area of high coffee production and recent extreme rust outbreaks (Georgiou et al., 2014). It examined how changes in monthly temperature, the associated 'incubation period' for the fungus (*Hemileia vastatrix*), and the inclusion of a vigilant farmer can affect the outbreak size distribution over time.

Hotter conditions have supported the increase of fungus spread that is killing coffee trees in altitudes that were once free of fungus. This has even caused farmers to switch to more resistant, but lower quality strains of coffee such as Coffea Robusta. This problem impacts the export earnings of coffee-producing countries but more importantly it directly impacts the employment of hundred of thousands of coffee workers who depend on the harvesting earnings to feed their families, with little income to cover a lost season (Magrath, 2014). Additionally, as coffee is a globally traded commodity and Central America is one of the top exporters, the proliferation of coffee rust fungus also has implications for other countries around the world.

Many attempts have been made to find simple and mechanistic solutions to both understand and predict the outbreaks dynamics, but as shown by Lockwood and Lockwood (2008), it has often proven fruitless to capture the effects of weather through linear models. Though many techniques have been utilized to capture the non-linear behavior for different spatial and temporal domains, this project follows their strategy of using a spatial, agent-based model to understand the interactions of space and time.

2.5 Weather and climate data

The current climate is represented by weather records from recent history. We use weather data since 1979 from the Climate Forecast System Reanalysis (CFSR). This data product combines station and satellite measurements using weather models to produce reliable weather estimates at a high spatial and temporal resolution. The spatial resolution is .32°x.32°, a grid with boxes that are about 35 km on a side at the equator. The temporal resolution is hourly, which we use to generate growing degree-days at a daily scale.

Climate Forecast System Reanalysis

The Climate Forecast System Reanalysis is a global weather product constructed by NOAA (Saha et al., 2010). CFSR merges the overlapping ranges of satellite products, as they are available across years:

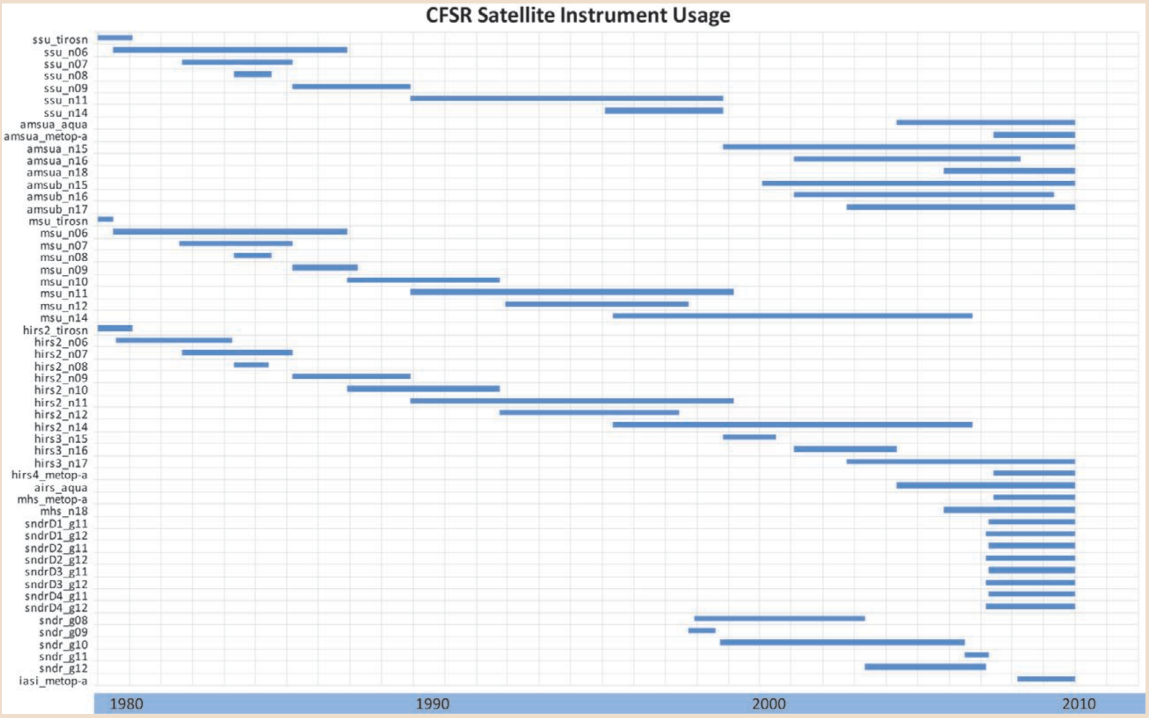

CFSR combines both conventional and satellite data from the following sources:

Conventional: Radiosondes and Pibals, AMMA special observations, Aircraft and ACARS data, Surface observations, PAOBS, SATOB observations, SSM/I ocean surface wind speed, Scatterometer winds

Satellite-radiance: TOVS radiances, Recalibrated MSU radiances, ATOVS radiances, GEOS radiances, Aqua AIRS, AMSU-A, and AMSR-E data, MetOp IASI, AMSU-A, and MHS data, CHAMP/COSMIC GPS radio occultation data.

Yields and production data are not available in a high-resolution, gridded form. Instead, yields, in the form of production quantities and harvested areas, are reported for political units. High resolution information about coffee producing regions needs to be combined with these low resolution recorded yield data. For example, coffee is grown exclusively in the southwest of Guatemala, in regions that cover 8.7% of the land area, but production data is reported for the entire country. Since we know that the country-wide production is coming only from these regions, we can limit the weather and other data used to infer coffee production relationships. To match the gridded weather data with growing regions, we use our coffee production database to aggregate the weather effects.

2.5.1 Climate indicies

We also study the effect of climate indicies. These are standardized measures of climate variables which relate to large scale weather patterns. We consider five indicators of broad relevance: NINO 3.4, NAO, SOI, and PDO from NOAA Climate Prediction Center (CPC) (2015), and unsmoothed AMO from Enfield et al. (2001). The indices are shown in figure A.33.

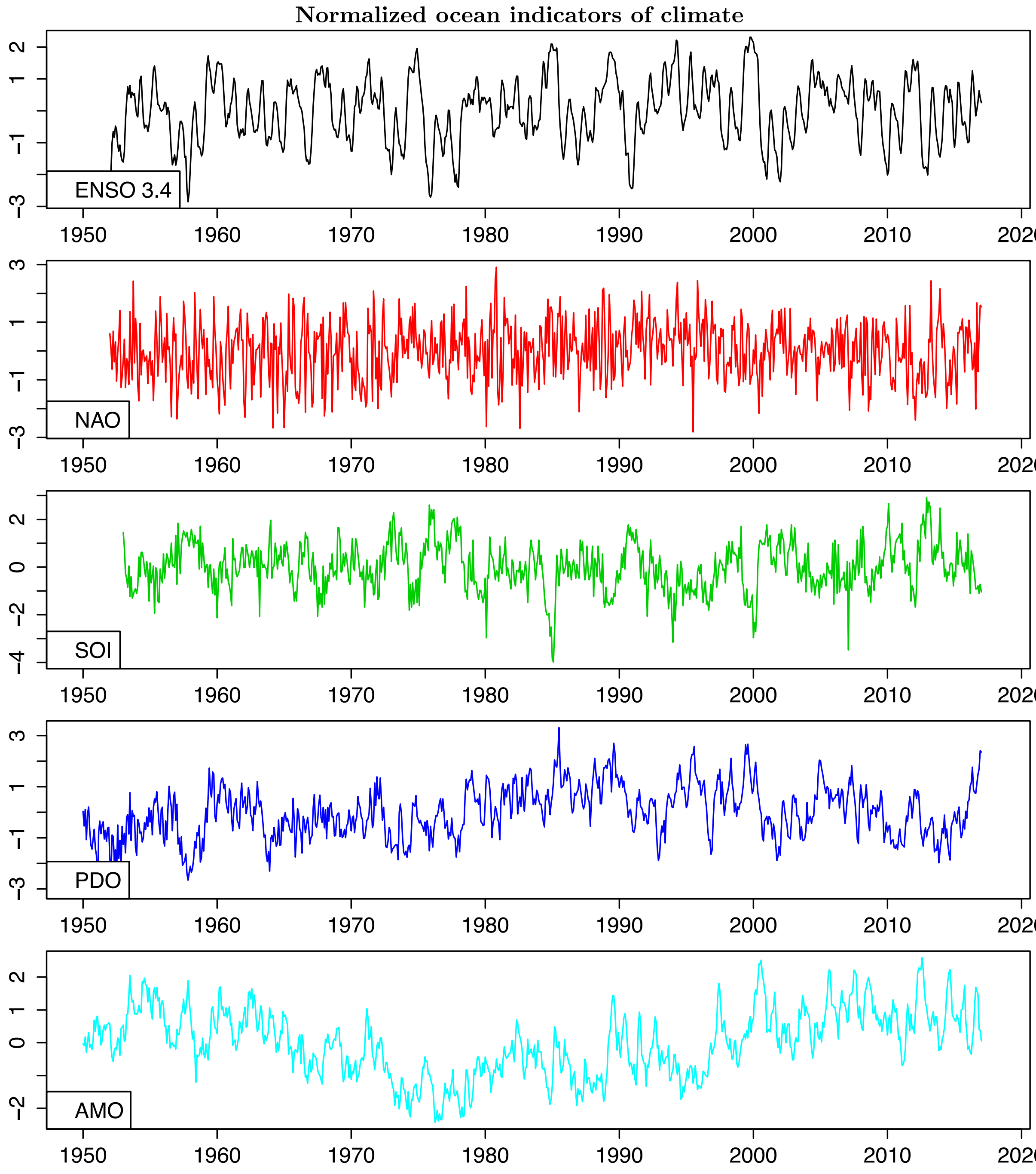

Figure 2.4: Normalized indicators used to study global and regional climate, sampled monthly. Each of these shows wide variability, but different periodicities. The interactions between these different signals can explain impacts in ways that individual signals cannot.

Chapter 3

Climate impacts

3.1 Future climate projections

Climate projections are produced by complicated models called Global Climate Models (GCMs). They apply scientific knowledge about the radiative heating of the atmosphere, its interaction with the ocean, and the movement of heat and water in response to human and natural drivers. The most recent report from the IPCC was produced in conjunction with a project to collect and harmonize results from all available GCMs. We use these 'CMIP5' models to study the changes in future climate and uncertainty surrounding them.

GCMs are calculated at a lower spatial resolution than we are interested in. A further process of downscaling expands the changes predicted by GCMs to produce high resolution projections. This process comes with additional uncertainty, since the feedbacks embodied in the GCM are not used when the resolution is improved. The downscaling dataset we use is WorldClim (Hijmans et al., 2005), available at a resolution of 5 arc-minutes (about 9km at the equator), the same resolution as the coffee database. WorldClim contains 17 GCMs for the "business-as-usual" emissions scenario (RCP 8.5). The changes in climate quantities over the coffee belt are shown in table 3.1.

Quantity	Baseline	Change	25 pct.	75 pct.
Annual mean temperature	23.6°C	2.1°C	1.7	2.5
Mean diurnal range	12.6°C	-0.5°C	-0.6	-0.5
Temperature seasonality	3055.0	3.9 %	1.9	4.4
Max temperature of warmest month	34.2°C	2.5°C	1.9	2.7
Min temperature of coldest month	12.3°C	1.9°C	1.7	2.4
Annual precipitation	1068.0 mm	1.7%	-0.1	3.2
Precipitation of wettest month	191.0 mm	8.0%	5.5	11.3
Precipitation of driest month	22.0 mm	-6.8%	-12.3	-2.0

Table 3.1: Mean changes over the coffee belt.

As an example, figure 3.2 shows the range of changes in one coffee growing region of Colombia across these 17 GCMs. For some of these aspects of the climate in this region, all 17 GCMs agree on the direction of the change. These are the annual mean temperature, and maximum and minimum temperatures, all of which are expected to increase about 2°C over a baseline period from 1950 - 2000. This represents a future average increase of 0.28°C per decade, 75% greater than the current rate. The temperature

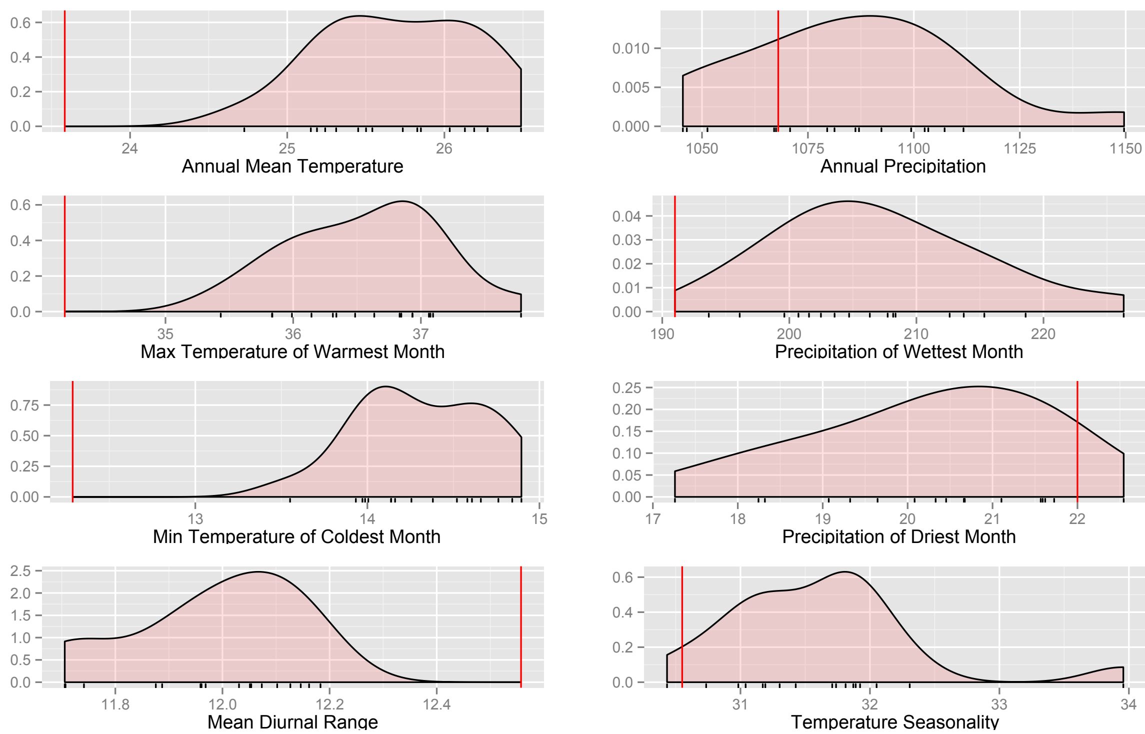

Figure 3.1: The baseline climatology (red lines) and distribution of possible future climate values in 2050 under RCP 8.5, averaged over all tropic belt land.

seasonality, defined as the standard deviation of temperature, is also expected to increase. The other values are less certain, with some models predicting increases and others decreases.

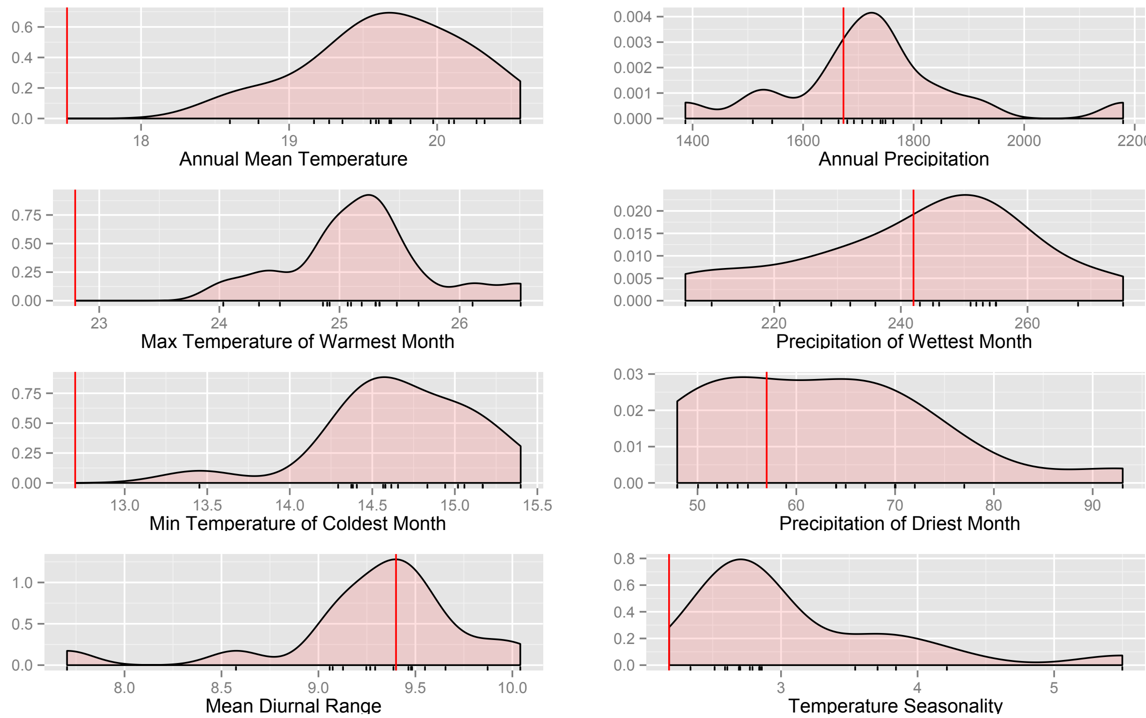

Figure 3.2: The baseline climatology (red lines) and distribution of possible future climate values in 2050 under RCP 8.5, for a location in Colombia at 4°N 76°W.

3.1.1 Spatial patterns of change and uncertainty

The median climate changes across 17 GCMs as they vary across the coffee belt are displayed in figures 3.4 and 3.5 for 2050, under RCP 8.5. We report impacts consistent with RCP 8.5, the highest IPCC emissions pathway, throughout this report because current emissions appear to be following this path.

Temperatures increase across the entire region with high confidence, within the explanatory power of these GCMs. The size of these temperature changes generally increases away from the equator, with most coffee growing regions seeing 1 - 2°C. The pattern for the diurnal (day-night) temperature range is more complicated, with increases in the Americas and decreases across northern Africa and South Asia. Precipitation changes are less certain, with decreases on the coasts of Brazil, and increases in northern Africa and India.

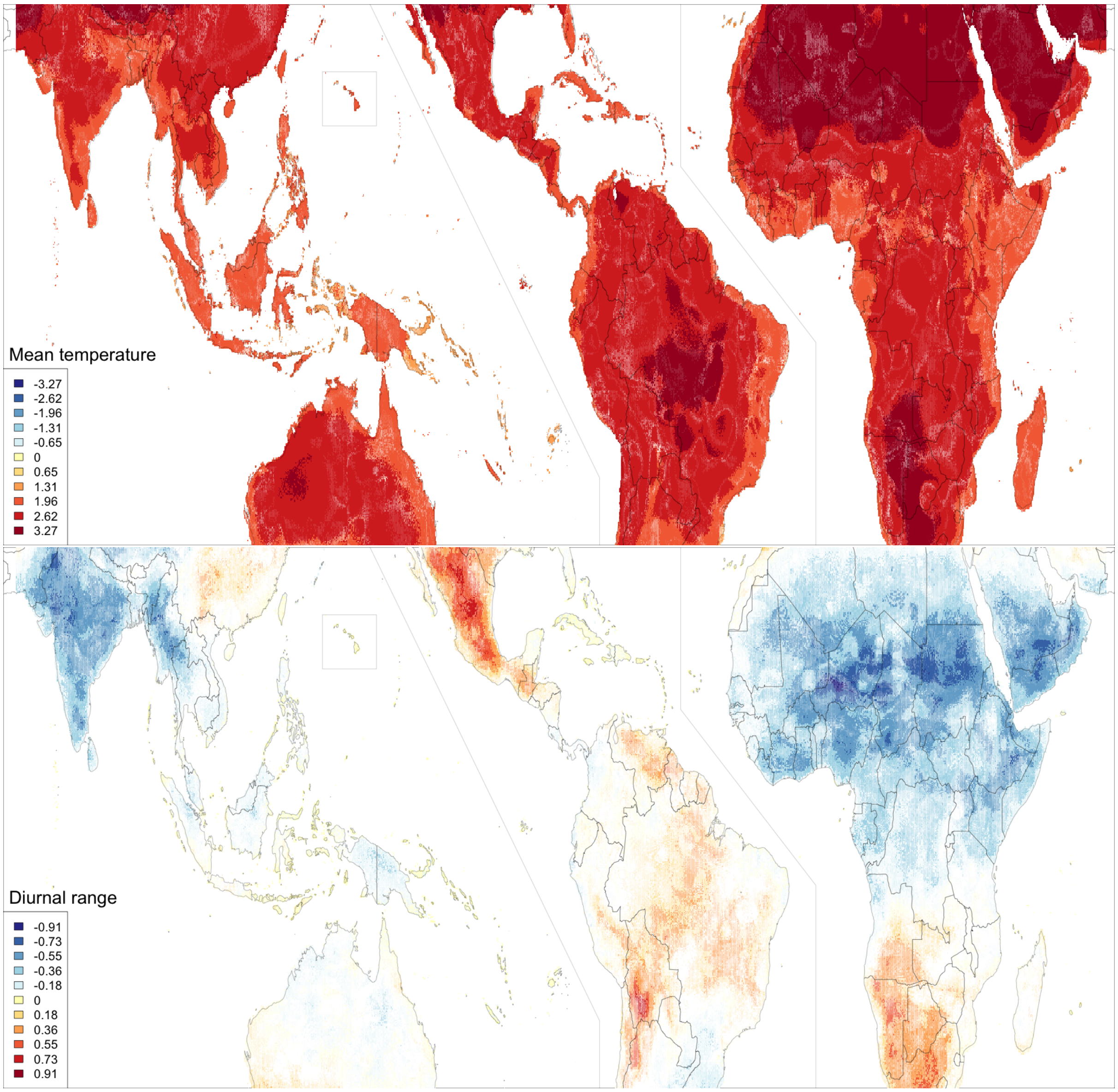

Figure 3.3: Global patterns of level changes in mean annual temperature and diurnal temperature range for 2050 from Hijmans et al. (2005). Areas are faded in proportion to the number of GCMs that do not agree with the sign of the median GCM.

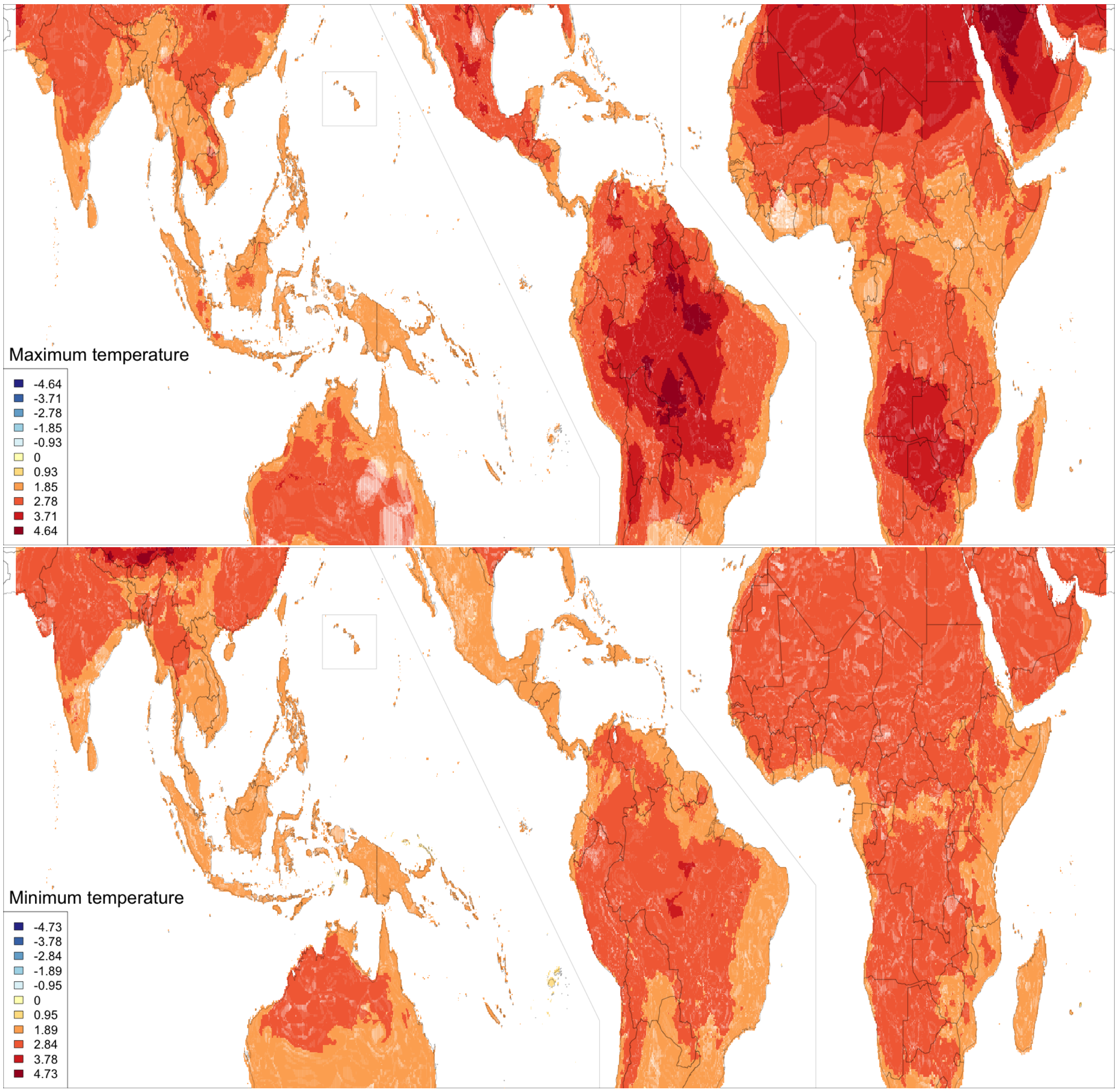

Figure 3.4: Global patterns of level changes in maximum yearly temperature and minimum yearly temperature for 2050 from Hijmans et al. (2005). Areas are faded in proportion to the number of GCMs that do not agree with the sign of the median GCM.

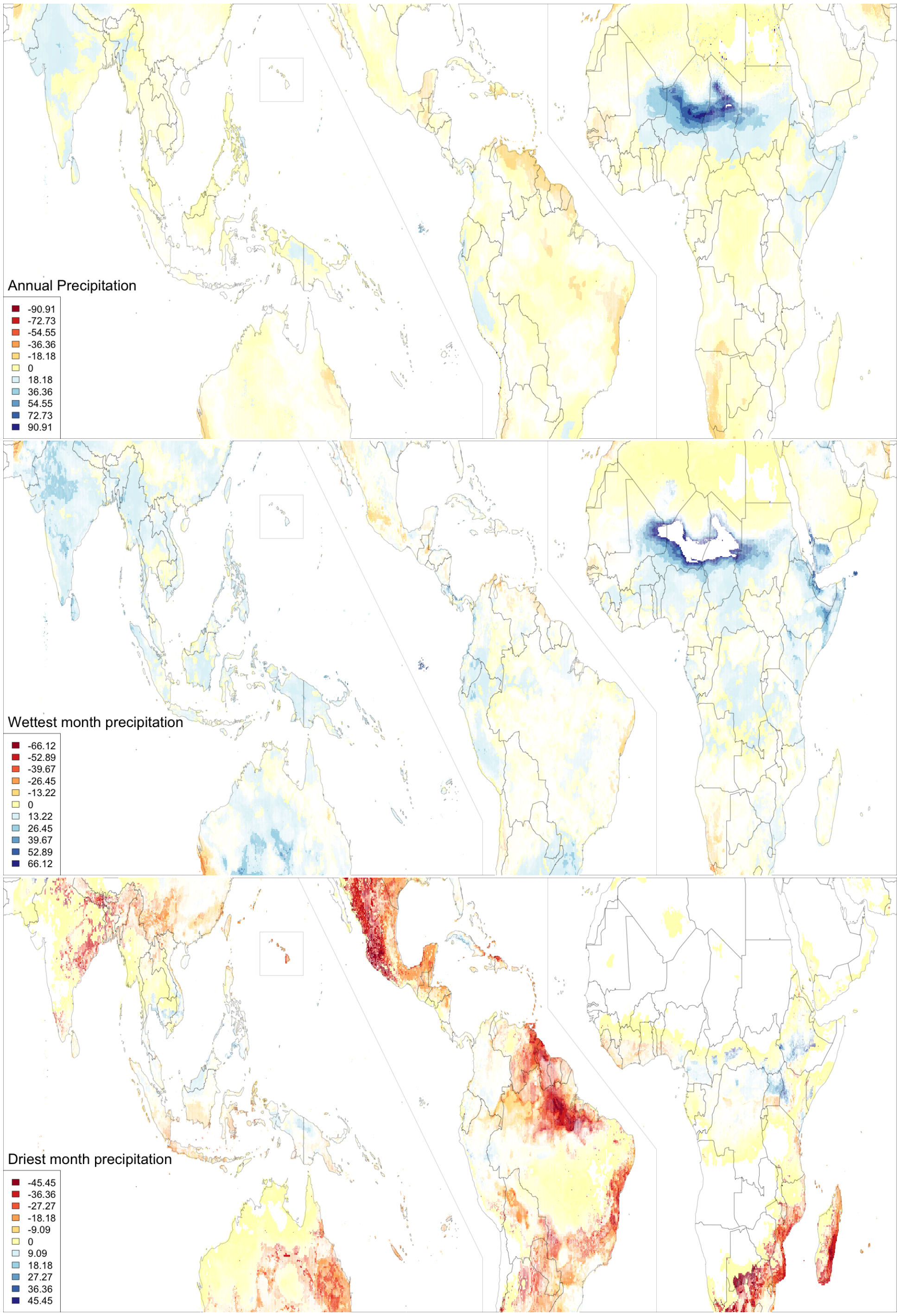

Figure 3.5: Global patterns of percent changes in annual total precipitation, precipitation in the wettest month, and precipitation in the driest month, for 2050 from Hijmans et al. (2005). Areas are faded in proportion to the number of GCMs that do not agree with the sign of the median GCM.

3.2 Observed yield changes

Coffee yields have shifted over the past decade, as a result of many factors including climate change. Some areas have seen increases in per-hectare yields from improved agricultural practices and varieties, while others have been hit by expanded diseases. In some cases, these diseases are also driven by changes in climate: for example, the coffee berry borer and coffee white stem borer have benefited from increases in temperatures in Africa (Jaramillo et al., 2011; Kutywayo et al., 2013), and coffee rust responds to changes in humidity (Alves et al., 2011). Trends in yields reflect a combination of all of these factors.

As shown in figure 3.6, yields have shifted in different directions for each country since 2000. Many equatorial regions have been hit hardest, particularly central and west Africa. However, the greatest decrease in yields has been experienced by Zimbabwe, with an average of an almost 8% decrease in yields per year, from 14,000 Hg/Ha in 2000-2003 to 4,500 Hg/Ha in 2009-2012. The greatest increase is nearby, in Angola, from 1,100 Hg/Ha in 2000-2003 to 13,000 Hg/Ha in 2009-2012.

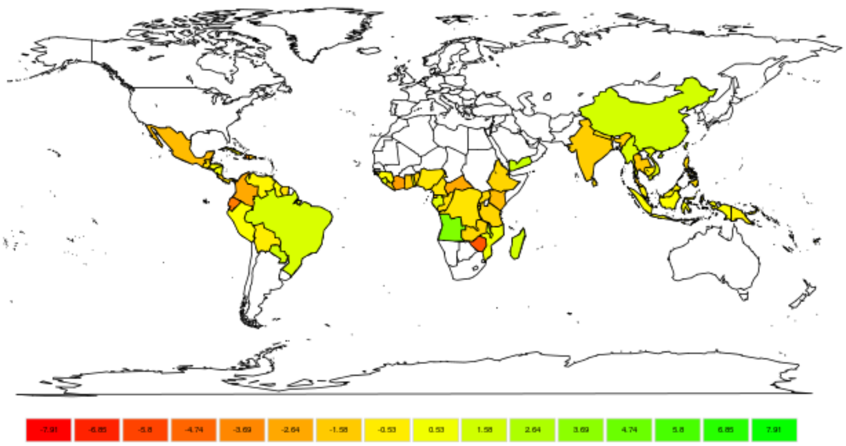

Figure 3.6: Trends in coffee yields since 2000 by country. Values represent the rate of yield change per year, since 2000 and relative to yields in 2000: Countries colored green have shown significant increases in per hectare yield, while those in red and orange have shown decreases.

We can explore the climate connection more closely in Brazil, where coffee yields are reported at the high-resolution municipality level. In Brazil, yield changes over the past decade appear to be predicted by elevation, suggesting a climate-related driver. Trends across Brazil vary from positive to negative, as shown below. With the exception of large and relatively unproductive regions in the north, the regions with the largest negative trends tend to be on the edges of the broad coffee producing region, suggesting that shifts in suitability are squeezing these border regions out. Many of the areas with positive trends are in higher hills than those with negative trends.

If temperatures are forcing coffee to higher elevations, it will be reflected in a fall in yields in municipalities at low elevations and increases at higher elevations. Figure 3.8 suggests that such a pattern might be occurring. On average, counties of every elevation have increasing yields, reflecting the broader trend in Brazil. However, counties with high elevations (greater than 700 m) have on average higher increases yields than those with lower elevations (below 500 m). These lower averages at low elevations also reflect

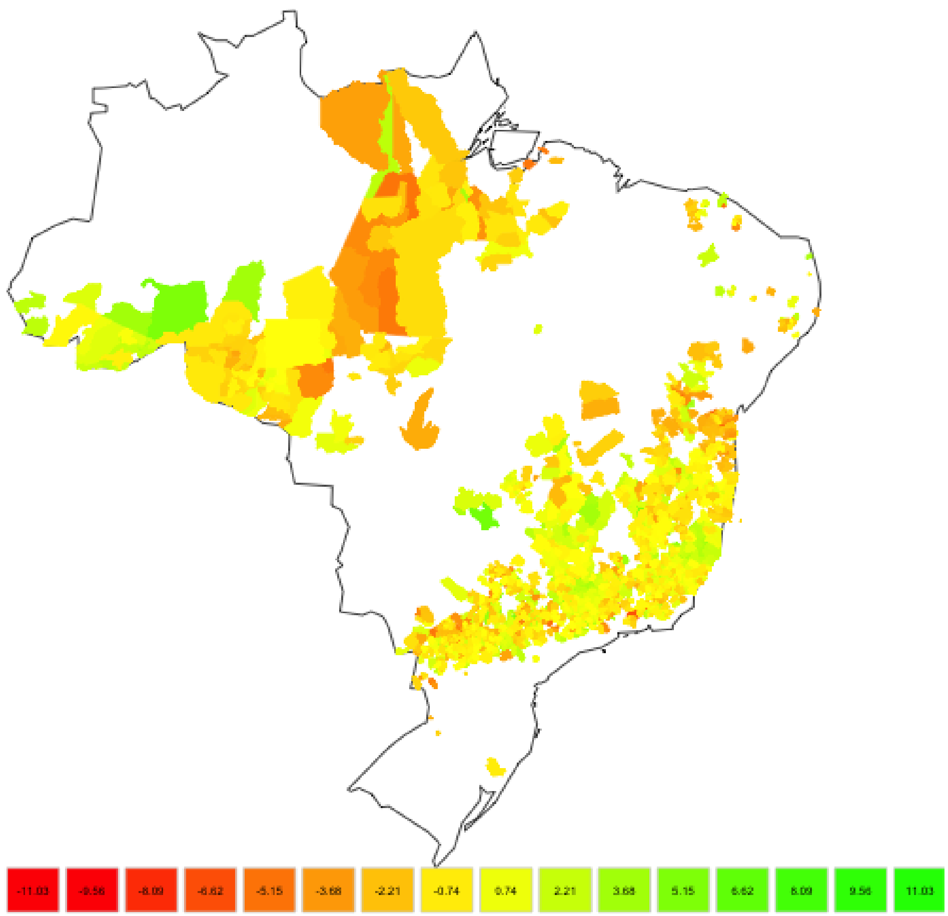

Figure 3.7: Trends in coffee yields since 2000 for Brazilian municipalities. Values represent the yearly decrease in percent terms: Countries colored green have shown significant increases in per hectare yield, while those in red and orange have shown decreases.

a greater number of municipalities with negative trends.

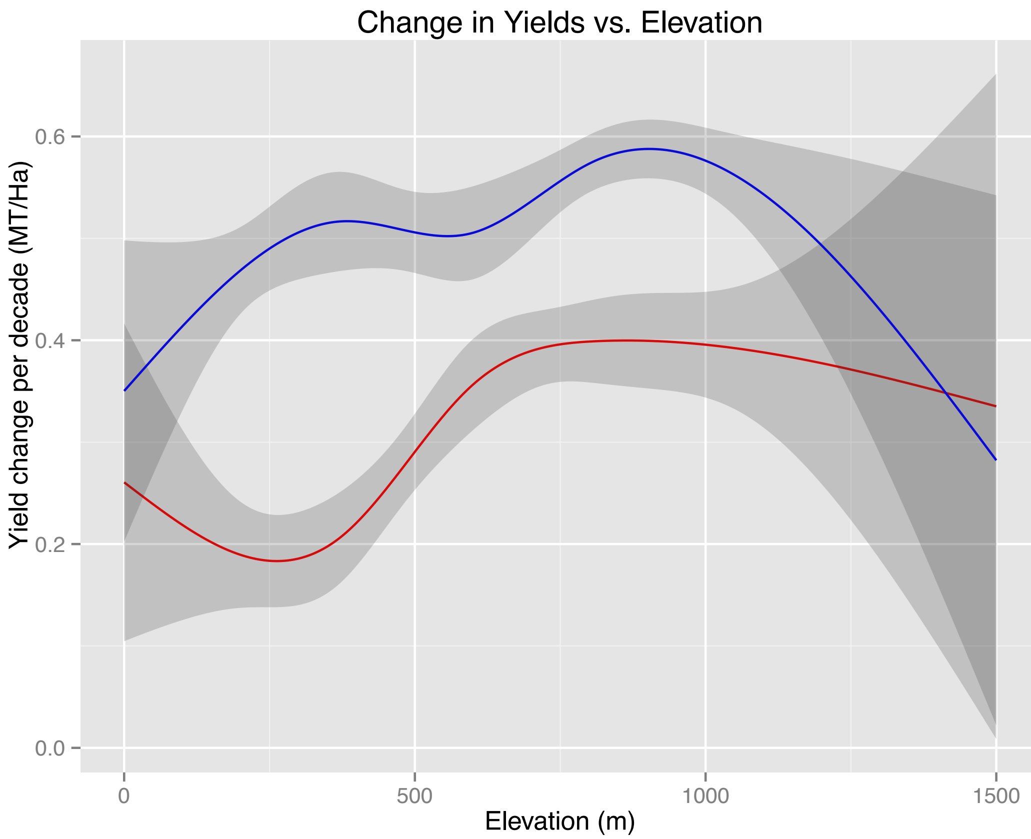

Figure 3.8: Changes in yields as a function of elevation. The red line shows municipality-level yields against elevation, showing a sharp increase in yields above 500 m. Blue shows the same relationship, but weighted by municipality harvests, and a more minor division around 700 m.

3.3 Impacts of hot temperatures

The Brazilian Institute of Geography and Statistics (IBGE) provides municipality-level production for coffee in Brazil since 1990. Nearly 2,700 municipalities with coffee production histories are included, and representing an average resolution of less than 40 km. This dataset allows for a broad case study of the impacts of climate change at a high spatial resolution.

We find that increases in temperature below a daily maximum temperature of 33°C limit are beneficial, resulting in higher yields and higher total production. Above 38°C, temperatures have a sharply harmful effect. As a result, even small increases in temperatures under climate change can produce large decreases in yields, particularly in regions where temperatures are currently optimal.

Every additional 1000 GDDs (of which there are about 3000 across coffee-growing municipalities in Brazil) increases yields by about 16%. Every additional 100 KDDs (an average year will have only 150

KDDs) decreases yields by 76%. These values are estimated using marginal changes, so the average year is the baseline from which these percent changes are applied.

The large and statistically significant negative effect on harvested acres is also important. This suggests that in hot years where the crop is damaged, the plants are simply not harvested. As a result, the actual damaging effects of high temperatures on yields are likely to be greater than reported. The yield numbers hide the fact that unproductive plots in poor years can be left unharvested, causing both total production and harvested acres to decrease without as large of decreases in yield.

Figure 3.9 shows a graphical representation of the growing degree-day production model, with 95% confidence intervals. The assumptions are as described before: growing degree-days and precipitation are calculated using hourly reanalysis data; state cubic trends capture the evolution of coffee production. Each day between 0°C and 33°C results in increased yields; each day above 38°C results in decreased yields.

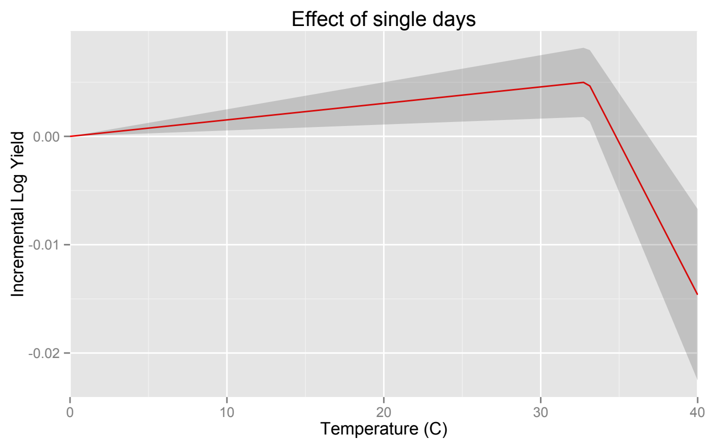

Figure 3.9: Marginal impact on log yields for an additional day at a given temperature. Up to 15°C, coffee plants experience no growth. From 15°C to 30°C, additional temperature results in greater yields. Above 30°C, this effect is sharply diminished and hot days above 32°C result in large decreases in yield. The grey band shows the 95% confidence intervals around the estimated effect for a single day at a given temperature.

These results support the common wisdom: Arabica, grown at higher elevations, is much more sensitive to weather than Robusta. We find that as elevation increases, the potential increased yield from higher temperatures as well as the potential damage due to extreme temperatures increases.

3.3.1 Yield estimates under a warmer climate

We can apply the production model to weather produced from climate change. As a proxy for climate change, we estimate yields using historical weather data increased by 2°C. Precipitation values are left unchanged, since they show an unclear trend. This change produces several effects: it increases the number of GDDs benefiting yields, increases the number of KDDs harming yields, and increases average minimum temperature. The resulting balance between these three impacts is not evident *a priori*. The figure below shows the distribution for municipality yields across Brazil, from observed data, and under climate changed weather predictions.

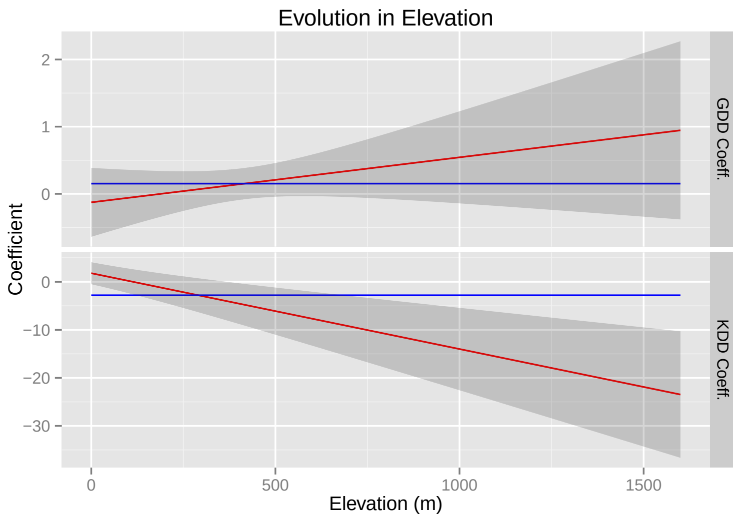

Figure 3.10: GDD and KDD coefficients as they vary by elevation. As elevation increases, plants become more sensitive to temperatures. The effect of GDDs increases, though very slightly. The effect of KDDs also increases.

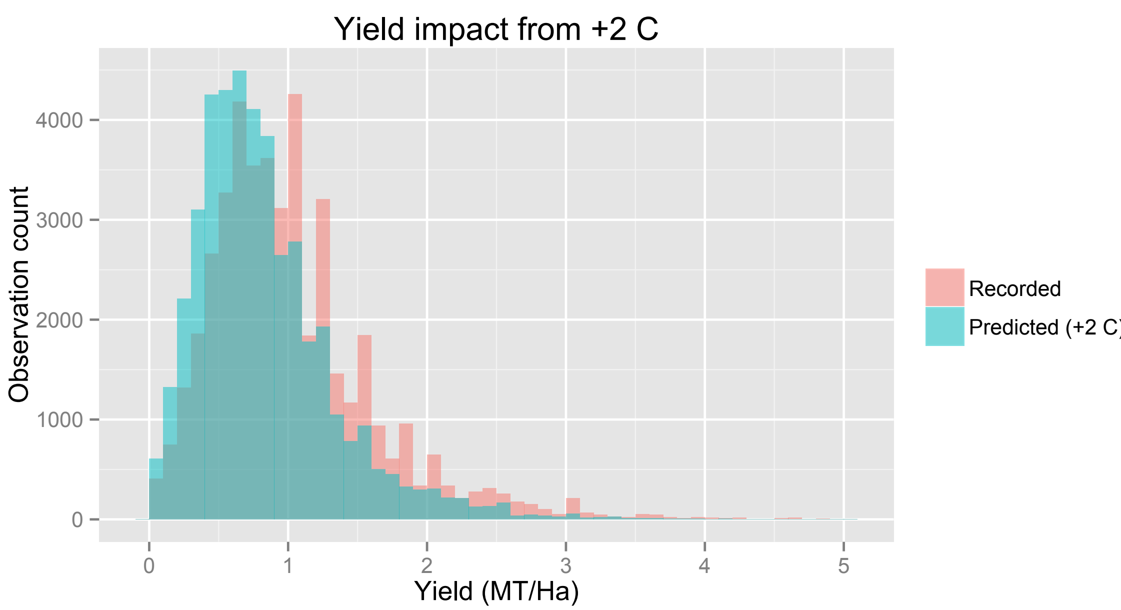

Figure 3.11: Observed yields over the period from 1990 - 2015 are shown in red, and model predictions under weather with temperatures increased by 2°C shown in blue.

As shown in figure A.6, the observed yields show wide variation. The blue distribution is shifted to the left, eliminating some of the most spectacular yields and lowering the average yield. The average yield in the warmer experiment is about 80% of the original yields.

3.3.2 Variation across countries

The growing degree-day effect is greater for the Robusta variety, while the coefficient for killing degree-days is greatest for combined records. A useful metric is the "break-even" temperature, $\frac{1}{\kappa}\left(\kappa H - \gamma(H - L)\right)$, where $L = 0°\mathrm{C}$ and $H = 33°\mathrm{C}$. A day at this temperature neither increases nor decreases yields. This is similar for Arabica and combined countries, at about 37°C. The corresponding temperature for Robusta is 40.5°C.

Figure 3.12 shows the variation across countries of the coefficient on killing degree-days and the break-even temperature. South America and Southern Africa show the least sensitivity to temperature, while Indonesia and the islands near it show the most.

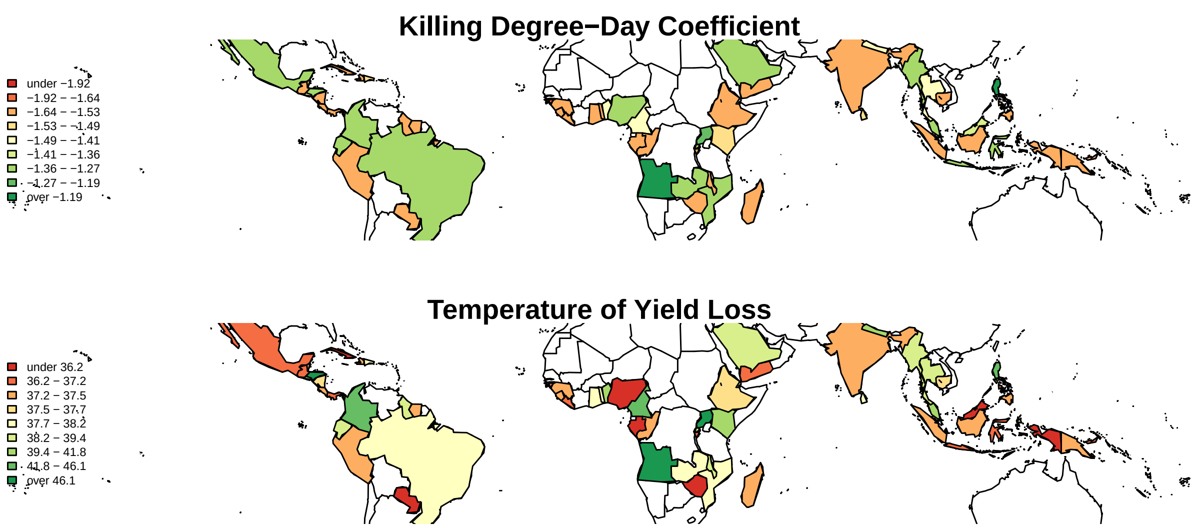

Figure 3.12: Coefficients of killing degree-days and the temperature at which yields decrease, across countries for the partially pooled model.

Another way to view these results is to compare the temperature at which each country is predicted to have losses in yield, to the average maximum daily temperature. This is shown in figure 3.13. Liberia, Nigeria, and Guinea are reported as having the highest temperature thresholds for yield losses, and are amongst the countries with the highest maximum temperatures, averaged over their coffee growing regions. This suggests some level of adaptation. However, other countries with similarly high temperatures do not show these high thresholds.

3.3.3 Future productivity

We can use the global hierarchical model to predict yields under future climate. We apply the level change in mean temperature and the proportional change in precipitation to all daily weather observations from

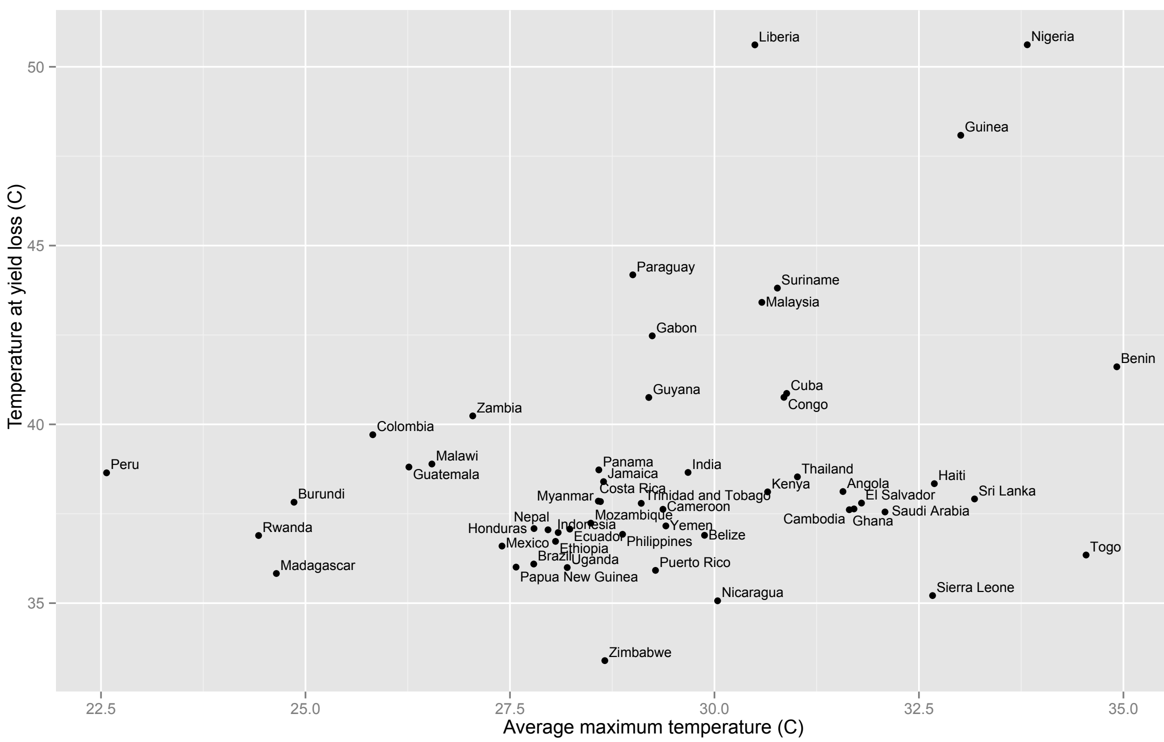

Figure 3.13: Observed average maximum daily temperature, 2004 - 2009, compared to the temperature at which yield losses are predicted.

CFSR. Then we calculate GDDs, KDDs, average minimum temperatures, and total precipitations, and apply them to the model. Figure 3.14 shows the result.

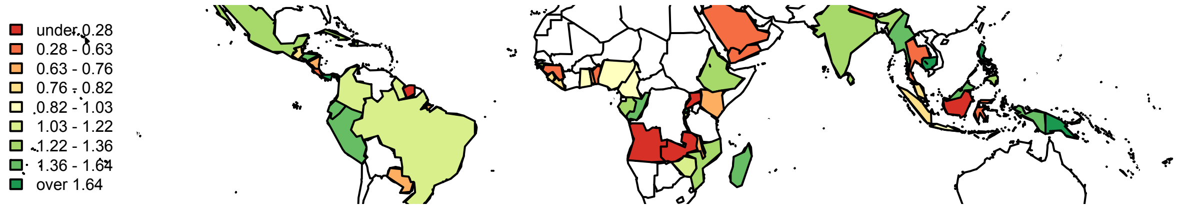

Figure 3.14: Changes in yield by country, for weather averaged over growing regions for each country.

As shown in the map, the impacts vary widely across countries, with some countries losing as much as 70% of their productivity, while others see increases of over 60%. Most areas in South America will experience improvements, while many countries in Central America, Southern and Eastern Africa, and Eastern Oceana will experience losses.

This result shows some general features about the variation across countries, but the actual country predictions have low confidence. In many cases, these country predictions are based on few data points, and the global distribution used to inform all of them is broad because of the uncertainty of predicting country aggregated yields.

3.4 Impacts of El Niño

The ENSO cycle is both a concern and an opportunity for coffee production. Many coffee-producing countries are significantly impacted by these events, with changes in temperature, precipitation, and blossoming conditions. Furthermore, since El Niño and La Niña are global, they can produce large impacts on the coffee market. Like all climate events, El Niño affects both coffee plants and their associated farming communities in a way that is difficult to disentangle.

The scientific understanding of the ENSO cycle continues to evolve. Here we do a quantitive analysis of ENSO on recorded prices and yields, although this is only a part of the picture. El Niño events can cause severe storms that increase erosion, produce a long-term effect that will only be reflected tangentially in our data. El Niños can also affect a coffee farming operation by affecting the welfare of its farmers.

Our first analysis uses a consensus categorization of years into El Niño, La Niña, and normal years, as an indicator for studying impacts. These years and the shape of the NINO 3.4 indicator that corresponds to them is shown in figure 3.15.

We see these impacts in the prices of Arabica and Robusta beans in El Niño years, relative to normal years, as shown in figure 3.16. In expectation, from the beginning of an El Niño year, prices climb for about 15 months, before beginning to decline. At their peak, prices are over 30% higher than they are predicted to have been in the absence of the El Niño event. We do not see a similar effect for La Niña events. These effects are similar in duration and form to those found by Ubilava (2012).

Little research has been done on the effects of the El Niño/La Niña cycle on coffee yields. Villegas et al. (2012) find that in Colombia the location of the Inter-Tropical Convergence Zone is a more important factor affecting yields, but global estimates of these effects do not appear to be available. We consider the impacts of El Niño and La Niña years globally and for each country.

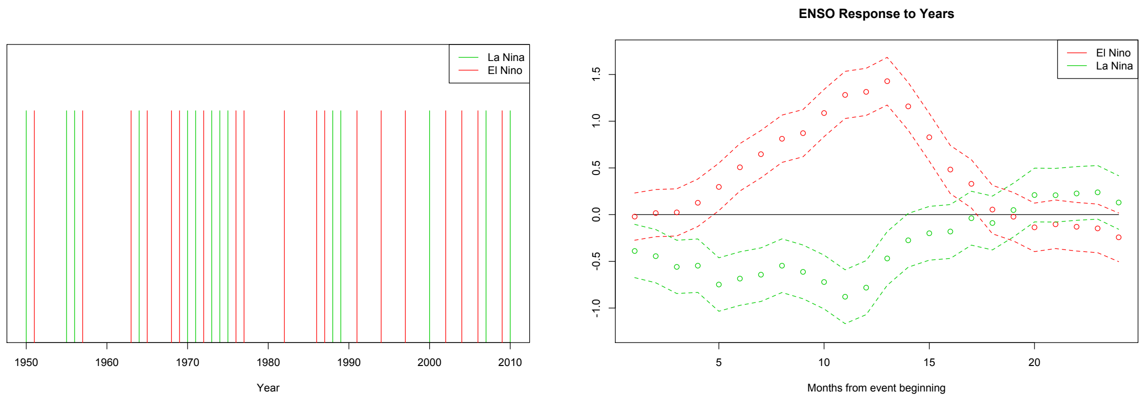

Figure 3.15: **Left:** The years categorized as La Niña years and El Niño years. **Right:** The estimated 24-month impulse response of the NINO 3.4 indicator to each of the three ENSO year types.

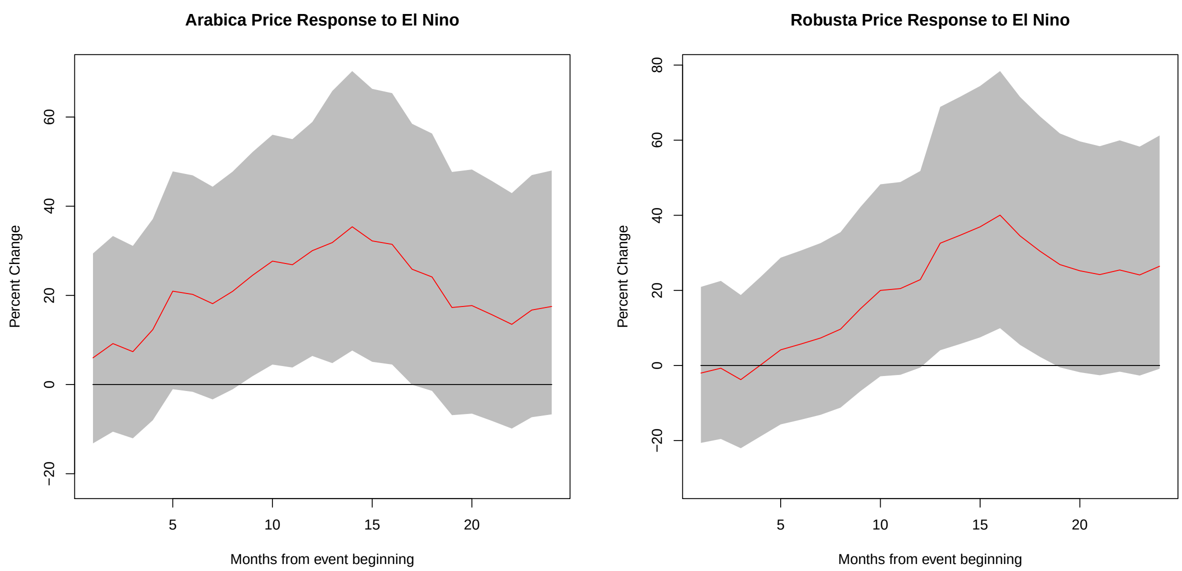

Figure 3.16: The graphs above show how international coffee prices respond to an El Niño event. Both Arabica and Robusta prices show increase of 20-40% over the course of the event, with potentially long-lasting impacts.

An impact analogous to the price change is evident in the yields across countries. In El Niño years, yields decrease on average by 100 Hg/Ha, against an average of 6800 Hg/Ha in recent years, after accounting for long-term trajectories in yields. While this is only a drop of 1.5%, the average hides larger effects in specific regions and variability between El Niño years. No effect is seen globally in La Niña years.

Looking at individual regions, using country-level data, only a few countries appear to have large impacts from El Niño, after accounting for each country's long-term evolution in yield and production. The French Polynesia, Gabon, Polynesia, and Thailand all show significant impacts in yields, although the directions of the impacts differ. Mauritius, Papua New Guinea, and Sri Lanka have significant impacts in total production, with large decreases for Papua New Guinea and Sri Lanka. Because of the lack of information on coffee planting areas as they vary by year, yields are calculated with respect to harvested areas. As a result, the countries that show impacts on production but not on yield probably reflect El Niño impacts that are hidden by selective harvesting decisions.

Regions with observed El Niño / La Niña impacts

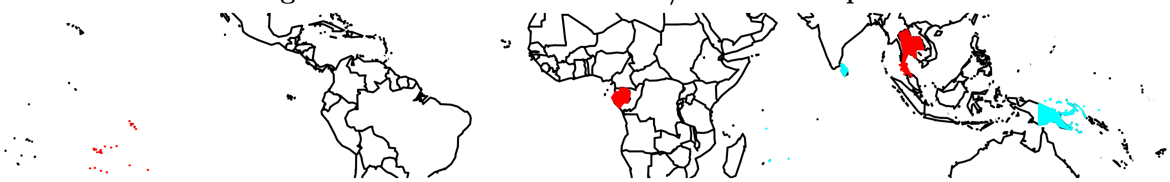

Yields	El Niño	El Niño + 1	La Niña	La Niña + 1
French Polynesia	-650 Hg/Ha	N.S.	N.S.	N.S.
Gabon	+940 Hg/Ha	N.S.	N.S.	N.S.
Polynesia	-650 Hg/Ha	N.S.	N.S.	-600 Hg/Ha
Thailand	N.S.	N.S.	N.S.	+1400 Hg/Ha
Productions	**El Niño**	**El Niño + 1**	**La Niña**	**La Niña + 1**
Mauritius	+17 MT	+13 MT	+18 MT	+17 MT
Papua New Guinea	-7,600 MT	N.S.	N.S.	N.S.
Sri Lanka	N.S.	N.S.	-2,000 MT	N.S.

Figure 3.17: Regions where country-level yield and production are teleconnected with El Niño and La Niña events. The location of the regions is shown at top, with yields affected by ENSO in blue and production affected by ENSO in red. In the table, values are the predicted change in yields or production in El Niño years, the year after an El Niño year, and the same for La Niña years. Entries with "N.S." show no statistically significant change at a 10% level.

3.4.1 Coherent movements

Section A.5.5 displays the results of an analysis of coherent movements in the coffee-climate system. These results are described as the first three orders of global changes, incorporating both the spatial pattern in yields and the temporal pattern of climate signals.

The order dynamic describes how yields have shifted on average over the past 50 years. Brazil, Mexico, and China have seen some the largest increases in yield, while Thailand, Myanmar and many countries in Africa have experienced the largest decreases. Most climate signals have not shown any trend, except for the Atlantic multidecadal oscillation (AMO) which is currently much higher than it was in the 1960s. As a result, all of the climate signals in the lower graph are near zero, except for AMO.

The second and third principal components are dominated by ENSO (the El Niño/La Niña cycle), represented by the NINO 3.4 index and the Southern oscillation index, which is known to be strongly correlated with ENSO but with an opposite sign. PC 2 is represented in the data when NINO 3.4 is high (El Niño) and the Pacific decadal oscillation (PDO) is also high, and its effects are reversed when these signals are both opposite in the direction of their anomalies. The largest effect of this combination, as shown in the map, is that Brazil, Paraguay, and Papua New Guinea have decreases in yields while India sees increases. This suggests that yields in these regions will often move in opposite directions, during many El Niño and La Niña years.

Observations with low values of PC 2 occur before 1975 and after 2000, while those with high values of PC 2 occur mostly in the 1980s and early 1990s. This may be driven by the slow oscillation of PDO. Since only one such cycle has occurred, it is difficult to distinguish the effects of the climate signals from socioeconomic effects, although most of this was be removed by the flexible trend used in the preprocessing step.

The third principal component also occurs when ENSO is in its El Niño state, and AMO is high or increasing. In this case, India, Peru, and southern areas in Africa show decreases, while other areas are not heavily affected. Both PC 2 and PC 3 can equally be understood in their La Niña form (and associated low values of PDO for PC 2 and low values of AMO for PC 3), which produce changes in yields in the opposite direction.

Between PCs 2 and 3, the effects of El Niño and La Niña appear across much of the globe. Because the impacts on most countries result from an interaction between the ENSO cycle and AMO or PDO, the results did not appear in the initial analysis.

3.5 Projection for 2015-2016

The El Niño predicted for the winter of 2015-16 is expected to have a similar magnitude to the event in 1997-98. However, there is considerable unresolved uncertainty in our analysis as to the most likely outcomes of this event.

The El Niño of 1997-98 produced catastrophic impacts in many areas, but its effect on coffee was fairly minor, coinciding with in a 9.6% drop in production. However, a large fraction of this global effect was due to Brazil, which had a 32% drop in yields, largely as a consequence of its biennial cycle. Excluding Brazil, the rest of global production only decreased 1.3%. The regional picture is more nuanced, with large decreases also in Oceania. The top part of figure 3.18 shows these results

From the analysis above, the most damaging El Niños coincide with consistently high values in PDO, such as we see today. By decomposing the existing constellation of climate signals into the three coherent groupings shown above, we project the estimates shown in figure 3.18. As with the second principal component, there may be large decreases in yields in Brazil and Central America. Our projection also identifies losses in India, and Southern Africa. This is at odds with the recorded values from 1997-98, which saw the most widespread losses across Indonesia and Papua New Guinea.

Inputs to the El Niño projection

Our projection is based on the most recent consensus projection of the NINO 3.4 index of ENSO, from International Research Institute for Climate and Society (2015). We try to apply reasonable values to the other indices, using the negative of NINO 3.4 for SOI, given its -0.6 correlation with NINO 3.4; a zero value for NAO, given its rapid shifts; and constant extrapolations for PDO and AMO at their most recent value, given the slow shifts in these signals.

Projecting these signals onto the principal component axes gives loadings of 1.3, 3.3, and 1.9, for the three components respectively.

To account for any spurious effect of our decision-making process, we estimate the values for 2014-15 as well, and report the difference.

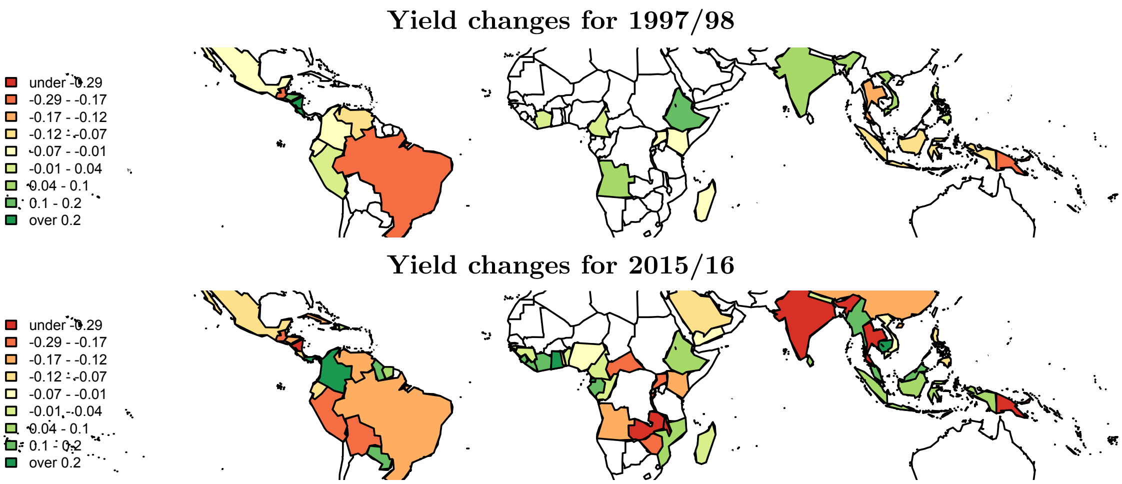

Figure 3.18: **Above:** Yield changes coinciding with the 1997/98 El Niño, relative to 1996/97, from International Coffee Council (1998). **Below:** Yield changes predicted for the 2015/16 El Niño, relative to 2014/15.

3.6 Price interconnections

Coffee forms a complex global network of international relations, not only between producer and consumer countries, but also amongst consumer and producer countries, as shown in figure 3.19. Both consumer and producer countries, for example, import coffee from Italy, a "consumer" country. Producer and consumer countries interact with each other through the global market of prices, and have long-standing trade relations that form the backbone of this market.

Coffee consumption has increased steadily for the past 20 years (see figure 3.20). The greatest drivers of this growth are producer countries, calling into question many traditional assumptions about the coffee market.

Despite the relatively smooth increase in coffee production, prices have historically swung wildly over the past 50 years, as shown in figure 3.21. There are many reasons for these swings, and some have been in response to political and economic changes, speculation, and the effects of disease and the environment.

In this section, we study the determinants of prices in the coffee market, both amongst producer and consumer countries.

Coffee is an important contribution to the economy of many countries. The prices paid to farmers account for over 3% of the GDP of four countries (Burundi, Honduras, Nicaragua, and Ethiopia; see Appendix A.7.10. The total value of coffee to seven countries exceeds 10% of their GDP (those above and Rwanda,

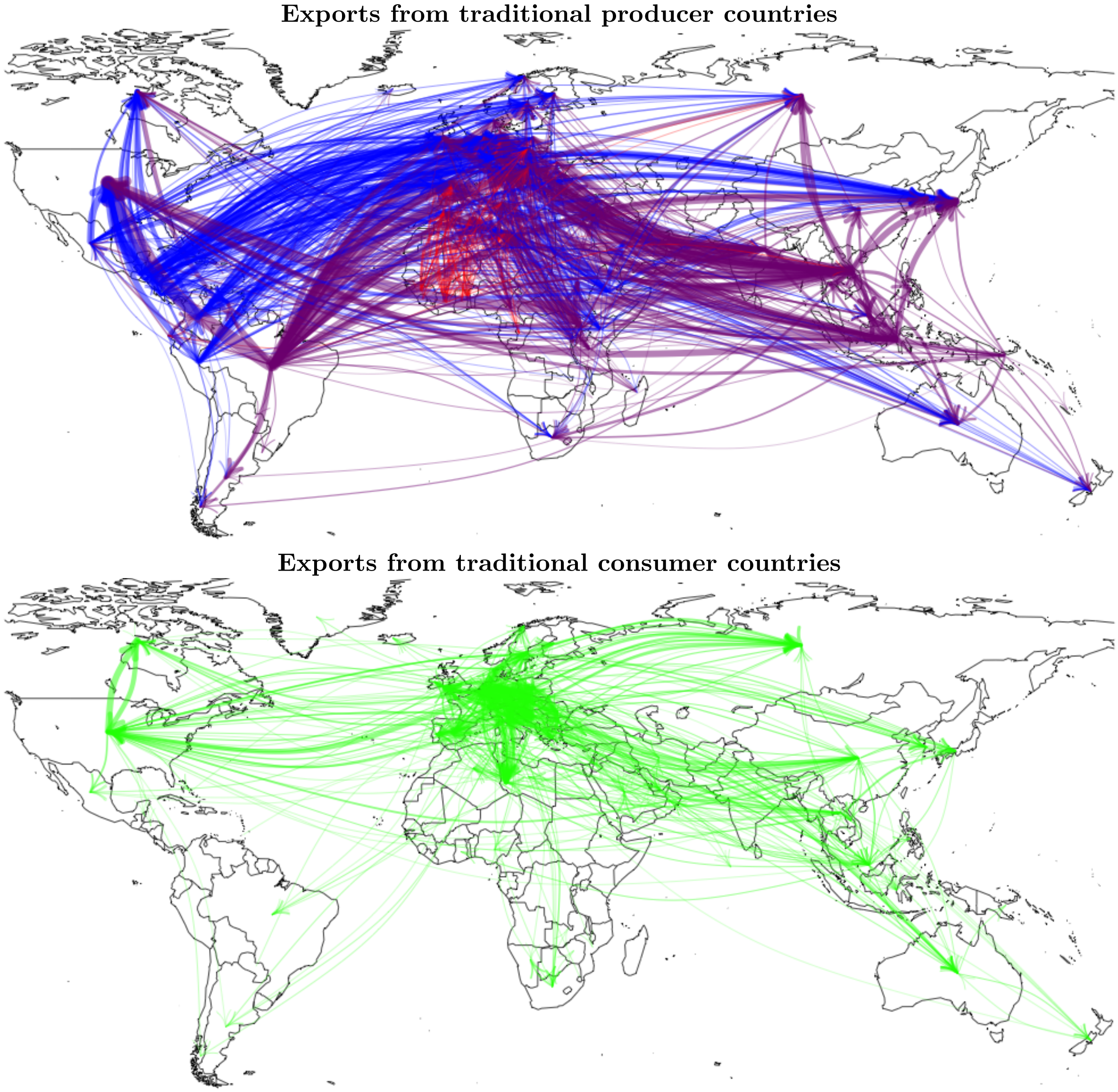

Figure 3.19: Exports from traditional producer (top) and consumer (bottom) countries. Above, blue arrows show Arabica exports, red arrows show Robusta exports, and purple arrows show exports that include both. The width of the lines increases with the yearly exports. Trade data from Comtrade (2015), producer classifications from International Coffee Organization (2015b).

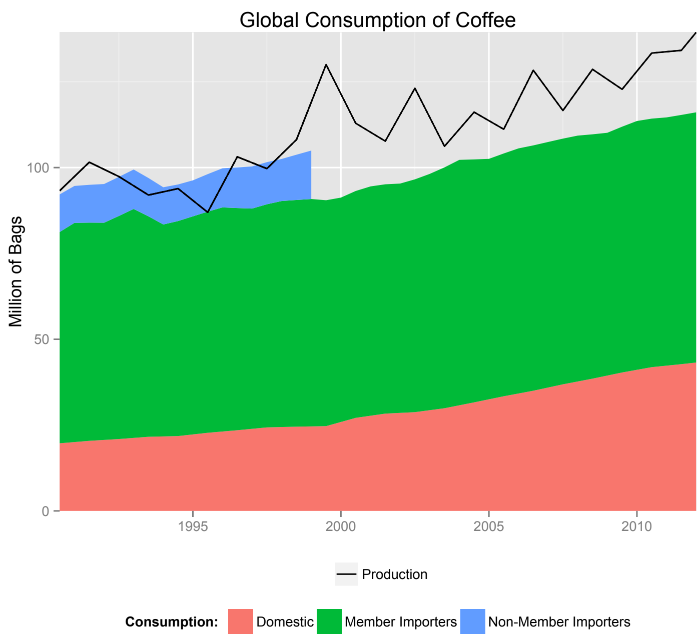

Figure 3.20: Global production (line) and consumption (colored areas) of coffee from ICO data. Non-member country consumption is unavailable after 1999. Most of the recent growth in consumption is driven by consumption within producing countries (domestic consumption), now equaling more than 50% of importing country consumption.

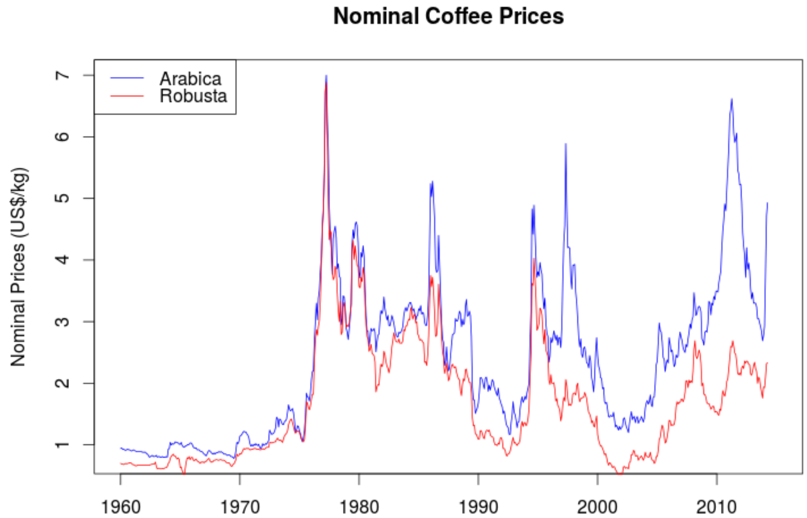

Figure 3.21: Nominal world prices of Arabica and Robusta coffee (in $/kg), from the World Bank Pink Sheet. The general shape is very erratic, with nominal prices not yet returning to the price they reached in 1977. Robusta prices have also diverged from Arabica prices, as Robusta production has spread, although the two remain closely correlated.

Uganda, and Guatemala) (International Coffee Organization, 2015a). Understanding what drives prices for consumer and producer countries is important to these regions as well as the world's 25 million coffee farmers.

For example, we find that global production has almost no predictive power in determining international prices, at odds with simple economic theory.

3.6.1 Prices to growers

Prices paid to farmers vary by an order of magnitude, as shown in figure 3.22.

The table shows coefficients on prices and production, the amount of variance explained (out of 1) by these two parameters, and the levels of significance of the coefficients. The effect of international prices on prices paid to farmers is very clear, across all countries and globally. Furthermore, this explains 46% of the variation in year-to-year farmer prices.

The effect of production, however, is much less clear. Although it has a significant effect for about 30% of countries, the direction of the effect varies, with almost half of countries showing prices that increase with the level of production. This is at odds with at least a simple view of the relevant economics: we would expect a glut on the market to drive down prices. Even so, the effect of production on farmer prices explain typically less than 1% of the variation in these prices.

Unweighted, Robustas have a mean VE by international prices of 57% to 69% for the other Arabica varieties. Weighted by production, the difference is 63% to 82%. This lower explained variance is only

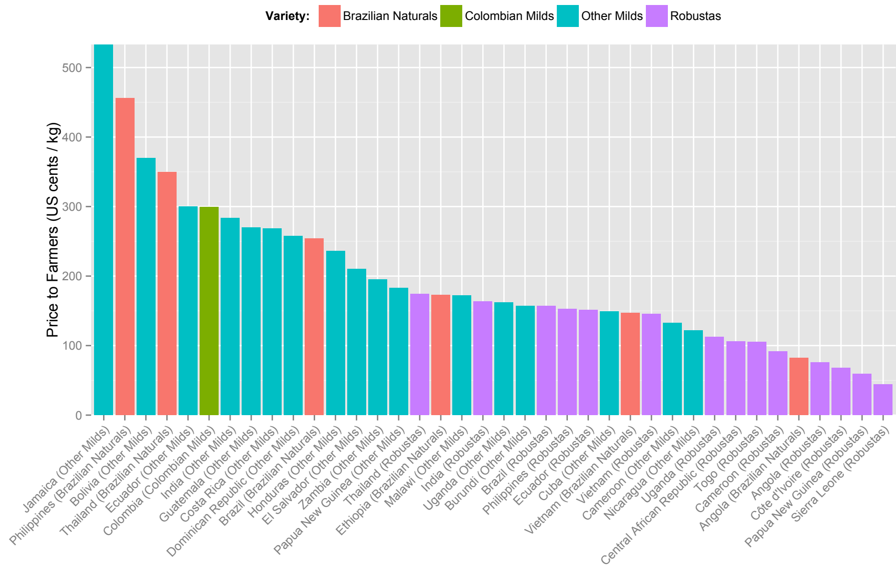

Figure 3.22: Price paid to farmers in U.S. cents per kg, between 2009 - 2013, from ICO.

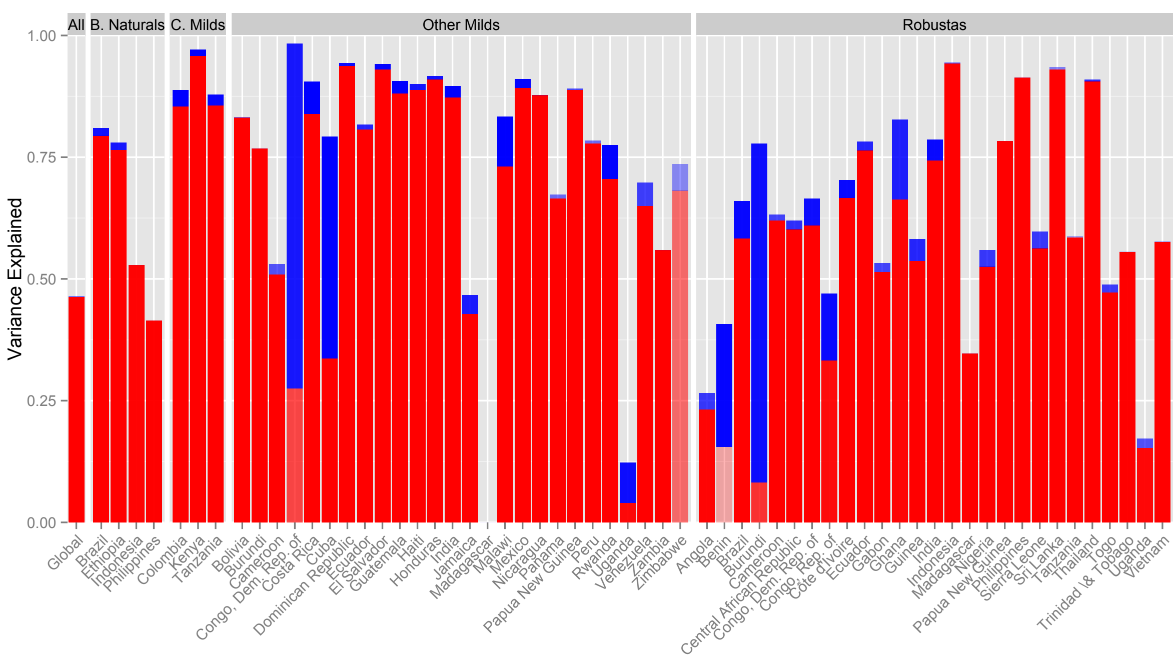

Figure 3.23: Variance of local prices explained by international prices (red) and local production (blue). Bars are faded according to their p-values.

slightly reflected in the production V.E.. This suggests that it is due to another factor, such as national price interventions.

3.6.2 Consumer response to prices

In 2009, consuming countries spent $27.1 billion for coffee (United Nations International Merchandise Trade Statistics, 2009). This value came after a decade of the lowest coffee prices, in real terms, ever seen, below $2.50 per kg. Consumers respond to these low prices by growing the total financial size of the coffee market. In recent years, retail prices for roasted beans in consumer countries have ranged from $6.65 per kg to $14.60 per kg (see 3.24).

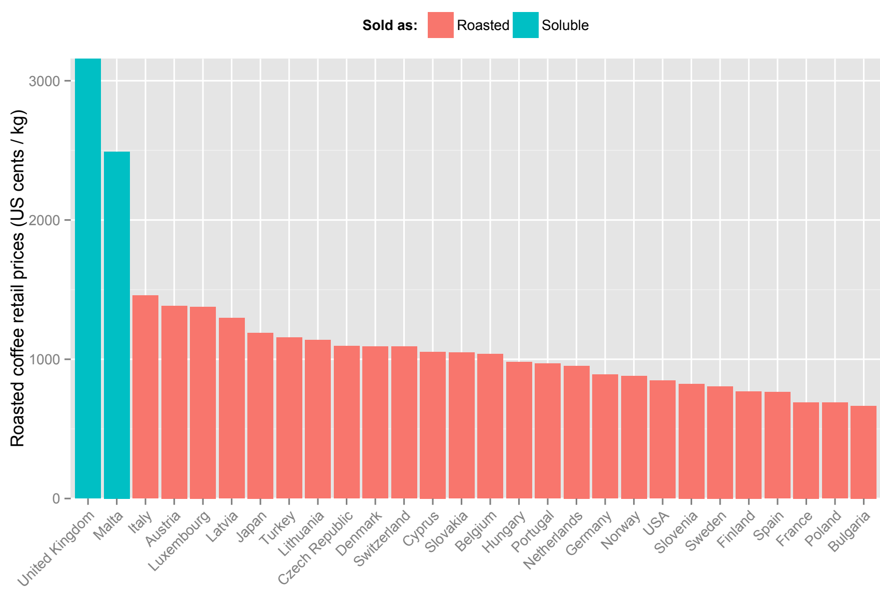

Figure 3.24: Retail price for roasted beans in U.S. cents per kg, between 2009 - 2013, from ICO.

Retail prices appear to have an uncertain effect on consumption, with consumption often climbing as retail prices climb. The direction of causality could be a problem in this case, where prices could be being driven higher by higher consumption. Only 1% of the variance in consumption explained globally by retail prices. Mostly, retail prices appear to be driven by their level in the previous year. In other words, they may follow a kind of random walk, determined more endogenously than by external factors.

3.6.3 Retail prices follow costs

Finally, we relate retail costs in consuming countries to prices paid to farmers in producing countries. Thurston et al. (2013) shows that for coffee sold in the U.S. and under modest assumptions, retail profit is 6% of the entire price of the product, and no actors upstream are taking a large share of profit either. We can therefore expect that retail prices are largely driven by economic necessities. The results are divided into producer country results and consumer country results. This is because each producing country sells to multiple consuming countries, and visa versa. The producer country results reflect the average of the effects they produce across all consuming countries, while the consuming country results

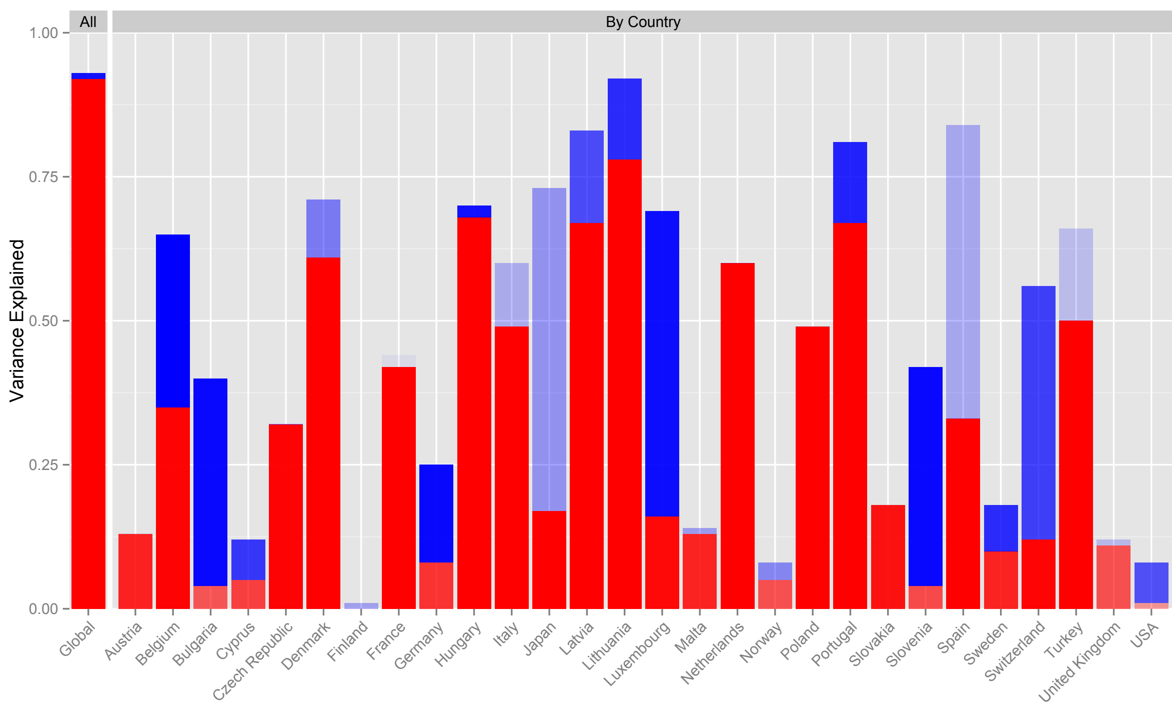

Figure 3.25: Variance of demand as explained by previous-year demand (red) and retail prices (blue). Bars are faded according to their p-values.

reflect the effects produced by their mix of producing country imports. The trade relation data is from Comtrade (2015).

Producer countries

Producer country prices are divided into the share to farmers, in US cents per kg, and an additional mark up inferred from retail prices. See figure 3.26 and the table in Appendix A.7.9.

The "To Farmers" column is reported in ICO data, and included in the table as the mean farmer price across all available years, in constant year 2000 cents. The remaining inferred producing cost for each country is the producer-side markup. While this may not be captured by producing-countries, it is associated with them: where this value is high, a large markup exists between retail prices that import from this country and farmer prices. Most markups are between 450 and 550 cents per kg, with Brazil and Vietnam as notable outliers. The greatest inferred markup comes from Indonesia.

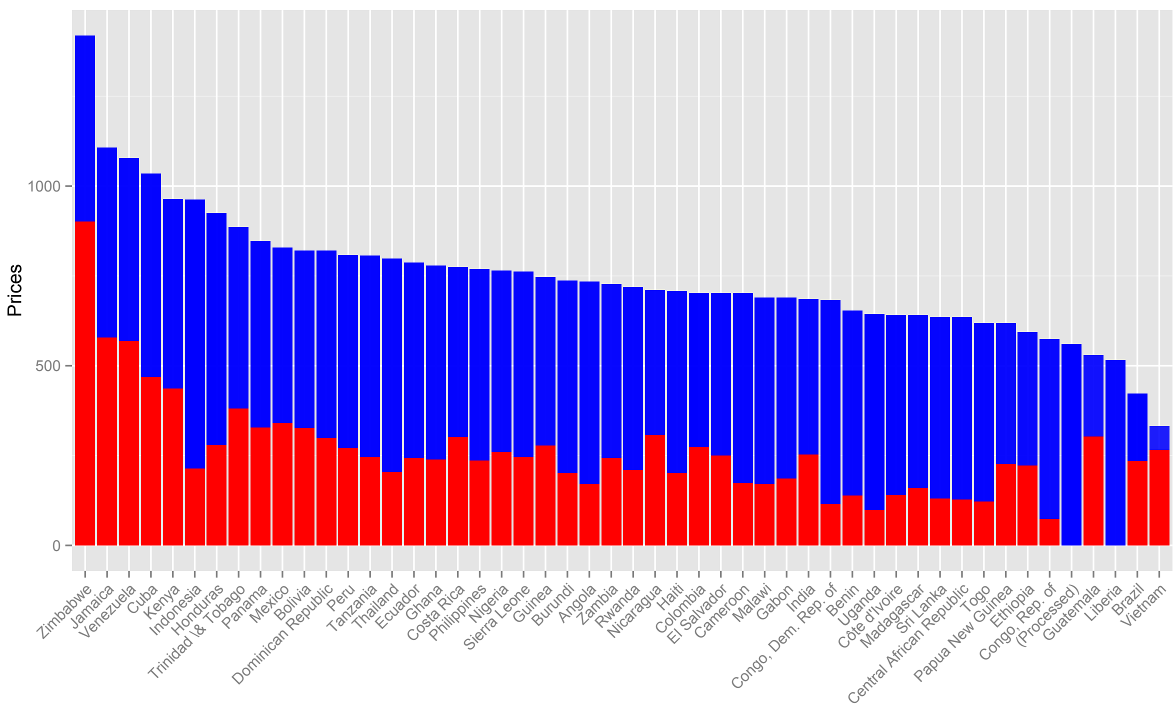

Figure 3.26: Producer country prices to farmers (red) and producer-associated markups (blue). Producer markups are faded by p-value.

Consumer countries

The consumer country values include prices to farmers ("To Farmers") as averaged across all imports; distribution costs (averaged over country-to-country specific inferred transportation costs), the final retail prices (from ICO, averaged over available years in constant year 2000 cents), and the additional markup associated with the consuming country.

The farmer price is taken as the weighted average of farmer prices that make up imports in a given year, and adjusted for 16% loss of weight. See figure 3.27 and table A.17 in the Appendix.

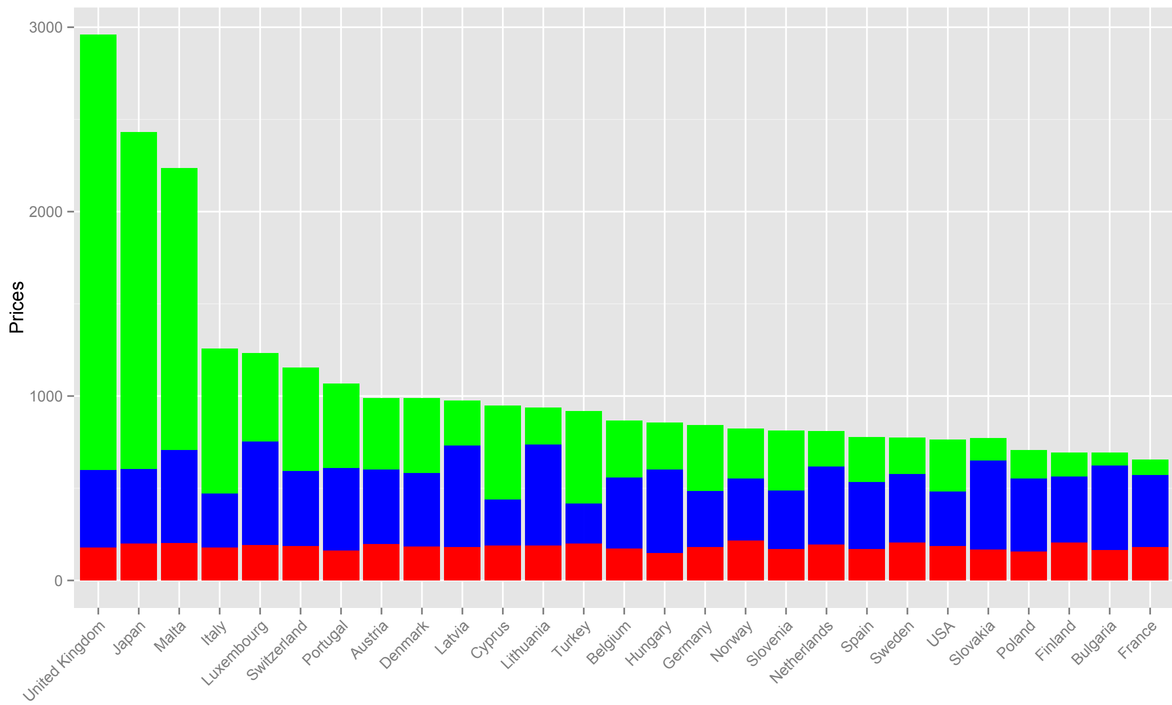

Figure 3.27: Consumer country prices to farmers (red), the distribution network (blue) and consumer-associated markups (green). Distribution prices are faded by p-value.

The largest markups are associated with soluble coffee prices (the United Kingdom and Malta). Japan also has very high markups. Low markups exist in Bulgaria, France, and Slovenia.

Chapter 4

Potential for shifting cultivation

4.1 Previous coffee suitability literature

Suitable lands for coffee are expected to shift poleward and to higher elevations as temperatures rise. A number of regional estimates of these effects have been made, mostly using the Maximum Entropy (MaxEnt) methodology (see table 4.1), which makes it difficult to assess their robustness. MaxEnt is a powerful technique in its ability to extrapolate suitability conditions from very sparse data. However, we believe that a different approach is more appropriate to the coffee context. We develop a Bayesian odds technique, which applies the data in our spatial coffee database.

Regions	Approach	Reference
Nicaragua, Mexico	MaxEnt	Laderach et al. (2009)
Kenya	MaxEnt	CIAT (2010)
Ethiopia	MaxEnt	Davis et al. (2012)
Haiti	MaxEnt	Eitzinger et al. (2013)
Uganda (data from Uganda, Tanzania, Kenya)	MaxEnt	Jassogne et al. (2013)
Rwanda	Qualitative criteria	Nzeyimana et al. (2014)
Indonesia	MaxEnt	Schroth et al. (2014)
Global	MaxEnt, SVM, Random Forest	Bunn et al. (2015)
Global	MaxEnt	Ovalle-Rivera et al. (2015)

Table 4.1: Recent analyses of current and future coffee suitability.

The most comprehensive previous estimates of changes in suitability are from the Global Agro-Ecological Zones (GAEZ) version 3.0 (2012), and from Bunn et al. (2015). GAEZ uses a potential yield model with soil physics and parameters derived from field experiments. Bunn et al. use a variety of data-mining methods, relating current occurrence to climate characteristics. The two approaches provide a useful comparison.

Figure 4.1 shows the GAEZ potential yield maps for the baseline period (1961 - 1990) and in 2050 under a business-as-usual trajectory (IPCC A2). These maps account for the additional benefit of CO2 fertilization and an intermediate level of fertilizer inputs.

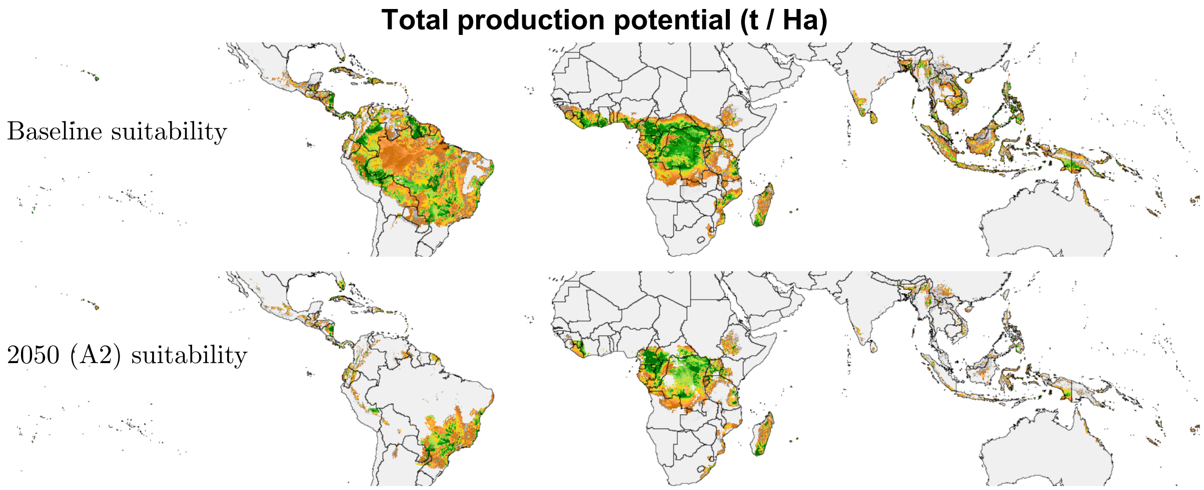

Figure 4.1: Coffee suitability maps for 1961-1990 (above) and for 2050 (below) under IPCC's A2 scenario (Hadley GCM). Color represent total production capacity, from 0 (white) to .98 t/ha (green). Source: GAEZ

A few results are visible in these figures. First, the current range of suitable climate is predicted to be large in many areas, particularly South America and central Africa. Actual coffee production areas are much more limited. The extent and quality of coffee producing areas in 2050 is much smaller than the suitable areas in the baseline period, but also tends to more closely match existing areas of cultivation. Some countries are predicted to no longer have any land suitable for growing coffee (e.g., Ghana and Nigeria) while other regions have new potential (e.g., Florida and South Africa).

These shifts in coffee production can be seen more clearly in the difference between current coffee production potential to future coffee production, as shown in figure 4.2.

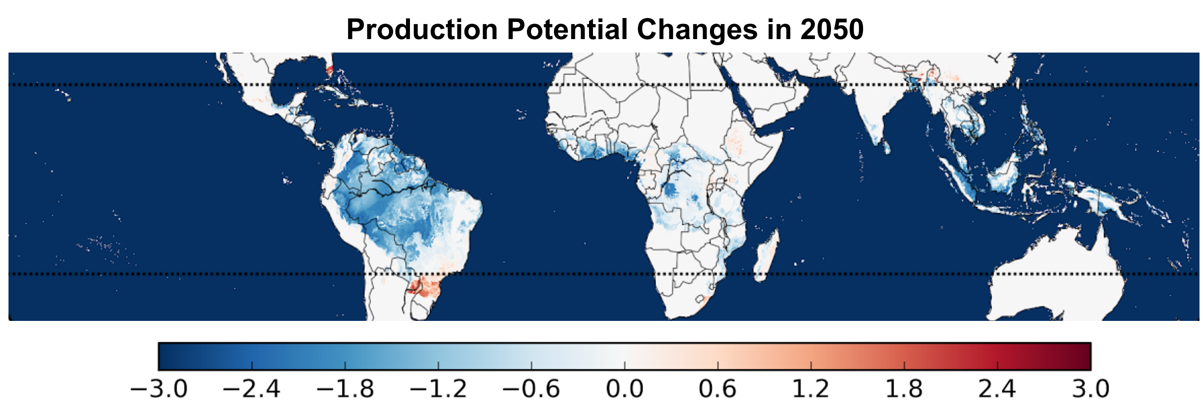

Figure 4.2: Changes in coffee suitability, in terms of production potential in t/ha, between 1961-1990 and 2050 under IPCC's A2 scenario, under a high-input farming system. Adapted from GAEZ.

Most areas show large decreases in coffee production potential, except for Florida, southern Brazil, South

Africa, Ethiopia, northern India, Myanmar, and China. The dashed lines show the tropics of Cancer and Capricorn, the traditional bounds of the coffee belt. Almost the entire region within these bounds decreases in suitability, while increases are generated in the region beyond it. A table of the country-by-country changes in amount of suitable area from GAEZ is included in Appendix A.4.5.

Bunn et al. (2015) provide a more nuanced picture (see figure 4.3). While Bunn et al. still estimate decreases in climatic suitability between now and 2050 across much of the current coffee producing area, they also find neighboring areas in many cases that show increases in suitability. For example, regions in Colombia, Central America, and Indonesia can shift to higher elevations, and Brazil production can shift south. The coffee production potential in much of Uganda and Tanzania shifts into Kenya and the Democratic Republic of the Congo.

Changes in arabica and robusta climate suitability

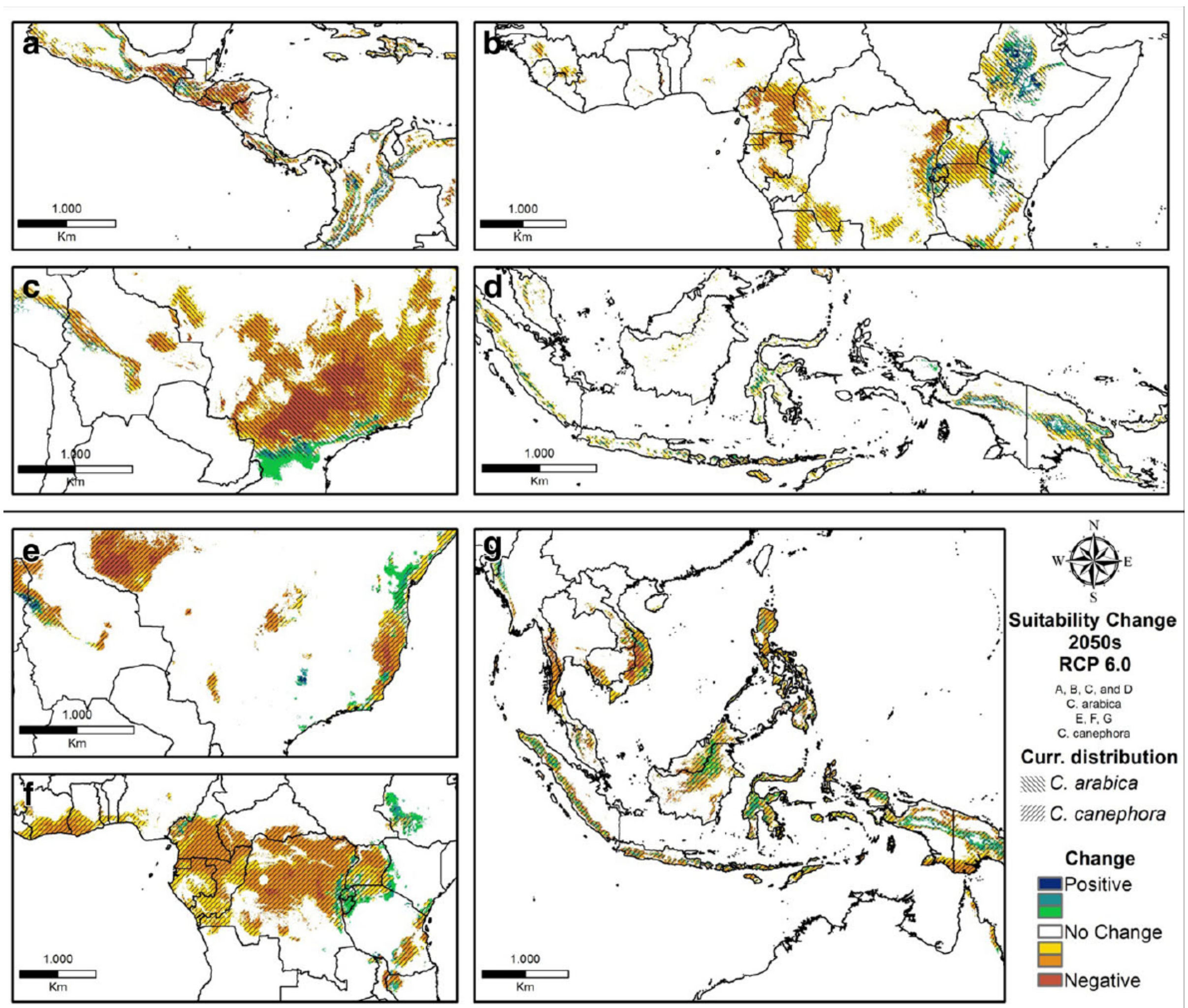

Figure 4.3: Suitability changes between present climate and 2050. Figures a - d show Arabica production and figures e - g show Robusta. Reproduced from Bunn et al. (2015).

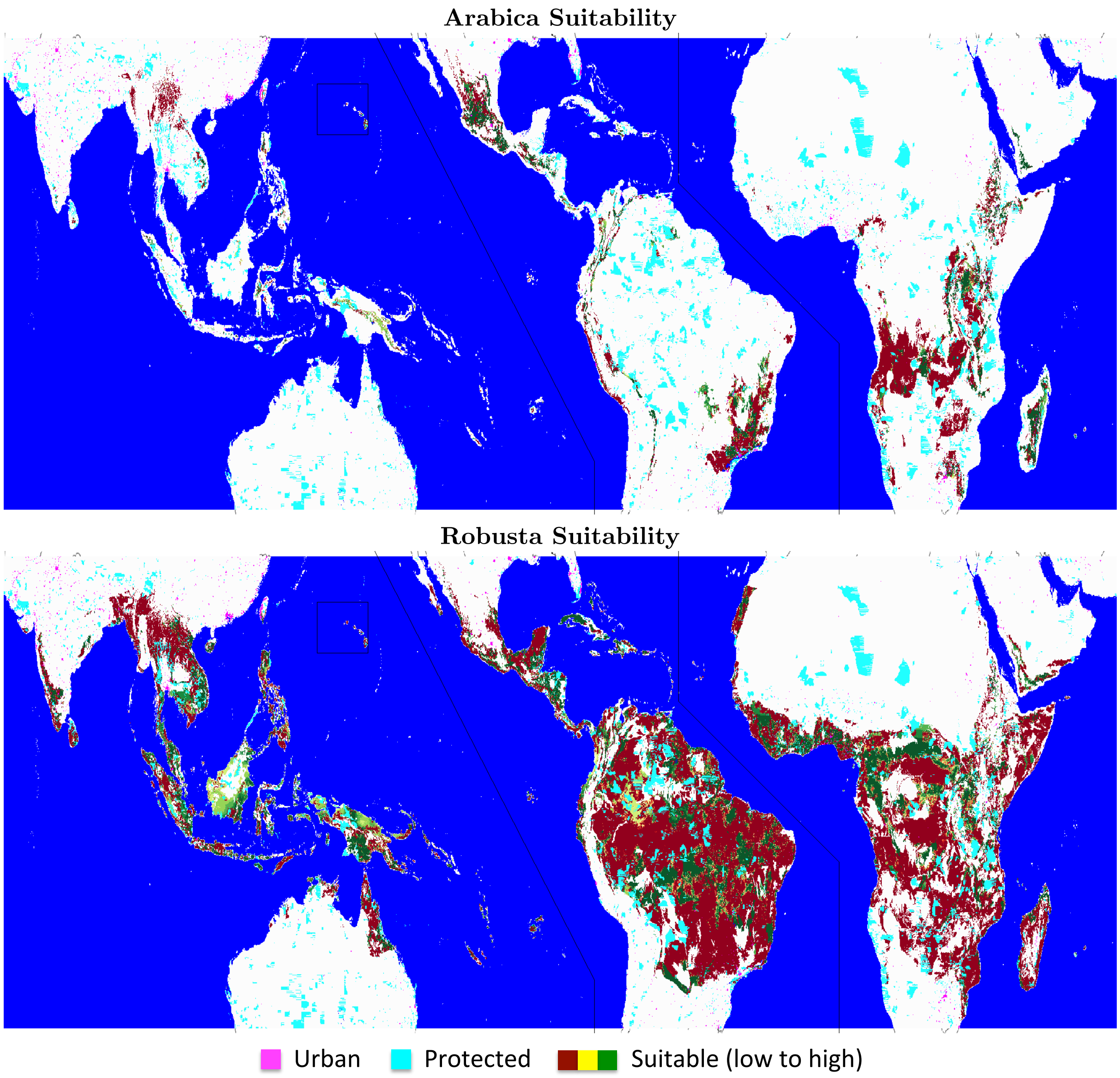

Figure 4.4: Combined Bayesian and GAEZ results for Arabica and Robusta.

4.2 Future suitability

Estimating future suitability requires taking careful account of the uncertainties involved in future predictions. We estimate suitability for each of 17 GCMs for Bioclim and 4 GCMs for GAEZ. We display three maps for each of Arabica and Robusta suitability. The first is just the measure of median changes in suitability, without protected and urban areas. The second shows the level of confidence that the direction of the suitability change is as shown. The third shows the full map, where areas are also faded in proportion to their level of uncertainty.

The maps show that many traditional coffee growing areas are going to experience large losses in suitability by 2050. This includes parts of Brazil, southern Mexico, Kenya, and Madagascar. Few places show increases, but these include other parts of Brazil and Angola.

Appendix A.4.7 shows the total area by country expected to increase and decrease, both by suitability and within harvested regions. These are summarized at the global level in table 4.2.

	Arabica	Robusta
Baseline suitable area (Ha)	187626000	14663700
New suitable area (Ha)	27247000	21598800
Existing suitability loss (Ha)	-132070000	-88827000
Loss from baseline (%)	-70.4	-60.6
Change from baseline (%)	-55.9	86.7
Current harvest (Ha)	10034618	10069911
Loss from harvested areas (%)	-24.3	-12.1

Table 4.2: Global changes in suitability for Arabica and Robusta varieties. Robusta is expected to see large increases in general, while Arabica will experience decreased suitability.

In absolute suitability changes, Brazil has the most lost of suitability in regions that are currently suitable, and the most gain in new regions becoming suitable. As a fraction of the current suitable area, a number of countries are tied in losing all of their suitable land: Belize, the Central African Republic, Côte d'Ivoire, Republic of Congo, Fiji, Gabon, Guinea, Equatorial Guinea, Cambodia, Paraguay, Sierra Leone, and Thailand. Although Taiwan also losses its entire allotment of suitable areas (of which it is currently using none), it also shows the largest percentage increase in suitable regions, gaining 50% more than it loses.

This result is more extreme than most suitability results in the literature, which typically do not predict losses in suitability beyond 95% in any country (Jaramillo, 2013). It is a consequence of our estimation approach, which relies on both biological and statistical factors. There are currently regions within these countries that satisfy both criteria, suggesting that they are likely to be highly productive. It may be that these areas will continue to be capable of producing quality coffee, but we predict that they will experience significant losses in their capacity.

Across the globe and under the median change, 130 million hectares of currently suitable land will be lost, and only 30 million hectares will be gained. Coffee is currently harvested on 10 million hectares.

These changes apply to suitable land, whether or not it coincides with our data on changes within areas of current cultivation. However, the story for current cultivation is similar: the countries that lose all of their harvested land are exactly the same as those that lose all of their suitable land. In total, 19 countries lose more than half of their currently harvested land to losses in suitability by 2050.

Suitability changes for Arabica

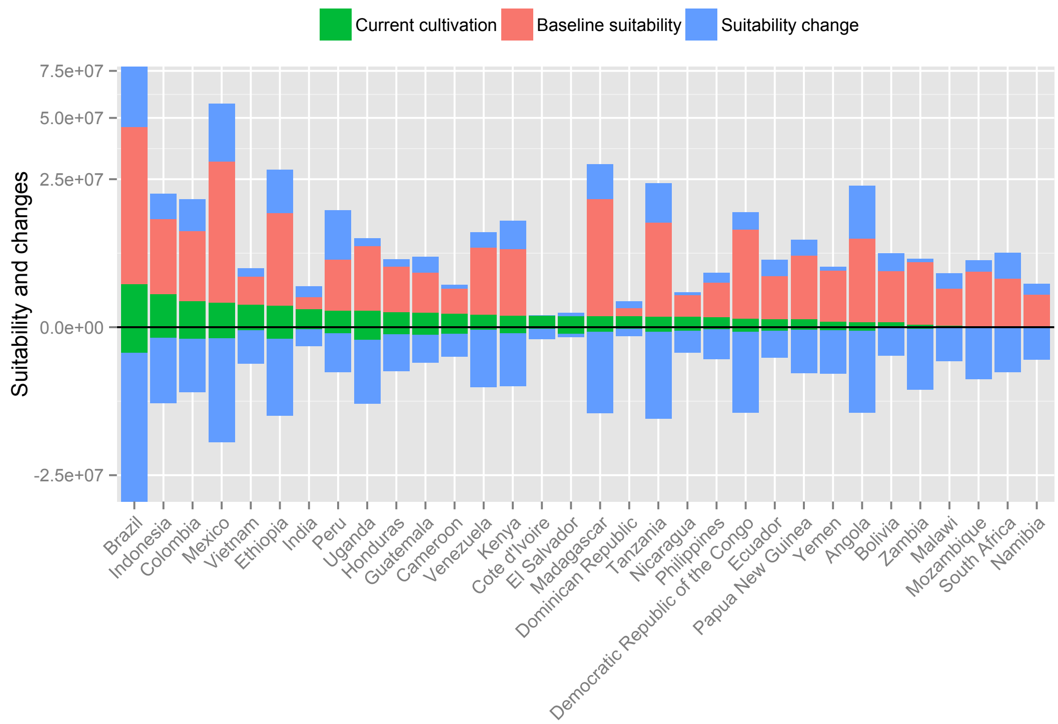

Suitability changes for Robusta

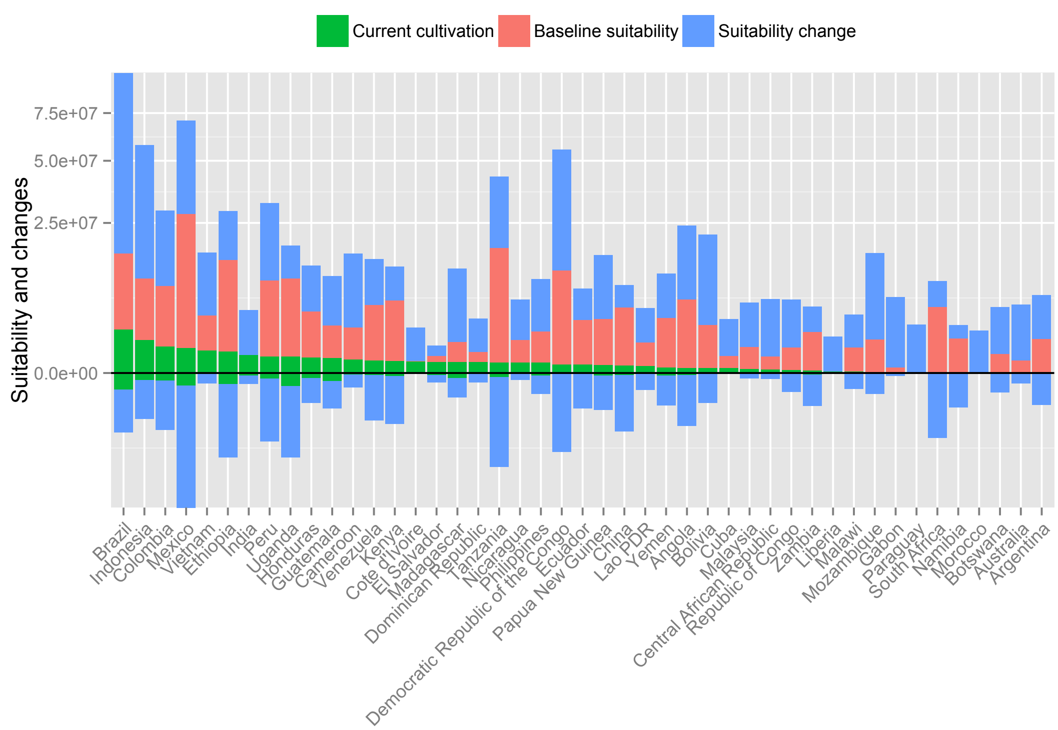

Figure 4.5: Increases and decreases in suitability and current cultivation by 2050. Green bars above the line describe current harvest areas; green below the line is the median predicted loss by 2050. Red above the line is the total baseline suitability. Blue above the line is new areas of suitability by 2050, and blue below the line lost areas.

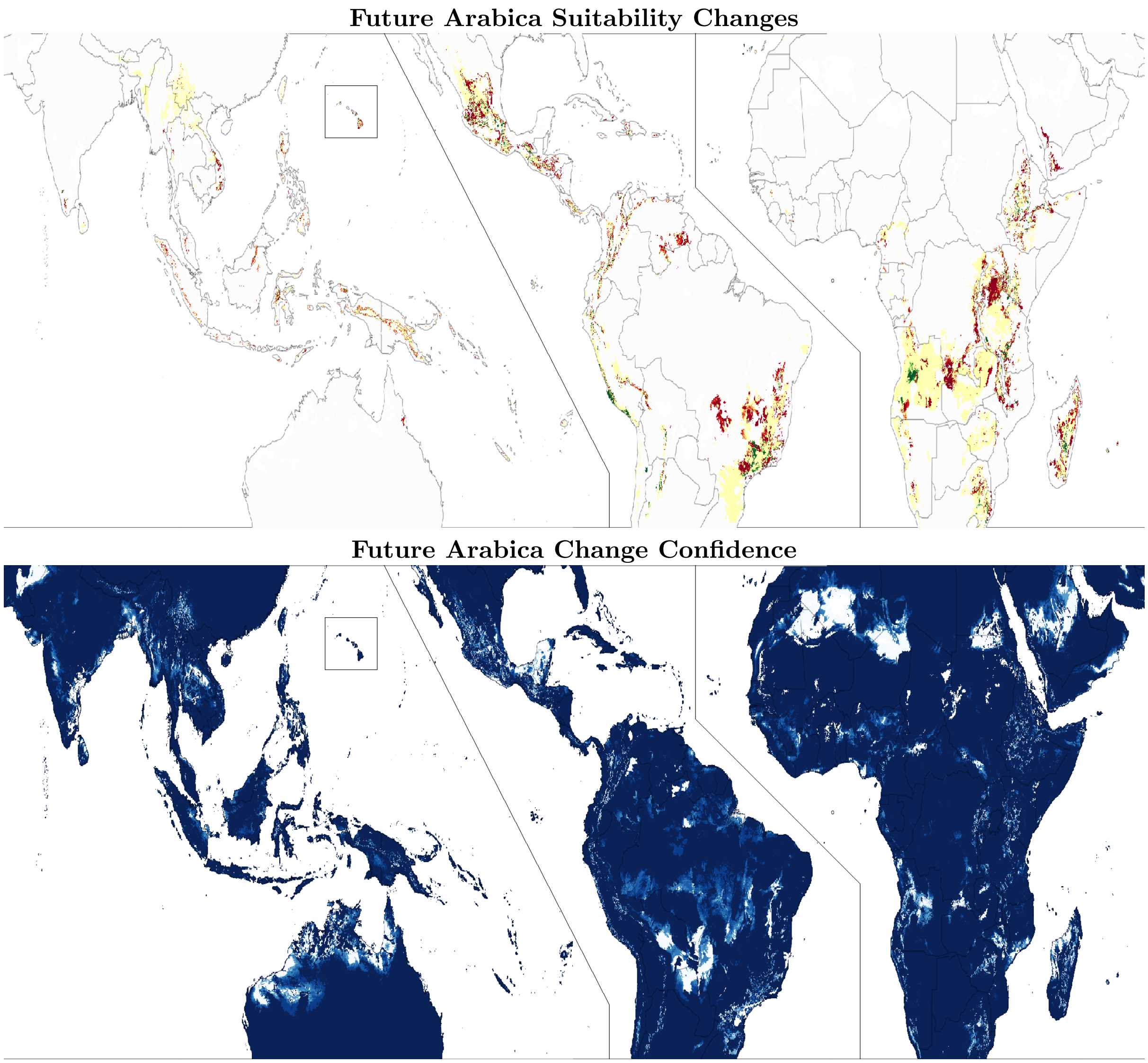

Figure 4.6: Maps of future Arabica suitability changes, showing the median suitability change (top) and the confidence level behind the direction of that change (bottom).

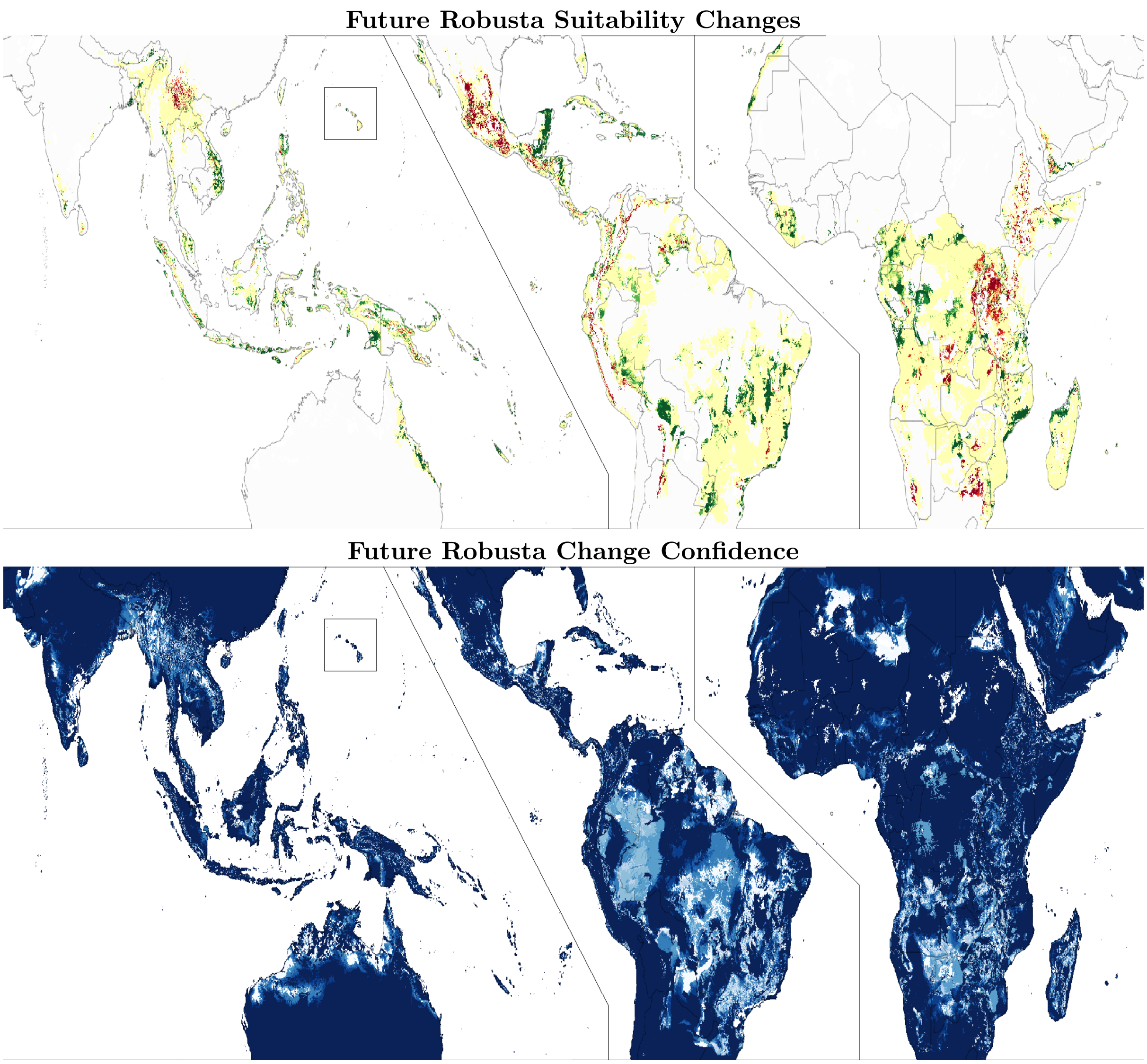

Figure 4.7: Maps of future Robusta suitability changes, showing the median suitability change (top) and the confidence level behind the direction of that change (bottom).

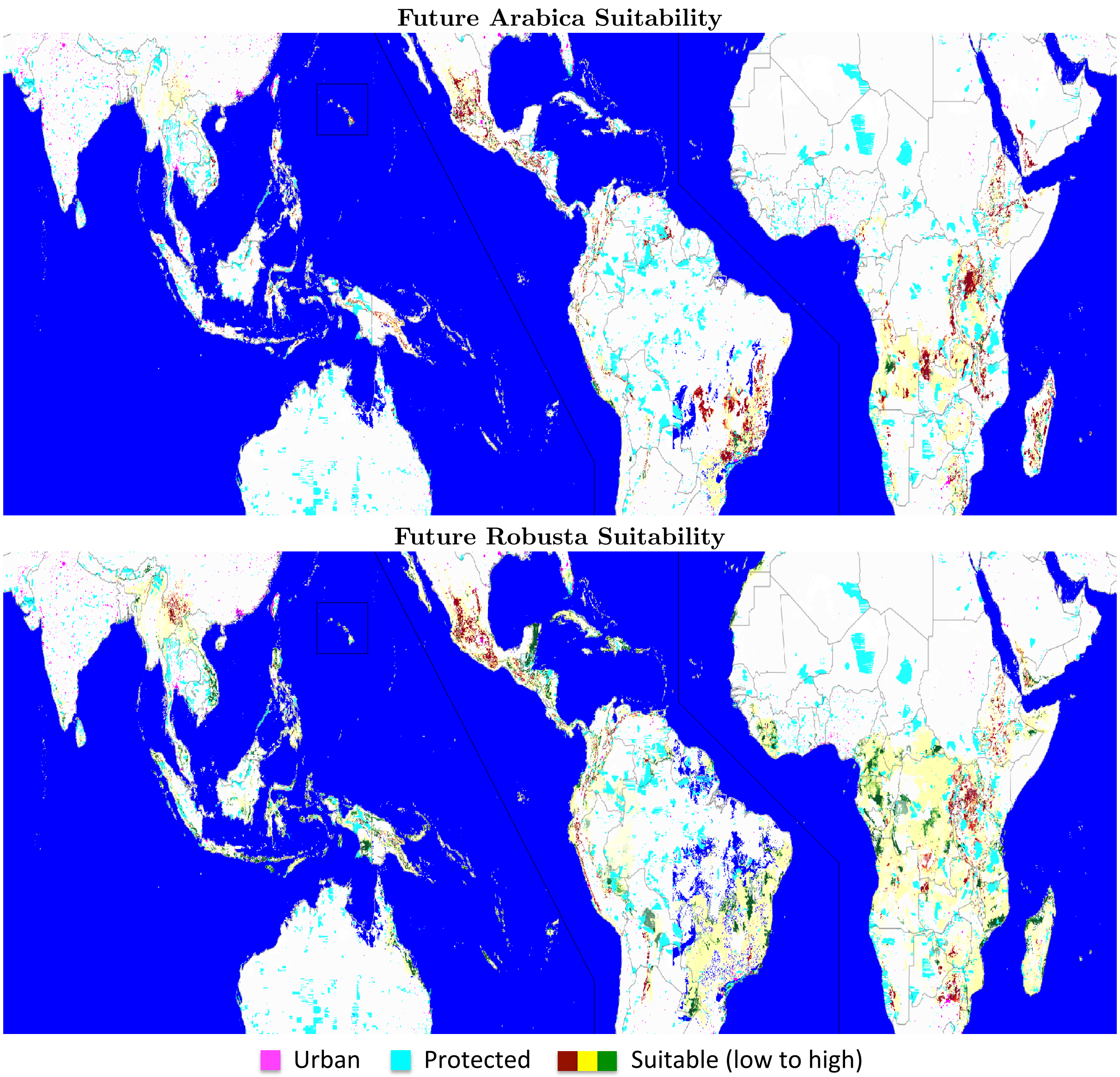

Figure 4.8: Maps of future Arabica and Robusta suitability as combined land use maps with suitability changes faded according to confidence.

Chapter 5

Adaptation strategies

5.1 The role of management

Fertilizer and irrigation use can open up new areas to coffee production. Figure 5.1 compares suitability according to GAEZ for low-input and high-input management. High-input management can produce yields 5 times that of low-input management.

Low Inputs, Rain-fed Suitability

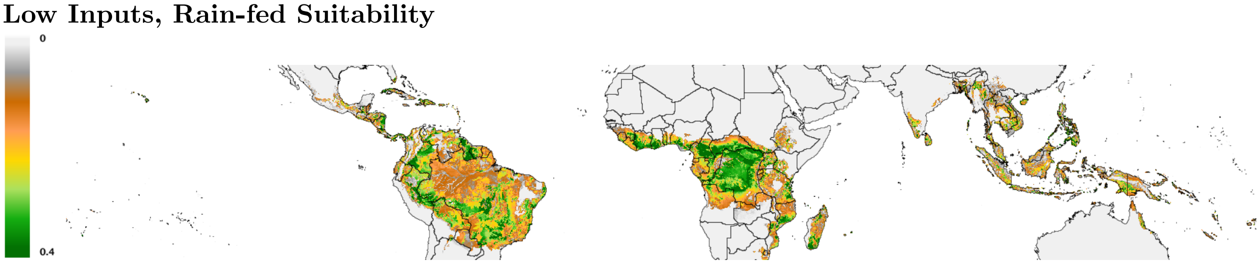

High Inputs, Rain-fed Suitability

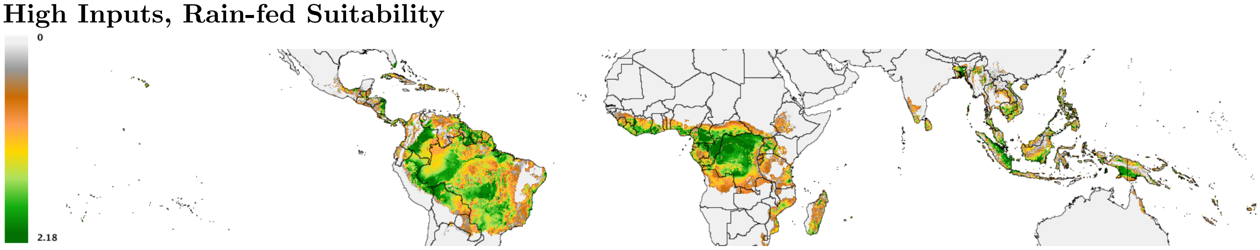

Figure 5.1: Both maps are copyright of IIASA and FAO.

Figure 5.2 shows the amount of fertilizer used by countries and distinguished for regions with Brazil, using FAO data (FertiStats). A wide range of fertilizer amounts are used, with the greatest amounts of fertilizer used by Vietnam, Venezuela, and Costa Rica, and the least by Ethiopia and Tanzania. This material is to be added to the production model.

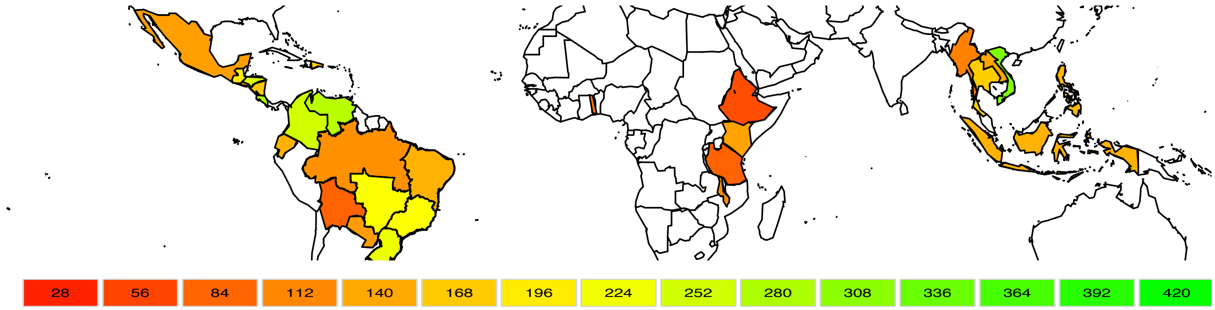

Figure 5.2: Average fertilizer use for coffee, from FertiStats (FAO), and including Brazil regional breakdown from `ftp://ftp.fao.org/agl/agll/docs/fertusebrazil.pdf` (FAO). The greatest amounts of fertilizer are used by Vietnam, Venezuela, and Costa Rica, and the least by Ethiopia and Tanzania.

5.2 Mitigation and adaptation

The two central responses to climate risk for any sector are mitigation and adaptation. Mitigation refers to the policies, practices, and international agreements that lead to lower greenhouse gas (GHG) emissions. Adaptation, the planning and practices engaged in to manage the risk of a changing climate, is an independent concern from mitigation. It is clear now that all sectors will need proactive adaptation, irrespective of the actions taken toward mitigation.

For the coffee sector, mitigation is synonymous with sustainable environmental practices, and many coffee farms are already performing well. GHGs can be released in the course of coffee production through the application of fertilizers and pesticides, direct fuel and electricity use, depulping and fermentation resulting in methane, and release of nutrients from the soil. Account for all of these, traditional and commercial coffee polycultures have a low carbon footprint, while monocultures produce 50% more GHGs (van Rikxoort et al., 2014).

One of the largest sources of CO_2 is deforestation, where there is evidence of both positive and negative interactions with coffee. Coffee plantations reinforces the ties between forests and the economy, resulting in lower deforestation rates in some regions like Ethiopia (Hylander et al., 2013). Elsewhere, such as in Indonesia, periods of high coffee prices have induced increases in deforestation (O'Brien and Kinnaird, 2003). We show that coffee suitability will shift rapidly as a result of climate change. Even where shade trees are maintained, the carbon impact of the loss of forest is far greater (Baker, 2013). For this reason, it is important for the shifts of coffee cultivation to take place solely within present agricultural regions, or in conjunction with reforestation programs, to maintain the balance of carbon.

The coffee industry also receives direct benefits from forests. Coffee farms near forests and their wild pollinators are 20% more productive and produce 27% fewer peaberries (Ricketts et al., 2004). By maintaining forest cover, coffee farms can benefit themselves both directly and through the climate.

While mitigation has long-term consequences, coffee farmers can achieve immediate benefits and lessen the impacts of climate change through adaptation. For example, shade trees in coffee plantations can decrease the temperatures to which plants are exposed by up to 4°C (Jaramillo, 2005). One reason why climate change is such a great risk to coffee producing countries is because many coffee farmers are poor and have a lower capacity to adapt to climate change.

coffee&climate (2015) provides an extensive overview not only of approaches to adaptation, but of the equally important process of evaluating climate vulnerability. Baca et al. (2014) identify nine axes of vulnerability through focus groups, and associate each with a parameter to measure and track:

Road type	Time from the farm to the collection center, time from the farm to the nearest market, type of road from the farm to the collection center or nearest market
Transport of products	Type of transportation from the farm to the market, time from the farm to the bus stop
Quality of housing	Housing material, basic services
Access to and availability of water	Source of water for drinking or post-harvest processing, availability of water during the year, distance to the water source, water quality
Conservation	Area of forest around the water source, area of forest to keep in the farm
Soil and fertility	Soil type, soil slope, mulch of leaves, soil depth
Food and health	Number of symptoms of human disease, number of times that person is attended by a doctor, dependency of external products
Migration	Type and time
Variability of yield	Average farm yield in four years compared to the local average

They also identify modes of adaptation for addressing each of these vulnerabilities, and the parameter that provide opportunities for new practices.

Variability of post-harvest infrastructure	Types or forms to dry coffee
Pollution	Waste management, release of fermentation residues into water, management of agrochemical containers, coffee waste management, area burning annually
Management of shade trees and reforestation	Number of trees cut, number of trees planted
Access to education	Level of education, quality of technical assistance, crops for which receive technical assistance, types of media accessed
Level of knowledge of farming system	Registration practices and activities, coffee intercropping, pests and diseases
Organization	Participation, time, benefits
Knowledge of laws and policies	Policies about coffee sector, environmental laws, land polices
Access to credit	Term of credit, interest rate of credit, opportunity of credits
Diversification of income	Number of sources of income
Access to specialty markets	Destined for sale, special market access
Access to technologies	Varieties, drip irrigation, water harvesting

This kind of broad thinking is essential to addressing the adaptation problem in coffee. Small-scale farmers will have a more difficult time adapting to climate change than large-scale ones. As a result, climate change will result not only in changes in coffee cultivation, but will also produce winners and losers amongst the groups planting them.

Chapter 6

Future research needs

6.1 Future opportunities for research

The coffee production database offers many new opportunities for studying the connection between coffee and its environment across the globe. Over the course of our research, we also uncovered a range of topics worth further research.

One of the most important open questions is how to combine suitability, variability, and production analyses. These three dynamics take place on different spatial and temporal scales, whereby suitability is based on static properties, our variability uses global patterns, and the production model represents the effect of weather on crops from year to year. These three are interrelated, and any region that has large production shocks more frequently than every three years, at the extreme, will be unsuitable for coffee, since coffee plants could never get to a sufficient level of maturity.

Another under-studied area is coffee disease. While all of our empirical estimates implicitly capture the effect of coffee disease, these may end up being the most difficult impacts to adapt to. The coffee berry borer's range has rapidly expanded in recent years, and some of these shifts are related to climate (Magina et al., 2011). Jaramillo et al. (2009) find that a 1-2°C increase in temperature would result in large losses from the coffee berry borer, particularly in regions with high-quality Arabica. Data on coffee diseases is not as plentiful as yield data, but can be collected from many sources.

Our study of the coffee market only scratches the surface of many interesting connections between climate and variability, producers and consumer, and prices and trade. The coffee market is global, complex, chaotic, and sophisticated, with many different kinds of stakeholders. Future work would extrapolate the effects of climate on coffee production amounts and locations to determine the consequences for price and demand.

Both of these are related to an all-important topic we struggled with: coffee quality. While coffee quality has physical determinants, its subjective nature make it very difficult to study. However, the structure of futures contracts provides an entry-point, where quality is quantified and varies over both space and time. This data would allow future research to understand the impact of climate on coffee quality, at least at the country-wide level.

Below are some additional analyses that would be informative.

Production Incorporating the role of wind speeds, known to be an important factor in many regions (e.g., Haiti), into the production model.

Production Incorporating the changes in climate-driven harvest area to correct reported yields to reflect damage that reduces yields to the extent that the plant is not harvested at all.

Production Studying the effect of fertilizer on production, captured in the "fixed effects" of each region in our production model.

Production Use the India district data to construct and India model, and incorporate that into the hierarchical global model (see figure **??** in the Appendix).

Prices Disaggregating the country-wide markup values to identify how they differ by coffee type.

Chapter 7

Industry recommendations

The results of this report support a range of actionable recommendations for the coffee industry.

The coffee industry should take a public stance on climate change.

Coffee is an intimate part of billions of lives, but it is also intricately affected by the hidden processes of the global climate. The coffee industry has the capacity and the incentive to be a global leader in discussing climate change.

That discussion should include a committment to understanding the effects of climate change both on coffee and on coffee growers. Coffee provides an important link between environmental justice, social justice, and health, providing a strong platform for discussing how these issues interrelate.

Invest in a global production data collection and coordination infrastructure.

High resolution, geospatial coffee production data, including information on yields, cultivated land, pest impacts, and management practices, are essential for understanding the present responses of weather and the future impacts of climate change.

Coffee production data is currently a fragmented mix of country agencies and NGOs reporting inconsistent metrics at different levels of regional aggregation. Few areas have long timeseries of production data, and even these are calculated across different periods per country.

The future data collection infrastructure persue two mutually-supportive levels. An aggregated level should provide basic production information for regions, including yields and total cultivated land, at as high a resolution as possible while maintaining comprehensive coverage and yearly reporting. A farm level dataset should provide a more detailed collection of management and outcome data for as many farms as possible, including the yearly reported production information for each farm.

The coffee database developed for this report provides a framework for describing and combining these data. It includes spatial boundary information for the aggregated level, and merges different reporting and information from multiple sources. The next step is to expand this model to a much larger collection of countries.

Another important kind of data that is currently unavailable at large levels is coffee quality information in a form that can be linked to production areas. Climate change will affect not only the productivity of coffee, but the quality of the coffee that is produced, but understanding this link requires new data that needs to be collected systematically and assembled historically.

Encourage proactive adaptation to climate change.

Shade trees and other management practices can go a long way toward diminishing the impacts of climate change. However, if farmers wait until the impacts are fully felt, it will be too late. Whether the proximate result of climate change is a heat wave, a drought, a pest attack, or something else, the results could be abupt and devastating unless new practices are already in place.

Work with existing farmers in planning for new suitability regions.

Many farmers will eventually see the loss of their capacity to grow productive coffee. The producers that weather this change best are likely to be larger and richer than those that currently grow coffee. This is both a social concern for the welfare of poor farmers, and a loss to the knowledge base for coffee cultivation.

The coffee industry should engage with existing small-scale stakeholders to ensure that they are not disenfranchised by these changes. Given the opportunity to use their knowledge and traditions to ensure the economic future of their families, they can be strong allies in the shifting landscape of coffee.

Appendix A

Supplemental material

A.1 Brazil case study

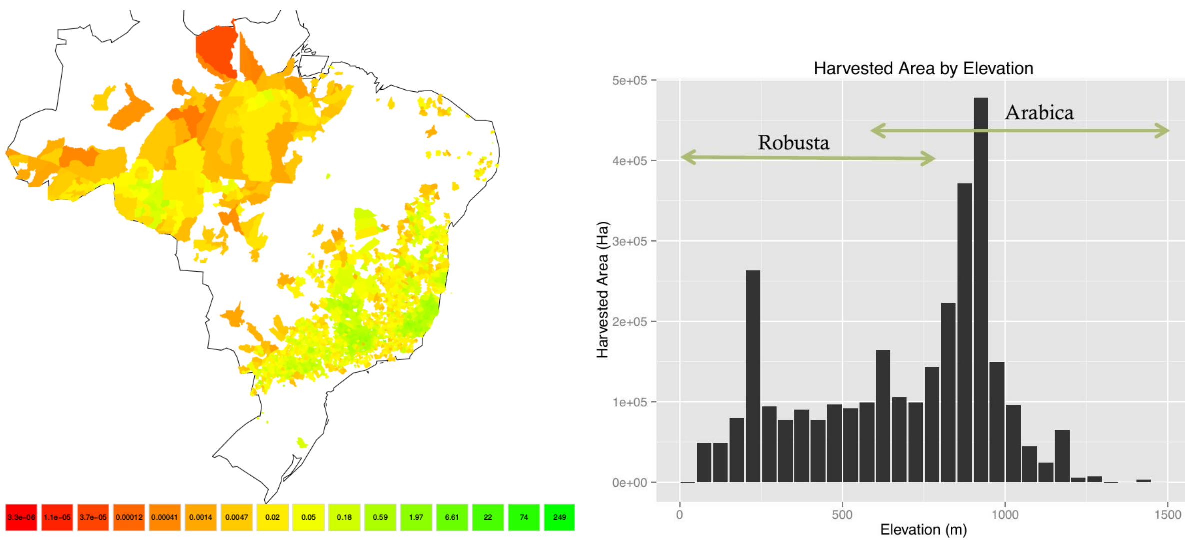

Figure A.1: Brazil dataset across space and elevation. **Left:** Density of coffee production, as the average production divided by municipality area. Regions in green account for the majority of production. Most production occurs in the south, however there are coffee producing regions also in the southern Amazon. **Right:** Distribution of coffee producing area, displayed across the average elevation of each municipality. The greatest extent of coffee production occurs in municipalities with around 900 m of elevation, but coffee is also produced in municipalities with a much lower elevation, including a peak around 200 m. The range of typical elevations for growing Arabica and Robusta are shown above the histogram.

A.1.1 An empirical model of production

Using the IBGE Brazilian coffee production estimates, combined with high resolution weather from the CFSR reanalysis product, we estimate a physically-based statistical model of coffee production. The model predicts yields using a nonlinear relationship with temperature and precipitation. We base our model on Schlenker and Roberts (2009), and divide GDDs into three groups: beneficial growing degree-days between 0°C and 33°C, killing degree-days above 33°C, and frost degree days below 0°C. We also use the average minimum temperature, which appears to be more significant than frost degrees. This kind of statistical relationship is based on the biological response of coffee to temperature, but puts a "black box" around farmer responses and ecosystem and pest dynamics. If farmers are providing sufficient irrigation and shade to coffee plants, the effect of high temperatures will be mitigated beyond what biological models suggest on their own.

Calculating growing degree-days

Growing degree-days (GDDs) are calculated using a continuous sinusoidal fit to minimum and maximum daily temperatures, as shown below:

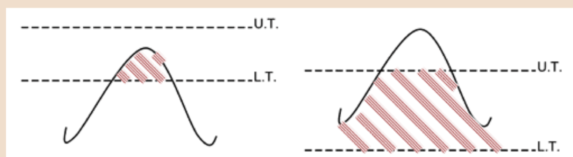

Calculations for growing degree-days and killing degree-days. Any temperatures above a given lower threshold (L.T.) are included, up to a maximum of an upper threshold (U.T.). As temperatures shift over the course of a day, fractional growing degree-days are accumulated.

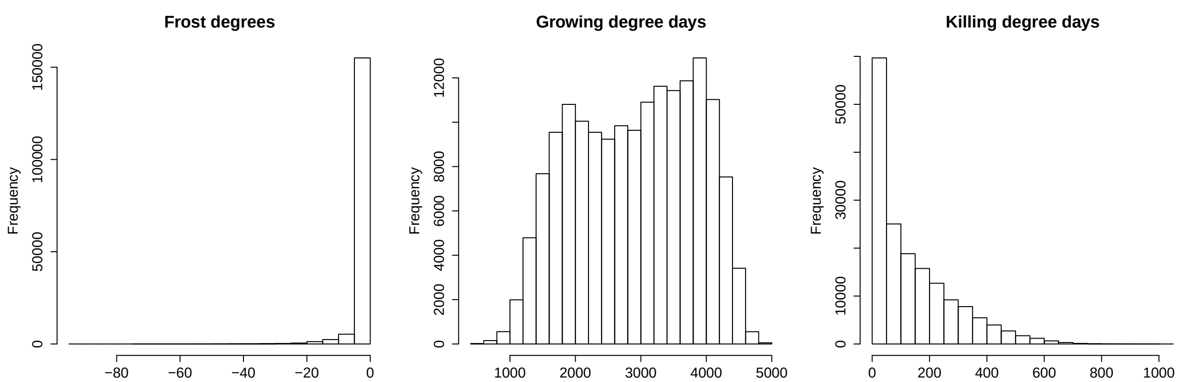

Figure A.2: Histograms displaying the number of growing seasons with a given number of frost degree-days, growing degree-days, and killing degree-days. The exponential decays in frost and killing degree days are useful for capturing the impact of extreme events. The broad range of growing degree-days represented in the center histogram allows for accurate estimates of the coffee growth response.

We also include precipitation, as the total accumulated precipitation over the six months before harvest. Precipitation is included as a quadratic, to capture the expectation that both too little precipitation and too much precipitation are harmfully impact yields.

A.1.2 Optimal temperature range

Guzmán Martínez et al. (1999) suggest that 10°C is the appropriate base temperature for calculating GDDs for coffee. We explore a large range of minimum and maximum temperatures for GDDs, seeking the limits that provide the greatest predictive capacity. See Appendix A.6.1 for predictive capacity of a range of possible limits. We find that a minimum temperature of 0°C and a maximum temperature of 33°C for beneficial GDDs is optimal. This means not only that all days over 0°C are estimated as beneficial, but that higher temperatures up to 33°C are progressively more beneficial. A day above 33°C is not immediately detrimental, but it has a progressively smaller benefit until it becomes negative, and we find that temperatures over about 38°C are detrimental in Brazil.

A.1.3 Predictive periods

Coffee production is very sensitive to weather during flowering, and the period during which we correlate weather with yields is important. To determine the optimal span of weather for predicting yields, we try out many combinations of starting and ending months. The harvesting period in Brazil ends in September, so we consider months starting with October to predict the yield in the next year. The coefficients of models for each of these periods are shown in figure A.3.

A few features are important in these results. In the top graph displaying coefficient values, areas in the upper-left are gray, denoting that models that use only the months shortly preceding harvest do not produce significant results. Second, we expect the effect of GDDs to be positive, KDDs negative, the linear component of precipitation (`precip`) to be positive, and the quadratic component of it (`precip2`) to be negative. This is confirmed for most date ranges, and we want to avoid regions that misestimate these values due to noisy or minor effects. Finally, the t-values figures show the confidence in these values, and are a measure of the statistical significance of the model as a whole. These values generally decrease as the starting month becomes later.

Figure A.4 shows the combined t-values for the GDD and KDD coefficients. The highest t-value is for GDD and KDD values calculated just for January and February. The probably reflects a highly sensitive period for the berry production. Nearly as high, and covering a six-month span, is December through May. We will use this as our span for calculating weather impacts.

A.1.4 Econometric model

The form of the statistical model is,

$$\log y_{it} = \alpha_i + \gamma g_{it} + \kappa k_{it} + \mu m_{it} + \pi p_{it} + \psi p_{it}^2 + P_{3,s(i)}(t) + \epsilon_{it}$$

Above and in the other models below, the observation variables and their corresponding effect estimating coefficients are:

	Var.	Coeff.
Growing degree-days	g_{it}	γ
Killing degree-days	k_{it}	κ
Average minimum temperature	m_{it}	μ
Total precipitation (linear)	p_{it}	π
Total precipitation (quadratic)	p_{it}^2	ψ

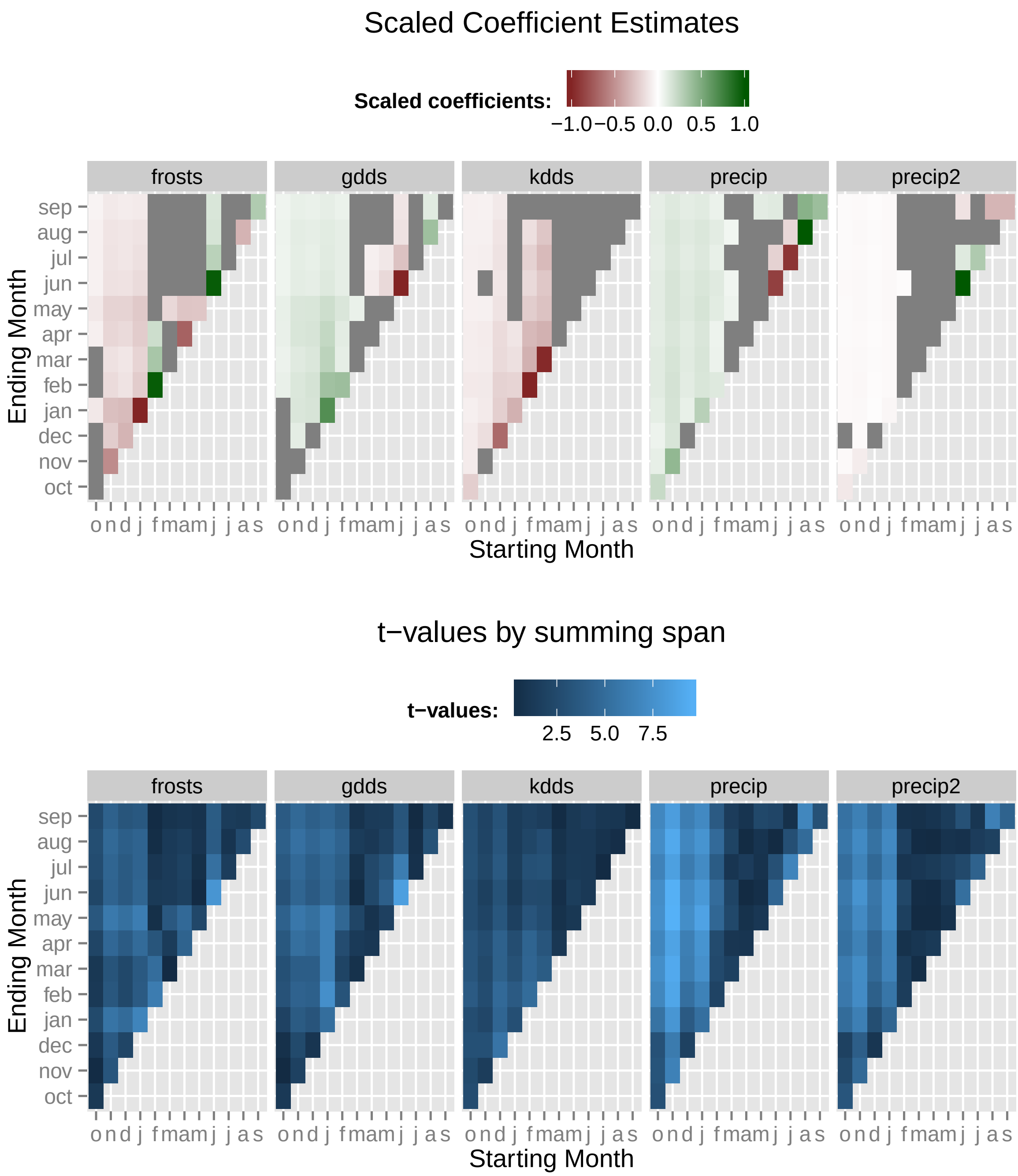

Figure A.3: Coefficients from estimating models with different month spans, and the t-values intervals associated with each coefficient. The top 118 municipalities in harvest density were used.

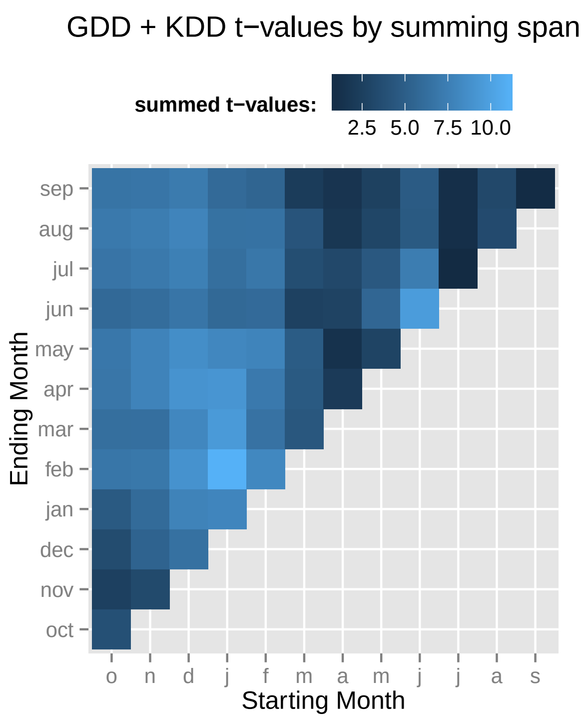

Figure A.4: The sum of t-values across the GDD and KDD coefficients, for identifying the most effective range.

where i indexes municipalities, t the years, and $P_{3,s(i)}(t)$ is a state-specific cubic trend to capture shifting productive capacity. We aggregate weather from December to May, and use 0°C to 33°C as the limits for computing growing degree-days.

Interpreting regression tables

Many of the results in this chapter are in the form of multiple regression tables. Each regression is of the form,

$$y_i = \alpha + \beta_1 x_{1,i} + \cdots + \beta_k x_{k,i} + \epsilon_i$$

which describes the relationship between a dependent variable, y_i, taking different values for each ith observation, and a linear combination of independent variables, $x_{1,i}, \ldots, x_{k_i}$. The ϵ_i term represents the remaining error that cannot be explained by the model. In addition, these models use "fixed-effects", which are parameters unique to each region, so that the model is effectively estimated by considering the effects of changes in the independent variables, rather underlying static differences between them.

The regression tables are mean to be read in columns. The first column specifies the variable for which an effect is reported, and the model columns specify the size of that effect. If a coefficient estimated is 10, that means that the dependent variable increases by 10 for every unit the independent variable increases.

The numbers directly below each effect and reported in parentheses are the values 'standard errors', a measure of the uncertainty of that value. If the standard error is less than half of the value, then there is 95% confidence that the sign of the coefficient in question is correct. This corresponds to the statistical significance of the estimate, and is denoted by asterisks (***).

The results are shown below as a table of statistical coefficients. Table A.1 displays the results across all municipalities, and A.2 is for the 118 municipalities with the greatest density of coffee harvesting.

A.1.5 Multilevel Brazil model

Next we extend the model to include "multilevel" effects. The multilevel model studies how the estimated coefficients vary across other characteristics of the municipalities. In this case, we consider how the effect of GDDs, KDDs, and average minimum temperature vary with elevation. Elevation is both an important determinant of coffee quality, and is a proxy for the variety of coffee grown: Brazil grows both Arabica and Robusta coffees, but does not report their production separately (until recent years).

The multilevel relationship is that:

$$\begin{aligned}
\log y_{it} &= \alpha_i + \gamma_i g_{it} + \kappa_i k_{it} + \mu_i m_{it} + \pi_i p_{it} + \psi_i p_{it}^2 + \epsilon_{it} \\
\gamma_i &= \gamma_0 + \beta_\gamma Elevation_i + \eta_{\gamma,i} \\
\kappa_i &= \kappa_0 + \beta_\kappa Elevation_i + \eta_{\kappa,i} \\
\mu_i &= \mu_0 + \beta_\mu Elevation_i + \eta_{\mu,i} \\
\pi_i &= \pi_0 + \beta_\pi Elevation_i + \eta_{\pi,i} \\
\psi_i &= \psi_0 + \beta_\psi Elevation_i + \eta_{\psi,i}
\end{aligned}$$

where the top line is the normal regression relationship, but with separate coefficients for each municipality i. The remaining lines relates all municipality coefficients together according to their varying elevations. The results are shown in table A.3 and in a graphical form in figure 3.10.

	Dependent variable:		
	Means	Log Yields	Harvested Hectares
		(1)	(2)
GDDs / 1000	2.946	0.152***	72.869
	(0.931)	(0.050)	(124.246)
KDDs / 1000	0.149	−2.806***	−2,197.369***
	(0.146)	(0.342)	(555.055)
Avg. Min.	0.944	−0.091***	−25.0
	(3.499)	(0.018)	(34.0)
Precip. (m)	1.421	0.347***	−9.587
	(0.719)	(0.028)	(64.092)
Precip.^{2} (m)	2.538	−0.366***	−8.520
	(2.439)	(0.036)	(84.618)
State cubic trends		Yes	Yes
Observations		43,165	43,185
R^2		0.383	0.655
Adjusted R^2		0.343	0.633
Residual Std. Error		0.535 (df = 40542)	4,300.446 (df = 40561)
Note:	*p<0.1; **p<0.05; ***p<0.01		

Table A.1: Estimates for statistical models relating growing degree-days, killing degree-days, average minimum temperature, and precipitation to the logarithm of yields, and to harvested area, for all municipalities. Stars (***) represent statistical significance levels, showing that most coefficients appear to have a relationship with production outputs.

	Dependent variable:	
	Log Yields	Harvested Hectares
	(1)	(2)
GDDs / 1000	0.475***	1,700.306*
	(0.109)	(976.997)
KDDs / 1000	−2.989**	−23,179.330***
	(1.423)	(8,681.404)
Avg. Min.	−0.183***	−290.009
	(0.0183)	(335.665)
Precip. (m)	0.441***	−1,168.520*
	(0.076)	(677.845)
Precip.^{2} (m)	−0.494***	1,978.722**
	(0.099)	(854.580)
Observations	3,181	3,181
R^2	0.320	0.485
Adjusted R^2	0.290	0.462
Residual Std. Error (df = 3043)	0.364	14,412.800
Note:		*p<0.1; **p<0.05; ***p<0.01

Table A.2: Estimates for statistical models relating growing degree-days, killing degree-days, average minimum temperature, and precipitation to the logarithm of yields, and to harvested area, for the top 118 municipalities by production density. Stars (***) represent statistical significance levels, showing that most coefficients appear to have a relationship with production outputs.

	Dependent variable:	
	Log Yields	Harvested Hectares
	(1)	(2)
GDDs / 1000	0.208***	40.303
	(0.051)	(130.508)
Elev. GDDs / 1000	0.001***	2.110***
	(0.0002)	(0.657)
KDDs / 1000	−6.106***	−4,600.562***
	(0.516)	(725.931)
Elev. KDDs / 1000	−0.016***	−17.054***
	(0.002)	(3.653)
Avg. Min.	−0.183***	−25.750
	(0.018)	(34.334)
Elev. Avg. Min.	−0.00000**	−0.183
	(0.00000)	(0.183)
Precip. (m)	0.358***	−32.650
	(0.030)	(76.846)
Elev. Precip. (m)	0.0001	−0.164
	(0.0001)	(0.285)
Precip.^{2} (m)	−0.391***	−10.825
	(0.039)	(98.941)
Elev. Precip.^{2} (m)	0.0001	0.648*
	(0.0001)	(0.390)
Observations	42,141	42,161
R^2	0.378	0.651
Adjusted R^2	0.338	0.628
Residual Std. Error	0.538 (df = 39582)	4,282.486 (df = 39601)
Note:		*p<0.1; **p<0.05; ***p<0.01

Table A.3: The effects of GDDs, KDDs, and average minimum, as each varies by elevation. While the estimates are not significant, they suggest increasing sensitivity to temperature in the form of both GDDs and KDDs as elevation increases. All municipalities in Brazil used.

A.1.6 Yield estimates under a warmer climate

We can apply the production model to weather produced from climate change. As a proxy for climate change, we estimate yields using historical weather data increased by 2°C. Precipitation values are left unchanged, since they show an unclear trend. This change produces several effects: it increases the number of GDDs benefiting yields, increases the number of KDDs harming yields, and increases average minimum temperature. The resulting balance between these three impacts is not evident *a priori*. The figure below shows the distribution for municipality yields across Brazil, from observed data, and under climate changed weather predictions.

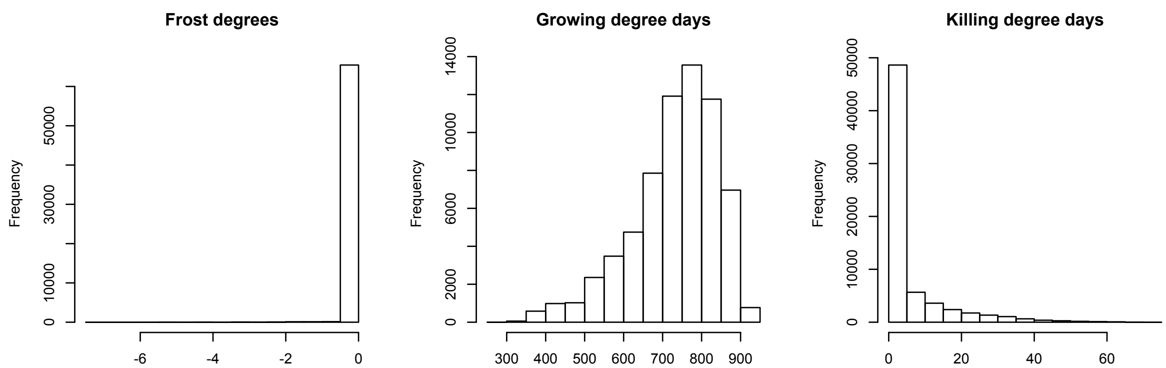

Figure A.5: Growing degree day histograms, after an increase of 2°C.

As shown in figure A.6, the observed yields show wide variation. The blue distribution is shifted to the left, eliminating some of the most spectacular yields and lowering the average yield. The average yield in the warmer experiment is about 80% of the original yields (see figure A.7).

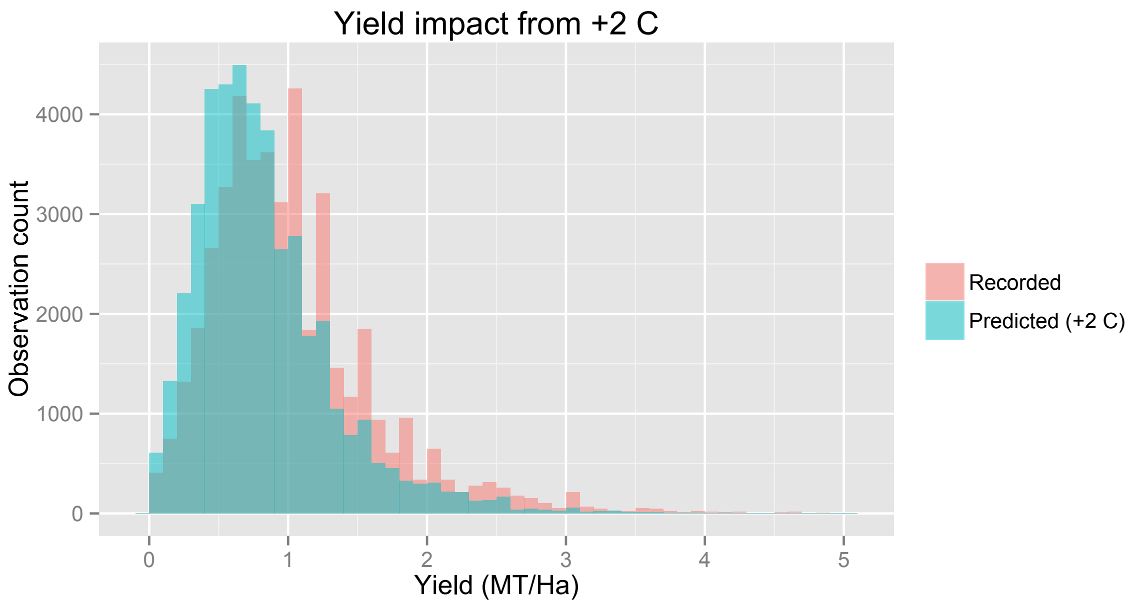

Figure A.6: Observed yields over the period from 1990 - 2015 are shown in red, and model predictions under weather with temperatures increased by 2°C shown in blue.

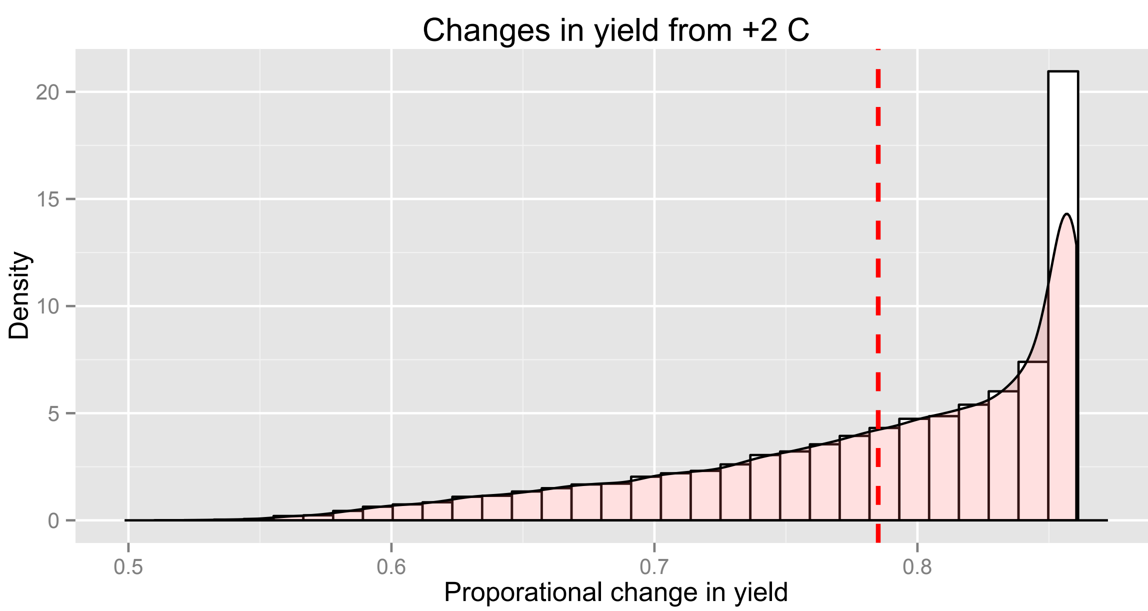

Figure A.7: Distribution of the proportional change in yields, with a mean yield 79% of historical yields.

A.2 Global production

In this section, we estimate the a model like the one for Brazil for all countries. Using the intra-year production estimates in the coffee database, we estimate the relationship between country yields and weather. We use the temperature span of 0°C to 33°C for growing-degree days, as estimated for Brazil.

The first estimate is exactly analogous to the Brazil estimate, in that a single coefficient is estimated across all countries for the global average effect of GDDs, KDDs, frost degrees, and quadratic precipitation. This is reported in table A.4 and shown schematically in figure A.8.

	Log Yield	Production
GDD / 1000	0.238^{**}	$1,710.548$
	(0.119)	$(5,917.907)$
KDD / 1000	-1.935	$-3,955.098$
	(1.786)	$(43,378.870)$
Frost Deg.	-0.005	284.772
	(0.008)	$(1,550.480)$
Year Precip	-3.454	$707,932.900$
	(12.928)	$(483,967.400)$
Year Precip^2	14.494	$-10,991,768.000$
	(135.355)	$(6,955,772.000)$
FE	$Region, variety$	$RegionVariety$
Trends	Y	Y
Errors	$Region$	$Region$
Observations	1,945	1,945
R^2	0.684	0.807
Adjusted R^2	0.676	0.802
Residual Std. Error (df = 1896)	0.441	33,325.380
Note:		*p<0.1; **p<0.05; ***p<0.01

Table A.4: Growing degree day model, pooled across all countries.

A.2.1 Hierarchical model framework

It is reasonable to expect different countries to have different effects from temperatures. We could estimate each country independently, and this would be an "unpooled" model. However, we also want the model for one country to inform, to an extent supported by the data, the model for another country. To capture this, we will construct a "hierarchical model", where each country's sensitivity to temperature will be drawn from a common distribution, simultaneously estimating each country's parameters and the distribution across all of them.

Furthermore, we allow varieties in different regions to operate differently, as supported by the data. For example, where plentiful data supports a higher optimal growing temperature for Robusta, the model should represent this. If very little data is available, the predicted response should by default conform to an average for that region and variety. Finally, we want to incorporate higher resolution data where it is available. The municipality data in Brazil informs the same common coefficients as the Brazil-specific country-level yield data.

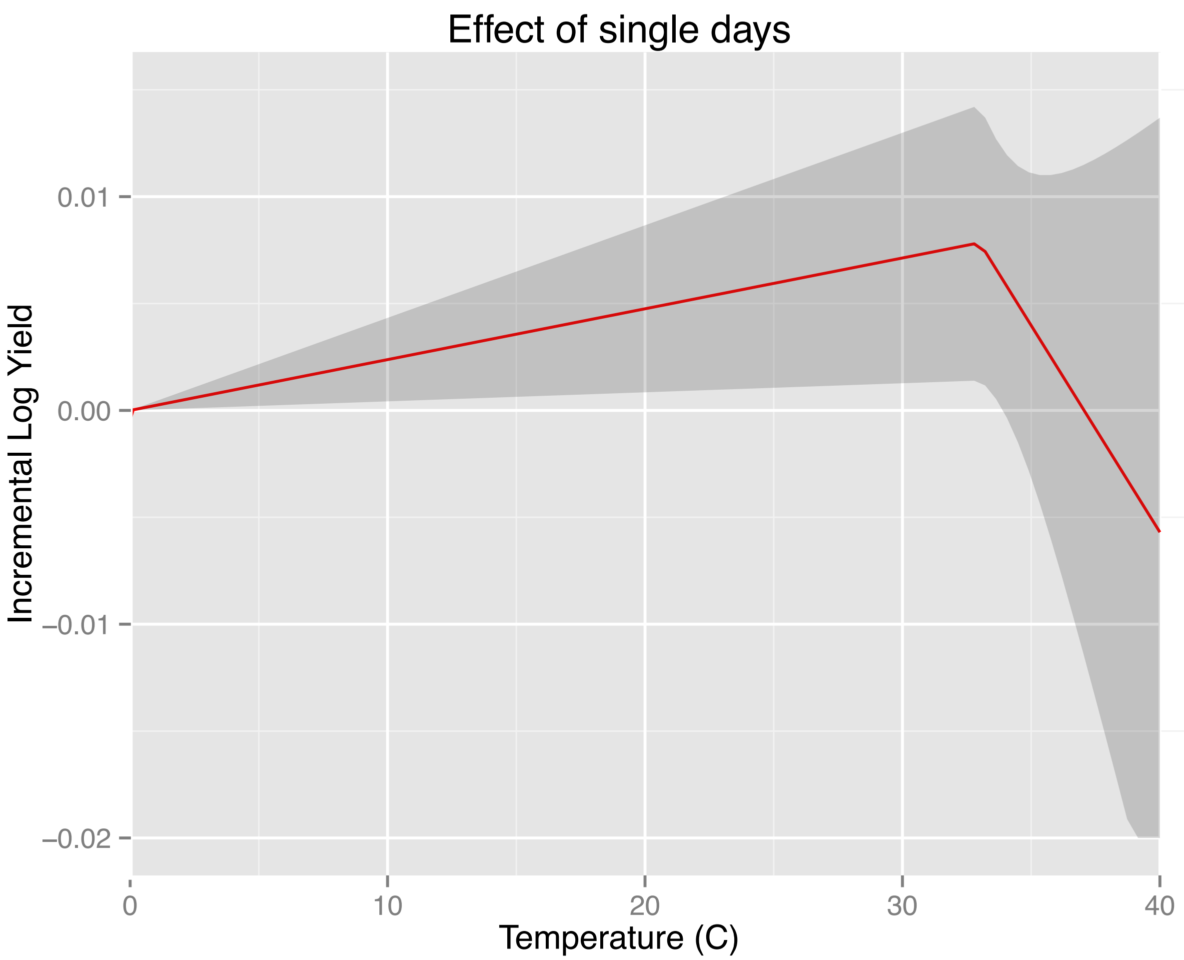

Figure A.8: Pooled model growing degree-day plot.

We have developed a technique for allowing this kind of data-driven multiple levels of aggregation and degrees of generalization, based on Bayesian Hierarchical Modeling (Gelman et al., 2014) and Inversion Theory (Menke, 2012). Under this technique, each country and sub-country region has its own parameters, but the parameters are further modeled as being related to each other.

Derivation of the hierarchical modeling system

Formally, we want to allow each variety in each country to have its own model, consisting of coefficients for growing degree-days, killing degree-days, average minimum temperature, and precipitation. The pooled model is as follows:

$$\log y_{it} = \alpha_i + \beta_v + \gamma g_{it} + \kappa k_{it} + \phi f_{it} + \pi p_{it} + \psi p_{it}^2 + \epsilon_{it}$$

while the partially pooled model starts with the unpooled relationship,

$$\log y_{ivt} = \alpha_i + \beta_v + \gamma_{iv} g_{it} + \kappa_{iv} k_{it} + \phi_{iv} f_{it} + \pi_{iv} p_{it} + \psi_{iv} p_{it}^2 + \epsilon_{ivt}$$

Consider the GDD coefficient for country i and variety v, γ_{iv}. To partial pool across countries for a given variety, this coefficient comes from a distribution of possible coefficient values, characterized by an unknown mean and standard deviation for that variety:

$$\gamma_{iv} \sim \mathcal{N}(\gamma_v, \tau_{\gamma_v})$$

Further, we partially pool these 'hyperparameters' as coming from a distribution across all varieties:

$$\gamma_v \sim \mathcal{N}(\gamma, \tau_\gamma)$$

We apply this for each parameter, $\gamma, \kappa, \phi, \pi, \psi$.

Estimating a partially-pooled model

Computationally, estimating this form of model can be very difficult. We construct an innovative framework for doing this using Ordinary Least-Squares matrix algebra.

The Gaussian relationships above, such as $\gamma_{iv} \sim \mathcal{N}(\gamma_v, \tau_{\gamma_v})$, are mathematically equivalent to the OLS-style relationship,

$$\gamma_{iv} = \gamma_v + \tau_{gamma_v} \eta \text{ with } \eta \sim \mathcal{N}(0, 1)$$

Under OLS, error terms are members of a Gaussian distribution, $\epsilon_i \sim \mathcal{N}(0, \sigma_e^2)$. We represent the hyper-model for the γ coefficient with the OLS-style relationships

$$\gamma_{iv} = \gamma_v + \epsilon_{iv}$$
$$\gamma_a = \gamma_c + \epsilon_a$$
$$\gamma_r = \gamma_c + \epsilon_r$$

and similarly for the other coefficients. It is then possible to rewrite these and the original unpooled relationship to take the same form, with the same complete set of coefficients:

$\log y_{ivt}$	$= \alpha_i$	$+\gamma_{iv} g_{it}$		$+\cdots$
$\log y_{ivt}$	$= \sum_j \alpha_j \mathbf{1}_{j=i}$	$+ \sum_{ju} \gamma_{ju} g_{it} \mathbf{1}_{ju=iv}$	$+\gamma_a 0 + \gamma_r 0 + \gamma_c 0$	$+\cdots$
0	$= \sum_j \alpha_j 0$	$+ \sum_{ju} \gamma_{ju} \mathbf{1}_{ju=1a}$	$-\gamma_a 1 - \gamma_r 0 - \gamma_c 0$	$+\cdots$
0	$= \sum_j \alpha_j 0$	$+ \sum_{ju} \gamma_{ju} \mathbf{1}_{ju=2a}$	$-\gamma_a 1 - \gamma_r 0 - \gamma_c 0$	$+\cdots$
		$\vdots$		
0	$= \sum_j \alpha_j 0$	$+ \sum_{ju} \gamma_{ju} \mathbf{1}_{ju=1r}$	$-\gamma_a 0 - \gamma_r 1 - \gamma_c 0$	$+\cdots$
		$\vdots$		
0	$= \sum_j \alpha_j 0$	$+ \sum_j u\gamma_{ju} \mathbf{1}_{ju=1c}$	$-\gamma_a 0 - \gamma_r 0 - \gamma_c 1$	$+\cdots$
		$\vdots$		
0	$= \sum_j \alpha_j 0$	$+ \sum_j u\gamma_{ju} 0$	$+\gamma_a 1 + \gamma_r 0 - \gamma_c 1$	$+\cdots$
0	$= \sum_j \alpha_j 0$	$+ \sum_j u\gamma_{ju} 0$	$+\gamma_a 0 + \gamma_r 1 - \gamma_c 1$	$+\cdots$

The first line is the start of the original model to be estimated. The second line re-writes this with more systematically, and in such a way that "constant" terms can be set to zero for fictional observations. The remaining lines are fictional observations added to estimate the entire model.

We have built this approach into a tool for the R statistical package which is available at `https://github.com/eicoffee/hierlm`.

Figure A.9 shows the effects of partial pooling at different levels. As the level of pooling increases, the range of country-specific values is brought closer together.

The results are shown in table A.5. Only the hyperparameter means are shown. Each statistically significant country coefficient is listed in Appendix A.6.4, and the remainder are in an online table at `http://eicoffee.net/`. The first column uses only observations at the country level. The second column places a prior on the Brazil coefficients, conforming to the Brazil municipality estimates above. These more-precise estimates then inform the global distribution for each coefficient, which in turn informs all of the countries, including Brazil.

A.2.2 Humidity

Humidity can have varying effects on coffee. The plant needs reasonably high levels of humidity during the flowering season to avoid floral atrophy, but humidity is also crucial to the development of coffee rust. For these reasons, the timing of high humidity levels appears to be particularly important. Here we see how Arabica coffee yields respond to a one-standard deviation increase in humidity during each particular month in the year leading up to harvest. Robusta appears to be less sensitive to humidity effects than Arabica.

Humidity data is from the NCEP CFSR. The reanalysis data is available at $1/12°$ resolution globally, which is then aggregated to the country-month level using weights from the coffee database. The values are reported as specific humidity at 6 hour intervals, which here is averaged over each month for the year prior to harvest.

Monthly effects of humidity are shown in figure A.10, and the table of coefficients is in Appendix A.6.2. The coefficients result from the following model:

$$log(y) = f(T) + \sum_{m=1}^{12} \beta_m q_m + h_c(t) + \alpha_c + \gamma_t + \epsilon_{ct}$$

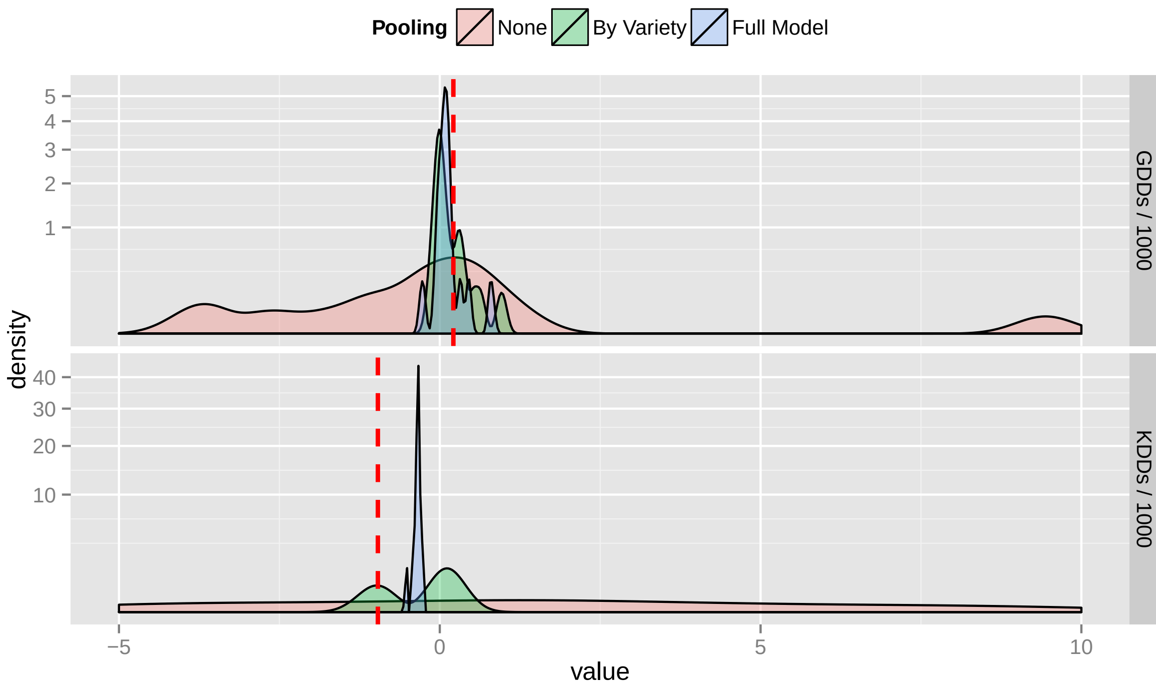

Figure A.9: Distribution across countries of values for the GDD and KDD coefficients for different levels of pooling.

	Dependent variable:	
	Countries only	
	(1)	(2)
GDDs / 1000 (Combined)	0.079	0.217**
	(0.123)	(0.095)
GDDs / 1000 (Arabica)	0.131	0.229**
	(0.112)	(0.103)
GDDs / 1000 (Robusta)	0.161	0.401***
	(0.152)	(0.133)
KDDs / 1000 (Combined)	−0.110	−1.801***
	(0.543)	(0.323)
KDDs / 1000 (Arabica)	−0.082	−1.731***
	(0.556)	(0.356)
KDDs / 1000 (Robusta)	−0.157	−1.766***
	(0.543)	(0.348)
Avg. Min. (Combined)	−0.077	−0.108
	(6.344)	(6.248)
Avg. Min. (Arabica)	−0.134	−0.152
	(7.147)	(7.164)
Avg. Min. (Robusta)	−0.114	−0.163
	(8.964)	(8.985)
Precip. (Combined)	−4.285	−2.124
	(5.792)	(2.390)
Precip. (Arabica)	−1.689	−0.156
	(6.058)	(3.254)
Precip. (Robusta)	−1.565	−0.279
	(5.971)	(3.403)
Precip.^{2}(Combined)	5.340	−5.530
	(82.317)	(28.605)
Precip.^{2}(Arabica)	21.749	11.218
	(79.174)	(37.825)
Precip.^{2}(Robusta)	12.794	0.264
	(88.198)	(42.271)
Observations	3,011	3,016
R^2	0.902	0.903
Adjusted R^2	0.885	0.886
Residual Std. Error	0.335 (df = 2561)	0.336 (df = 2566)
F Statistic	52.575*** (df = 450; 2561)	52.962*** (df = 450; 2566)
Note:		*p<0.1; **p<0.05; ***p<0.01

Table A.5: Hierarchical model results, for the mean of the global distribution of coefficients for each parameter and each variety.

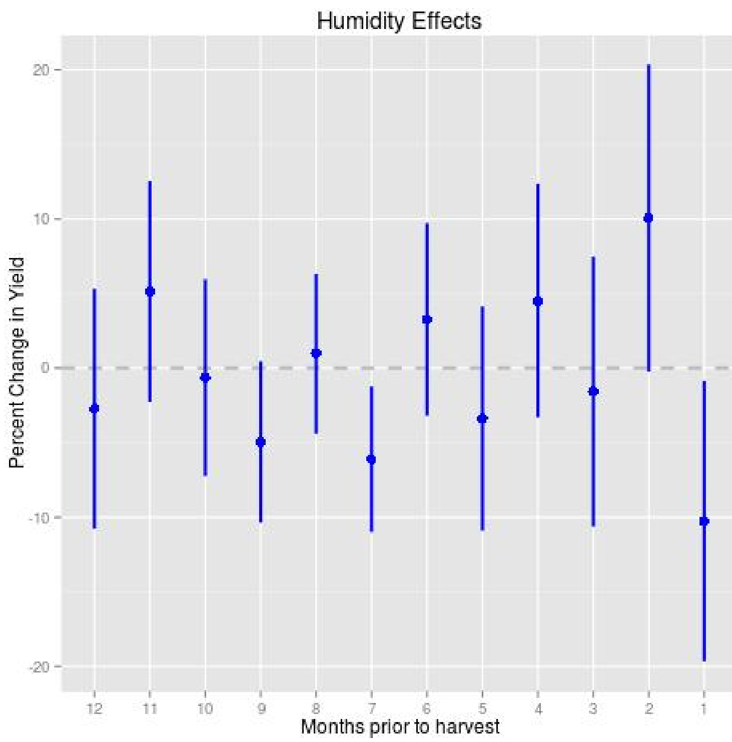

Figure A.10: Arabica humidity effects. Only the humidity one and seven months before harvest are significant at 95% confidence.

where $f(T)$ is a non-linear function of temperature, estimated using the number of days spent in 1-degree C temperature bins, $h_c(t)$ is a country-specific linear time trend, α_c and γ_t are country and year fixed-effects. Each β_m is the effect of specific humidity m months prior to the beginning of harvest on log yield.

A.2.3 Interpreting empirical model results

Climate change impacts coffee production through many different channels. Foremost, climate change reflects changes in temperature and patterns of precipitation– that is, changes in climate mean changes in weather. The models above estimate the relationship between changes in weather and changes in yields, and then extrapolate those changes to their responses under climate change.

There are important differences between unexpected weather shocks and prolonged climate changes. Coffee farming will find ways to adapt to repeated shocks of higher temperatures, and we hope our estimates provide an upper bound on the production impacts of climate change. However, the evidence for such adaptation is limited. Burke and Emerick (2012) study maize in the United States, and while there is a clear potential for adaptation to warmer temperatures, they find almost no evidence of it. The reasons for this empirical result are unclear.

The effects that we measure of temperature on yields cannot be unambiguously interpreted as the biological response to temperatures. Temperatures could be simultaneously affecting other species that then affect coffee. For example, the harmful affects of average minimum temperature could reflect a greater capacity for coffee rust or the coffee berry borer to proliferate in these warmer years. It could also reflect decreased activity on the part of farmers on hot days.

Our results should be taken as representing a holistic effect as it has occurred in the past. The extent to which it will occur in the future may be up to us.

A.3 Pest modeling results

A.3.1 A rust model

We make a number of simplifications to study the fungus outbreaks. First, we will only consider the fungus's interaction with the host plant, even though it has been found to utilize other plants for different stages of its growth cycle. Secondly, we assume that the only factors influencing it spread are temperature and the health of the host plant, thereby ignoring wind and rain impacts that are also known to be important (Ferreira and Boley, 1991). Similarly ignored are higher order effects from the application of fungicide, where fungicide can also impact some flora and fauna that regulate the fungus, leading to potentially unpredictable disruptions in the natural system.

The model is initialized as a two-dimensional grid of farm space, each grid cell having a certain probability of an appearance of a fungal outbreak. For each time-step, chosen to be one month after examining the reproductive cycle of coffee rust, the outbreak will begin to increase in size as a function of both its current size, the temperature, the amount of host plants available and spread to neighboring grid-cells. The temperature used in the model was obtained from surface temperature Reanalysis Data from the National Center of Atmospheric Research, spatially averaged over the area of Guatemala (without ocean cells) and temporally averaged to each month (NCAR, 2015). A time series of these average temperatures is shown in Figure A.11, left. Here, one can note a relatively consistent seasonal amplitude of ˜2.5°C around a mean of ˜22°C, with a slight upwards skew.

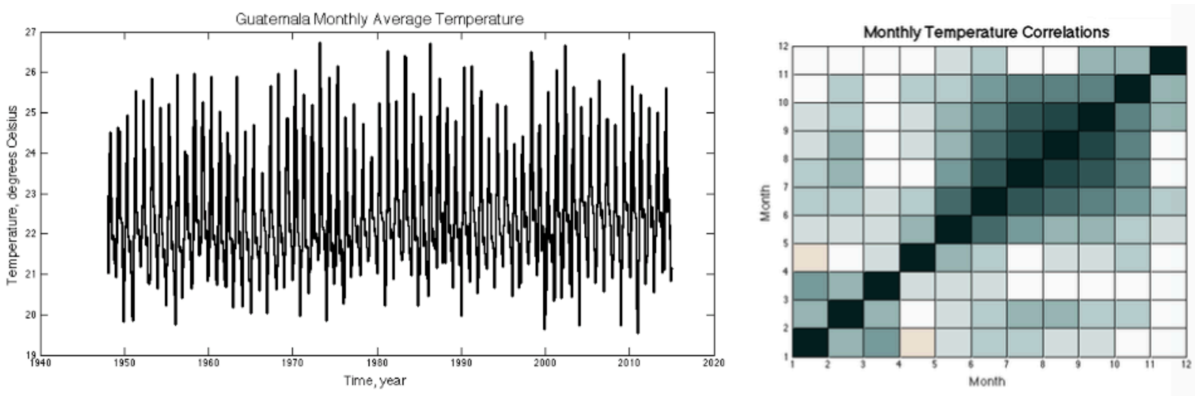

Figure A.11: **Left:** Timeseries of temperatures. **Right:** Autocorrelation of monthly temperature.

The high level of correlation between months requires that the temperature selected in each monthly time step depend on the temperature in the previous month (see figure A.11, right). In particular, the summer months are highly correlated, reaching correlations of 0.8 with the previous month in some cases. To account for this, the model is set up to draw a random season from the 67-year time series, employing a three month time series corresponding to an instance of summer, fall, winter or spring, depending on which is needed.

Our basic growth equation can be described by the following equation, with the basic assumption being that higher temperatures increase the growth rate of the fungus (at least at the temperatures seen in Guatemala).

$$N_{t+1} = N_t e^{r_i T_t / T_c}$$

where N is the population of a particular grid cell, r_i is the initial growth rate, T_t is the temperature at that specific time, T_c is the average temperature (over all months). Normally, the quantification of the growth rate is usually conducted with a consideration of both the daily maximum and daily minimum temperature (Magrath, 2014). However this was simplified for inclusion in our model.

When an additional population of fungus is created in subsequent time steps, it is distributed among the original and nearby grid-cells proportional to the health of the host plant in the new grid cell, the population of the source grid-cell and a multiplicative term similar to the prior growth equation. The maximum fungus population for each grid cell is 1, representing 100% infection of the host plant.

The disturbance of each grid-cell is also be subject to density-dependent pressure from predators, in this case the farmer spraying fungicide. Once a particular grid cell reaches a certain percentage of infection it is detected by the farmer. Detected, the population is decreased by a certain fraction, through the application of the fungicide. In addition, the fungus population will also decrease at a rate proportional to its current population and the relative health of the host species, independent of temperature.

$$N_{t+1} = N_t - N_t(F - 1)$$

where F is the percentage of available host plants for the fungus to grow on.

A.3.2 Experiments and results

To evaluate how temperature affects the spread of pests, experiments with three temperature scenarios were run. The first one uses each time step temperature (month) from the historical seasonal data for the region. The other two temperature scenarios considered global warming, one where the mean temperature was increased by 2°C and the other by 4°C. Those three temperature scenarios were run under two pest control conditions, the first one without any kind of pest control and the second one with a farmer's control by using fungicide that eliminated a fraction of the fungus when detected.

A.3.3 Historical temperature data without pest control

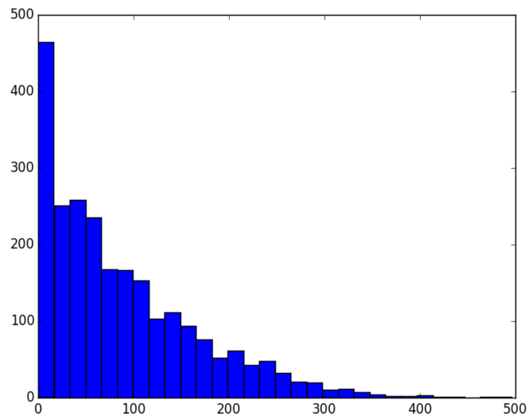

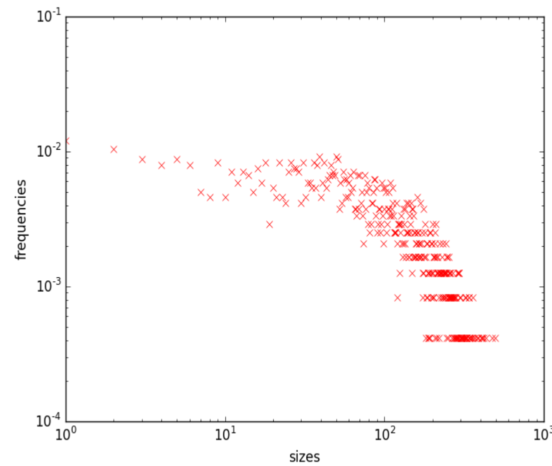

Figure A.12: Historical temperature data without pest control. **Left:** Histogram of outbreak sizes. **Right:** Log-Log Plot of outbreak sizes.

We set the 'infected threshold' to about 0.3, from the simple fact that we found several instances in which leaves about 1/3 covered in coffee rust where considered 'heavily infected'. In figure A.12 we have plotted the distribution of outbreak sizes, counting each heavily infected grid-cell at each time step. Please note that as we utilized a 30 by 30 grid cell, complete infection can be represented by a score of 900. Therefore, 490, the largest event, signifies that 54% of the crop is heavily infected.

The Log-Log result, though resembling a power law from 100 on, demonstrates some inconsistent behavior in smaller events. Indeed, in the histogram shelves can be observed where lower values have relatively the same probability. With no warming, the most common event is between 0 – 17, or between 0 and 2% of the crop (though this refers to a single month, not a harvest cycle). The largest event, at 54% of the crop is actually lower than the actual 70% loss in Guatemala in 2012, though there was not an indication of how this figure was calculated. Nevertheless, the model predicts scenarios where the fungus infects over 30% (300 sites) of the field.

Figure A.13 shows the time series of the previous figure in months. It is clear that the system can be entrenched within certain domain (i.e., large or small events) for many years. As the behavior between 1750 and 2000, a 21-year period, consistently shows some of the highest outbreaks, while still containing intervening low events. This is possibly because the growth of fungus and plant, which are both tied to temperature, sometimes became more synchronous. However, this cannot be determined outright, and thus for future study we might want to run for more time steps, to understand more fully the nature of this large- scale periodicity.

On smaller scales, it can also be noted that many of the largest events come directly after a period of relative calm, as the host plant has had a chance to regain health and provide much more nourishment to the attacking fungus. This small scale rebound, can be seen with more detail. Though the rapid up and

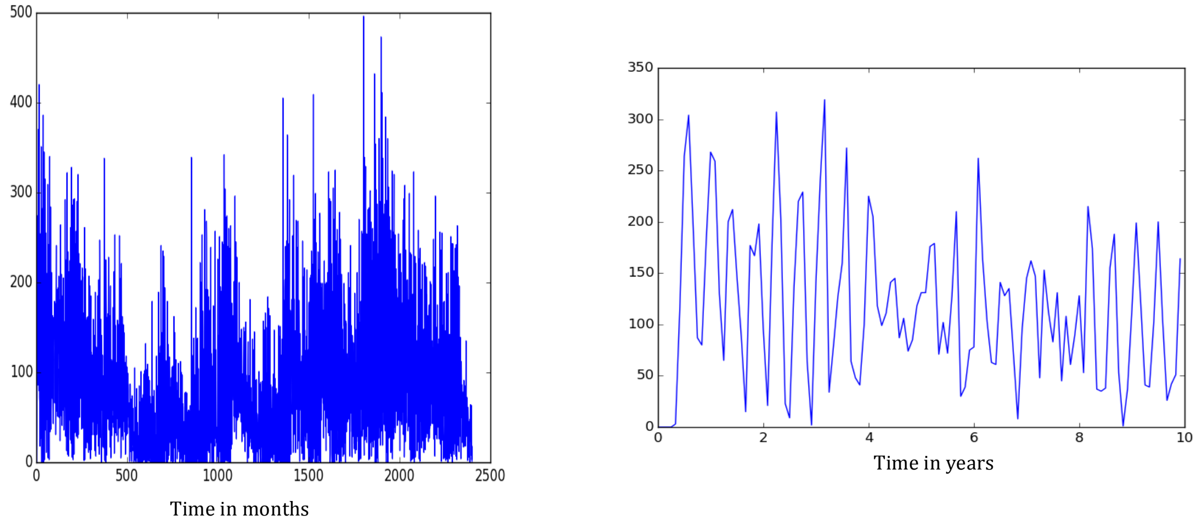

Figure A.13: **Left:** Time series of outbreak sizes by month. **Right:** Time series of outbreak sizes by year.

down movement can be shown on a scale of a few months, there always seems to be a larger periodicity on the scale of a few years; however, the randomness in the system makes it difficult to conclude anything concrete.

A.3.4 Historical temperature data with pest control

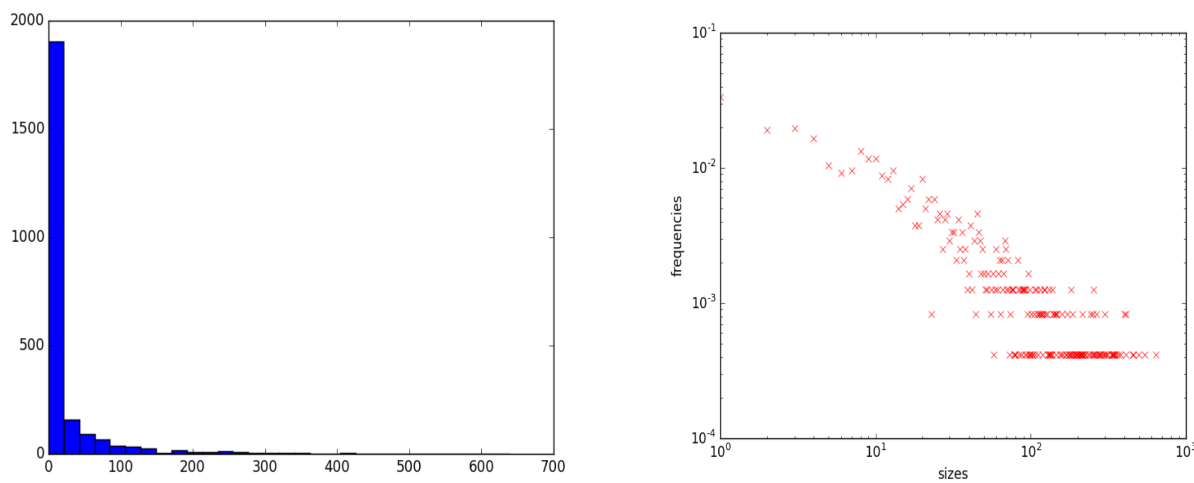

Figure A.14: Historical temperature data with pest control. **Left:** Histogram of outbreak sizes. **Right:** Log-Log Plot of outbreak sizes.

Next, we implemented the farmer control, where obvious pest presence would immediately be sprayed with a fungicide and reduced to a fraction of its value in the next month. This fungicide and the necessary training to use it correctly may currently be absent within the poorer farms in the area. Thus, this allows us to see how implementation might change the situation in the future. In Figure A.14, the distribution has a much smaller mean and median than the without the pest control measures. We note a stronger power law relationship, though like the last iteration, it is slightly concave down. This suggests that moderate events are marginally more likely than they would have been. However, the histogram might be slightly skewed by a larger prevalence of zero events. Additionally, one can note a larger spread than the previous model run for lower probability events.

Unexpectedly, the largest event, 643, signifying about 77% of the crop, is much higher than the previous iteration. This suggests that though fungicide keeps the fungus levels low for the average month, the healthy status of the host plant will make it so the correct temperature conditions or perturbation can cause a huge event, even before the farmer can react (here at a 1 month lag). This is very reminiscent of real world pest control experiences, where application can have unforeseen consequences, such as diminishing the population of a pest predator, and thus upsetting the natural structure of the system and allowing a pest to flourish later (Modern Farmer, 2014). However, catastrophic losses at a few points do not offset the considerable gains shown across the histogram.

Nevertheless, this line of thinking is further corroborated by figure A.15, where decent periods of little activity are punctuated by huge events, a common feature in nonlinear spatial systems. However, when zoomed in to a period of 10 years, one can note the similarity between the control and non- control scenarios, where the lower bound in the control situation (within inter-month cycles) is replaced with 0.

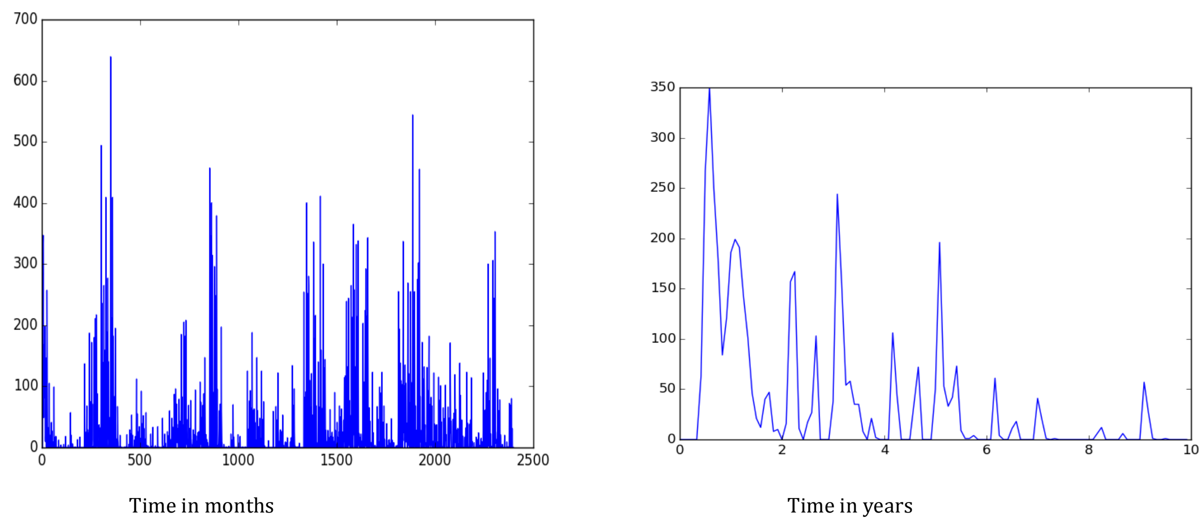

Figure A.15: **Left:** Time series of outbreak sizes by month. **Right:** Time series of outbreak sizes by year.

A.3.5 2°C global warming temperature data without pest control

For the next run, we linearly increased the temperature of each month by 2 degrees, in order to represent possible regional warming over the next century. Increasing the temperatures to above normal, and thus often increasing the ability of the fungus to reproduce, causes the histogram of outbreak sizes to shift rightward. The log-log plot, while showing linear behavior for the right tail of the distribution, mimics this change. In an average month 10% of the crop is considered heavily infected, with the tail hitting about 75% of the crop as a maximum value. The time series (Figure A.17) shows very few events with absolutely no fungus though the behavior in terms of both large-scale and small-scale periodicities does not seem to be drastically different.

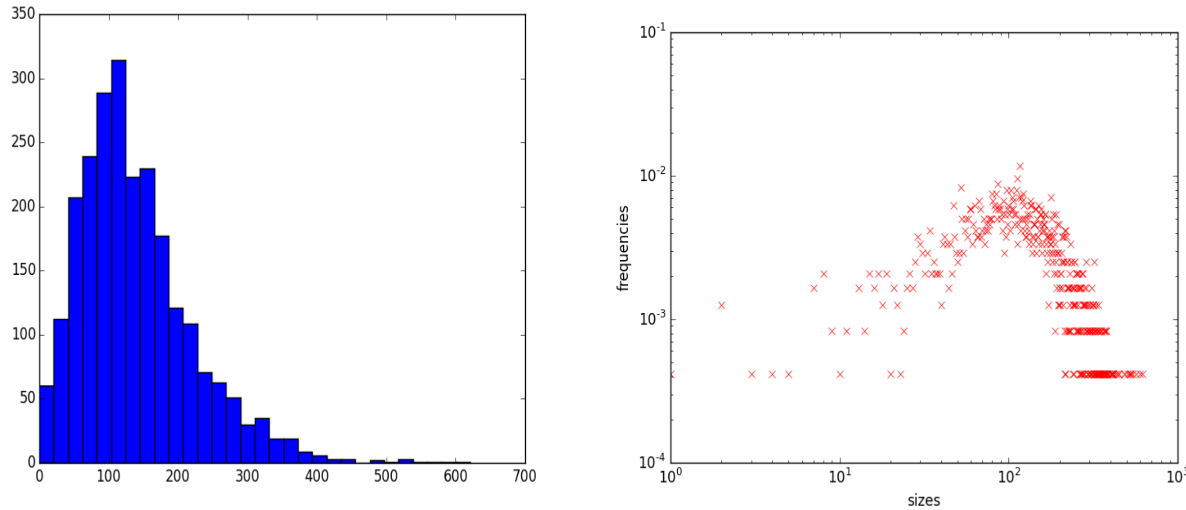

Figure A.16: 2°C global warming temperature data without pest control. **Left:** Histogram of outbreak sizes. **Right:** Log-Log Plot of outbreak sizes.

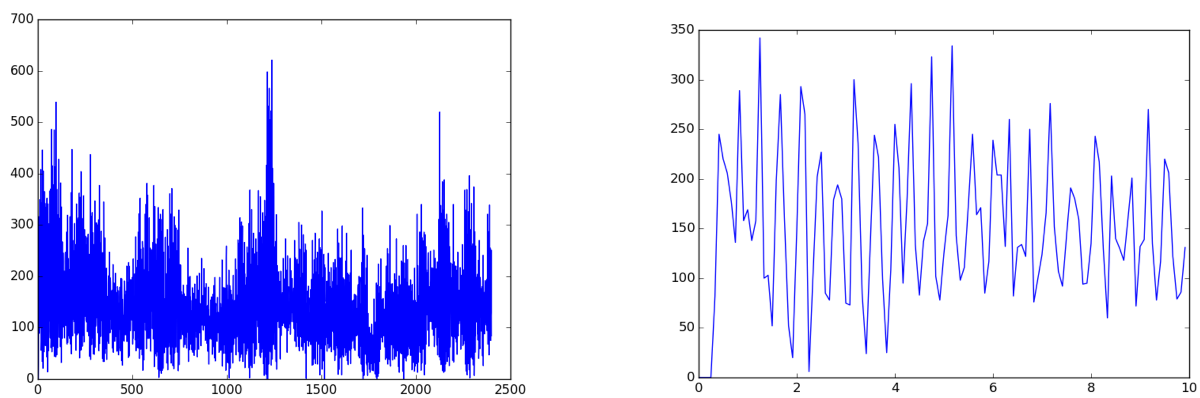

Figure A.17: **Left:** Time series of outbreak sizes by month. **Right:** Time series of outbreak sizes by year.

A.3.6 2°C global warming temperature data with pest control

The addition of pest controls to the warmed scenario has a similar effect as we have noted in the previous iteration. The distribution begins to resemble a power law, however here with a slightly thinner tail. Nevertheless, even in the warmed environment the measures do a reasonable job of controlling the pests, with levels far below the untreated, cooler scenario. The Log-log plot, is however slightly more concave than the previous scenario with pest control.

Results for a warming of 4°C are included in Appendix A.5.4. Under these conditions and without

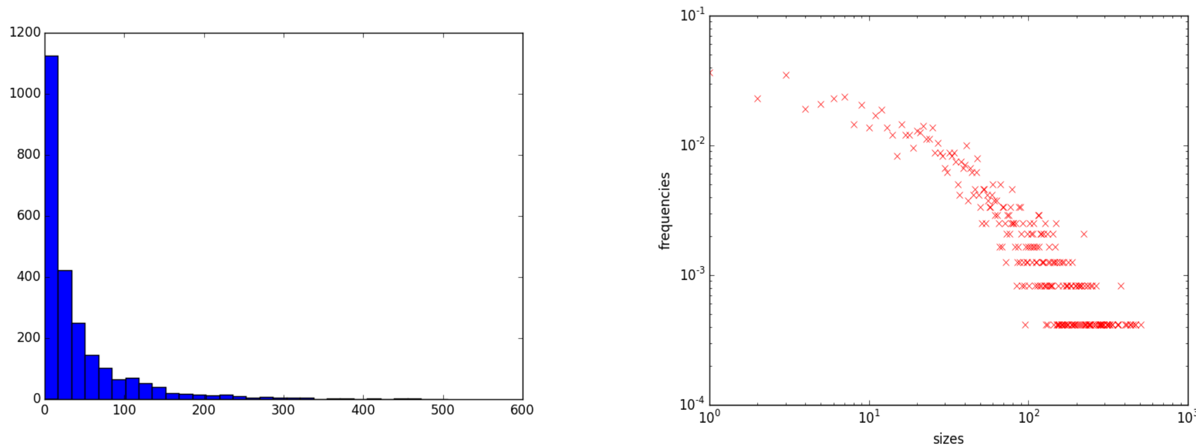

Figure A.18: 2°C global warming temperature data with pest control. **Left:** Histogram of outbreak sizes. **Right:** Log-Log Plot of outbreak sizes.

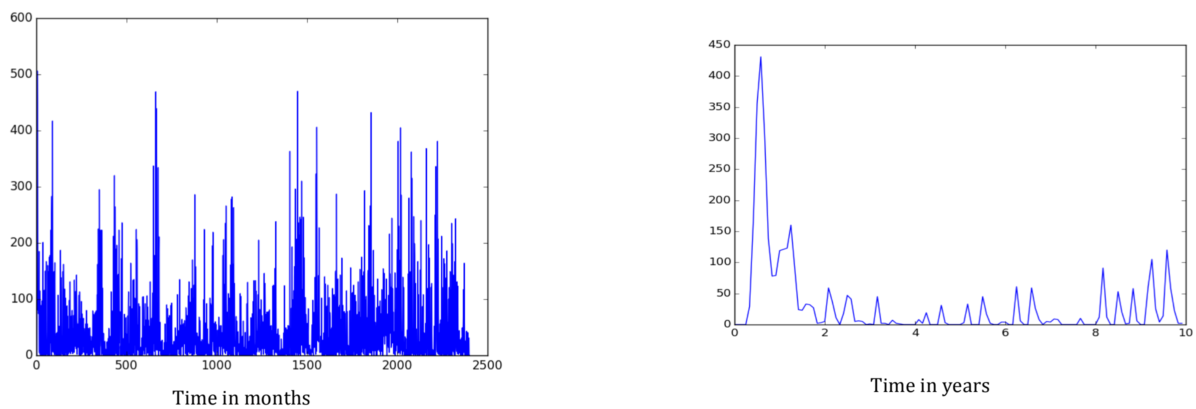

Figure A.19: **Left:** Time series of outbreak sizes by month. **Right:** Time series of outbreak sizes by year.

pesticide, the health of the crop is so poor that it cannot maintain a full outbreak. Even with pesticide, it is impossible to full contain the disease.

A.3.7 Discussion

Throughout the drafting and modeling process, we made many other simplifications. We ignored rain and wind as possible spreading agents, instead opting for a random approach. We chose significant parameters such as our time step through very simplified observations of the fungus. We ignored the vegetation cycle (as Guatemala has a very defined wet and dry season which must affect plant growth), though this might be somewhat mitigated by the fact that we tied temperature to the growth of the host plant. We also made considerable simplifying assumptions about the qualities of fungicide application and fungus growth and spread.

Nevertheless, we believe that our results in the change of distribution are representative of what might occur in the real world, given a particular coffee field. We have noted that warming induces a rightward shift in event distribution. The subsequent health decline of the plants may inhibit huge shocks to the system, as the conditions are not ideal for a full fungus takeover. Pest control, while curtailing the infection of an average month can lead to thicker tails and larger rare events. This is possibly because plants are kept at a healthier level, an ideal condition for a quick fungus take over and a drawback of an artificially controlled environment. Additionally, pest control appears to be efficient at compensating for the increased fungus growth rates caused by warming, as even in the 4°C warmer environment, it is able to bring the distribution back to the less disastrous approximate power law, albeit with a mode higher than zero. In the future, under the extreme scenario, it is very possible that some sort of artificial control will be necessary to continue to grow coffee in this region. This will possibly bring more complications and unpredictable dynamics that we cannot comment on with such a simple model.

A.4 Suitability analysis details

Given any environmental condition, we can use Bayes rule to provide a empirical estimate of suitability. We write Bayes rule as an odds ratio:

$$\frac{p(\text{coffee} = 1|\vec{x})}{p(\text{coffee} = 1)} = \frac{p(\vec{x}|\text{coffee} = 1)}{p(\vec{x})}$$

The left-hand-side describes the ratio of the probability of coffee in a region given the observed conditions, to the probability of coffee generally. If this is greater than 1, the area is more suitable than the average location.

To calculate the coffee probability, the right-hand-side describes a ratio between the distribution of a property across harvested areas, and the distribution of that property across the entire region. As conditioning data, we use soil properties, climatic properties, elevation, and latitude.

Climatic and soil properties are not mutually independent, complicating our ability to calculate this ratio given the large number of properties we have available. We use the statistical "copulas" technique to disentangle the marginal distributions of each property from their dependence structure (Nelsen, 2013).

We use a Gaussian copula, which captures the correlation between the various properties.

To incorporate a new property, we determine its unweighted distribution across the entire region from 30°N to 30°S. Then we create a weighted distribution, with properties from the region weighted by harvested area. Finally, we calculate Spearman's rho, between the new property and all existing properties, to represent the dependence structure.[1]

Then, to determine $p(\vec{x})$ and $p(\vec{x}|\text{coffee} = 1)$ for a given location, we reverse the normal copula process. In this case, we determine the span in $\vec{u}$-space (rank space) that a small region of $\vec{x}$-space represents ($\vec{x} \pm \vec{\Delta x}$), using each marginal distribution and the probability integral transform. If there is very little mass in the marginal distribution in the region of x_i, the corresponding Δu_i will be small. Then we evaluate

$$\int_{\vec{\Delta u}} c_R^{\text{Gauss}}$$

Above, c_R^{Gauss} is the Gaussian copula, which can be written as,

$$c_R^{\text{Gauss}}(u) = \frac{1}{\sqrt{\det R}} \exp\left(-\frac{1}{2} \begin{pmatrix} \Phi^{-1}(u_1) \\ \vdots \\ \Phi^{-1}(u_d) \end{pmatrix}^T \cdot \left(R^{-1} - \mathbf{I}\right) \cdot \begin{pmatrix} \Phi^{-1}(u_1) \\ \vdots \\ \Phi^{-1}(u_d) \end{pmatrix} \right)$$

where Φ^{-1} is the inverse cumulative distribution function of a standard normal (Arbenz, 2013), and R is the matrix of correlations, equal to $2 \sin \rho_{ij} \frac{\pi}{6}$ for each Spearman's rho, ρ_{ij}, between property i and property j.[2]

A.4.1 Baseline Bayesian odds map

The result of the Bayesian odds procedure for current coffee suitability is shown in figure A.20. Dark green regions (high suitability) are rare, unlike the analyses by GAEZ and Bunn et al.. While they typically match areas of actual coffee growth (in Brazil, Colombia, and Central America), there are several places where there are large mismatches (in North Africa and Western India). While this provides a high resolution and data-driven map, it cannot stand alone.

A.4.2 Use of Copulas in the Bayesian odds measure

We use a Gaussian copula, which captures the correlation between the various properties.

To incorporate a new property, we determine its unweighted distribution across the entire region from 30°N to 30°S. Then we create a weighted distribution, with properties from the region weighted by harvested area. Finally, we calculate Spearman's rho, between the new property and all existing properties, to represent the dependence structure.[3]

Then, to determine $p(\vec{x})$ and $p(\vec{x}|\text{coffee} = 1)$ for a given location, we reverse the normal copula process. In this case, we determine the span in $\vec{u}$-space (rank space) that a small region of $\vec{x}$-space represents ($\vec{x} \pm \vec{\Delta x}$), using each marginal distribution and the probability integral transform. If there is very little

[1] Either Spearman's rho and Kendall's tau can be used in this process. We use Spearman's rho because it has a more linear relationship with the Gaussian copula's correlation matrix.

[2] See `http://www.mathworks.com/help/stats/copulas-generate-correlated-samples.html#buqq6py`.

[3] Either Spearman's rho and Kendall's tau can be used in this process. We use Spearman's rho because it has a more linear relationship with the Gaussian copula's correlation matrix.

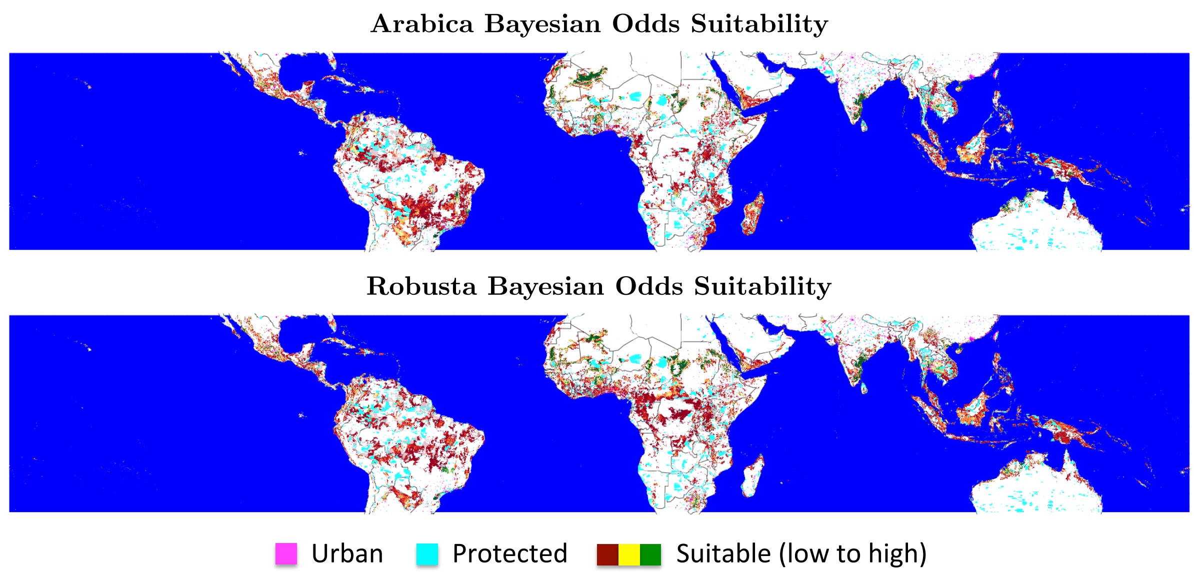

Figure A.20: Suitability for Arabica coffee (top) and Robusta coffee (bottom). Colors range from red (slight suitability odds) to yellow to green (very strong suitability odds). The map also shows protected areas (cyan), urban areas (purple), and managed areas (faded).

mass in the marginal distribution in the region of x_i, the corresponding Δu_i will be small. Then we evaluate

$$\int_{\vec{\Delta u}} c_R^{\text{Gauss}}$$

Above, c_R^{Gauss} is the Gaussian copula, which can be written as,

$$c_R^{\text{Gauss}}(u) = \frac{1}{\sqrt{\det R}} \exp\left(-\frac{1}{2} \begin{pmatrix} \Phi^{-1}(u_1) \\ \vdots \\ \Phi^{-1}(u_d) \end{pmatrix}^T \cdot \left(R^{-1} - \mathbf{I}\right) \cdot \begin{pmatrix} \Phi^{-1}(u_1) \\ \vdots \\ \Phi^{-1}(u_d) \end{pmatrix} \right)$$

where Φ^{-1} is the inverse cumulative distribution function of a standard normal (Arbenz, 2013), and R is the matrix of correlations, equal to $2 \sin \rho_{ij} \frac{\pi}{6}$ for each Spearman's rho, ρ_{ij}, between property i and property j.[4]

A.4.3 Incorporating biological process

The Global Agro-ecological Zones (GAEZ) project uses biologically-motivated calculations to estimate suitability. GAEZ suitability indexes are normalized to be between 0 and 100, so a comparison between the Bayesian results and GAEZ requires constructing a common scale. We do this by comparing the results in ranks, rather than levels. In other words, we look for differences in the percentile quality of land (see figure A.21).

Some areas match closely (southern Brazil, Colombia, and parts of Indonesia), while GAEZ attributes suitability to large regions not supported by the Bayesian methods, such as Amazonian and Congo

[4] See `http://www.mathworks.com/help/stats/copulas-generate-correlated-samples.html#buqq6py`.

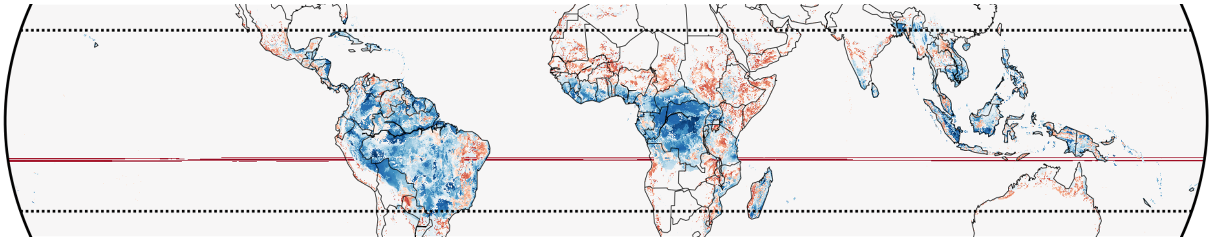

Figure A.21: Comparison between GAEZ and the Bayesian odds technique for Arabica. Blue regions have greater quantile suitability in GAEZ than for the Bayesian odds approach; red regions show lower suitability in GAEZ, and white regions agree.

rainforest. This indicates a complementarity between GAEZ and the Bayesian odds approach, where GAEZ provides physical constraints while the Bayesian approach forces the results to match observed data.

Computing a combined metric

We combine the two approaches by mapping the following:

$$s(x, y) = p(x, y)\frac{b(x, y)}{1 + b(x, y)}$$

This attributes zero suitability where either approach specifies it, and otherwise allows them to reinforce each other. The results are shown in figure 4.4. It also normalizes the result to match GAEZ 0 - 100 scale.

The combined result shows high suitability in many fewer places, scattered based on where both techniques support their suitability. This provides a stronger basis for identifying the shifts in suitability, conservatively matched to only the highly suitable regions.

A.4.4 Suitability comparison with Bunn et al.

A recent paper by Bunn et al. (2015) uses data mining methods, such as MaxEnt, on coffee-growing presence at 42 000 individual farms to estimate suitability. Above, we build upon this work by incorporating the coffee presence map from their paper into our database. We also use the same collection of 19 bioclimactic variables, on top of which we add soil variables, and we extend the study of future uncertainty by using 12 additional global climate model results. While we believe that our approach, based on Bayesian updating of presence and absence information, is better grounded theoretically and less arbitrary than their MaxEnt and other data-mining techniques, Bunn et al. provides an important comparison for our results.

Figure A.22 displays a comparison of current suitability between the two methods. Most of the world in this figure is colored yellow, where both techniques specify very little suitability. Some areas, such as Brazil and Kenya, show differing patterns between the two approaches. In these cases, our approach produces a result that more closely matches the patterns in the coffee database.

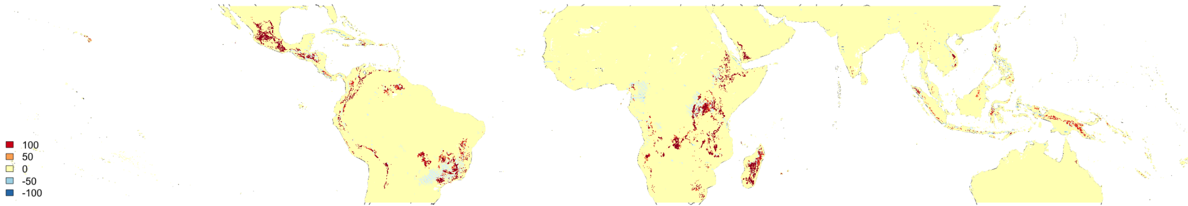

Figure A.22: Comparison between Bunn et al. (2015) and the combined Bayesian-GAEZ approach. Blue areas have higher suitability in the baseline map produce by Bunn et al., while red is higher using our approach.

A.4.5 Changes in suitability by country for GAEZ

Country	Baseline (1000 Ha)	A2 2050 (1000 Ha)	Change (1000 Ha)	%
Angola	63738	40508	-23230	(-36%)
Argentina	9047	12173	+3126	(+35%)
Australia	13870	7593	-6277	(-45%)
Bahamas	3487	1821	-1666	(-48%)
Bangladesh	11677	298	-11379	(-97%)
Belize	2652	1642	-1010	(-38%)
Benin	4129	0	-4129	(-100%)
Bhutan	0	1216	+1216	(new)
Bolivia	76211	7791	-68420	(-90%)
Brazil	785103	235221	-549882	(-70%)
Cambodia	15559	1084	-14475	(-93%)
Cameroon	39370	34157	-5213	(-13%)
Central African Republic	56584	33494	-23090	(-41%)
Chad	861	17	-844	(-98%)
China	21597	30291	+8694	(+40%)
Colombia	100541	27018	-73523	(-73%)
Congo, Dem. Rep.	230509	199389	-31120	(-14%)
Congo, Rep.	34477	33530	-947	(-3%)
Costa Rica	5659	2653	-3006	(-53%)
Cote d'Ivoire	30012	5965	-24047	(-80%)
Cuba	14109	5786	-8323	(-59%)
Dominican Republic	5481	3381	-2100	(-38%)
Ecuador	20067	16909	-3158	(-16%)
El Salvador	2331	1369	-962	(-41%)
Equatorial Guinea	2933	2675	-258	(-9%)
Ethiopia	39590	41674	+2084	(+5%)
French Guiana	8592	4058	-4534	(-53%)
Gabon	27151	26178	-973	(-4%)
Ghana	13116	770	-12346	(-94%)
Guatemala	10667	6718	-3949	(-37%)
Guinea	18599	8595	-10004	(-54%)
Guinea-Bissau	1348	0	-1348	(-100%)
Guyana	21534	2672	-18862	(-88%)
Haiti	3382	754	-2628	(-78%)
Honduras	11616	7657	-3959	(-34%)

Country	Baseline (1000 Ha)	A2 2050 (1000 Ha)	Change (1000 Ha)	%
India	34293	18979	-15314	(-45%)
Indonesia	213246	104505	-108741	(-51%)
Jamaica	1176	0	-1176	(-100%)
Japan	164	39	-125	(-76%)
Kenya	20565	17816	-2749	(-13%)
Lao PDR	22976	12597	-10379	(-45%)
Lesotho	0	268	+268	(new)
Liberia	9908	9293	-615	(-6%)
Madagascar	53116	48359	-4757	(-9%)
Malawi	8475	4583	-3892	(-46%)
Malaysia	35720	14051	-21669	(-61%)
Mexico	54345	34878	-19467	(-36%)
Mozambique	62931	35267	-27664	(-44%)
Myanmar	47616	31854	-15762	(-33%)
Nepal	0	3312	+3312	(new)
Nicaragua	12968	7975	-4993	(-39%)
Nigeria	28792	1717	-27075	(-94%)
Panama	8959	4500	-4459	(-50%)
Papua New Guinea	51723	25520	-26203	(-51%)
Paraguay	29591	10163	-19428	(-66%)
Peru	74724	24262	-50462	(-68%)
Philippines	38768	15724	-23044	(-59%)
Rwanda	2296	2486	+190	(+8%)
Senegal	411	0	-411	(-100%)
Sierra Leone	7631	2006	-5625	(-74%)
Solomon Islands	5322	2921	-2401	(-45%)
South Africa	6796	14140	+7344	(+108%)
South Sudan	24980	3986	-20994	(-84%)
Sri Lanka	6507	1144	-5363	(-82%)
Sudan	272	0	-272	(-100%)
Suriname	14810	447	-14363	(-97%)
Swaziland	1516	708	-808	(-53%)
Tanzania UR	82305	61876	-20429	(-25%)
Thailand	34606	5546	-29060	(-84%)
Timor-Leste	1803	1242	-561	(-31%)
Togo	4082	409	-3673	(-90%)
Uganda	21578	21028	-550	(-3%)
United States of America	3960	7218	+3258	(+82%)
Venezuela	83978	12959	-71019	(-85%)
Viet Nam	27213	11551	-15662	(-58%)
Zambia	56972	39304	-17668	(-31%)
Zimbabwe	3194	992	-2202	(-69%)

A.4.6 Suitability condition distributions

Soils and nutrients

Coffee is very sensitive to soil conditions. The Harmonized World Soil Database (FAO/IIASA/ISRIC/ISSCAS/JRC, 2012) contains six soil components for both the topsoil and subsoil, to study this.

The comparison between the distribution across the entire tropics, and across coffee regions for Arabica farms is shown in figures A.23 and A.24.

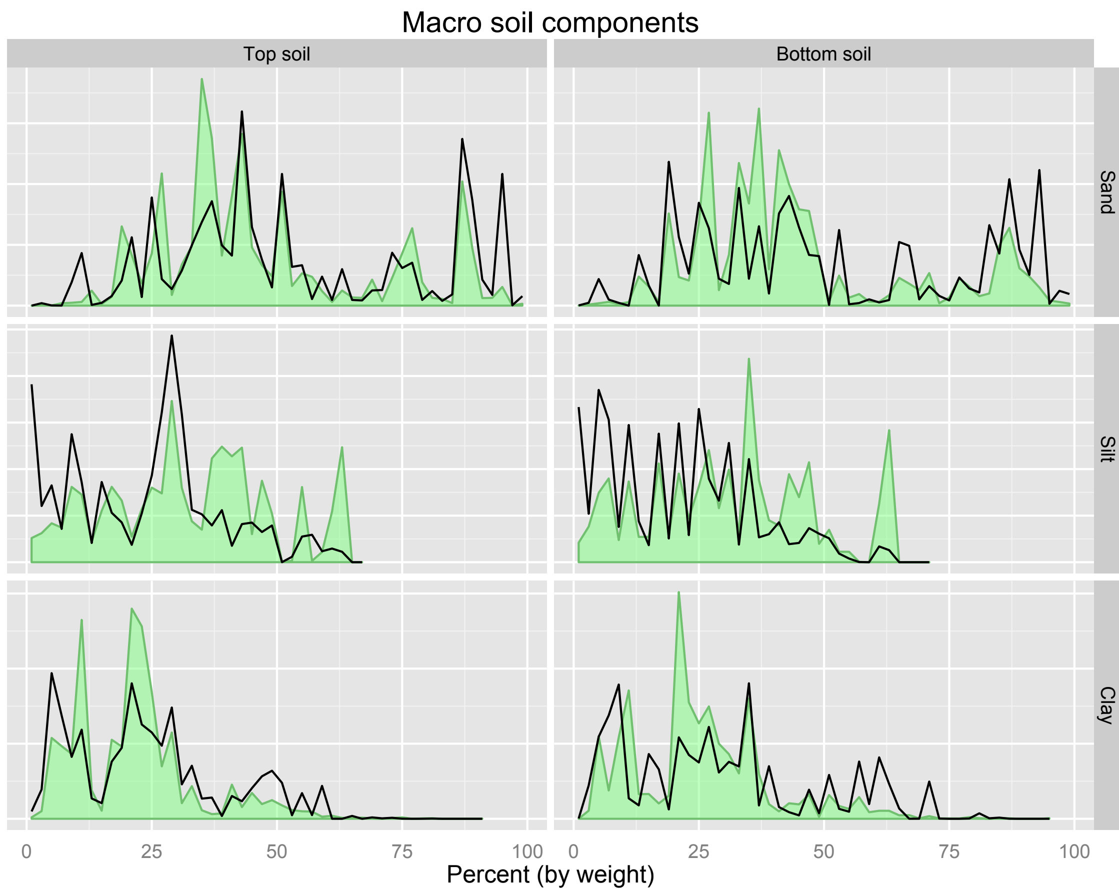

Figure A.23: Comparison of distributions of texture soil components. The faded area shows the distribution of soils generally between 30°N and 30°S. The line shows the distribution of soils, weighted by coffee planting densities.

From the first figure, coffee is more common in soils that have a larger share of sand and smaller share of silt than the norm. Clay also shows effects where coffee is less frequently grown in regions with intermediate quantities of clay. From the second figure, it appears that coffee is suitable in regions with intermediate quantities of calcium carbonate and low levels of gypsum.

Elevation

The distributional analysis shows a very wide range of elevations, possibly reflecting inaccuracies in the maps of Arabica and Robusta cultivation. See figure A.25.

Arabica shows clear diminished presence at low elevations (below 550 m) and increased presence at all higher elevations. However, there is still probability mass below 550 m. Similarly, Robusta has extra presence of elevations below 50 m, but still has some elevated presence between 550 m and 1200 m.

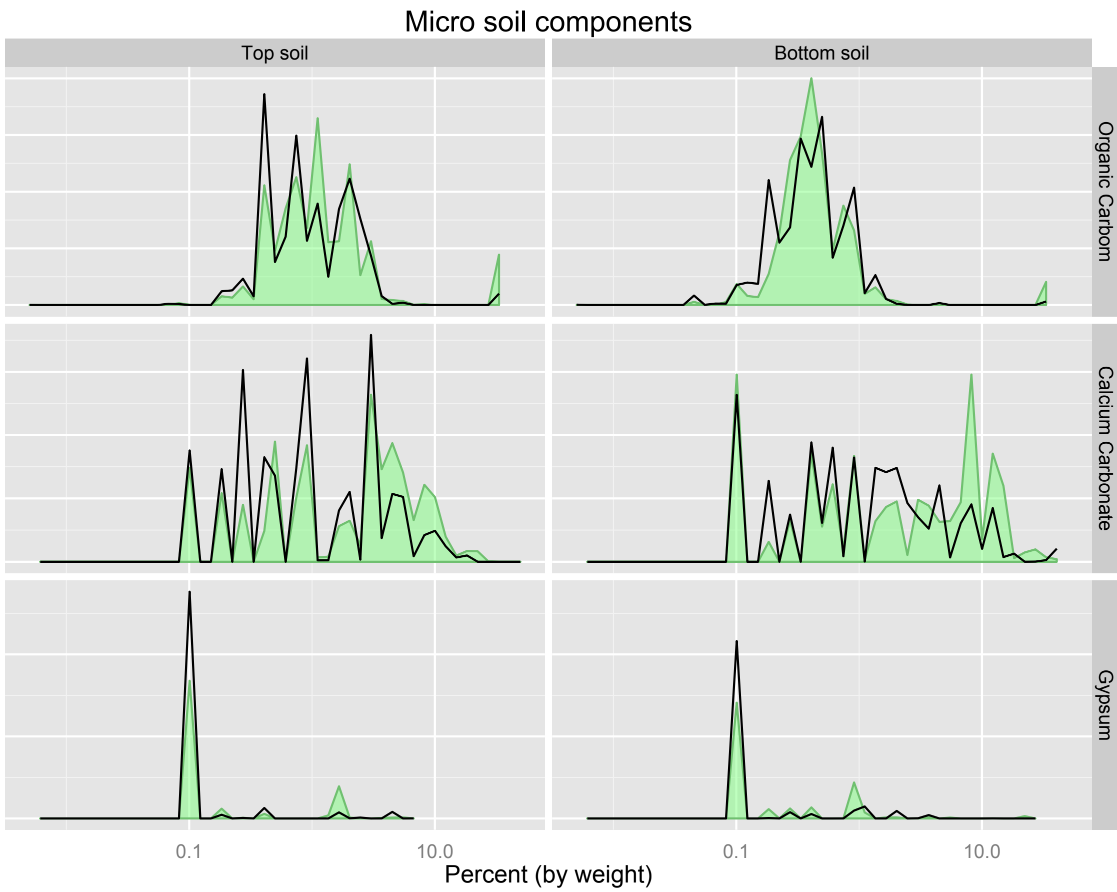

Figure A.24: Comparison of distributions of trace soil components. The faded area shows the distribution of soils generally between 30°N and 30°S. The line shows the distribution of soils, weighted by coffee planting densities.

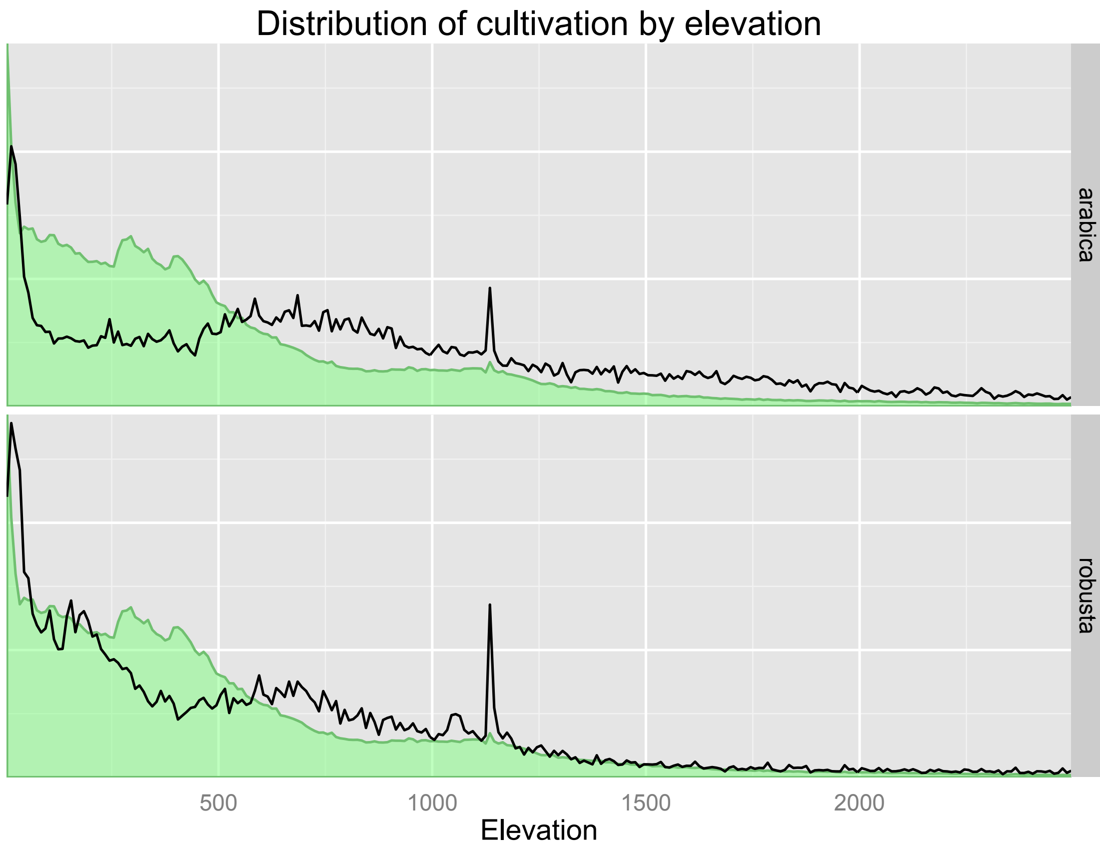

Figure A.25: Distributions of elevation for Arabica and Robusta (lines) and for the tropics in general (green).

The most important result of elevation for coffee cultivation is the temperatures it produces. Hawaii, for example, has excellent coffee-growing temperatures from sea level to 610m, and Arabica coffee is grown across this entire range (Thurston et al., 2013). However, the distributions shown in figure A.25 are probably much more broad than is accurate. This data problem does not undermine the method, except that it increases the amount of uncertainty in the results.

Bioclimatic variables

Figure A.27 shows the distributions for all bioclimatic variables. These distributions are more erratic, because of the uneven spread of the observations within them: several bins in these histograms have no locations within their range, because of the discrete valuation of the Bioclim variables.

Latitude

We also incorporate latitude itself (see figure A.28). Even if there are increases in temperature, different latitudes will provide different levels of suitability, because of the tilt of the Earth and other processes. We cannot be certain whether coffee will grow effectively outside of these latitudes, even if they appear climatically similar in the future to lower latitudes now. Including the distribution of latitude imposes a slight conservativism on our estimate which is supported by the data.

A.4.7 Changes in suitability by country for our model

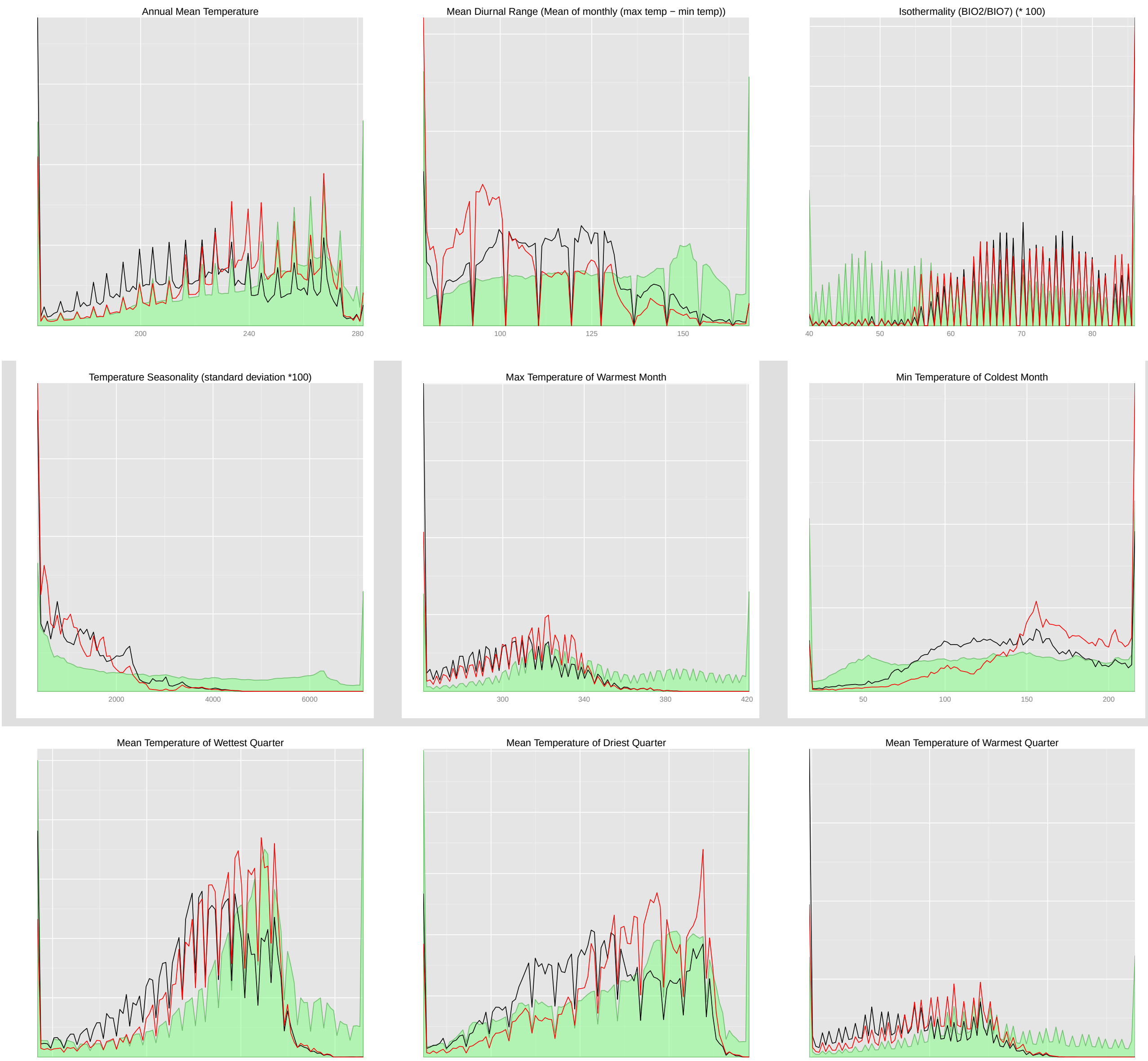

Figure A.26: First set of nine of the 19 variables in the Bioclim dataset, with coffee region distributions shown in black (Arabica) and red (Robusta). We dropped one, the Annual Temperature Range, since the technique implicitly infers it from the minimum and maximum temperatures.

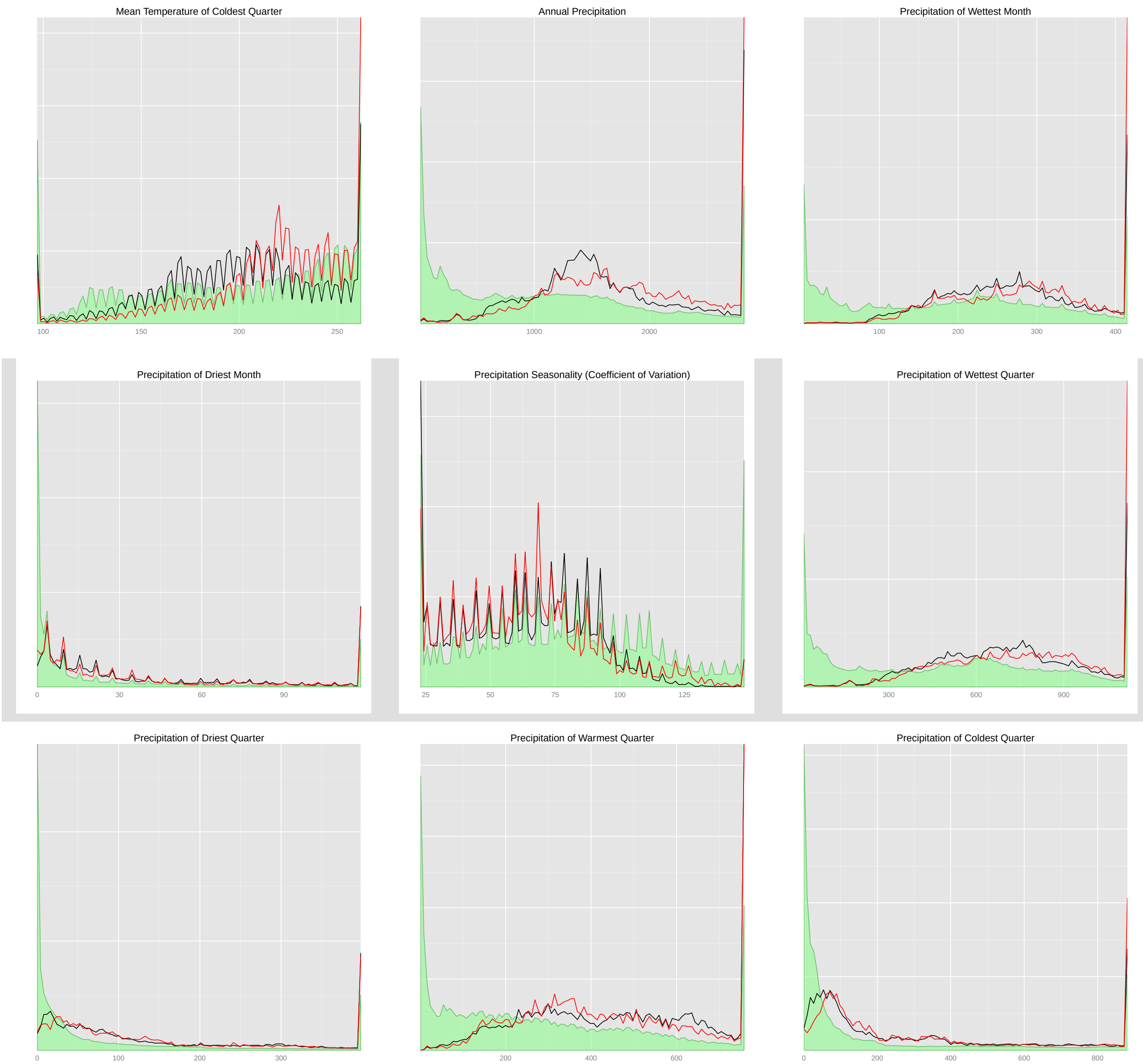

Figure A.27: Second set of nine of the 19 variables in the Bioclim dataset, with coffee region distributions shown in black (Arabica) and red (Robusta). We dropped one, the Annual Temperature Range, since the technique implicitly infers it from the minimum and maximum temperatures.

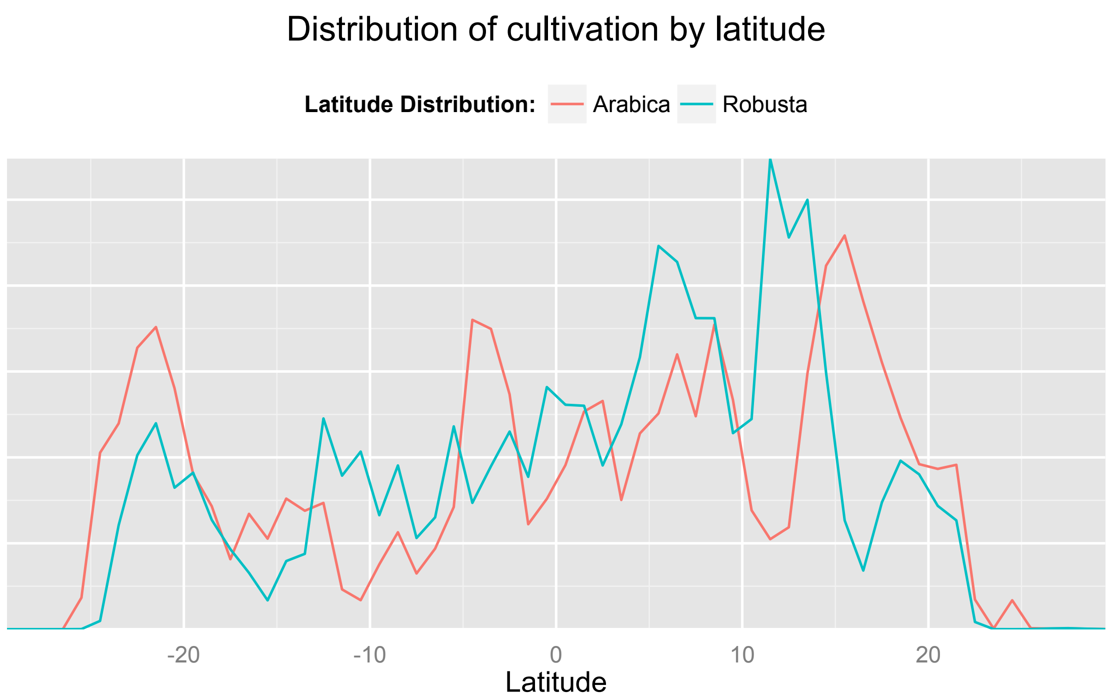

Figure A.28: The distribution of coffee production for Arabica (red) and Robusta (blue) across latitude.

Arabica Changes, Baseline - 2050, RCP 8.5

	Suitable Areas						Harvested Areas	
Country	Baseline (Ha)	Increase (Ha)	Decrease (Ha)	Conf. (%)	Loss (%)	Chng. (%)	Harvest (Ha)	H. Loss (%)
Angola	7832331	3163478	-7540076	96.66	-96.30	-55.90	31000.00	-43.90
Argentina	703607	500422	-362311	91.07	-51.50	19.60		0.00
Australia	324109	0	-320158	97.77	-98.80	-98.80		0.00
Burundi	642525	46216	-463559	87.50	-72.10	-65.00	27000.00	-25.70
Belize	28658	0	-28658	100.00	-100.00	-100.00	47.00	-100.00
Bolivia	2975159	361779	-849786	100.00	-28.60	-16.40	30000.00	-5.40
Brazil	30031272	4064511	-25719629	97.67	-85.60	-72.10	2120080.00	-34.70
Bhutan	0	93542	0	70.01				0.00
Botswana	2559	0	-2559	100.00	-100.00	-100.00		-100.00
Central African Republic	17019	0	-17019	100.00	-100.00	-100.00	14000.00	-100.00
Chile	327	242076	-327	99.11	-99.80			0.00
China	267924	31940	-250819	91.15	-93.60	-81.70	62000.00	-37.90
CÙte d'Ivoire	34259	0	-34259	100.00	-100.00	-100.00	160000.00	-100.00
Cameroon	901606	15973	-637133	100.00	-70.70	-68.90	210000.00	-25.50
Democratic Republic of the Congo	9054217	328050	-7382600	95.55	-81.50	-77.90	86000.00	-29.40
Republic of Congo	274260	0	-274260	100.00	-100.00	-100.00	10500.00	-100.00
Colombia	6333379	1130339	-3333722	94.51	-52.60	-34.80	778084.00	-19.30
Comoros	51817	603	-39930	96.12	-77.10	-75.90	885.00	0.00
Cape Verde	552	8183	-552	99.44	-100.00		0.00	-100.00
Costa Rica	680983	125192	-388387	97.31	-57.00	-38.60	93774.00	-14.70
Cuba	155472	0	-155387	98.11	-99.90	-99.90	28000.00	-7.40
Dominican Republic	212045	47801	-64205	93.88	-30.30	-7.70	133342.00	-2.10
Ecuador	2169018	291030	-820424	90.98	-37.80	-24.40	78709.71	-17.50
Eritrea	616234	11180	-443696	100.00	-72.00	-70.20		0.00
Spain	0	145055	0	97.54				0.00
Ethiopia	10236225	2117081	-6834556	92.96	-66.80	-46.10	528571.00	-28.00
Fiji	28317	0	-28317	100.00	-100.00	-100.00	30.00	-100.00
France	138260	32780	-45329	92.31	-32.80	-9.10	120.00	0.00
Gabon	9451	0	-9451	100.00	-100.00	-100.00	310.00	-100.00
Guinea	101123	0	-101123	100.00	-100.00	-100.00	66000.00	-100.00
Equatorial Guinea	141982	0	-141982	100.00	-100.00	-100.00	12500.00	-100.00
Guatemala	2019079	287541	-934956	90.05	-46.30	-32.10	250000.00	-25.70
Guyana	694669	1504	-664846	99.68	-95.70	-95.50	360.00	-5.20
Honduras	2549303	62862	-1593540	99.31	-62.50	-60.00	266000.00	-22.90
Haiti	336450	17876	-208607	98.68	-62.00	-56.70	92000.00	-27.00
Indonesia	7617814	705740	-4902428	96.51	-64.40	-55.10	1233900.00	-10.90
India	523680	133453	-329003	96.62	-62.80	-37.30	368687.00	-1.00
Jamaica	49008	0	-42530	100.00	-86.80	-86.80	7500.00	-19.80
Kenya	5106633	888046	-3200314	91.90	-62.70	-45.30	160000.00	-27.10
Cambodia	2239	0	-2239	100.00	-100.00	-100.00	430.00	-100.00
Lao PDR	216682	0	-211843	100.00	-97.80	-97.80	56875.00	-19.00
Sri Lanka	48813	1895	-26470	97.22	-54.20	-50.30	8460.00	-0.70
Lesotho	0	1623	0	76.47				0.00
Morocco	0	0	0	0.35				0.00

Arabica Changes, Baseline - 2050, RCP 8.5

	Suitable Areas						Harvested Areas	
Country	Baseline (Ha)	Increase (Ha)	Decrease (Ha)	Conf. (%)	Loss (%)	Chng. (%)	Harvest (Ha)	H. Loss (%)
Madagascar	15676837	1359696	-7488575	96.47	-47.80	-39.10	138000.00	-18.90
Mexico	23046243	3759088	-12251072	96.23	-53.20	-36.80	695350.00	-21.10
Myanmar	82547	4844	-79233	93.42	-96.00	-90.10	12000.00	-17.60
Mozambique	3368146	143380	-2974523	96.50	-88.30	-84.10	980.00	-18.40
Mauritius	63460	0	-48142	100.00	-75.90	-75.90	0.00	0.00
Malawi	1545688	256879	-1272351	90.01	-82.30	-65.70	2580.00	-1.10
Malaysia	561747	19748	-492026	96.17	-87.60	-84.10	19300.00	-0.50
Namibia	1209730	134161	-1171642	96.62	-96.90	-85.80		0.00
New Caledonia	116243	4	-100629	99.37	-86.60	-86.60	95.00	0.00
Nigeria	3391	109	-3372	92.22	-99.40	-96.20	2200.00	-2.20
Nicaragua	657690	9958	-545072	100.00	-82.90	-81.40	123000.00	-13.70
Nepal	0	0	0	63.34			1780.00	0.00
Oman	0	0	0	100.00	-100.00	-100.00		-100.00
Panama	379618	40024	-221501	94.76	-58.30	-47.80	30000.00	-20.30
Peru	3254385	2747945	-1723632	92.61	-53.00	31.50	312251.00	-13.80
Philippines	1451866	102893	-996757	97.58	-68.70	-61.60	119999.00	-5.40
Papua New Guinea	4652101	274890	-2134348	96.37	-45.90	-40.00	73000.00	-10.60
Puerto Rico	148890	0	-123066	100.00	-82.70	-82.70	42000.00	-36.70
Paraguay	0	0	-	100.00	-100.00	-100.00	300.00	-100.00
Rwanda	858792	108725	-573378	89.08	-66.80	-54.10	41762.00	-9.20
Saudi Arabia	802649	1111	-768697	99.03	-95.80	-95.60	0.00	0.00
South Sudan	140253	5615	-110543	93.32	-78.80	-74.80		0.00
Solomon Islands	44906	5927	-44870	100.00	-99.90	-86.70		0.00
Sierra Leone	0	0	-	100.00	-100.00	-100.00	14000.00	-100.00
El Salvador	88234	11743	-59752	90.19	-67.70	-54.40	139958.00	-33.90
Somaliland	535507	10985	-533484	99.92	-99.60	-97.60		0.00
Somalia	94467	4137	-94467	95.80	-100.00	-95.60		-100.00
S„o TomÈ and Principe	22915	0	-16475	100.00	-71.90	-71.90	250.00	0.00
Swaziland	94563	8035	-79389	78.66	-84.00	-75.50		0.00
Thailand	236767	0	-236761	100.00	-100.00	-100.00	52000.00	-100.00
Timor-Leste	201630	15264	-161490	99.85	-80.10	-72.50	55000.00	-12.10
Taiwan	17859	45193	-17859	85.53	-100.00	153.00	0.00	-100.00
Tanzania	10120904	1745435	-8474385	96.69	-83.70	-66.50	127335.00	-21.80
Uganda	5007871	67539	-4767946	99.69	-95.20	-93.90	310000.00	-60.20
United States	457497	20861	-400461	98.97	-87.50	-83.00	2550.00	-85.70
Venezuela	5232487	259415	-3729513	96.81	-71.30	-66.30	182000.00	-3.70
Vietnam	1469106	73643	-1256133	98.44	-85.50	-80.50	574314.36	-1.90
Vanuatu	14532	0	-14417	90.77	-99.20	-99.20	65.00	0.00
Yemen	2949889	16273	-2137856	98.63	-72.50	-71.90	34987.00	-27.40
South Africa	2635760	760688	-2252927	98.86	-85.50	-56.60		0.00
Zambia	4406514	13720	-4193830	95.68	-95.20	-94.90	7000.00	-34.40
Zimbabwe	398934	6065	-390551	99.82	-97.90	-96.40	5397.00	-31.40

Robusta Changes, Baseline - 2050, RCP 8.5

	Suitable Areas						Harvested Areas	
Country	Baseline (Ha)	Increase (Ha)	Decrease (Ha)	Conf. (%)	Loss (%)	Chng. (%)	Harvest (Ha)	H. Loss (%)
Angola	5150021	5959656	-2805429	85.92	-54.50	61.20	31000.00	-17.80
Argentina	1286056	2105318	-1114987	91.68	-86.70	77.00		0.00
American Samoa	0	0	0	100.00				0.00
Antigua and Barbuda	0	0	0	100.00				0.00
Australia	170410	3414649	-114523	93.17	-67.20			0.00
Burundi	494565	145247	-284285	92.28	-57.50	-28.10	27000.00	-14.20
Bangladesh	0	561488	0	15.07				0.00
Bahamas	0	0	0	50.00				0.00
Belize	0	885404	0	82.07	0.00		47.00	0.00
Bolivia	2038575	8924087	-962916	65.29	-47.20	390.50	30000.00	-0.10
Brazil	8450738	35586649	-2304340	72.03	-27.30	393.80	2120080.00	-14.00
Barbados	0	12	0	100.00				0.00
Brunei Darussalam	0	13	0	100.00				0.00
Bhutan	0	104353	0	99.09				0.00
Botswana	405172	2386421	-405166	62.82	-100.00	489.00		-100.00
Central African Republic	198116	3599572	-33401	84.84	-16.90		14000.00	-0.00
Chile	12937	6	-12937	99.95	-100.00	-100.00		-100.00
China	3768742	550157	-3466649	98.36	-92.00	-77.40	62000.00	-7.20
CÙte d'Ivoire	7815	1220362	-296	94.34	-3.80		160000.00	-0.10
Cameroon	1324883	5991635	-175708	96.84	-13.30	439.00	210000.00	-1.60
Democratic Republic of the Congo	9668515	16006969	-6745133	82.72	-69.80	95.80	86000.00	-0.70
Republic of Congo	570588	2522891	-354354	92.87	-62.10	380.10	10500.00	-6.70
Colombia	4831268	6170063	-2722280	78.40	-56.30	71.40	778084.00	-8.40
Comoros	1083	41001	0	78.33	0.00		885.00	0.00
Cape Verde	47599	10128	-17921	84.26	-37.70	-16.40	0.00	0.00
Costa Rica	563486	158883	-271265	80.43	-48.10	-19.90	93774.00	-7.90
Cuba	188896	1498809	-375	83.71	-0.20	793.30	28000.00	-0.00
Cayman Islands	0	15092	0	100.00				0.00
Djibouti	0	0	0	88.23				0.00
Dominica	0	18146	0	100.00			610.00	0.00
Dominican Republic	249043	1195690	-73639	92.28	-29.60	450.50	133342.00	-0.70
Ecuador	2266507	1056561	-1267955	90.67	-55.90	-9.30	78709.71	-1.70
Eritrea	606180	92476	-303872	96.16	-50.10	-34.90		0.00
Spain	0	54557	0	79.99				0.00
Ethiopia	9630697	2589937	-5991843	90.52	-62.20	-35.30	528571.00	-27.30
Fiji	31202	215943	-1686	91.50	-5.40	686.70	30.00	0.00
France	87221	96079	-14879	99.72	-17.10	93.10	120.00	0.00
Gabon	31063	5413957	-9317	99.52	-30.00		310.00	-0.00
Ghana	0	196263	0	98.17			4000.00	0.00
Guinea	433521	831493	-243442	87.70	-56.20	135.60	66000.00	-6.90
Equatorial Guinea	1050	318762	-11	99.57	-1.10		12500.00	-0.10
Grenada	0	23207	0	97.94				0.00
Guatemala	1428221	2652766	-876418	82.59	-61.40	124.40	250000.00	-31.40
Guyana	510369	419814	-48270	78.66	-9.50	72.80	360.00	-0.40

Robusta Changes, Baseline - 2050, RCP 8.5

	Suitable Areas						Harvested Areas	
Country	Baseline (Ha)	Increase (Ha)	Decrease (Ha)	Conf. (%)	Loss (%)	Chng. (%)	Harvest (Ha)	H. Loss (%)
Hong Kong	0	14612	0	74.94				0.00
Honduras	2594743	2282517	-702365	91.15	-27.10	60.90	266000.00	-10.60
Haiti	434375	779343	-28904	92.06	-6.70	172.80	92000.00	-0.50
Indonesia	5364764	19407103	-1702290	93.03	-31.70	330.00	1233900.00	-4.60
India	191152	2193510	-84498	92.31	-44.20		368687.00	-1.80
Jamaica	6010	61053	0	92.30	0.00		7500.00	0.00
Kenya	4190724	1238752	-2507363	91.06	-59.80	-30.30	160000.00	-6.90
Cambodia	175055	427216	-24262	57.23	-13.90	230.20	430.00	-0.00
Saint Kitts and Nevis	0	0	0	100.00				0.00
Lao PDR	666770	1268847	-273633	66.60	-41.00	149.30	56875.00	-2.60
Liberia	0	1323785	0	99.43			2800.00	0.00
Saint Lucia	0	104	0	100.00			0.00	0.00
Sri Lanka	53824	44149	-36806	87.67	-68.40	13.60	8460.00	-0.10
Morocco	0	1953628	0	87.06				0.00
Madagascar	579295	5905617	-430242	93.92	-74.30	945.20	138000.00	-21.80
Mexico	20342425	9564738	-16492118	94.79	-81.10	-34.10	695350.00	-24.90
Myanmar	782366	972653	-693545	93.04	-88.60	35.70	12000.00	-0.00
Mozambique	1196437	8105709	-466356	86.79	-39.00	638.50	980.00	-8.60
Mauritania	0	9144	0	99.83				0.00
Montserrat	0	0	0	88.23				0.00
Mauritius	34422	107428	0	89.97	-0.00	312.10	0.00	0.00
Malawi	652634	1158706	-259512	82.41	-39.80	137.80	2580.00	-14.10
Malaysia	552660	2165838	-28576	95.38	-5.20	386.70	19300.00	-0.10
Namibia	1325792	192435	-1300052	98.90	-98.10	-83.50		0.00
New Caledonia	39667	596897	-1088	99.88	-2.70		95.00	0.00
Nigeria	22291	127003	-2176	89.15	-9.80	560.00	2200.00	-0.20
Nicaragua	680281	1773570	-53620	96.00	-7.90	252.80	123000.00	-0.00
Nepal	0	0	0	100.00			1780.00	0.00
Oman	0	82194	0	90.57	0.00			0.00
Panama	385527	538364	-163103	83.74	-42.30	97.30	30000.00	-9.50
Peru	6609345	6578036	-4375019	80.81	-66.20	33.30	312251.00	-10.40
Philippines	1200467	2966352	-368050	88.92	-30.70	216.40	119999.00	-5.60
Papua New Guinea	2390681	4469796	-1276059	91.17	-53.40	133.60	73000.00	-11.90
Puerto Rico	105939	352303	0	98.38	0.00	332.60	42000.00	0.00
Paraguay	0	2483538	0	84.98	-100.00		300.00	-100.00
Rwanda	667299	8125	-512784	92.74	-76.80	-75.60	41762.00	-36.00
Western Sahara	0	31668	0	99.03				0.00
Saudi Arabia	828878	46020	-300087	100.00	-36.20	-30.70	0.00	0.00
Sudan	0	19421	0	97.53				0.00
South Sudan	81932	306289	-31559	60.11	-38.50	335.30		0.00
Senegal	0	0	0	100.00				0.00
Solomon Islands	39621	378509	-61	98.42	-0.20	955.10		0.00
Sierra Leone	2290	483628	-2288	88.83	-99.90		14000.00	-0.00
El Salvador	178283	112387	-59934	62.25	-33.60	29.40	139958.00	-4.10

Robusta Changes, Baseline - 2050, RCP 8.5

	Suitable Areas						Harvested Areas	
Country	Baseline (Ha)	Increase (Ha)	Decrease (Ha)	Conf. (%)	Loss (%)	Chng. (%)	Harvest (Ha)	H. Loss (%)
Somaliland	510372	402411	-161477	83.59	-31.60	47.20		0.00
Somalia	0	57573	0	45.79	-100.00			-100.00
S„o TomÈ and Principe	7584	11738	-174	98.88	-2.30	152.50	250.00	0.00
Suriname	0	6728	0	31.93			488.00	0.00
Swaziland	16051	15316	-16051	100.00	-100.00	-4.60		-100.00
Togo	0	100627	0	100.00			27000.00	0.00
Thailand	221535	640290	-70468	80.08	-31.80	257.20	52000.00	-0.00
Timor-Leste	24148	145298	-8755	93.06	-36.30	565.40	55000.00	-2.20
Tonga	0	7290	0	96.30			10.00	0.00
Trinidad and Tobago	0	32	0	50.01			350.00	0.00
Taiwan	6208	256909	0	90.01	-0.00		0.00	0.00
Tanzania	14434260	5551037	-8871902	85.55	-61.50	-23.00	127335.00	-13.80
Uganda	6944190	1159159	-5756638	80.92	-82.90	-66.20	310000.00	-60.40
United States	129750	359497	-29880	88.00	-23.00	254.00	2550.00	-26.80
Saint Vincent and the Grenadines	0	72	0	100.00				0.00
Venezuela	3515842	2313894	-2227300	78.01	-63.40	2.50	182000.00	-2.50
United States Virgin Islands	0	0	0	100.00				0.00
Vietnam	1883848	4343466	-92368	88.85	-4.90	225.70	574314.36	-0.40
Vanuatu	63133	327533	-1013	96.96	-1.60	517.20	65.00	0.00
Samoa	0	11403	0	58.88			35.00	0.00
Yemen	2748339	2130013	-985741	91.92	-35.90	41.60	34987.00	-18.50
South Africa	4799951	713212	-4627116	100.00	-96.40	-81.50		0.00
Zambia	1625781	704492	-1063716	86.34	-65.40	-22.10	7000.00	-51.40
Zimbabwe	962921	347792	-955963	95.36	-99.30	-63.20	5397.00	-20.90

A.5 Extra variability analysis

A.5.1 Computing ENSO impacts

We estimate the impacts of El Niño and La Niña by estimating an "impulse response", which accounts for the multiple overlapping effects of different ENSO years and the monthly climatology of the NINO 3.4 signal.

$$y_t = \alpha + \sum_{Y=Year(t)-N/12+1}^{Year(t)} \sum_{M=1}^{N} \beta_{12(Year(t)-Y)+M}^{Class(Y)} + \gamma \sum_{s=1}^{24} \frac{y_{t-s}}{24} + \mu_{Month(t)}$$

$Year(t)$ is the year for time t and $Month(t)$ is the month for time t; $Class(Y)$ is the class of ENSO event that happened in year Y (El Niño and La Niña). N is the number of months to include in the impulse responses.

Here, the β_m^k variables describe impulse responses of length N for each class of ENSO event.

A.5.2 Additional PCA details

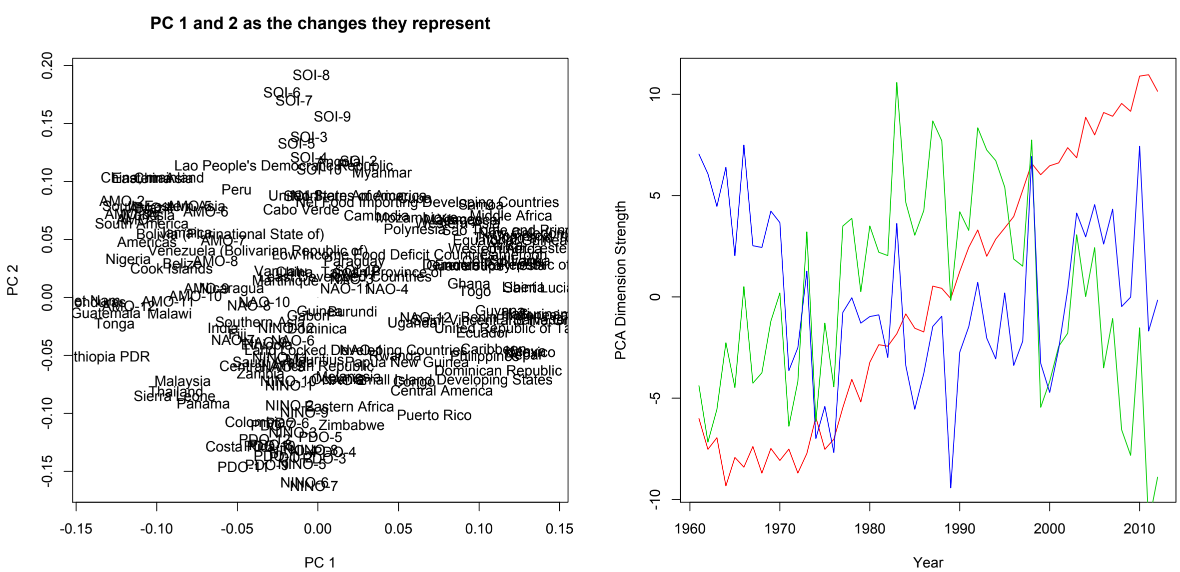

Figure A.29: **Left:** The first and second principal component, in terms of the marginal effects of countries and climate signals. These are displayed more clearly in the main report. **Right:** The values of the first three principal components (PC 1 = red, PC 2 = green, PC 3 = blue) across years. As years progress, PC 1 generally increases, and PC 2 first decreases and then increases.

A.5.3 Monthly production

Production records are generally maintained on a yearly basis, but different price information is available monthly. Different countries harvest and ship beans during different months, and this information can be used to infer the monthly production added to the global market.

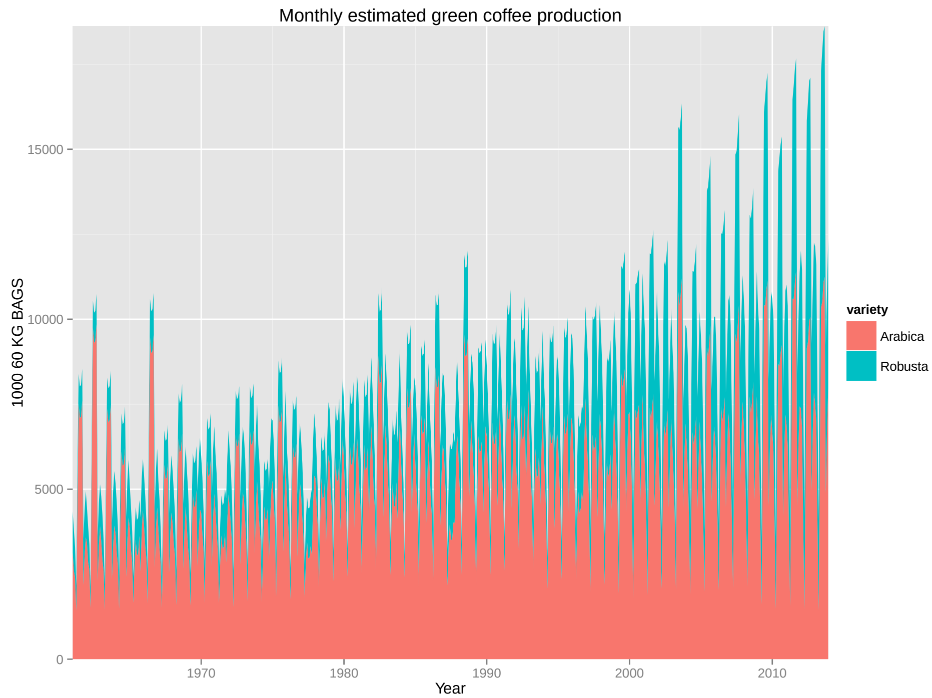

Figure A.30: Inferred monthly production for Arabica and Robusta coffee, based on the harvesting calendars of their producing countries.

We use the coffee harvested calendar from the Sweet Maria's Coffee Production Timetable, which is admittedly uncertain and subject to yearly change. However, they provide a general cycle around which actual yearly production is assumed to vary. We distribute the production for each country amongst its harvesting months, and evenly distribute throughout the year production for countries not represented in the calendar (most notably, Vietnam). We also distinguish between countries that produce Arabica and Robusta coffees, or those that produce a combination of both every year. The result in the figure above shows wide variations from month to month.

It is also interesting that the range of variation has increased significantly. The peak of production each year has increased much faster than the yearly minimum: In the 1960s, the best years produced monthly peaks over 10 million bags, while the slowest months produced only 3 million bags. In the last decade, the greatest monthly production has been over 15 million bags, but the worst months have only produced 5 million bags. The situation is even starker for Arabica coffee, where the worst months in the last decade are comparable to those in the 1960s, although the best months have increased over 20%.

We can use this monthly production data to inform the coffee market model, described below.

A.5.4 Additional pest control results

4°C global warming temperature data without pest control

With 4°C of warming, the distribution becomes almost completely normal, continuing to move right, though with a smaller right tail. Even with a huge amount of warming, there were no instances above 600 or 66% of the crop. This suggests that with the average monthly infection around 20%, the plants are not healthy enough to sustain a super event like the size of one previously seen. This absolute limit does little to help the predictability on short time scales however.

Histogram of outbreak sizes and Log-log plot of outbreak sizes

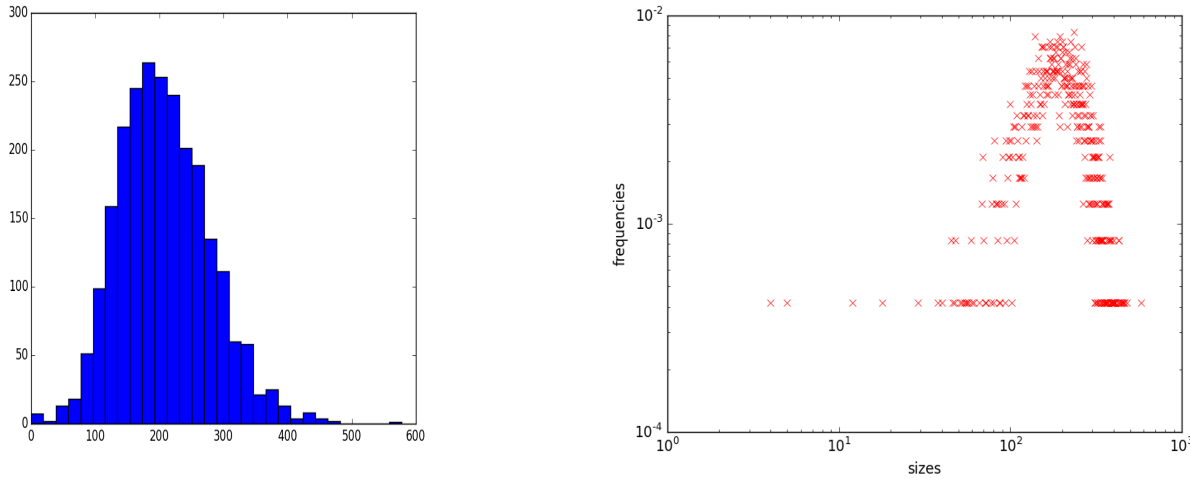

Time series of outbreak sizes

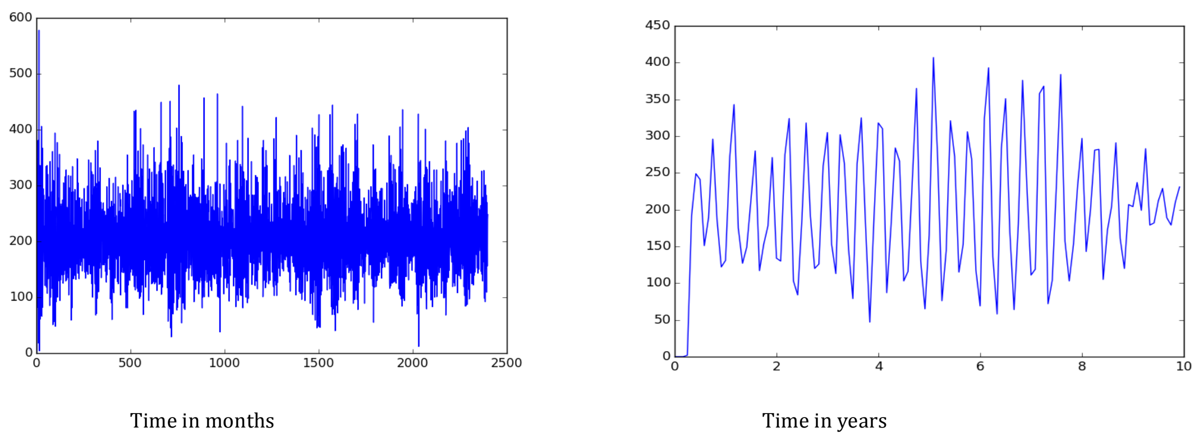

Figure A.31: Results for 4°C warming without pest control.

4°C global warming temperature data with pest control

4°C of warming begins to offset the ability of fungicides to control the fungus population, the highest values in the histogram moves away from zero, shown by the concavity of the Log-log plot, as the curve continues to be thicker in areas than it was with less warming. The time series, as well as the other plots itself begin to more resemble the model runs in uncontrolled but cooler environments, with the highest values still not going higher than 70%.

Histogram of outbreak sizes and Log-log plot of outbreak sizes

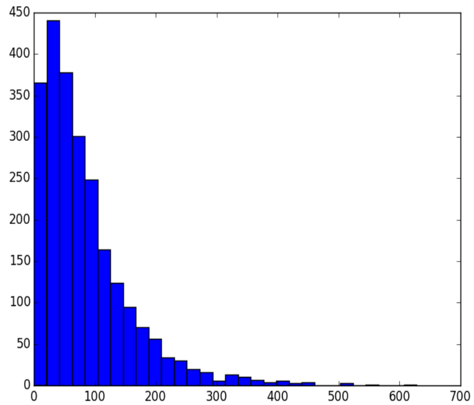

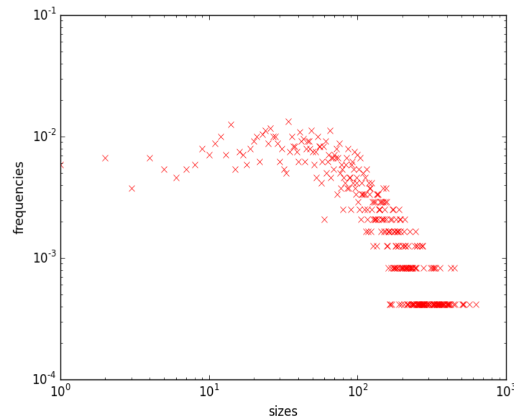

Time series of outbreak sizes

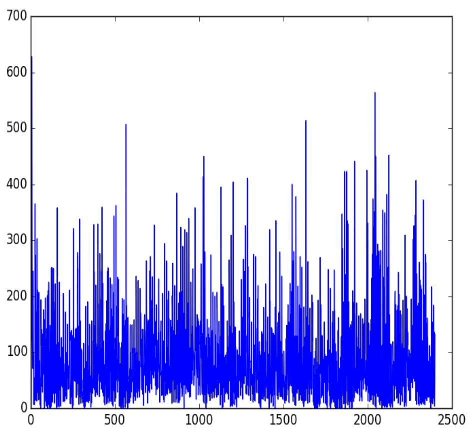

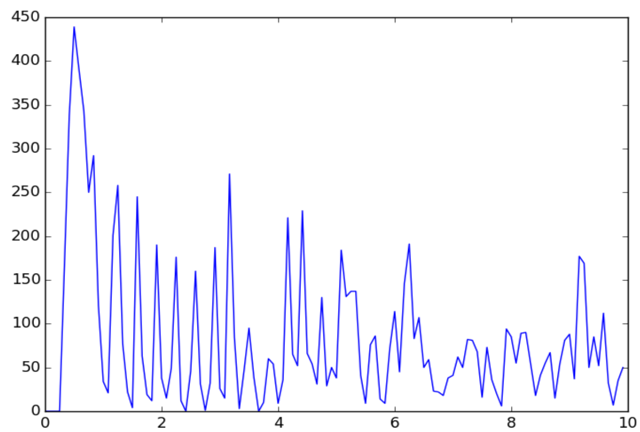

Figure A.32: Results for 4°C warming with pest control.

A.5.5 Coherent movements

The relatively weak statistical relationship found between El Niño and country-specific yields is not uncommon among agricultural crops, but it drove an interest in our group into dissecting more clearly the relationship between global climate signals and country production. We collected five oceanic signals to explore this further, as shown in figure A.33.[5]

A principal component analysis identifies regions of coherent marginal changes, across multiple time-series. This technique can be used to better understand patterns in large datasets, like the one describing country coffee production.

[5] NINO 3.4, NAO, SOI, PDO from NOAA Climate Prediction Center (CPC) (2015), unsmoothed AMO from Enfield et al. (2001).

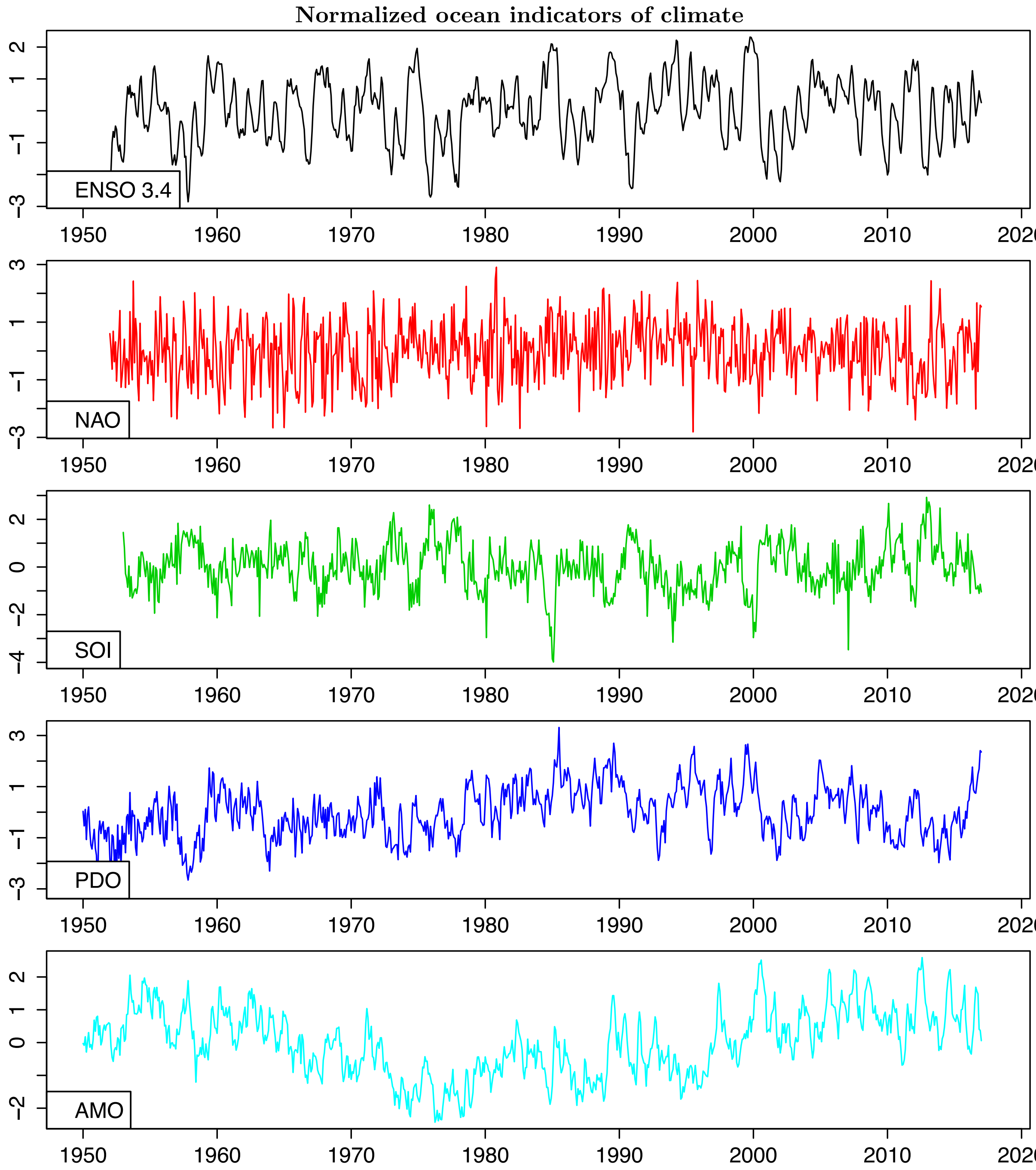

Figure A.33: Normalized indicators used to study global and regional climate, sampled monthly. Each of these shows wide variability, but different periodicities. The interactions between these different signals can explain impacts in ways that individual signals cannot.

For each year, monthly values of the climate signals (delayed 6 months, to capture their impacts on coffee flowering) and country yields (detrended with locfit and normalized) are included. The first principal component represents the largest coherent movement of change, followed by the second component, and so on. Between the first three components, over 50% of the variation in yields can be described. The share of each of these components by year is shown in Appendix A.5.2. Each of the components and what it suggests about the relationship between climate and yields is described below.

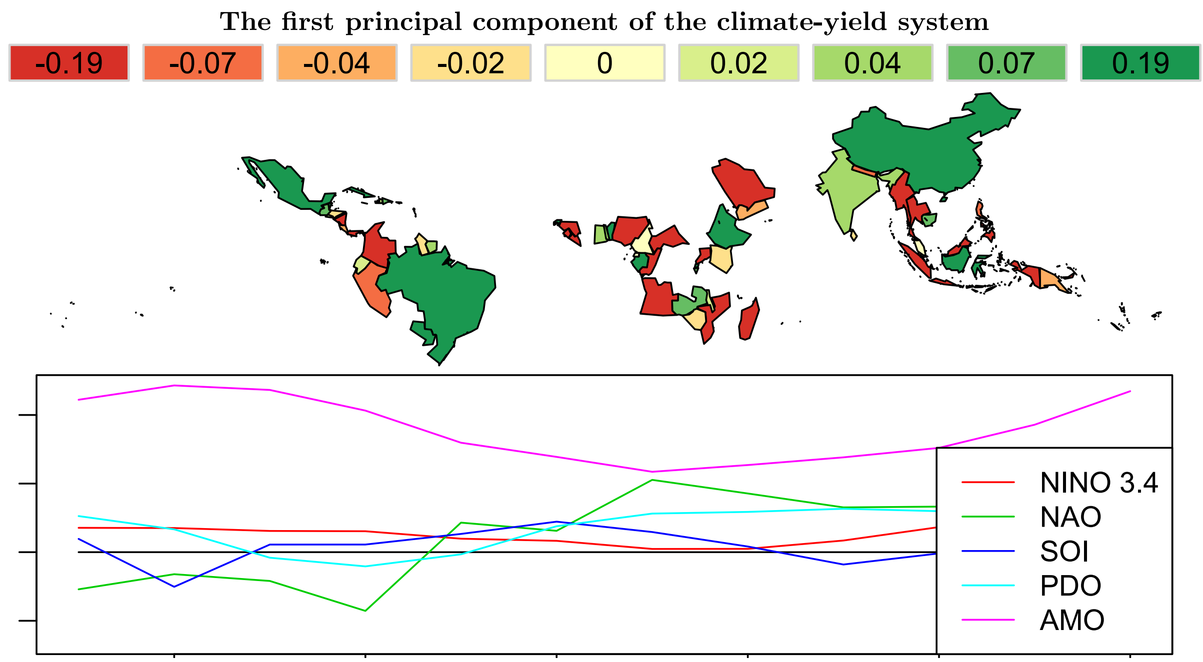

Figure A.34: Spatial and temporal representation of the first principal component of the climate-yield system. Colors in the map represent increases (green) and decreases (red), and the plot below shows the climate signals across the year (delayed 6 months, so month 1 is July and month 12 is June). Explanation in the text.

The first principal component describes how yields have shifted on average over the past 50 years. Brazil, Mexico, and China have seen some the largest increases in yield, while Thailand, Myanmar and many countries in Africa have experienced the largest decreases. Most climate signals have not shown any trend, except for the Atlantic multidecadal oscillation (AMO) which is currently much higher than it was in the 1960s. As a result, all of the climate signals in the lower graph are near zero, except for AMO.

The second and third principal components are dominated by ENSO (the El Niño/La Niña cycle), represented by the NINO 3.4 index and the Southern oscillation index, which is known to be strongly correlated with ENSO but with an opposite sign. PC 2 is represented in the data when NINO 3.4 is high (El Niño) and the Pacific decadal oscillation (PDO) is also high, and its effects are reversed when these signals are both opposite in the direction of their anomalies. The largest effect of this combination, as shown in the map, is that Brazil, Paraguay, and Papua New Guinea have decreases in yields while India sees increases. This suggests that yields in these regions will often move in opposite directions, during many El Niño and La Niña years.

Observations with low values of PC 2 occur before 1975 and after 2000, while those with high values of PC 2 occur mostly in the 1980s and early 1990s. This may be driven by the slow oscillation of PDO. Since only one such cycle has occurred, it is difficult to distinguish the effects of the climate signals

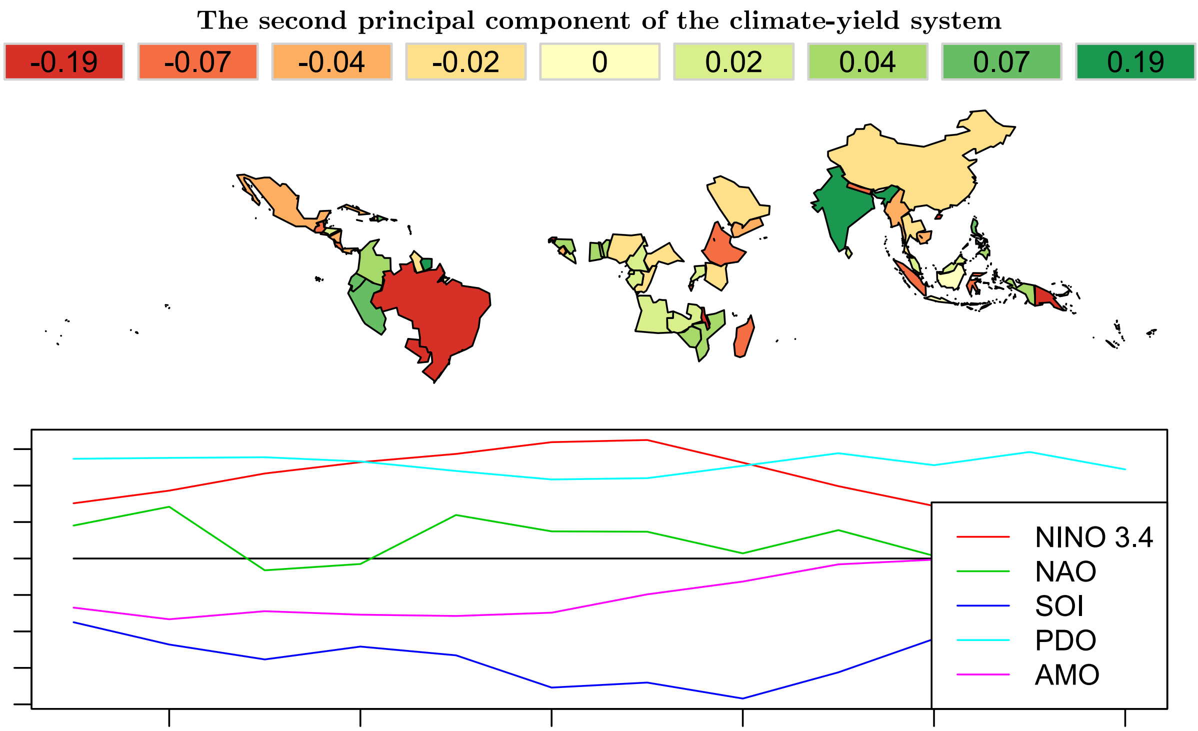

Figure A.35: Spatial and temporal representation of the second principal component of the climate-yield system. Colors in the map represent increases (green) and decreases (red), and the plot below shows the climate signals across the year (delayed 6 months). Explanation in the text.

from socioeconomic effects, although most of this was be removed by the flexible trend used in the preprocessing step.

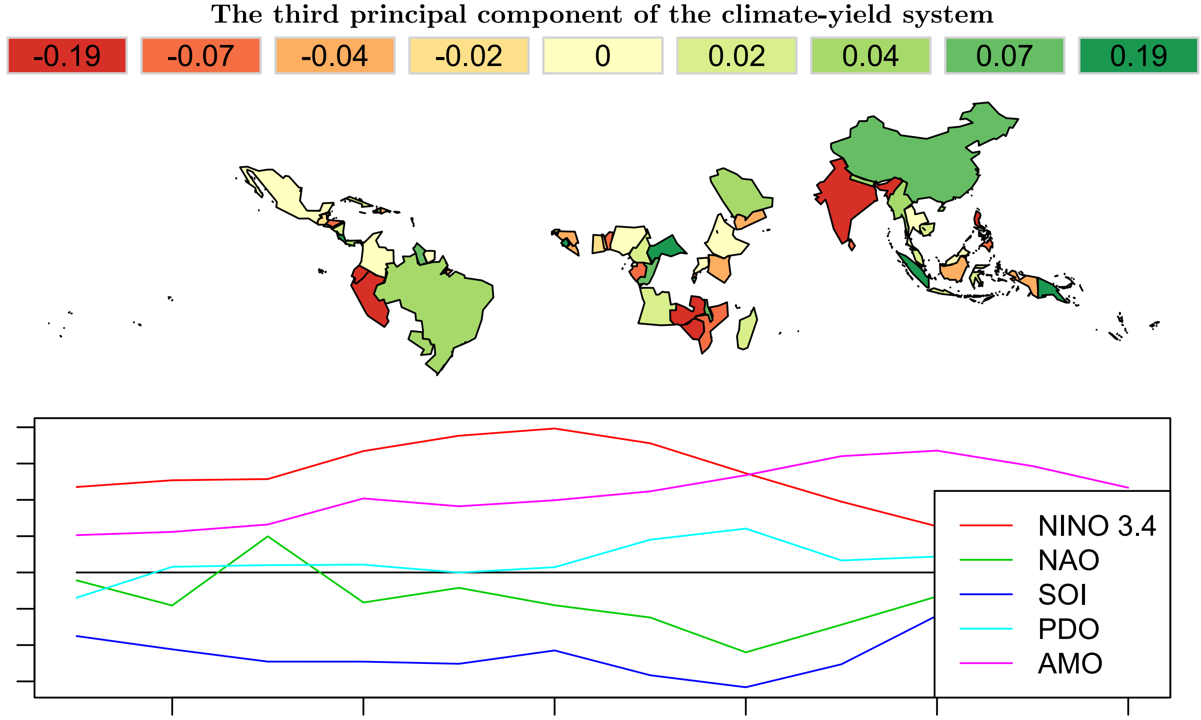

Figure A.36: Spatial and temporal representation of the third principal component of the climate-yield system. Colors in the map represent increases (green) and decreases (red), and the plot below shows the climate signals across the year (delayed 6 months). Explanation in the text.

The third principal component also occurs when ENSO is in its El Niño state, and AMO is high or increasing. In this case, India, Peru, and southern areas in Africa show decreases, while other areas are not heavily affected. Both PC 2 and PC 3 can equally be understood in their La Niña form (and associated low values of PDO for PC 2 and low values of AMO for PC 3), which produce changes in yields in the opposite direction.

Between PCs 2 and 3, the effects of El Niño and La Niña appear across much of the globe. Because the impacts on most countries result from an interaction between the ENSO cycle and AMO or PDO, the results did not appear in the initial analysis.

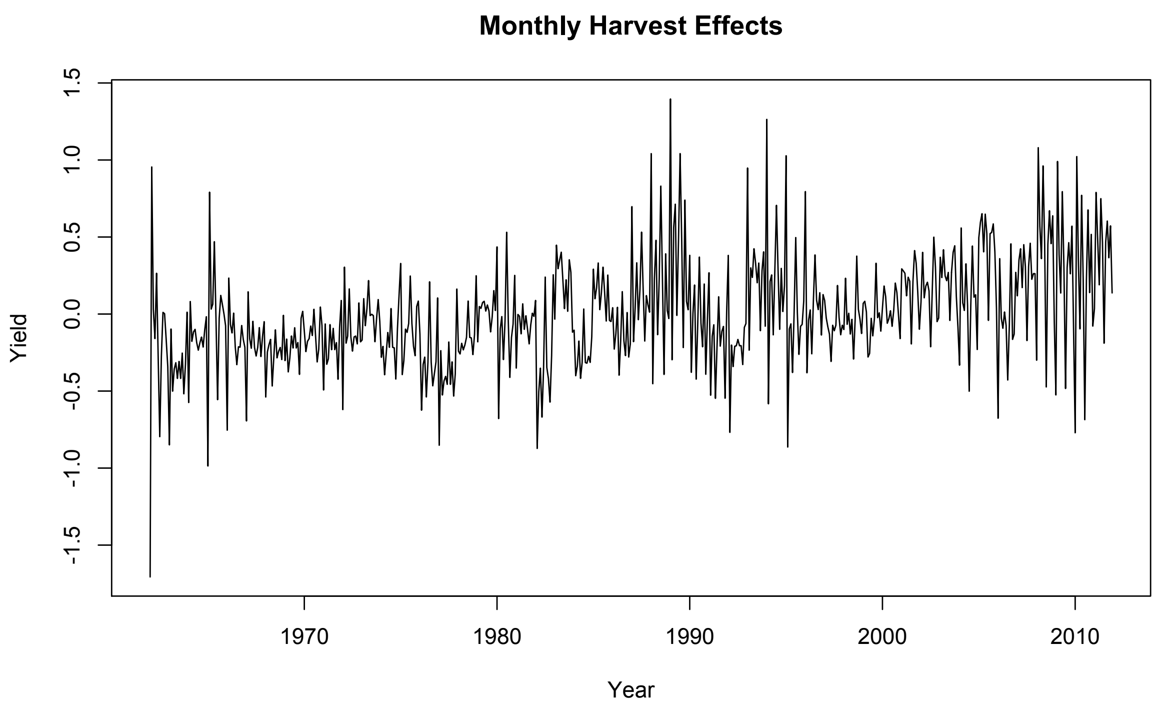

Figure A.37: Monthly harvesting effects. Each point on this curve represents the difference in yields predicted by harvesting in a given month, according to coffee harvest calendars, after accounting for country-specific and month effects. Uses calendars from `https://www.sweetmarias.com/coffee.prod.timetable.php`

Low \High	28	29	30	31	32	33	34
-4					87.4211	87.4289	87.3933
-3							
-2						87.4290	
-1							
0				87.2986	87.4213	87.4290	87.3934
1						87.4290	
2					87.4212	87.4289	87.3933
3						87.4288	
4				87.2983	87.4210	87.4286	
5			87.0758	87.2979	87.4206		
6				87.2978	87.4205	87.4281	
7			87.0755	87.2978	87.4204		
8				87.2981			
9			87.0749	87.2979	87.4199		
10	86.7490		87.0737	87.2975			
11			87.0729	87.2975	87.4182		
12	86.7398		87.0700	87.2954			
13							
14							
15	86.6988		87.0369	87.2645			

Table A.9: F-statistics for a growing degree-day and killing degree-day model of coffee production, across all countries. The highest F-stats use a maximum temperature of 30°C and a minimum temperature between -3°C and 1 °C.

A.6 Extra production analysis

A.6.1 Selecting temperature limits

A.6.2 Humidity

A.6.3 Harvest month effects

Figure A.37 shows the estimated "effect" of harvesting in a given month on yields, from 1962 to 2011, after accounting for country-specific and monthly effects. The gradual increase reflects improvements in coffee production technology, but this increase is not without large shocks. An increase in yields between 1985 and 1990 was followed by a decrease and then another period of increased yields. Countries that harvest in different months also show different fortunes, with the greatest yields to countries that harvest in January and the lowest to those that harvest in February. Since the only country that harvests in January but not February is Colombia, this probably reflects the difference between Colombia yields and yields in other February-harvesting countries.

A.6.4 Hierarchical model coefficients

Only statistically-significant coefficients are listed below. The remaining are available online at `http://eicoffee.net/`.

Table A.10: Humidity Effects

	Dependent variable:
Month prior to harvest	log(yield)
1	−8.562
	(12.703)
2	17.386
	(12.509)
3	−2.607
	(13.406)
4	−23.317*
	(12.756)
5	4.781
	(13.223)
6	−30.035**
	(12.008)
7	15.021
	(14.797)
8	−14.813
	(16.496)
9	19.024
	(16.429)
10	−6.111
	(17.747)
11	35.636*
	(18.228)
12	−33.730**
	(15.444)
Observations	738
R^2	0.895
Adjusted R^2	0.881
Residual Std. Error	0.191 (df = 653)
F Statistic	66.164*** (df = 84; 653)
Note:	*p<0.1; **p<0.05; ***p<0.01

	Dependent variable:	
	Countries only	
	(1)	(2)
GDDs / 1000, Liberia (Robusta)	0.515**	0.743***
	(0.213)	(0.202)
GDDs / 1000, Gabon (Robusta)	0.223	0.448**
	(0.215)	(0.204)
GDDs / 1000, Yemen (Arabica)	0.274	0.368**
	(0.189)	(0.183)
GDDs / 1000, Benin (Robusta)	0.146	0.409**
	(0.221)	(0.207)
GDDs / 1000, Cuba (Arabica)	0.222	0.322*
	(0.194)	(0.189)
GDDs / 1000, Angola (Robusta)	0.121	0.354*
	(0.217)	(0.205)
GDDs / 1000, Malaysia (Robusta)	0.266	0.495**
	(0.220)	(0.209)
GDDs / 1000, Brazil (Combined)	0.079	0.158***
	(0.208)	(0.052)
GDDs / 1000, Guinea (Robusta)	0.356*	0.603***
	(0.199)	(0.185)
GDDs / 1000, Nigeria (Robusta)	0.377*	0.659***
	(0.212)	(0.197)
GDDs / 1000, Suriname (Combined)	0.346*	0.484**
	(0.204)	(0.189)
GDDs / 1000, Zambia (Arabica)	0.217	0.300*
	(0.178)	(0.173)
GDDs / 1000, Paraguay (Arabica)	0.248	0.405***
	(0.165)	(0.156)
GDDs / 1000, Guyana (Robusta)	0.140	0.374*
	(0.223)	(0.211)
GDDs / 1000, Congo (Robusta)	0.145	0.382*
	(0.215)	(0.203)
KDDs / 1000, Cambodia (Combined)	−0.112	−1.798***
	(0.567)	(0.363)
KDDs / 1000, Ethiopia (Arabica)	−0.082	−1.731***
	(0.581)	(0.394)
KDDs / 1000, Cameroon (Combined)	−0.111	−1.801***
	(0.568)	(0.364)
KDDs / 1000, Ghana (Robusta)	−0.180	−1.787***
	(0.568)	(0.386)
KDDs / 1000, Saudi.Arabia (Combined)	−0.110	−1.801***
	(0.568)	(0.364)
KDDs / 1000, Guatemala (Arabica)	−0.082	−1.731***
	(0.581)	(0.394)
KDDs / 1000, Guatemala (Combined)	−0.110	−1.801***
	(0.568)	(0.364)
KDDs / 1000, Dominica (Combined)	−0.110	−1.801***
	(0.568)	(0.364)

	Dependent variable:	
	Countries only	
	(1)	(2)
KDDs / 1000, Liberia (Robusta)	−0.123	−1.732***
	(0.568)	(0.386)
KDDs / 1000, Gabon (Robusta)	−0.155	−1.764***
	(0.568)	(0.386)
KDDs / 1000, Gabon (Combined)	−0.110	−1.800***
	(0.568)	(0.364)
KDDs / 1000, Yemen (Combined)	−0.110	−1.801***
	(0.568)	(0.364)
KDDs / 1000, Yemen (Arabica)	−0.078	−1.728***
	(0.581)	(0.394)
KDDs / 1000, Jamaica (Arabica)	−0.082	−1.731***
	(0.581)	(0.394)
KDDs / 1000, Samoa (Combined)	−0.110	−1.801***
	(0.568)	(0.364)
KDDs / 1000, Kenya (Arabica)	−0.082	−1.731***
	(0.581)	(0.394)
KDDs / 1000, Kenya (Combined)	−0.114	−1.804***
	(0.568)	(0.364)
KDDs / 1000, India (Combined)	−0.110	−1.801***
	(0.568)	(0.364)
KDDs / 1000, Saint.Lucia (Combined)	−0.110	−1.801***
	(0.568)	(0.364)
KDDs / 1000, Rwanda (Arabica)	−0.082	−1.731***
	(0.581)	(0.394)
KDDs / 1000, Peru (Arabica)	−0.082	−1.731***
	(0.581)	(0.394)
KDDs / 1000, Vanuatu (Combined)	−0.110	−1.801***
	(0.568)	(0.364)
KDDs / 1000, Malawi (Arabica)	−0.082	−1.731***
	(0.581)	(0.394)
KDDs / 1000, Benin (Robusta)	−0.156	−1.754***
	(0.565)	(0.384)
KDDs / 1000, Benin (Combined)	−0.114	−1.773***
	(0.559)	(0.358)
KDDs / 1000, Cuba (Arabica)	−0.076	−1.725***
	(0.581)	(0.394)
KDDs / 1000, Togo (Robusta)	−0.244	−1.827***
	(0.560)	(0.380)
KDDs / 1000, Tonga (Combined)	−0.110	−1.801***
	(0.568)	(0.364)
KDDs / 1000, Indonesia (Combined)	−0.110	−1.801***
	(0.568)	(0.364)
KDDs / 1000, Mauritius (Combined)	−0.110	−1.801***
	(0.568)	(0.364)
KDDs / 1000, Angola (Combined)	−0.109	−1.799***
	(0.568)	(0.364)

	Dependent variable:	
	Countries only	
	(1)	(2)
KDDs / 1000, Angola (Robusta)	−0.159	−1.768***
	(0.568)	(0.386)
KDDs / 1000, Trinidad.and.Tobago (Combined)	−0.110	−1.801***
	(0.568)	(0.364)
KDDs / 1000, Nicaragua (Arabica)	−0.084	−1.733***
	(0.581)	(0.394)
KDDs / 1000, Malaysia (Robusta)	−0.159	−1.768***
	(0.568)	(0.386)
KDDs / 1000, Mozambique (Combined)	−0.111	−1.801***
	(0.568)	(0.364)
KDDs / 1000, Uganda (Combined)	−0.111	−1.801***
	(0.568)	(0.364)
KDDs / 1000, Brazil (Combined)	−0.110	−1.971***
	(0.568)	(0.309)
KDDs / 1000, Guinea (Robusta)	−0.101	−1.703***
	(0.566)	(0.384)
KDDs / 1000, Panama (Arabica)	−0.082	−1.731***
	(0.581)	(0.394)
KDDs / 1000, Costa.Rica (Arabica)	−0.081	−1.731***
	(0.581)	(0.394)
KDDs / 1000, Nigeria (Robusta)	−0.085	−1.674***
	(0.562)	(0.382)
KDDs / 1000, Ecuador (Combined)	−0.110	−1.801***
	(0.568)	(0.364)
KDDs / 1000, El.Salvador (Arabica)	−0.081	−1.729***
	(0.581)	(0.393)
KDDs / 1000, Puerto.Rico (Combined)	−0.110	−1.801***
	(0.568)	(0.364)
KDDs / 1000, Thailand (Combined)	−0.109	−1.796***
	(0.567)	(0.363)
KDDs / 1000, Thailand (Robusta)	−0.165	−1.773***
	(0.568)	(0.386)
KDDs / 1000, Haiti (Arabica)	−0.087	−1.731***
	(0.580)	(0.393)
KDDs / 1000, Belize (Combined)	−0.110	−1.799***
	(0.568)	(0.364)
KDDs / 1000, Sierra.Leone (Robusta)	−0.239	−1.835***
	(0.563)	(0.383)
KDDs / 1000, Philippines (Combined)	−0.110	−1.801***
	(0.568)	(0.364)
KDDs / 1000, Timor.Leste (Combined)	−0.109	−1.799***
	(0.568)	(0.364)
KDDs / 1000, Colombia (Arabica)	−0.082	−1.731***
	(0.581)	(0.394)
KDDs / 1000, Burundi (Combined)	−0.110	−1.801***
	(0.568)	(0.364)

	Dependent variable:	
	Countries only	
	(1)	(2)
KDDs / 1000, Burundi (Arabica)	−0.082	−1.731***
	(0.581)	(0.394)
KDDs / 1000, Fiji (Combined)	−0.110	−1.801***
	(0.568)	(0.364)
KDDs / 1000, Madagascar (Combined)	−0.110	−1.801***
	(0.568)	(0.364)
KDDs / 1000, Nepal (Combined)	−0.110	−1.801***
	(0.568)	(0.364)
KDDs / 1000, Suriname (Combined)	−0.089	−1.779***
	(0.568)	(0.364)
KDDs / 1000, Zambia (Arabica)	−0.082	−1.731***
	(0.581)	(0.394)
KDDs / 1000, Papua.New.Guinea (Combined)	−0.110	−1.801***
	(0.568)	(0.364)
KDDs / 1000, Zimbabwe (Arabica)	−0.094	−1.742***
	(0.581)	(0.393)
KDDs / 1000, New.Caledonia (Combined)	−0.110	−1.801***
	(0.568)	(0.364)
KDDs / 1000, New.Caledonia (Arabica)	−0.082	−1.731***
	(0.581)	(0.394)
KDDs / 1000, Paraguay (Arabica)	−0.043	−1.660***
	(0.571)	(0.387)
KDDs / 1000, Guyana (Robusta)	−0.157	−1.766***
	(0.568)	(0.386)
KDDs / 1000, Guyana (Arabica)	−0.081	−1.730***
	(0.581)	(0.394)
KDDs / 1000, Guyana (Combined)	−0.111	−1.801***
	(0.568)	(0.364)
KDDs / 1000, Honduras (Arabica)	−0.084	−1.733***
	(0.581)	(0.394)
KDDs / 1000, Myanmar (Combined)	−0.110	−1.800***
	(0.568)	(0.364)
KDDs / 1000, Mexico (Combined)	−0.110	−1.801***
	(0.568)	(0.364)
KDDs / 1000, Congo (Robusta)	−0.165	−1.773***
	(0.568)	(0.386)
KDDs / 1000, Congo (Combined)	−0.111	−1.800***
	(0.568)	(0.364)
KDDs / 1000, Sri.Lanka (Combined)	−0.108	−1.793***
	(0.567)	(0.363)
KDDs / 1000, Comoros (Combined)	−0.110	−1.801***
	(0.568)	(0.364)
Avg. Min., Liberia (Robusta)	−0.817***	−0.873***
	(0.141)	(0.140)
Avg. Min., Gabon (Robusta)	−0.642***	−0.714***
	(0.181)	(0.180)

	Dependent variable:	
	Countries only	
	(1)	(2)
Avg. Min., Yemen (Combined)	0.402*	0.369*
	(0.208)	(0.207)
Avg. Min., Jamaica (Arabica)	0.297**	0.269**
	(0.117)	(0.116)
Avg. Min., Kenya (Arabica)	−1.325***	−1.369***
	(0.288)	(0.288)
Avg. Min., Kenya (Combined)	−0.755***	−0.794***
	(0.156)	(0.154)
Avg. Min., Malawi (Arabica)	−0.255*	−0.288**
	(0.141)	(0.140)
Avg. Min., Angola (Combined)	−0.367*	−0.400**
	(0.199)	(0.198)
Avg. Min., Angola (Robusta)	0.218**	0.178*
	(0.110)	(0.108)
Avg. Min., Malaysia (Robusta)	2.766***	2.680***
	(0.164)	(0.162)
Avg. Min., Brazil (Combined)	−0.077	−0.091***
	(34.091)	(0.020)
Avg. Min., Guinea (Robusta)	0.329***	0.300**
	(0.125)	(0.124)
Avg. Min., El.Salvador (Arabica)	−0.525***	−0.526***
	(0.145)	(0.145)
Avg. Min., Sierra.Leone (Robusta)	−1.196***	−1.197***
	(0.147)	(0.147)
Avg. Min., Suriname (Combined)	−1.532***	−1.559***
	(0.174)	(0.172)
Avg. Min., Zambia (Arabica)	−0.204	−0.237*
	(0.125)	(0.123)
Avg. Min., Congo (Robusta)	−1.389***	−1.441***
	(0.155)	(0.154)
Avg. Min., Sri.Lanka (Combined)	−0.426***	−0.402***
	(0.140)	(0.139)
Precip., Brazil (Combined)	−4.285	0.347***
	(6.691)	(0.030)
Precip., Suriname (Combined)	−12.378*	−10.271**
	(6.552)	(4.007)
Precip.^{2}, Brazil (Combined)	5.340	0.366***
	(88.871)	(0.039)
Observations	3,011	3,016
R^2	0.902	0.903
Adjusted R^2	0.885	0.886
Residual Std. Error	0.335 (df = 2561)	0.336 (df = 2566)
F Statistic	52.575*** (df = 450; 2561)	52.962*** (df = 450; 2566)
Note:		*p<0.1; **p<0.05; ***p<0.01

A.6.5 Spatially-weighting weather

To generate weather observations at the same spatial aggregation as yields, we perform the following procedure. For each political unit,

1. Translate CFSR grid cells into a lattice of points.
2. Find all grid lattice points within a given country.
3. Identify the measure of harvested area in the coffee database nearest to each lattice point.
4. Take the weighted average of weather observations, weighted by coffee harvested area.

An example is shown below for grid cells that fall within Colombia.

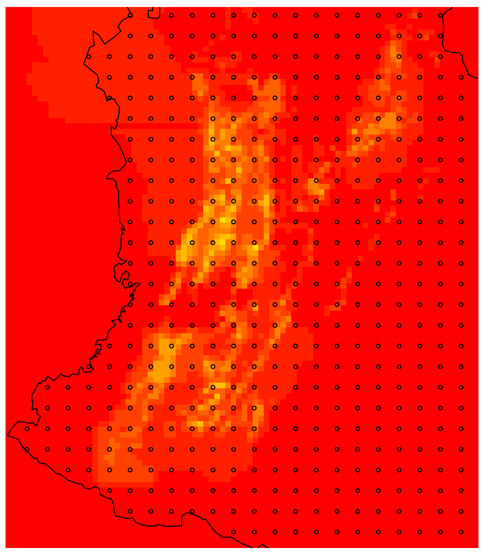

Circles show the location of CFSR grid lattice points. Colors show the coffee weights.

A.7 Extra market analysis

A.7.1 Market data

The coffee market model incorporates coffee production divided out by producer countries, coffee consumption divided out by consuming countries, and the national and international drivers of the prices paid to growers and by consumers. The following inputs are used to construct an empirically-grounded market model. All are available at least at a yearly resolution, and are here implicitly indexed by year.

q_i	Production in country i	USDA and FAO
p_i	Price to growers in country i	ICO
d_j	Consumption in country j	UN Comtrade
c_j	Retail price in country j	ICO
e_{ij}	Export from country i to j	UN Comtrade
u	International coffee price	World Bank

Below, we use a consumer price index[6] to translate prices to year 2000 US dollars, as shown for Arabica and Robusta international prices in figure A.38. Coffee consumers have enjoyed a significant reduction in prices, in real terms, since the 1970s and 1980s.

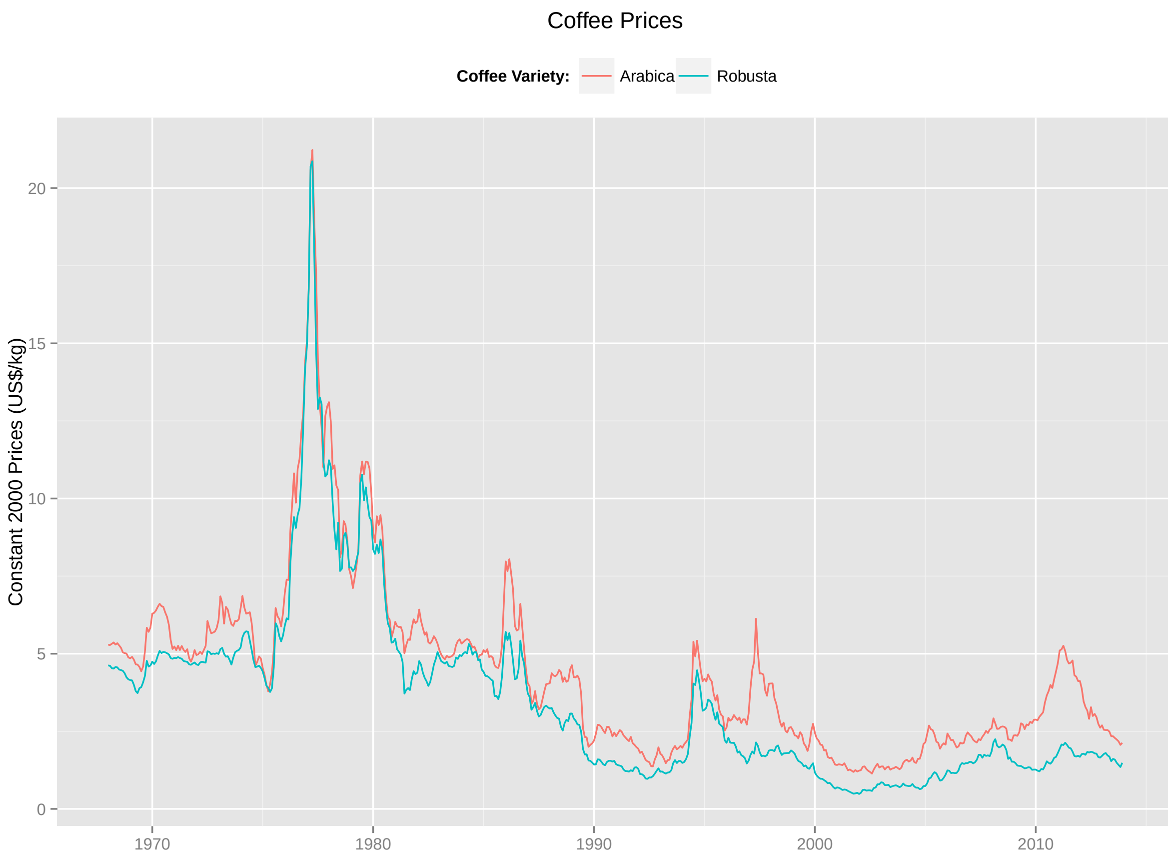

Figure A.38: Arabica and Robusta green bean coffee prices, in terms of constant year 2000 US$ per kilogram.

The following sections estimate empirical price relationships. While these are greatly simplified, they provide approximation to the drivers of the international coffee market.

A.7.2 International prices and production

International prices a partially driven by global production, but with considerable autocorrelation. The simplest form of this relationship is:

$$u = \alpha_0 + \alpha_1 \sum_i q_i + \alpha_2 u_{t-1}$$

[6]We use a single CPI across all countries, calculated by International Financial Statistics for their “All Items” goods in advanced economies.

This expression represents the fundamental driver of international coffee prices: scarcity increases prices and a glut of coffee reduces them. α_1 is negative to capture this relationship. α_2 represents the extent to which prices adjust slowly and are driven by other shocks. If α_2 is near 1, coffee prices have a long memory; while if it is near 0, they respond immediately to production changes. The result is estimated in table A.12.

	Dependent variable:	
	Arabica	Robusta
	(1)	(2)
α_0	0.059	0.074
	(0.075)	(0.060)
α_1	−0.00000	−0.00001
	(0.00001)	(0.00002)
α_2	0.988***	0.987***
	(0.007)	(0.007)
Observations	551	551
R^2	0.975	0.980
Adjusted R^2	0.975	0.980
Residual Std. Error (df = 548)	0.458	0.410
F Statistic (df = 2; 548)	10,669.730***	13,612.970***
Note:	*p<0.1; **p<0.05; ***p<0.01	

Table A.12: Estimate of the effect of production on international prices.

This estimate places the entire weight of the predictive capacity on the autoregressive term. In other words, the only significant information about the future international price is the current international price.

To improve this analysis, we model the dynamics of Arabica and Robusta stocks as a closer proxy for the driving quantities on the market, in Appendix A.7.6. We find that international prices continue to be best explained by their own internal dynamics.

A.7.3 Prices to growers

Prices to growers are affected by both international prices and local production:

$$p_i = \beta_0 + \beta_1 q_i + \beta_2 u$$

Farmers are paid more when coffee fetches a higher price on the international market ($\beta_2 > 0$) , but less if there is a relative excess of coffee produced in their country in a given year ($\beta_1 < 0$). We further allow for country-specific unexplained variation. The results of this estimate are shown in figure 3.23 and in the table in Appendix A.7.7. The data is from International Coffee Organization (2015b).

A.7.4 Consumer response to prices

We expect consumption to decrease with retail prices:

$$d_j = \gamma_0 + \gamma_1 c_j + \gamma_2 d_{j,t-1}$$

Demand does not re-calibrate immediately to changes in retail prices ($\gamma_2 > 0$), but we assume that high prices produce a downward force while low prices produce an upward force ($\gamma_1 < 0$). However, we allow for this "economic" force to be dominated by internal consumption dynamics, represented here as external demand shocks that persist through the autoregression term γ_2. These results are shown in figure 3.25 and in table A.15 in the Appendix. The data is from International Coffee Organization (2015b).

A.7.5 Retail prices follow costs

Retail costs are a composite of the costs for imports from each country, plus a markup:

$$c_j = \phi_j + \sum_i \frac{e_{ij}}{d_j} \left(p_i + \theta_i + l_{ij}\right)$$

Retailers respond to the costs of their inputs, which combine country-specific production prices (p_i), added prices for processing and tariffs (θ_i), a cost related to the transportation between them (l_{ij}), and added costs specific to the retailing country (ϕ_j). The extent to which each of the producing country variables (p_i, θ_i, l_{ij}) impact the final retail price is determined by the faction imported from each country (e_{ij}/d_j).

A.7.6 Stock analysis

As an improvement, we note that prices are determined more directly by the stocks of coffee beans available to coffee markets. Therefore, we explore adding stocks of Arabica and Robusta to the model. These are not recorded separately by variety, although the USDA Foreign Agricultural Service reports total coffee stocks. We use a Bayesian model to infer the stocks, informed simultaneously by monthly production and the ability of these stocks to inform prices. The inferred stocks are shown in figure A.39.

Reported stocks were much higher than those inferred by the model. This is because the model attempts to use low initial stocks to explain the high international coffee prices in the 1970s. Later, bursts in stock correspond closely with increases in recorded stocks– for example, in 1982, 1988, and 2003. However, the model predicts a rapid decrease in the stock after the burst, while recorded stocks remain high after each event. This could reflect the sensitivity of the market to "fresh" green beans, rather than stored ones.

The stocks are estimated simultaneously with the effect they have on the prices, thereby using the price to inform the level of stock. We further estimate the price in logs, and add an effect of the CPI (c_t), to produce our final model:

$$\log u = \alpha_0 + \alpha_1 s_i + \alpha_2 \log u_{t-1} \alpha_3 \log c_t$$

The estimates and their standard deviations are shown in table A.13. The effect of stock levels is still negative as expected, but not statistically significant. The autocorrelation in α_2 is decreased because of the other informative elements. The coefficients also suggest that as CPI increases, international prices decrease, although this might just reflect the general downward trend in prices.

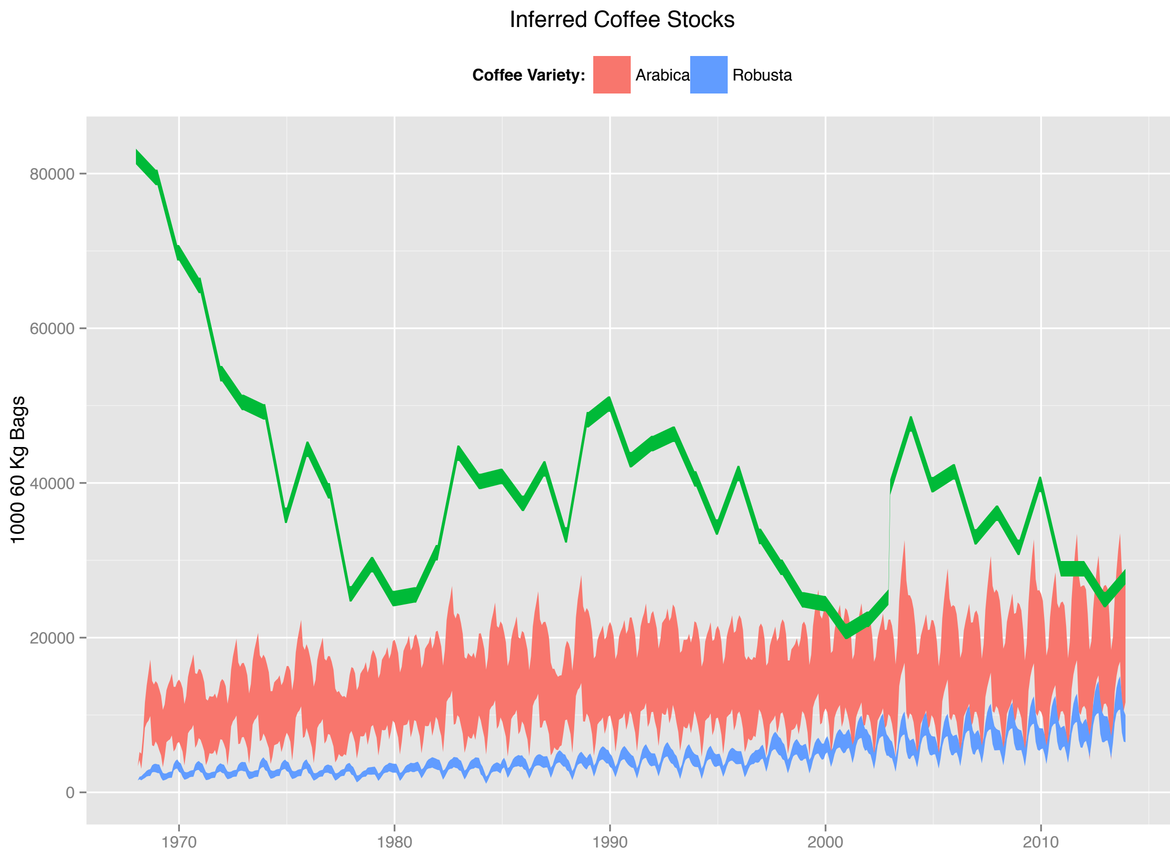

Figure A.39: Inferred stocks of Arabica (red) and Robusta (blue) coffee, compared with reported stocks (green) summed over all countries. Arabica and Robusta curves are shown with 50% confidence intervals, while the recorded curve is shown with a constant width.

	Arabica		Robusta	
	Mean	Std. Dev.	Mean	Std. Dev.
α_0	0.96	1.08	0.48	0.6
α_1	-8.47×10^{-7}	4.32×10^{-6}	-8.85×10^{-6}	1.17×10^{-5}
α_2	0.73	0.31	0.89	0.14
α_3	-0.16	0.17	-0.08	0.1

Table A.13: Coefficient estimates for the full stock model. Only α_2, the coefficient on delayed international price, is significant at a 95% level.

A.7.7 Explaining prices to farmers

Estimates for the determinants of prices to growers of coffee.

Country	Type	International	Log Product.	Int. V.E.	Prod. V.E.	Int. P(>|t|)	Prod. P(>|t|)
Colombia	Colombian Milds	16.190	-0.004	0.855	0.033	0.000	0.001
Kenya	Colombian Milds	42.872	-0.037	0.958	0.013	0.000	0.001
Tanzania	Colombian Milds	26.367	0.110	0.856	0.022	0.000	0.022
Bolivia	Other Milds	26.126	0.126	0.831	0.002	0.000	0.635
Burundi	Other Milds	13.918	0.006	0.768	0.000	0.000	0.819
Cameroon	Other Milds	17.297	-0.043	0.509	0.021	0.000	0.351
Congo, Dem. Rep. of	Other Milds	5.788	-0.148	0.275	0.708	0.297	0.098
Costa Rica	Other Milds	21.069	-0.052	0.839	0.066	0.000	0.000
Cuba	Other Milds	14.087	0.584	0.337	0.455	0.000	0.000
Dominican Republic	Other Milds	32.377	-0.040	0.937	0.006	0.000	0.046
Ecuador	Other Milds	23.186	-0.025	0.807	0.010	0.000	0.151
El Salvador	Other Milds	33.379	-0.018	0.930	0.011	0.000	0.010
Guatemala	Other Milds	20.445	-0.019	0.881	0.025	0.000	0.002
Haiti	Other Milds	19.746	0.097	0.888	0.012	0.000	0.094
Honduras	Other Milds	35.087	0.009	0.910	0.007	0.000	0.072
India	Other Milds	17.230	-0.039	0.873	0.023	0.000	0.006
Jamaica	Other Milds	18.733	1.791	0.428	0.038	0.000	0.113
Madagascar	Other Milds	0.211	-0.074	0.000	0.001	0.987	0.933
Malawi	Other Milds	28.364	0.277	0.731	0.102	0.000	0.004
Mexico	Other Milds	25.079	-0.023	0.892	0.018	0.000	0.016
Nicaragua	Other Milds	39.074	-0.010	0.877	0.001	0.000	0.641
Panama	Other Milds	13.132	-0.131	0.665	0.008	0.000	0.451
Papua New Guinea	Other Milds	21.258	-0.023	0.888	0.003	0.000	0.302
Peru	Other Milds	47.729	-0.013	0.778	0.006	0.000	0.458
Rwanda	Other Milds	13.679	0.084	0.706	0.069	0.000	0.005
Uganda	Other Milds	2.894	0.043	0.040	0.083	0.039	0.053
Venezuela	Other Milds	22.230	0.138	0.650	0.048	0.001	0.261
Zambia	Other Milds	13.538	-0.041	0.559	0.000	0.000	0.852
Zimbabwe	Other Milds	14.874	3.177	0.681	0.055	0.455	0.585
Brazil	Brazilian Naturals	22.184	0.001	0.794	0.016	0.000	0.067
Ethiopia	Brazilian Naturals	14.567	-0.006	0.765	0.015	0.000	0.097
Indonesia	Brazilian Naturals	31.851	0.005	0.528	0.001	0.011	0.919
Philippines	Brazilian Naturals	28.897	-0.040	0.414	0.001	0.005	0.901
Angola	Robustas	6.650	0.010	0.232	0.033	0.019	0.241
Benin	Robustas	0.449	-0.637	0.155	0.252	0.711	0.016
Brazil	Robustas	27.762	0.002	0.583	0.077	0.000	0.028
Burundi	Robustas	5.382	1.301	0.082	0.696	0.210	0.055
Cameroon	Robustas	10.715	0.012	0.620	0.012	0.000	0.283
Central African Republic	Robustas	7.394	0.039	0.602	0.018	0.000	0.196

Congo, Dem. Rep. of	Robustas	10.625	-0.023	0.610	0.055	0.000	0.059
Congo, Rep. of	Robustas	1.318	0.227	0.333	0.137	0.047	0.030
Côte d'Ivoire	Robustas	9.459	0.006	0.667	0.036	0.000	0.030
Ecuador	Robustas	36.988	-0.022	0.764	0.018	0.000	0.154
Gabon	Robustas	9.228	0.409	0.514	0.018	0.000	0.286
Ghana	Robustas	6.622	-0.721	0.663	0.164	0.023	0.123
Guinea	Robustas	14.037	-0.434	0.537	0.045	0.000	0.157
India	Robustas	23.426	0.007	0.743	0.043	0.000	0.030
Indonesia	Robustas	25.263	0.003	0.942	0.002	0.000	0.339
Madagascar	Robustas	6.512	0.004	0.347	0.001	0.001	0.813
Nigeria	Robustas	8.682	-0.439	0.525	0.034	0.001	0.240
Papua New Guinea	Robustas	28.154	0.028	0.783	0.000	0.000	0.923
Philippines	Robustas	23.835	-0.007	0.913	0.000	0.000	0.780
Sierra Leone	Robustas	11.475	0.181	0.563	0.034	0.000	0.245
Sri Lanka	Robustas	31.224	-0.183	0.930	0.005	0.001	0.547
Tanzania	Robustas	16.526	-0.018	0.585	0.003	0.000	0.689
Thailand	Robustas	28.468	-0.022	0.906	0.004	0.000	0.193
Togo	Robustas	5.642	0.022	0.472	0.016	0.000	0.255
Trinidad & Tobago	Robustas	24.719	0.426	0.555	0.001	0.002	0.786
Uganda	Robustas	2.255	-0.005	0.153	0.019	0.026	0.354
Vietnam	Robustas	77.812	-0.001	0.576	0.002	0.000	0.745
Global	All	25.651	-0.002	0.463	0.000	0.000	0.000

A.7.8 Explaining consumer demand

Country	Retail Pr.	Previous Yr.	Ret. V.E.	Prev. V.E.	Ret. Pr(>|t|)	Prev. Pr(>|t|)
Austria	0.01	0.35	0.00	0.13	0.88	0.14
Belgium	-0.47	1.13	0.30	0.35	0.00	0.01
Bulgaria	0.15	0.20	0.36	0.04	0.03	0.37
Cyprus	-0.02	0.23	0.07	0.05	0.24	0.28
Czech Republic	-0.01	0.69	0.00	0.32	0.37	0.01
Denmark	0.03	0.83	0.10	0.61	0.53	0.00
Finland	0.04	0.03	0.01	0.00	0.70	0.88
France	-0.00	0.66	0.02	0.42	0.95	0.00
Germany	-0.08	-0.35	0.17	0.08	0.04	0.22
Hungary	-0.06	0.86	0.02	0.68	0.07	0.00
Italy	0.02	0.79	0.11	0.49	0.74	0.00
Latvia	0.01	0.72	0.16	0.67	0.32	0.00
Lithuania	0.01	0.83	0.14	0.78	0.18	0.00
Luxembourg	-1.42	0.52	0.53	0.16	0.06	0.03
Malta	0.00	0.43	0.01	0.13	0.68	0.15
Netherlands	-0.05	0.74	0.00	0.60	0.76	0.00
Poland	0.00	0.77	0.00	0.49	0.86	0.00
Portugal	-0.02	0.79	0.14	0.67	0.14	0.00
Slovakia	0.00	-0.46	0.00	0.18	0.93	0.08
Slovenia	0.02	0.21	0.38	0.04	0.03	0.32
Spain	0.01	0.91	0.51	0.33	0.72	0.00
Sweden	-0.04	0.30	0.08	0.10	0.18	0.15
United Kingdom	0.01	0.36	0.01	0.11	0.80	0.35
Japan	0.00	0.78	0.56	0.17	0.64	0.00
Norway	0.03	0.23	0.03	0.05	0.58	0.34
Switzerland	-0.04	0.58	0.44	0.12	0.27	0.02
Turkey	-0.00	1.02	0.16	0.50	0.82	0.00
USA	-0.01	0.12	0.07	0.01	0.35	0.64
Global	-0.01	0.70	0.01	0.92	0.08	0.00

Table A.15: Determinants of consumption of coffee.

A.7.9 Inferred markups

Producer country markups

Mark-ups over the prices paid to farmers, by producer country, in US cents per pound. These are estimated simultaneous with the consumer country mark-ups.

Country	To Farmers	Mark Up	Std. Dev.
Bolivia	148.59	223.80	112.91
Brazil	107.06	84.80	31.14
Burundi	91.43	242.62	113.93
Cameroon	79.02	239.24	105.61
Sri Lanka	59.24	228.88	117.07
Colombia	124.50	194.32	70.11

Country	To Farmers	Mark Up	Std. Dev.
Congo, Dem. Rep. of	52.37	257.35	116.00
Costa Rica	137.20	214.23	102.04
Cuba	212.77	256.45	122.19
Dominican Republic	135.59	236.17	113.14
Ecuador	110.42	246.34	115.02
El Salvador	113.71	204.70	99.97
Ethiopia	101.05	168.01	94.98
Gabon	84.70	228.00	113.03
Ghana	108.59	244.26	121.38
Guatemala	137.95	102.30	70.70
Guinea	126.11	212.57	109.47
Haiti	91.81	229.51	114.36
Honduras	126.66	292.54	113.00
Indonesia	97.53	339.22	88.09
Côte d'Ivoire	63.74	226.83	96.66
Jamaica	262.39	239.55	116.14
Kenya	198.15	239.01	109.90
Madagascar	72.44	218.01	109.38
Malawi	77.87	235.31	117.05
Mexico	155.06	221.07	106.49
Nicaragua	139.47	182.82	96.48
Panama	149.15	235.36	106.61
Papua New Guinea	102.78	177.36	100.33
Peru	123.27	243.61	106.00
Rwanda	95.20	230.81	113.27
India	114.96	196.25	92.03
Vietnam	120.97	29.68	25.36
Thailand	93.03	268.90	122.50
Togo	55.70	225.31	108.66
Uganda	44.89	246.98	80.22
Tanzania	111.59	254.27	120.02
Venezuela	258.16	230.70	115.24
Zambia	110.58	219.19	112.56
Congo, Rep. of	33.52	226.88	120.91
Nigeria	118.40	228.59	114.78
Sierra Leone	111.94	234.04	110.40
Zimbabwe	408.97	234.58	118.08
Central African Republic	58.13	229.93	116.94
Trinidad & Tobago	173.12	228.67	114.16
Philippines	107.48	241.64	119.16
Angola	77.44	255.29	117.56
Benin	63.19	233.40	112.44
Liberia	NA	234.01	115.80
(Processed)	NA	254.26	34.22

Consumer country markups

Country	To Farmers	Distribution	Retail	Mark Up	Std. Dev.
Austria	89.40	184.31	448.67	175.07	34.15
Belgium	79.54	173.86	392.38	139.93	38.09
Bulgaria	74.88	208.52	283.88	31.51	25.96
Cyprus	86.47	112.54	429.70	230.73	35.58
Denmark	84.43	179.78	447.29	184.20	33.37
Finland	93.54	162.29	309.97	58.43	31.33
France	82.91	176.00	283.45	37.98	26.30
Germany	83.16	136.86	380.83	162.09	35.53
Hungary	68.32	205.45	387.22	114.71	39.63
Italy	81.08	132.38	571.66	356.53	37.01
Latvia	82.82	249.52	441.37	109.76	42.82
Lithuania	86.29	248.47	422.60	89.78	43.23
Luxembourg	87.45	254.18	559.21	217.24	48.44
Malta*	92.70	228.81	1019.96	692.57	41.21
Netherlands	88.05	192.84	366.49	86.88	34.92
Poland	71.99	178.79	317.54	70.10	32.04
Portugal	74.36	202.26	484.34	206.79	34.62
Slovakia	76.42	219.32	342.90	54.81	31.93
Slovenia	77.50	144.39	367.10	146.78	38.11
Spain	77.46	165.04	350.89	109.90	31.78
Sweden	93.92	168.28	350.25	89.53	34.55
United Kingdom*	81.04	190.61	1354.07	1070.48	37.39
Japan	91.23	182.71	1107.51	828.59	35.21
Norway	98.18	152.83	372.36	122.48	36.67
Switzerland	84.83	184.49	524.88	254.33	35.19
Turkey	91.25	99.09	416.92	226.54	39.70
USA	85.46	133.48	345.80	127.57	37.40

Table A.17: Mark-ups over the prices paid to farmers, by consumer country, in US cents per pound. These are estimated simultaneous with the producer country mark-ups.

A.7.10 Economic importance of coffee

Country	Variety	Farm ($/kg)	Itnl. ($/kg)	Production (kg)	Local Value ($)	Intl Value ($)	GDP ($)	(%)
Angola	arabica	0.82	2.74	0	0	0	44080659100	0.00
Angola	robusta	0.59	1.46	1698000	1004067	2483891	44080659100	0.01
Bolivia	arabica	3.70	2.74	8442000	31232762	23162986	11362240323	0.20
Brazil	arabica	2.12	2.74	2026500000	4294893862	5560268994	1019917358692	0.55
Brazil	robusta	1.39	1.46	711900000	991280609	1041391089	1019917358692	0.10
Burundi	arabica	1.28	2.74	16026000	20465292	43971809	1320071226	3.33
Burundi	robusta		1.46	0		0	1320071226	0.00
Cameroon	arabica	1.41	2.74	5532000	7807333	15178588	18629569264	0.08
Cameroon	robusta	0.97	1.46	39630000	38314825	57972087	18629569264	0.31
Central African Republic	robusta	0.91	1.46	1518000	1378446	2220581	1631792478	0.14
Colombia	arabica	2.38	2.74	597966000	1422490591	1640686804	175186920716	0.94
Congo, Dem. Rep. of	arabica		2.74	5262000		14437767	14788569483	0.10
Congo, Dem. Rep. of	robusta		1.46	11724000		17150259	14788569483	0.12
Congo, Rep. of	robusta		1.46	0		0	7163015187	0.00
Costa Rica	arabica	2.15	2.74	104058000	223638738	285512199	23899924562	1.19
Côte d'Ivoire	robusta	0.61	1.46	121800000	73750900	178173107	18513289732	0.96
Cuba	arabica	1.39	2.74	7740000	10766855	21236853	49991611345	0.04
Dominican Republic	arabica	2.14	2.74	27162000	58194207	74526537	42066031892	0.18
Ecuador	arabica	2.45	2.74	25110000	61503896	68896301	47883528950	0.14
Ecuador	robusta	1.30	1.46	17400000	22547442	25453301	47883528950	0.05
El Salvador	arabica	1.70	2.74	87264000	148428732	239433167	18219072282	1.31
Ethiopia	arabica	1.47	2.74	315408000	465181914	865409979	18472707950	4.68
Ghana	robusta		1.46	2214000		3238713	14161252979	0.02
Guatemala	arabica	2.24	2.74	232476000	521865895	637862864	31344823589	2.03
Guinea	robusta		1.46	23412000		34247855	3208509564	1.07
Haiti	arabica		2.74	19368000		53141520	4429227578	1.20
Honduras	arabica	1.92	2.74	227994000	438103331	625565245	11134160781	5.62
India	arabica	2.35	2.74	98028000	230277245	268967209	1109531099998	0.02
India	robusta	1.43	1.46	187410000	268898827	274149605	1109531099998	0.02
Indonesia	arabica	2.09	2.74	69150000	144393359	189732347	353469522531	0.05
Indonesia	robusta	0.82	1.46	461700000	377800422	675390175	353469522531	0.19
Jamaica	arabica	5.55	2.74	1686000	9360707	4626012	11075778481	0.04
Kenya	arabica	1.45	2.74	47946000	69690082	131553248	22500842427	0.58
Liberia	robusta		1.46	1836000		2685762	839609172	0.32
Madagascar	arabica	0.99	2.74	1632000	1611367	4477848	5652013484	0.08
Madagascar	robusta	0.79	1.46	30264000	23879354	44271190	5652013484	0.78
Malawi	arabica	1.54	2.74	1560000	2402418	4280296	3465670842	0.12
Mexico	arabica	2.00	2.74	251100000	502945556	688963012	943131575944	0.07
Nicaragua	arabica	1.17	2.74	99240000	115978241	272292670	7096139115	3.84
Nigeria	robusta		1.46	2226000		3256267	144037995041	0.00

Country	Variety	Farm ($/kg)	Itnl. ($/kg)	Production (kg)	Local Value ($)	Intl Value ($)	GDP ($)	(%)
Panama	arabica		2.74	7044000		19327182	21253648150	0.09
Papua New Guinea	arabica	1.59	2.74	59610000	94843298	163556691	6141247952	2.66
Papua New Guinea	robusta	0.56	1.46	2748000	1542012	4019866	6141247952	0.07
Peru	arabica	1.13	2.74	224640000	253661686	616362609	96436263271	0.64
Philippines	arabica	2.01	2.74	1950000	3915230	5350370	123566704265	0.00
Philippines	robusta	1.33	1.46	27990000	37124998	40944707	123566704265	0.03
Rwanda	arabica	0.76	2.74	17640000	13479953	48400269	3504265695	1.38
Sierra Leone	robusta	0.44	1.46	3414000	1517699	4994113	1998841063	0.25
Sri Lanka	arabica		2.74	594000		1629805	31081582880	0.01
Sri Lanka	robusta		1.46	1446000		2115257	31081582880	0.01
Tanzania	arabica	0.91	2.74	31134000	28441963	85424828	18155123928	0.47
Tanzania	robusta	0.38	1.46	19248000	7401039	28156617	18155123928	0.16
Thailand	arabica	3.50	2.74	0	0	0	199643270642	0.00
Thailand	robusta	1.30	1.46	53166000	69270076	77773000	199643270642	0.04
Togo	robusta	0.96	1.46	20520000	19786230	30017341	2406177565	1.25
Trinidad & Tobago	robusta		1.46	336000		491512	18345375584	0.00
Uganda	arabica	1.37	2.74	37038000	50823541	101624102	12065197411	0.84
Uganda	robusta	1.03	1.46	143748000	148064470	210279374	12065197411	1.74
Venezuela	arabica		2.74	50298000		138006617	171452404755	0.08
Vietnam	arabica	1.47	2.74	30684000	45130389	84190128	72353243154	0.12
Vietnam	robusta	1.26	1.46	1108206000	1395836280	1621120737	72353243154	2.24
Zambia	arabica	1.91	2.74	3132000	5972119	8593517	11256721495	0.08
Zimbabwe	arabica		2.74	2538000		6963712	5603223515	0.12

Appendix B

Coffee production database

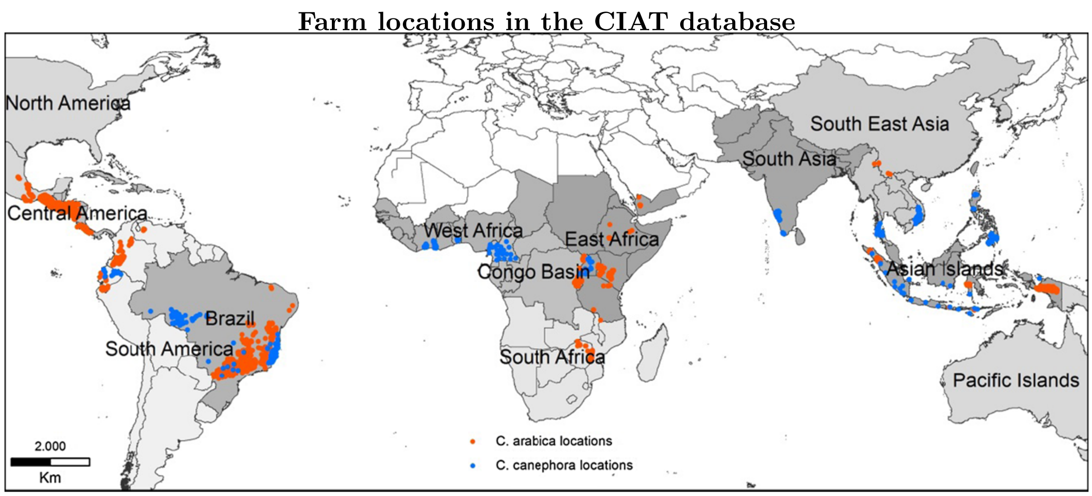

Figure B.1: Arabica and Robusta coffee producing farms in the CIAT database.

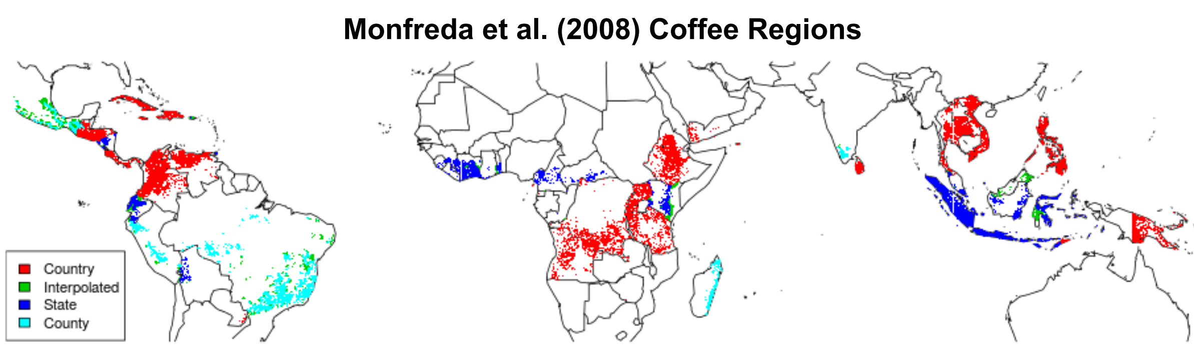

Figure B.2: Quality of geospatial production data for coffee, from Monfreda et al. (2008). Global agricultural areas are intersected with country-specific datasets to create a global map of coffee production areas.

B.0.1 Confidence maps

The first result of the database is its own measure of confidence in the geographic data across the globe. The confidence maps reflect the combined amount of information available, across the multiple map inputs. Each contributing map is assigned its own confidence, with maps of global harvest having low or medium confidence and maps detailing a given country with high confidence. Where multiple input maps corroborate each other, the confidence increases (see appendix B.2.1). In figure B.3, dark green represents low confidence, and yellow and tan colors represent high confidence. The band of lighter green in the middle shows the overlap between maps from Thurston et al. (2013), Monfreda et al. (2008), and Bunn et al. (2015).

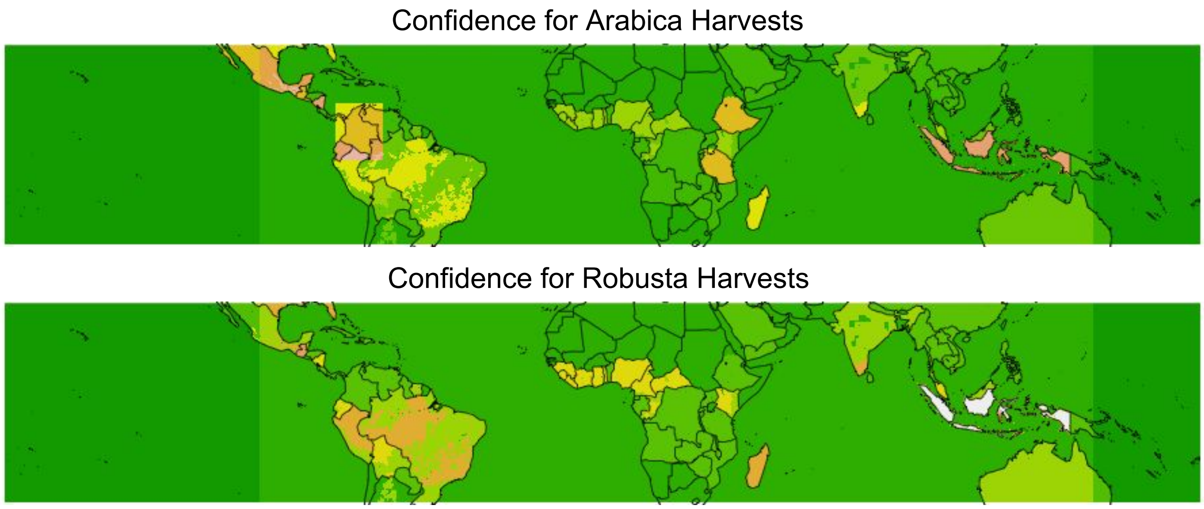

Figure B.3: Database geospatial harvest confidence, based on the amount and scale of data available.

B.0.2 Harvest maps

The harvest maps are the main output of the spatial portion of coffee database. For each month, these combine country-specific information (some of which specifies harvest months as they differ across the country), with global harvesting regions applied to a calendar of harvest months from Sweet Maria (2015). Some country calendars are unavailable, so these harvested regions show throughout the year. The added weight of these multiple instances will be handled next.

To provide a visual summary of the combined harvest maps, we use average country-wide total harvest areas from FAO to translate harvest patterns to units of harvested hectares. Where information is detailed, hectare harvests in intensely cultivated coffee regions approach the land area of the grid cells. Where only diffuse, country-level data is available, the entire country has a uniform low average harvested area. These values are used as weights to aggregate climate impacts when comparing country production with spatially distributed weather data.

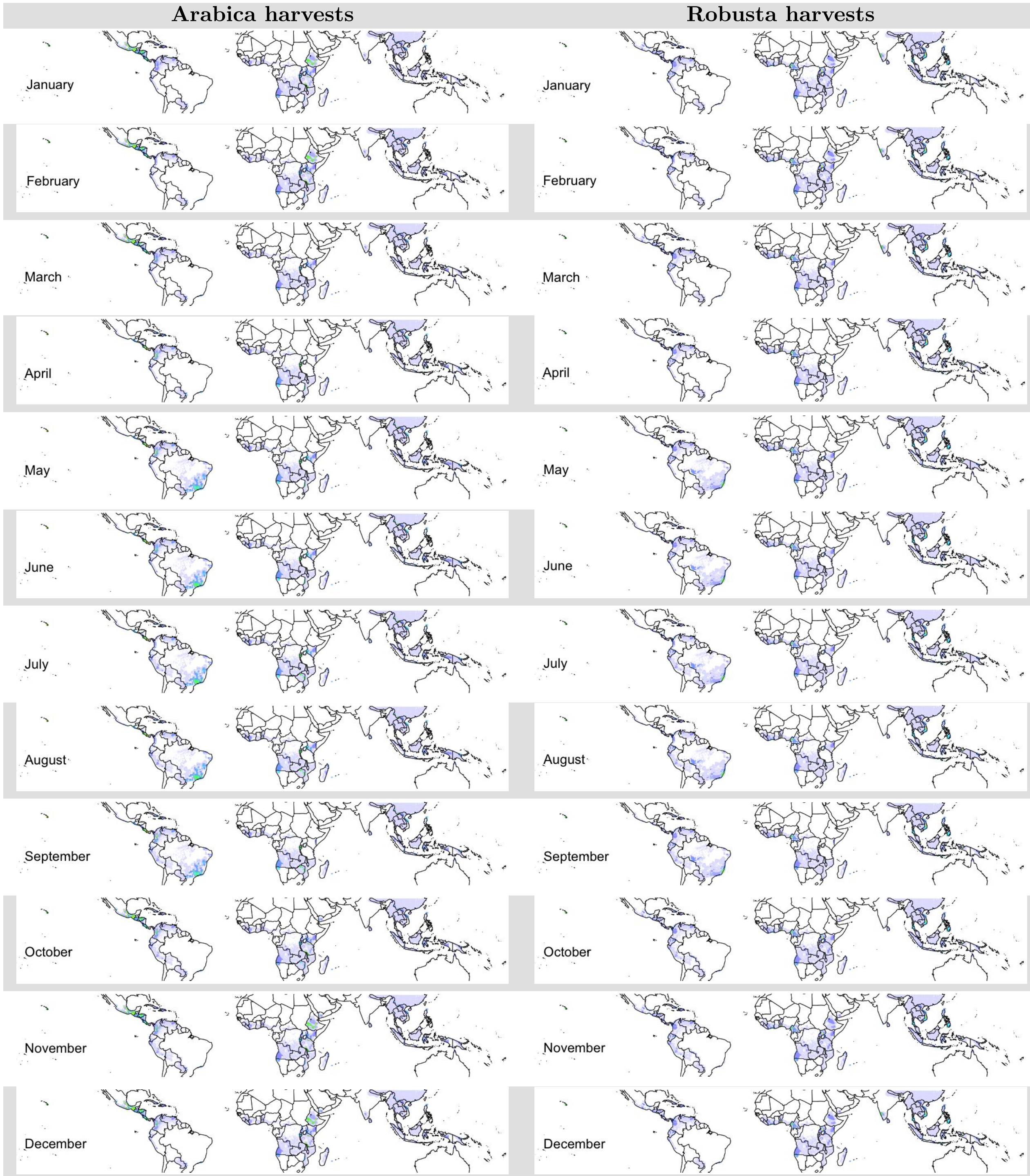

Figure B.4: Harvest maps for Arabica and Robusta varieties, during each month. Darker colors represent higher levels of evidence that these regions are undergoing harvest in the given month.

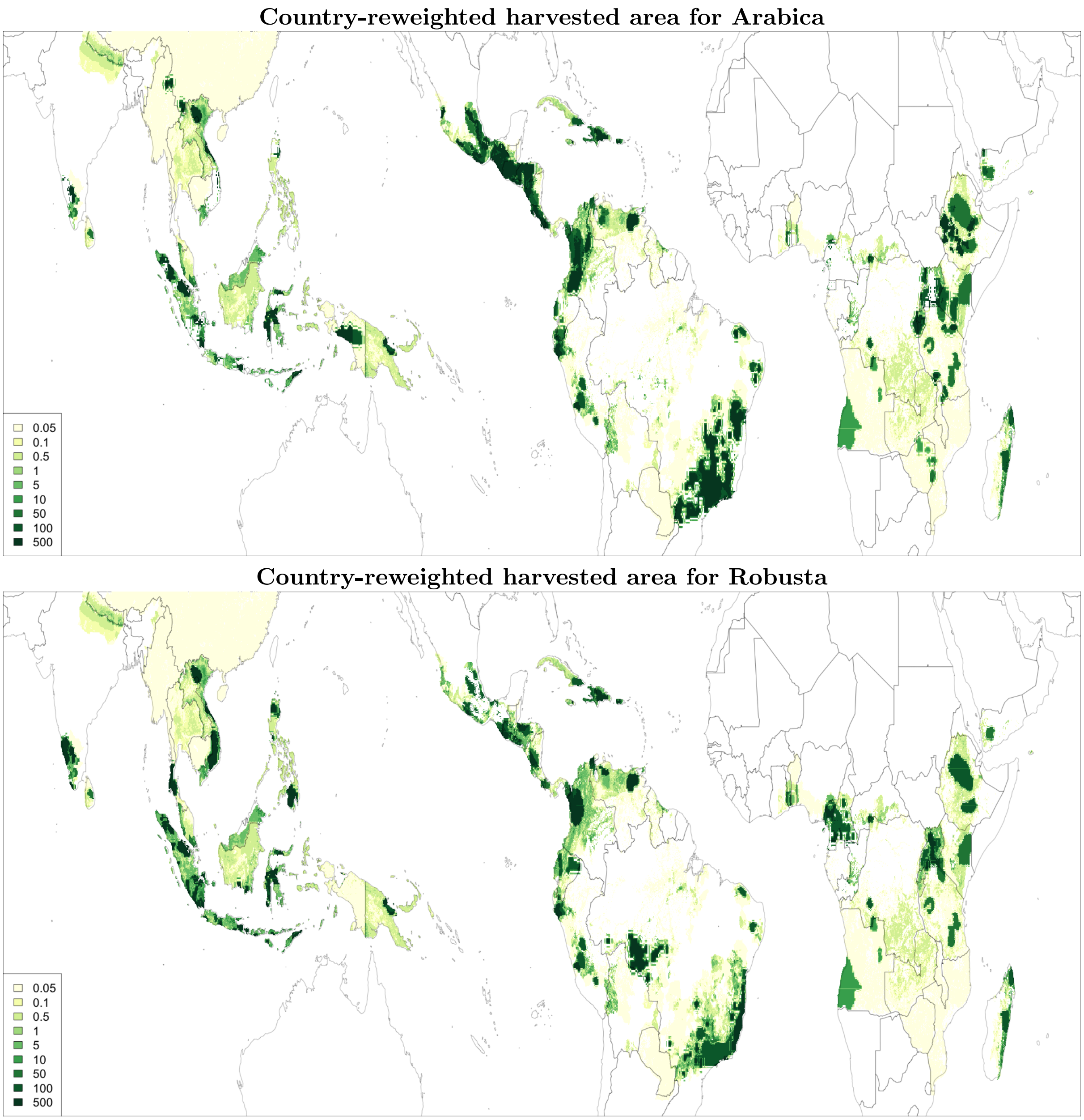

Figure B.5: Harvest maps combined across all months, and re-weighted so that the sum of grid cell values within a country is equal to the average harvested area in the most recent year of harvest.

B.0.3 Time series data

Both FAO and the USDA Foreign Agricultural Service report production information for coffee, but the information they provide is quite different. FAO reports total production and harvested area, for all varieties of coffee combined, with a total of 4242 observations. The USDA reports only production information, but divides it out by Arabica and Robusta production, with 3211 observations per variety. The number of countries included also varies by year (see figure B.6).

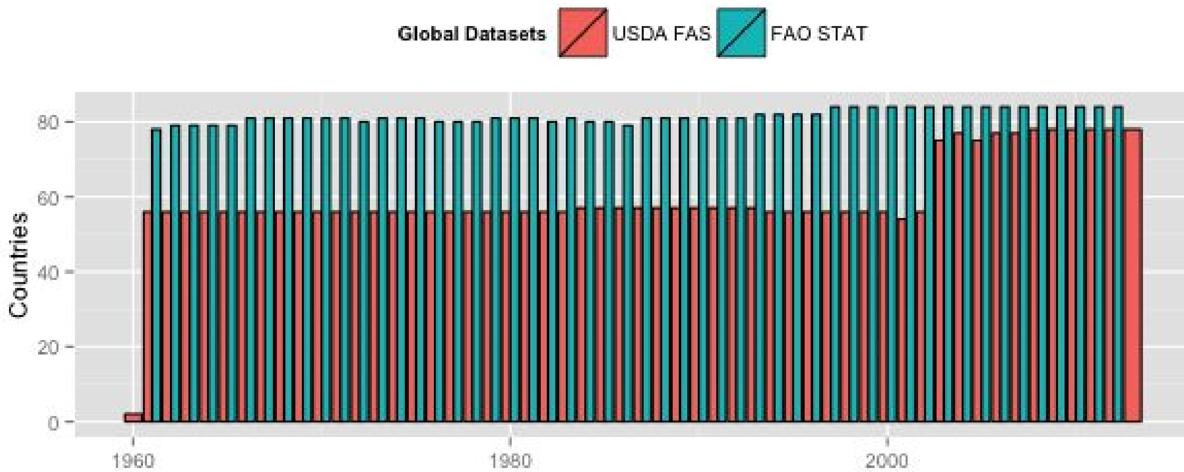

Figure B.6: The number of countries with coffee production data available by year.

A second complication arises from the definition of the reported year. FAO reports production for calendar years, while USDA reports it for market years which vary by country. This can be an opportunity, allowing us to determine more precisely when production occurs. For example, in Brazil, coffee is harvested mainly between May and September. However, the USDA market year for Brazil is from July to June. So, discrepancies between the FAO and USDA production totals allow us to distinguish, approximately, between the share of production before and after July, the start of the market year cycle.

Calculating intra-year production

The diagram below shows how the USDA and FAO calendars align. The actual division is different for each country, depending on the start of the USDA market year.

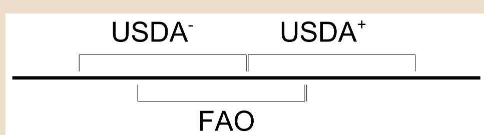

We divide each USDA value into "left" and "right" parts, with $USDA^L = \alpha USDA$ and $USDA^R = (1-\alpha)USDA$, where the coefficient α is unknown. Further, we know from the diagram that $USDA^R_- + USDA^L_+ = FAO$; that is, the FAO year consists of the 'right' (latter) portion of one market year and the 'left' (early) portion of the next one. Finally, we can use the difference to estimate α from

$$FAO_t - USDA_{t+} = \alpha(USDA_{t-} - USDA_{t+}) + \epsilon_t$$

We estimate this division for each country. In the case of Brazil, we find that 12% of production occurs between May and June, and 88% between July and September. A full table of these portions is shown in table B.1. Where there are blanks, the two datasets could not be consistently combined.

Using these values, we can construct a monthly timeseries of production, as shown in figure B.7.

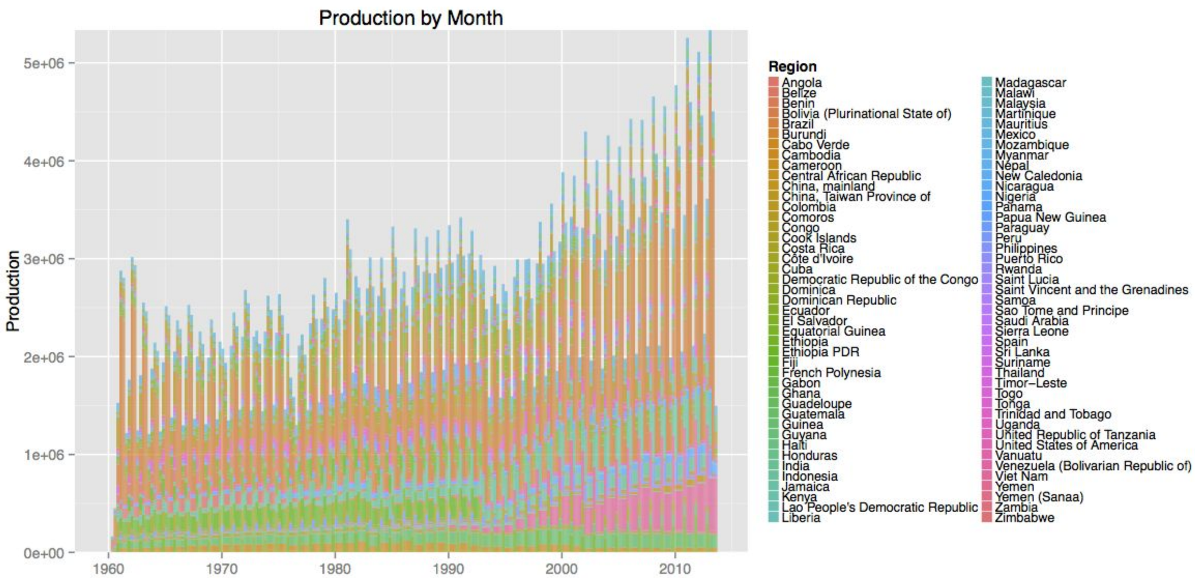

Figure B.7: Production by month and country, inferred by the discrepancies between USDA FAS and FAO accounting systems.

The coffee database consists of paired production and growing region files. The database consists of both the final files and the code for generating standardized versions of input source files. The standardized versions have the same format as the merged database.

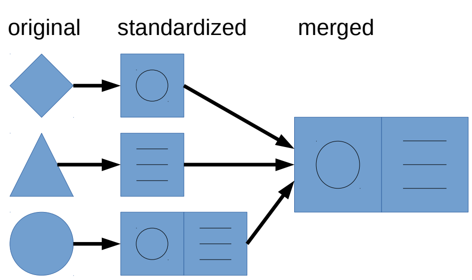

The coffee database is available in a sharable form, at `https://bitbucket.org/jrising/coffeedb/`. Request for access.

	Market Year	Previous Year	Following Year	Std. Err.
Brazil	Jul - Jun	0.12	0.88	0.05
Madagascar	Apr - Mar	0.50	0.50	0.25
Kenya	Oct - Sep	0.91	0.09	0.04
Guinea	Oct - Sep	0.37	0.63	0.33
Panama	Oct - Sep	0.68	0.32	0.28
Costa Rica	Oct - Sep	0.50	0.50	0.06
Ethiopia	Oct - Sep			
Rwanda	Apr - Mar	0.17	0.83	0.08
United Republic of Tanzania	Jul - Jun	0.67	0.33	0.11
Sri Lanka	Oct - Sep			
Peru	Apr - Mar	0.07	0.93	0.10
Lao People's Democratic Republic	Oct - Sep			
Bolivia (Plurinational State of)	Apr - Mar			
Cameroon	Oct - Sep	0.09	0.91	0.11
Côte d'Ivoire	Oct - Sep	0.89	0.11	0.07
Ecuador	Apr - Mar	0.41	0.59	0.25
Benin	Oct - Sep	0.60	0.40	0.20
Ghana	Oct - Sep	0.80	0.20	0.16
Cuba	Jul - Jun	0.46	0.54	0.16
El Salvador	Oct - Sep	0.40	0.60	0.05
Venezuela (Bolivarian Republic of)	Oct - Sep	0.57	0.43	0.15
Papua New Guinea	Apr - Mar	0.26	0.74	0.07
Malawi	Oct - Sep	0.10	0.90	0.16
Togo	Oct - Sep	0.44	0.56	0.16
Guatemala	Oct - Sep	0.42	0.58	0.17
Zimbabwe	Oct - Sep	0.19	0.81	0.10
Viet Nam	Oct - Sep	0.63	0.37	0.07
Dominican Republic	Jul - Jun	0.55	0.45	0.15
Nigeria	Oct - Sep	0.68	0.32	0.19
Liberia	Oct - Sep	0.56	0.44	0.14
Democratic Republic of the Congo	Oct - Sep	0.61	0.39	0.14
Paraguay	Oct - Sep	0.60	0.40	0.34
Trinidad and Tobago	Oct - Sep	0.77	0.23	0.10
Philippines	Jul - Jun			
Indonesia	Apr - Mar	0.23	0.77	0.29
Central African Republic	Oct - Sep	0.22	0.78	0.14
New Caledonia	Oct - Sep			
United States of America	Oct - Sep	0.19	0.81	0.65
Guyana	Oct - Sep			
Honduras	Oct - Sep	0.56	0.44	0.08
Yemen	Oct - Sep	0.36	0.64	0.86
Haiti	Jul - Jun	0.36	0.64	0.19
Thailand	Oct - Sep	0.77	0.23	0.07
Jamaica	Oct - Sep	0.69	0.31	0.98
Angola	Apr - Mar	0.62	0.38	0.11
Equatorial Guinea	Oct - Sep			
Mexico	Oct - Sep	0.62	0.38	0.22
India	Oct - Sep	0.98	0.02	0.02
Sierra Leone	Oct - Sep	0.98	0.02	0.60
Malaysia	Oct - Sep	0.58	0.42	0.33
Congo	Oct - Sep	0.28	0.72	0.26
Colombia	Oct - Sep	0.72	0.28	0.06
Burundi	Apr - Mar	0.06	0.94	0.09
Gabon	Oct - Sep	0.23	0.77	0.17
Uganda	Oct - Sep	0.83	0.17	0.09
Nicaragua	Oct - Sep	0.13	0.87	0.08
Zambia	Oct - Sep	0.93	0.07	0.35

Table B.1: Portion of the production for each market year attributed to the previous calendar year and to the next one.

B.1 Standardized format

B.1.1 Growing Region Files

Growing regions are stored as raster (gridded) files describe "masks" of which regions are under harvest in a given month. They are at a resolution of 12 pixels per degree (a grid width of 5 minutes), and cover the entire area from 180°W to 180°E longitude, and 30°S to 30°N latitude.

The grids are stored as NetCDF files. Each NetCDF file contains a "harvest" variable and a "confidence" variable. The harvest variable specifies areas under harvest in a given month, and has dimensions Longitude x Latitude x 12, with a separate mask for each month. Values may range between 0 and 1, based on how much evidence there is of harvest there. The confidence mask describes the level of confidence in the information, also from 0 to 1.

Note that neither the "harvest" nor "confidence" variables describe the portion of a given grid cell under harvest. Instead, both relate to the evidence that the grid cell contains areas under harvest. The difference between the harvest value and confidence value is expanded upon in the Merging Growing Region Files section.

B.1.2 Production Files

Production data consists of a `.csv` file that specifies the production, planted area, harvested area, and yields (as data is available for each) in a given year and a given region. Where the data describes sub-country regions, an additional region definition file (`*-regions.csv`) and a shapefile database (collections of a `.shp`, `.shx`, and `.dbf` file) describe an association between the production records and growing regions. Each polygon in the shapefile database identifies a region for which production data is available in one or more years, and region definition files specify which region is described in each record.

The production file has the following column header:

```
year,region,variety,produced,prod-se,harvested,harv-se,planted,plant-se,yield,yield-se
```

`year` is the year being described. Not all years need to be represented for a region. `variety` is Arabica, Robusta, or combined. `region` is the region identifier in the associated region definitions file. This may change across years. `produced` is the calendar year production, measured in metric tonnes. `prod-se` is the standard error of the production estimate. It may be `NA` if the error estimate is available, but this will cause any other estimate to be chosen over it if one is available. `harvested` is the harvested area in hectares, and `harv-se` is its standard error. This may be `NA`. `planted` is the planted area in hectares, and `plan-se` is its standard error. This may be `NA`. `yield` is the yield in terms of MT per hectare, and `yield-se` is its standard error. The yield is computed as production divided by planted area. This may be `NA`.

The region definitions file has the following column header:

```
region,PID,weight
```

`region` is a region identifier, unique across the entire database. If there are multiple rows with the same region identifier, all of these PIDs will be combined in the region. `PID` is a polygon IDs in the associated growing region file. The same `PID` may occur in multiple regions, since different regions may be used to describe different years. `weight` is a measure of the accuracy of the production region definitions. In general, `weight` is calculated as *(mean planted area) / (total polygon area)*, and is between 0 (no confidence) and 1 (full confidence).

B.2 Generating merged database files

B.2.1 Merging growing region files

Region definition files are merged according to the weight of evidence of harvest in each month. At every point, the new weight in the combined region definitions is,

$$w(x,y) = \sum_i \frac{w_i(x,y)c_i(x,y)}{c_i(x,y)}$$
$$c(x,y) = \sum_i c_i(x,y)$$

This formulation allows confidence to increase where multiple data sources are available, and causes contradictory maps (for example, one that says that coffee is grown in a region and one that says it is not) to result in averaged values.

	Arabica 1	Arabica 0	Combined 1	Combined 0
Arabica 1, Robusta 0	1, 0	0.5, 0	1, 0	0.5, 0
Arabica 0, Robusta 0	0.5, 0	0, 0	0.5, 0.5	0, 0

Additional logic is used where maps that describe Arabica and Robusta growth separately are combined with those that lump them together.

B.2.2 Merging production files

Production files are merged using a Bayesian approach, with a uniform prior. Each estimate (a given year-region value for production, harvested area, or planted area) is translated into a distribution, $p(y_i)$. Then the merged estimate of production is,

$$p(y) = \prod_i p(y_i)$$

This allows the database to account for uncertainty in the estimates, as well as allowing corroborating records to decrease the amount of uncertainty. Additional logic used where time series that split out Arabica and Robusta growth (such as the USDA Foreign Agricultural Service) are combined with ones that lump them together (such as FAO).

Combining estimates

1. Associate uncertainty with each observation ($k\sqrt{v_{it}}$).
2. Case 1: Same or Combined + (Arabica or Robusta):

$$\mu* = \frac{\frac{\mu_1}{\sigma_1^2} + \frac{\mu_2}{\sigma_2^2}}{\frac{1}{\sigma_1^2} + \frac{1}{\sigma_2^2}}$$
$$\sigma*^2 = \frac{\sigma_1^2\sigma_2^2}{\sigma_1^2 + \sigma_2^2}$$

3. Case 2: Combined + Arabica + Robusta:

$$\max_{a,r} \mathcal{N}(a|\mu_a, \sigma_a)\mathcal{N}(r|\mu_r, \sigma_r)\mathcal{N}(a+r|\mu_c, \sigma_c)$$

σ_a* and σ_r* from Inverse Hessian.

B.3 Production maps

We performed a geospatial matching between diagrams in the gray literature and countries maps.

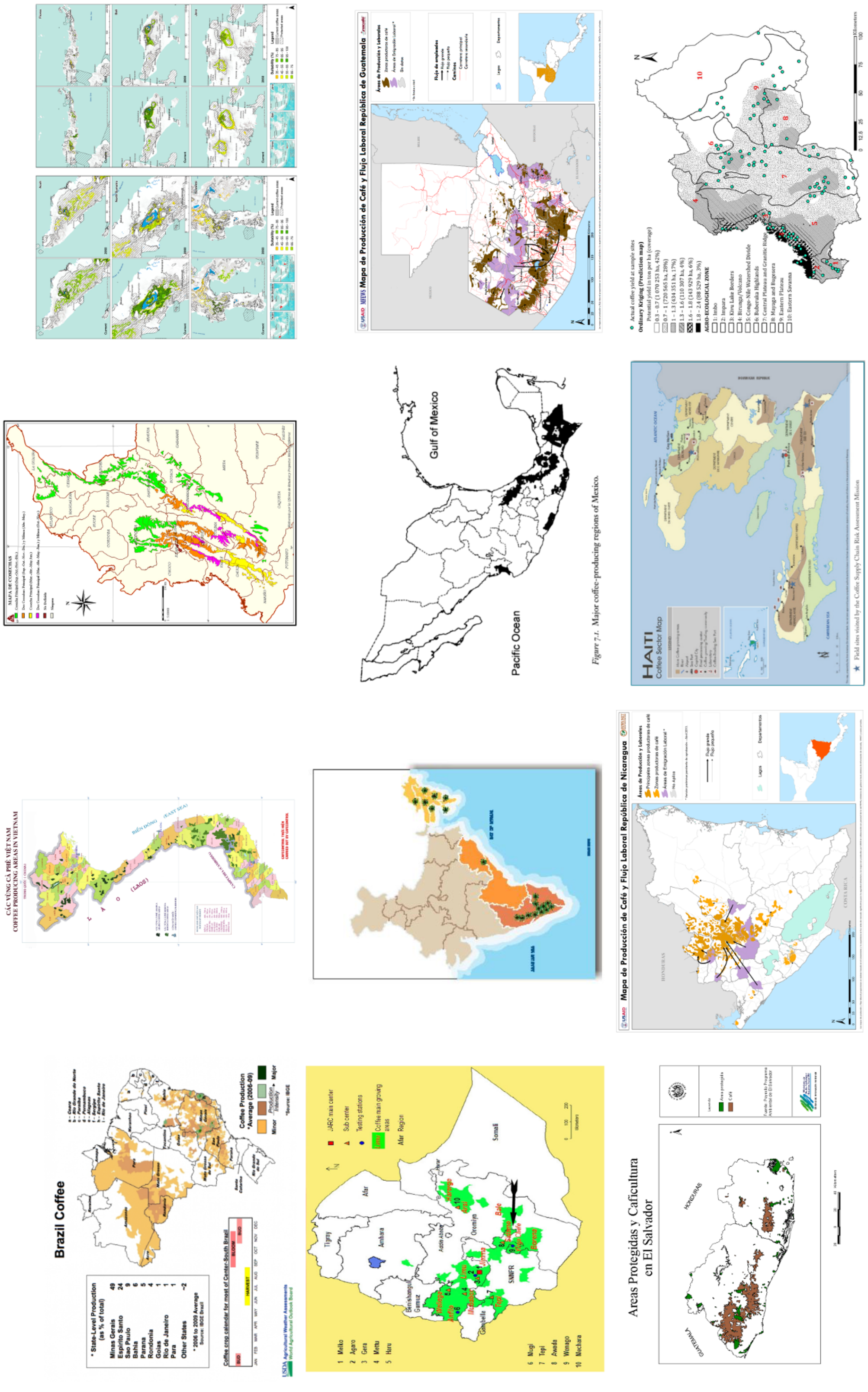

Figure B.8: Coffee growing region maps for Brazil, Vietnam, Colombia, Indonesia, Ethiopia, India, Mexico, Guatemala, El Salvador, Nicaragua, Haiti, and Rwanda, collected from various sources (see main text for the table).

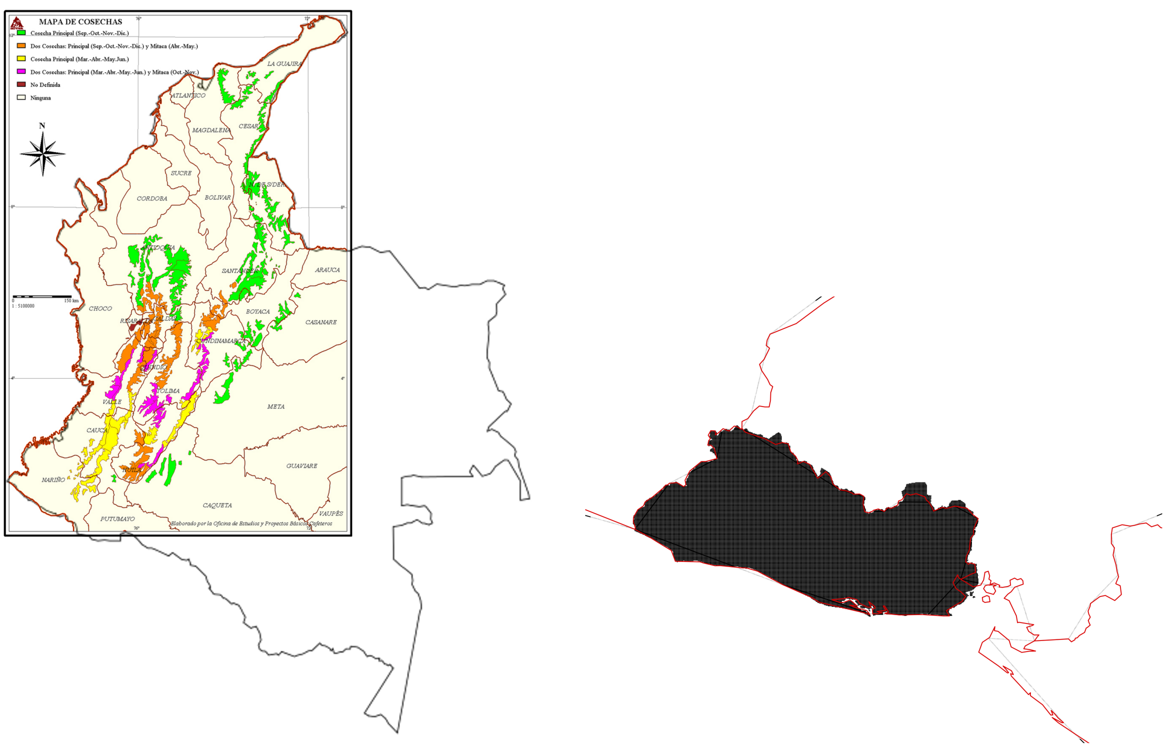

Figure B.9: Two examples of the geospatial matching process, using hand correspondences for Colombia (left) and country-wide shape matching for El Salvador (right).

Bibliography

Alves, M. d. C., de Carvalho, L., Pozza, E., Sanches, L., and Maia, J. d. S. (2011). Ecological zoning of soybean rust, coffee rust and banana black sigatoka based on brazilian climate changes. *Procedia Environmental Sciences*, 6:35–49.

Arbenz, P. (2013). Bayesian copulae distributions, with application to operational risk management—some comments. *Methodology and Computing in Applied Probability*, 15(1):105–108.

Baca, M., Läderach, P., Haggar, J., Schroth, G., Ovalle, O., et al. (2014). An integrated framework for assessing vulnerability to climate change and developing adaptation strategies for coffee growing families in mesoamerica. *PloS one*, 9(2):e88463.

Baker, P. S. (2013). Coffee as a global system. In *Coffee: A Comprehensive Guide to the Bean, the Beverage, and the Industry*.

Bell, G. D., Halpert, M. S., Kousky, V. E., Gelman, M. E., Ropelewski, C. F., Douglas, A. V., and Schnell, R. C. (1999). Climate assessment for 1998. *Bulletin of the American Meteorological Society*, 80(5):1040–1040.

Bernardes, T., Moreira, M. A., Adami, M., Giarolla, A., and Rudorff, B. F. T. (2012). Monitoring biennial bearing effect on coffee yield using modis remote sensing imagery. *Remote Sensing*, 4(9):2492–2509.

Bunn, C., Läderach, P., Rivera, O. O., and Kirschke, D. (2015). A bitter cup: climate change profile of global production of arabica and robusta coffee. *Climatic Change*, 129(1-2):89–101.

Burke, M. and Emerick, K. (2012). Adaptation to climate change: Evidence from us agriculture. *Available at SSRN 2144928*.

CIAT (2010). Climate adaptation and mitigation in the kenyan coffee sector. Technical report, International Center for Tropical Agirculture, Cali, Colombia.

coffee&climate (2015). Climate change adaptation in coffee production. Technical report.

Comtrade, U. (2015). United nations commodity trade statistics database. Available at `http://comtrade.un.org`.

Dauzat, J., Griffon, S., Roupsard, O., Vaast, P., and Rodrigues, G. (2014). Building the foundations of a coffea arabica fspm. In *Embrapa Informática Agropecuária-Resumo em anais de congresso (ALICE)*. In: INTERNATIONAL CONFERENCE ON FUNCTIONAL-STRUCTURAL PLANT MODELS, 7., 2013, Saariselkä. Proceedings... Vantaa: Finnish Society of Forest Science, 2013.

Davis, A. P., Gole, T. W., Baena, S., and Moat, J. (2012). The impact of climate change on indigenous arabica coffee (coffea arabica): predicting future trends and identifying priorities. *PloS one*, 7(11):e47981.

Eitzinger, A., Läderach, P., Carmona, S., Navarro, C., and Collet, L. (2013). Prediction of the impact of climate change on coffee and mango growing areas in haiti. Technical report, Full Technical Report. Centro Internacional de Agricultura Tropical (CIAT), Cali, Colombia. http://dapa. ciat. cgiar. org/wp-content/uploads/2014/03/CC_impact_coffeemango_Haiti_CRS-CIAT_final. pdf.

Enfield, D. B., Mestas-Nunez, A. M., Trimble, P. J., et al. (2001). The atlantic multidecadal oscillation and its relation to rainfall and river flows in the continental u. s. *Geophysical Research Letters*, 28(10):2077–2080.

Epstein, P. R. (1999). Climate and health. *Science(Washington)*, 285(5426):347–348.

FAO/IIASA/ISRIC/ISSCAS/JRC (2012). Harmonized world soil database (hwsd). *FAO, Rome, Italy and IIASA, Laxenburg, Austria*.

Ferreira, S. and Boley, R. (1991). Hemileia vastatrix. *Crop Knowledge Master. Available at: www. extento. hawaii. edu/kbase/crop/type/h_ vasta. htm. Acessed on*, 7(27):2012.

Gay, C., Estrada, F., Conde, C., Eakin, H., and Villers, L. (2006). Potential impacts of climate change on agriculture: A case of study of coffee production in veracruz, mexico. *Climatic Change*, 79(3-4):259–288.

Gelman, A., Carlin, J. B., Stern, H. S., and Rubin, D. B. (2014). *Bayesian data analysis*, volume 2. Taylor & Francis.

Georgiou, S., Jacques, A., and Imbach Bartol, P. A. (2014). An analysis of the weather and climate conditions related to the 2012 epidemic of coffee rust in guatemala. technical report.

GISTEMP Team (2015). GISS Surface Temperature Analysis (GISTEMP). Dataset accessed 2015-06-05 at http://data.giss.nasa.gov/gistemp/.

Gonzalez, R. J. (2010). *Zapotec science: Farming and food in the Northern Sierra of Oaxaca*. University of Texas Press.

Guilford, G. (2014). How climate change and a deadly fungus are threatening the world's coffee supply. Retrieved from `http://www.citylab.com/weather/2014/06/how-climate-change-and-a-deadly-fungus-are-threatening-the-worlds-coffee-supply/371994/`.

Guzmán Martínez, O., Jaramillo Robledo, A., and Baldión Rincón, J. V. (1999). Anuario meteorologico cafetero, 1998.

Hansen, J., Ruedy, R., Sato, M., and Lo, K. (2010). Global surface temperature change. *Reviews of Geophysics*, 48(4).

Hijmans, R. J., Cameron, S. E., Parra, J. L., Jones, P. G., Jarvis, A., et al. (2005). Very high resolution interpolated climate surfaces for global land areas. *International journal of climatology*, 25(15):1965–1978.

Hsiang, S. M. and Meng, K. C. (2015). Tropical economics. *American Economic Review*, 105(5):257–61.

Hylander, K., Nemomissa, S., Delrue, J., and Enkosa, W. (2013). Effects of coffee management on deforestation rates and forest integrity. *Conservation biology*, 27(5):1031–1040.

International Coffee Council (1998). The "el niño southern oscillation event (enso)" and its impact on coffee production. Technical report. Available at `http://www.ico.org/documents/eb3657r1e.pdf`.

International Coffee Organization (2015a). Climate change and coffee: Enhancing the coffee sector's response to climate change. Technical report.

International Coffee Organization (2015b). ICO Historical Data. Supplied by ICO, May 7, 2015.

International Research Institute for Climate and Society (2015). IRI/CPC ENSO Predictions Plume. Available at `http://iri.columbia.edu/our-expertise/climate/forecasts/enso/current/`, accessed on Sep. 23, 2015.

IPCC (2014). Climate change 2014: Impacts, adaptation, and vulnerability. part a: Global and sectoral aspects. contribution of working group ii to the fifth assessment report of the intergovernmental panel on climate change. Technical report.

Jaramillo, A. (2005). Solar radiation and rainfall distribution within coffee plantations (coffea arabica l.). *Rev Acad Col Ci Ex Fıs Ntles (Colombia)*, 29:371–382.

Jaramillo, J. (2013). Coffee under threat. In *Coffee: A Comprehensive Guide to the Bean, the Beverage, and the Industry*.

Jaramillo, J., Chabi-Olaye, A., Kamonjo, C., Jaramillo, A., Vega, F. E., Poehling, H.-M., Borgemeister, C., et al. (2009). Thermal tolerance of the coffee berry borer hypothenemus hampei: predictions of climate change impact on a tropical insect pest. *PLoS One*, 4(8):e6487.

Jaramillo, J., Muchugu, E., Vega, F. E., Davis, A., Borgemeister, C., and Chabi-Olaye, A. (2011). Some like it hot: the influence and implications of climate change on coffee berry borer (hypothenemus hampei) and coffee production in east africa. *PLoS One*, 6(9):e24528.

Jarvis, A., Reuter, H. I., Nelson, A., and Guevara, E. (2008). Hole-filled srtm for the globe version 4. *available from the CGIAR-CSI SRTM 90m Database (http://srtm. csi. cgiar. org)*.

Jassogne, L., Lderach, P., and van Asten, P. (2013). The impact of climate change on coffee in uganda: Lessons from a case study in the rwenzori mountains. *Oxfam Policy and Practice: Climate Change and Resilience*, 9(1):51–66.

Körner, C., Morgan, J., and Norby, R. (2007). Co2 fertilization: When, where, how much? In *Terrestrial ecosystems in a changing world*, pages 9–21. Springer.

Kutywayo, D., Chemura, A., Kusena, W., Chidoko, P., and Mahoya, C. (2013). The impact of climate change on the potential distribution of agricultural pests: the case of the coffee white stem borer (monochamus leuconotus p.) in zimbabwe. *PloS one*, 8(8):e73432.

Laderach, P., Lundy, M., Jarvis, A., Ramirez, J., Portilla, E. P., Schepp, K., and Eitzinger, A. (2009). *Predicted impact of climate change on coffee supply chains*. na.

Lockwood, D. R. and Lockwood, J. A. (2008). Grasshopper population ecology: catastrophe, criticality, and critique. *Ecology and Society*, 13(1):34.

Magina, F., Makundi, R., Maerere, A., Maro, G., and Teri, J. (2011). Temporal variations in the abundance of three important insect pests of coffee in kilimanjaro region, tanzania. In *Proceedings, 23rd International Scientific Colloquium on Coffee. Association Scientifique Internationale du Café (ASIC), Bali, Indonesia*, pages 1114–1118.

Magrath, J. (2014). Coffee rust fungus threatens employment collapse in central america.

Malkin, E. (2014). A coffee crop withers. Retrieved from `http://www.nytimes.com/2014/05/06/business/international/fungus-cripples-coffee-production-across-central-america.html`.

Maro, G., Mrema, J., Msanya, B., Janssen, B., and Teri, J. (2014). Developing a coffee yield prediction and integrated soil fertility management recommendation model for northern tanzania. *International Journal of Plant & Soil Science*, 3(4):380–396.

Maxey, M. (2015). Arabica coffee from yemen: Hope in a time of turmoil. Available at https://www.linkedin.com/pulse/arabica-coffee-from-yemen-hope-time-turmoil-michael-maxey.

McGrath, J. M. and Lobell, D. B. (2013). Regional disparities in the co2 fertilization effect and implications for crop yields. *Environmental Research Letters*, 8(1):014054.

Menke, W. (2012). *Geophysical data analysis: discrete inverse theory*. Academic press.

Modern Farmer (2014). Battling the coffee rust: Photos of farmers fighting an epidemic. Retrieved May 16, 2015, from http://modernfarmer.com/2014/08/battlingcoffee-growers-struggleepidemic/.

Monfreda, C., Ramankutty, N., and Foley, J. A. (2008). Farming the planet: 2. geographic distribution of crop areas, yields, physiological types, and net primary production in the year 2000. *Global biogeochemical cycles*, 22(1).

Muschler, R. G. (2001). Shade improves coffee quality in a sub-optimal coffee-zone of costa rica. *Agroforestry systems*, 51(2):131–139.

NCAR (2015). Ncep/ncar reanalysis monthly jeans and other derived variables. Retrieved 17 Apr. 2015 from http://www.esrl.noaa.gov/psd/data/gridded/data.ncep.reanalysis.derived.html.

Nelsen, R. B. (2013). *An introduction to copulas*, volume 139. Springer Science & Business Media.

NOAA Climate Prediction Center (CPC) (2015). Climate indices: Monthly atmospheric and ocean time series. Available at http://www.esrl.noaa.gov/psd/data/climateindices/list/.

Nzeyimana, I., Hartemink, A. E., and Geissen, V. (2014). Gis-based multi-criteria analysis for arabica coffee expansion in rwanda. *PloS one*, 9(10):e107449.

O'Brien, T. G. and Kinnaird, M. F. (2003). Caffeine and conservation. *Science(Washington)*, 300(5619):587.

Ovalle-Rivera, O., Läderach, P., Bunn, C., Obersteiner, M., and Schroth, G. (2015). Projected shifts in coffea arabica suitability among major global producing regions due to climate change.

Page, S. E., Siegert, F., Rieley, J. O., Boehm, H.-D. V., Jaya, A., and Limin, S. (2002). The amount of carbon released from peat and forest fires in indonesia during 1997. *Nature*, 420(6911):61–65.

Pendergrast, M. (1999). *Uncommon grounds: The history of coffee and how it transformed our world*. Basic Books.

Pohlan, H. A. J. and Janssens, M. J. (2012). Growth and production of coffee. *Soil, Plant Growth Crop Produc*, 3:1–11.

Ricketts, T. H., Daily, G. C., Ehrlich, P. R., and Michener, C. D. (2004). Economic value of tropical forest to coffee production. *Proceedings of the National Academy of Sciences of the United States of America*, 101(34):12579–12582.

Rodríguez, D., Cure, J. R., Cotes, J. M., Gutierrez, A. P., and Cantor, F. (2011). A coffee agroecosystem model: I. growth and development of the coffee plant. *Ecological modelling*, 222(19):3626–3639.

Saha, S., Moorthi, S., Pan, H.-L., Wu, X., Wang, J., Nadiga, S., Tripp, P., Kistler, R., Woollen, J., Behringer, D., et al. (2010). The ncep climate forecast system reanalysis. *Bulletin of the American Meteorological Society*, 91(8):1015–1057.

Schlenker, W. and Roberts, M. J. (2009). Nonlinear temperature effects indicate severe damages to us crop yields under climate change. *Proceedings of the National Academy of sciences*, 106(37):15594–15598.

Schneider, A., Friedl, M., Woodcock, C. E., et al. (2003). Mapping urban areas by fusing multiple sources of coarse resolution remotely sensed data. In *Geoscience and Remote Sensing Symposium, 2003. IGARSS'03. Proceedings. 2003 IEEE International*, volume 4, pages 2623–2625. IEEE.

Schroth, G., Läderach, P., Cuero, D. S. B., Neilson, J., and Bunn, C. (2014). Winner or loser of climate change? a modeling study of current and future climatic suitability of arabica coffee in indonesia. *Regional Environmental Change*, pages 1–10.

Sharf, S. (2014). Mondelez to take bigger sip of $81b global coffee industry with de master joint venture. Retrieved from `http://www.forbes.com/sites/samanthasharf/2014/05/07/mondelez-to-take-bigger-sip-of-81b-global-coffee-industry-with-de-master-joint-venture/`.

Stocker, T., Qin, D., Plattner, G.-K., Tignor, M., Allen, S. K., Boschung, J., Nauels, A., Xia, Y., Bex, V., and Midgley, P. M. (2014). *Climate change 2013: The physical science basis*. Cambridge University Press Cambridge, UK, and New York.

Sweet Maria (2015). World coffee production timetable. Available at `http://sweetmarias.com/coffee.prod.timetable.php`.

Thurston, R. W., Morris, J., and Steiman, S. (2013). *Coffee: A Comprehensive Guide to the Bean, the Beverage, and the Industry*. Rowman & Littlefield Publishers.

Ubilava, D. (2012). El niño, la niña, and world coffee price dynamics. *Agricultural Economics*, 43(1):17–26.

United Nations International Merchandise Trade Statistics (2009). Commodity pages, 071, coffee and coffee substitutes. In *Yearbook 2009*. `http://comtrade.un.org/pb/CommodityPagesNew.aspx?y=2009`, accessed June 11, 2011.

van Rikxoort, H., Schroth, G., Läderach, P., and Rodríguez-Sánchez, B. (2014). Carbon footprints and carbon stocks reveal climate-friendly coffee production. *Agronomy for Sustainable Development*, 34(4):887–897.

Varangis, P. N. et al. (2003). *Dealing with the coffee crisis in Central America: Impacts and strategies*, volume 2993. World Bank Publications.

Villegas, N., Barrientos, J. C., and Málikov, I. (2012). Relationship between ocean-atmospheric parameters and green coffee production in colombia. *Revista Colombiana de Ciencias Hortícolas*, 6(1):88–95.

WDPA Consortium (2004). World database on protected areas. *World Conservation Union and UNEP-World Conservation Monitoring Centre, New York, New York, USA*.

Willson, K. (1985). Climate and soil. In *Coffee*, pages 97–107. Springer.

Wrigley, G. (1988). Coffee. tropical agricultural series. *Long man Scientific and Technical publishing: New York*, page 639.

Acknowledgments

We would like to thank **Walter Baethgen** at the International Research Institute for Climate and Society for his thoughtful reviews of the work here and all of his comments and suggestions.

Many thanks also to:

Andrea Illy, illycaffè S.p.A., Chairman/CEO

Mario Cerutti, Lavazza S.p.A., Corporate Relations

Belay Begashaw, Columbia Global Centers, Director

Mauricio Galindo, International Coffee Organization, Head of Operations

Alexandra Tunistra, Root Capital, Advisory Services

Amir Jina, University of Chicago, Economics

Joann de Zegher, Stanford University, Environment and Resources

Marion Dumas, Columbia University, School of International and Public Affairs